Pharmacodynamic in vitro studies contributing to the rational use of linezolid in infections by vancomycin resistant Enterococcus faecium

DISSERTATION

zur Erlangung des akademischen Grades

doctor rerum naturalium (Dr. rer. nat.)

vorgelegt der

Naturwissenschaftlichen Fakultät I
Biowissenschaften

der Martin-Luther-Universität Halle-Wittenberg

von Frau Dipl. pharm.
Julia Michael
geborene Glöde, am 05.08.1981 in Halle

Gutachter:

1. Prof. Dr. Charlotte Kloft
2. Prof. Dr. Andreas Langner
3. Prof. Dr. Markus Zeitlinger

Halle (Saale), 20.07.2011   verteidigt am 05.12.2011

Meinen Eltern

Contents

Abstract

Bacterial infections still present a serious problem and the leading cause of death worldwide. Increasing resistance development and the shortage of new antibiotics necessitate a rational dosing of the existing drugs such as linezolid (LZD). One bacterial strain with a high resistance potential is *Enterococcus faecium*, which may cause severe skin as well as systematic infections (sepsis and septic shock).

The present work systematically investigated the effect of linezolid on vancomycin resistant *Enterococcus faecium* (VRE; ATCC 700221) over (i) a wide range of constant LZD concentrations in a static *in vitro* model and under (ii) *in vivo*-like changing drug concentrations in a dynamic *in vitro* model. At first, several preliminary microbiological investigations were performed ensuring a stable and reproducible experimental conduction. Bacterial counting was performed under assistance of a digital automatic colony counter, which was efficiently qualified for the developed methods with respect to guidelines. To determine the experimental drug concentrations, an HPLC assay for LZD in the bacterial growth medium was assessed and successfully validated according to FDA guidelines. Thus, LZD samples could be routinely taken during *in vitro* experiments and determined. This allowed linking of the observed effect to the actual experimental drug concentrations and furthermore, it confirmed the robustness of the models with respect to drug concentrations. To investigate the effect of changing LZD concentrations on VRE, a known dynamic *in vitro* model working on the principles of drug dilution was advanced and optimised concerning bacteria retainment and bacterial backgrowth in this work. The reliability and robustness of the dynamic model was investigated concerning variations in drug concentrations and in bacterial concentrations, which were below 11 and 5%, respectively. The dynamic *in vitro* model was utilised for time-kill studies under changing drug exposure, whereby different routes of administrations and different declines of drug concentrations were applied.

The effect of LZD on VRE was examined by time-kill curves and the relative bacterial reduction analysis (RBR). Comparison of the results with parts of previous studies showed a high reliability of the data. LZD concentrations of 1.5 to 1.7 µg/mL were identified to lead to a disproportionately high increase of the drug effect, even though the MIC was determined with 2-4 µg/mL. Furthermore, a dose escalation did not increase the maximum effect of LZD, which was observed by 8 µg/mL. The maximum effect was reached at 12 h, independent of the drug administration route and drug decline. The use of a commercially available VRE strain and the determination of actual experimental drug concentrations guaranteed reproducible and comprehensive results. For further interpretation of the bacterial concentration-time courses different mathematical models were applied to describe the growth and kill of bacteria, the RBR and the effect at different time points, respectively.

Based on the developed mathematical RBR model computer simulations of the effect based on different dosings were carried out. Deterministic simulations for a typical patient examined several different dosing regimens of LZD. Stochastic simulations described the range of these effects in a patient population. The revision of the standard dosing of LZD (2x 600mg) by deterministic simulations showed the appropriateness of this dosing regimen against VRE infections in typical patients, but also the benefit for nearly all patients by reaching the maximum effect due to a higher daily dose of LZD (1800 mg) was indicated. In a worst-case scenario concerning the antibiotic effect, the effect of LZD on VRE in a patient with worst pharmacokinetic conditions such as a high drug clearance was also simulated. For this type of patient different dosing regimens with an increased daily dose (1800 mg) of LZD and thus an increased antibiotic effect were simulated. The positive effects suggest these dosing regimens to be tested in clinical trials in the future.

Zusammenfassung

Bakterielle Infektionen stellen weltweit immer noch ein großes Problem und die häufigste Todesursache dar. Steigende Resistenzraten und der Mangel an neuen Antibiotika erfordern einen rationaleren Einsatz der vorhandenen Arzneistoffe wie z.B. Linezolid (LZD). Ein Bakterienstamm mit hohem Resistenzpotenzial ist *Enterokokkus faecium*, der zu schweren Haut- und Systeminfektionen (Sepsis und septischer Schock) führen kann.

Die vorliegende Arbeit untersuchte systematisch die Wirkung von Linezolid auf Vancomycin-resistenten *Enterokokkus faecium* (VRE, ATCC 700221) über (i) einen breiten LZD-Konzentrationsbereich mit konstanten Bedingungen in einem statischen *In-vitro*-Modell und unter (ii) *in-vivo*-adaptierten, sich verändernden Arzneistoffkonzentrationen in einem dynamischen *In-vitro*-Modell. Vorab wurden verschiedene mikrobiologische Untersuchungen wurden durchgeführt, um die Stabilität und Qualität der experimenellen Durchführung zu gewährleisten. Die Bakterienauszählung wurde mittels eines digitalen automatischen Kolonienzählgeräts durchgeführt, welches für die eigens entwickelte Zählmethode erfolgreich, leitliniengerecht qualifiziert wurde. Für die Bestimmung der Arzneistoffkonzentration in den *In-vitro*-Experimenten wurde ein HPLC-Assay für LZD in Bakterienkulturmedium bestimmt und erfolgreich nach FDA Guidelines qualifiziert. Dadurch konnten die LZD-Konzentrationen in den *In-vitro*-Versuchen routinemäßig gewonnen und bestimmt werden. Dies ermöglichte die Verknüpfung der beobachteten Wirkung (Bakteriensterben) mit den tatsächlichen Arzneistoffkonzentrationen und bestätigte außerdem die Robustheit der in den *In-vitro*-Modellen erzeugten Arzneistoffkonzentrationen. Für die Untersuchungen des Effekts von abnehmenden LZD-Konzentrationen auf VRE diente ein bestehendes dynamisches *In-vitro*-Modell, das auf mit dem Prinzip der Arzneistoffverdünnung arbeitet und in der vorliegenden Arbeit weiter entwickelt und hinsichtlich Bakterienverlust und Bakterienwachstum in das Vorratsgefäß optimiert wurde. Die Zuverlässigkeit und Robustheit des dynamischen Modells wurde untersucht und in die Variationen in der Arzneistoffkonzentration und der Bakterienzahl mit sehr guten Werten von 11 bzw. 5% ermittelt. In diesem dynamischen *In-vitro*-Modell wurden Wachstumskurven (time-kill curves) unter veränderlichen Arzneistoffkonzentrationen untersucht, wobei verschiedene Wege der Arzneistoffgabe und unterschiedliche Abnahmen der Arzneistoffkonzentration angewendet wurden.

Die Wirkung von Linezolid auf VRE wurde mittels Wachstumskurven und Analyse der relativen Bakterienreduktion (RBR) analysiert. Der Vergleich von Ergebnisteilen mit vorherigen Studien zeigte eine hohe Verlässlichkeit der Daten. LZD-Konzentrationen von 1.5-1.7 µg/mL konnten als Schlüsselkonzentrationen mit überproportionaler Wirkungssteigerung identifiziert werden, obwohl die minimale Hemmkonzentration mit 2-4 µg/mL bestimmt wurde. Außerdem konnte durch Dosiseskalation keine Steigerung des maximalen Effekts, wie er für 8 µg/mL LZD

beobachtet wurde, erreicht werden. Dieser maximale Effekt wurde nach 12 h erreicht, wobei weder die Art der Arzneistoffgabe noch ihr Abbau einen Einfluss hatten. Durch die Verwendung eines kommerziell verfügbaren Bakterienstammes und die Bestimmung der tatsächlichen Arzneistoffkonzentrationen im Modell sind die Ergebnisse reproduzierbar und nachvollziehbar. Eine weitergehende Auswertung des Bakterienkonzentrations-Zeitverlaufs erfolgte mithilfe von verschiedenen mathematischen Modellen, die den Effekt zu verschiedenen Zeitpunkten, die relative Bakterienreduktion und das Wachstums- bzw. Absterbeverhalten beschrieben.

Mit dem entwickelten RBR-Modell konnte in computergestützten Simulationen die Wirkung von verschiedenen Arzneistoffdosierungen vorhergesagt werden. In deterministischen Simulationen für einen typischen Patienten wurden mehrere verschiedene LZD-Dosierungen untersucht. Stochastische Simulationen wurden zur Abschätzung des Ausmasses der Wirkung in dieser Patientengruppe benutzt. Die Überprüfung der Standarddosierung von LZD (2x 600 mg) durch deterministische Simulation zeigte die Angemessenheit dieser Dosierung bei VRE-Infektionen in typischen Patienten, aber auch ein höherer Nutzen für fast alle Patienten durch Erreichen der maximalen Wirkung bei 1800 mg Tagesdosis konnte gezeigt werden. In einem Worst-Case-Szenario hinsichtlich des antibiotischen Effekt, wurde die Wirkung von LZD auf VRE in einem Patienten mit besonders ungünstige pharmakokinetische Eigenschaften wie einer hohen Arzneistoffclearance simuliert. Für diese Patientengruppe wurden verschiedene Dosierungsregime mit 1800 mg Tagesdosis und damit einer erhöhten antibiotischen Wirkung simuliert. Aufgrund der positiven ermittelten Effekte sollten in Zukunft klinische Studien zu diesen Dosierungsregimen durchgeführt werden.

Abbreviations and symbols

α	Hybrid constant for the rapid distribution and elimination phase in the two-compartmental model
AIC	Akaike's information criterion
AICc	Corrected Akaike's information criterion
AUBC	Area between the growth control and antibiotic effect curves
AUC	Area under the curve
AUC_E	Area under the effect curve
$AUC_{E(14\ days)}$	Area under the effect-time curve over 14 days
$AUC_{E,max}$	Maximum area under the effect time curve over 14 days
β	Hybrid constant for the slower distribution and elimination phase in the two-compartmental model
BE	Baseline effect
C	Drug concentration
C_1 and C_2	Concentration in compartment one and two
C_e	Drug concentration in the effect compartment
$Ce_{ss,max}$	Maximum concentration in the effect compartment at steady state
C_{est}	Estimated drug concentration
cfu/mL	Colony forming units per millilitre
95% CI	95% confidence interval
CL	Clearance
C_{nom}	Nominal drug concentration
C_{max}	Maximum drug concentration
Cmt/s	Compartment/s
$Cp_{ss,max}$	Maximum concentration in plasma at steady state
CV	Coefficient of variation
DD	Daily dose
DD_{50}	Daily dose producing the half maximum AUC_E
DE	Drug effect
dk	Delay in kill constant
E	Effect
E. faecalis	*Enterococcus faecalis*
E. faecium	*Enterococcus faecium*
EC_{50}	Concentration provoking the half-maximum effect
$EC_{I,90}$	Drug concentration provoking 90% of the maximum inhibitory effect
EC_{inf}	Drug concentration at the inflexion point

E_I	Inhibitory effect
$E_{I,90}$	90% of the maximum inhibitory effect
E_{inf}	Effect at inflexion point
E_{max}	Maximum kill rate constant
$E_{ss,max}$	Maximum effect at steady state
$E_{ss,min}$	Minimum effect at steady state
GC	Growth control
GC_{max}	Maximum bacterial growth
h	Hour/s
H	Hill coefficient
IIV	Inter-individual variability
I_E	Intensity of the effect
i.v.	Intravenous
k_0	Bacterial growth rate constant
k_{10}	Elimination rate constant from first (central) compartment
k_{12} and k_{21}	Transfer (distribution) rate constants between first and second compartment
k_{1i}	Transfer rate constant from the central to the hypothetical inhibition compartment
k_a	Absorption rate constant
k_e	Elimination rate constant
k_{e0}	Elimination rate constant from the effect compartment
k_{i0}	Elimination rate constant from the hypothetical inhibition compartment
k_{ic}	Elimination rate constant from central to inhibition compartment
LZD	Linezolid
MH	Mueller-Hinton
MIC	Minimum inhibitory concentration
MRSA	Methicilline resistant *Staphylococcus aureus*
MSC	Model selection criterion
n	Number/s
N	Bacterial concentration
N_0	Minimum bacterial concentration in the effect at different time-points model
N_{max}	Maximum bacterial concentration in the effect at different time-points model
N_{min}	Minimum bacterial concentration in the time-kill curve model
No.	Number
PBSP	Phosphate-buffered saline solution with peptone
PD	Pharmacodynamic/s
PK	Pharmacokinetic/s
PP	Polypropylene
X	

R	Coefficient of correlation
R^2	Coefficient of determination
RBR	Relative bacterial reduction
RE	Relative error
rpm	Rounds per minute
S. aureus	*Staphylococcus aureus*
S.D.	Standard deviation
SSR	Sum of squared residuals
t	Time
T	Duration of infusion
V	Volume
V2	Volume of distribution in the central compartment
V3	Volume of distribution in the peripheral compartment
VBA	Visual basic for applications
VRE	Vancomycin resistant Enterococcus/i

1 Introduction

1.1 Trends in infectious diseases and antiinfective treatment

Infectious diseases still belong to the chief causes of death world wide. In the developing world, they even present the main cause of death.[1, 2] Also in the industrial countries their relevance rises again, due to the higher spreading of pathogens and the enhanced development of resistances against existing antiinfective drugs, which are both originated in the modernisation in the society such as urban development and travelling activities.[2] The severity of infectious diseases, in contrast to other illnesses, consists in the spreading and transmission of pathogens to other people;[2] the emergency is even higher for resistant germs. Strategies for the reduction of resistances include the adherence to hygienic principles, the eradication of the source of infections, the inhibition of resistance development by a rational use of the existing antiinfective drugs and the minimisation of resistant pathogens by new drugs.[2]

The number of bacterial targets is limited and different antibiotics intervene in the same process. An acquired antibiotic resistance can therefore affect also other antibiotics (cross resistance).[3] The identification of new targets and therewith the development of new antibiotics has decreased in the last years.[4, 5] However, the new antibiotic classes of oxazolidinones (first agent: linezolid), cyclic lipopeptides (first agent: daptomycin) and glycylglycine (first agent: tigecycline) have been developed during the last ten years and their agents released to the market. Due to rare newly developed antibiotics, the trend in drug development and application focuses more and more on personalised medicine.[6, 7] Along this, drugs have to be better investigated concerning their mode of action in the body, as well as the patients have to be characterised on their physiological conditions resulting in a classification for an appropriate medical treatment.

1.2 Enterococci – a genus with resistance potential

Resistances develop, where antibiotics are frequently used and a variety of bacterial strains come together. Hence, expression and exchange of resistance genes become likely. Especially in hospitals resistant strains emerge more often, where they lead to complicated infections (nosocomial infections), and often exhibit resistances to several drugs (multi-drug resistance).[2, 8] Typical examples of these pathogens are methicilline resistant *Staphylococcus aureus* (MRSA), vancomycin resistant enterococci (VRE) and bacteria developing extended spectrum beta-lactamases (ESBL producer).[9]

In Europe, the occurrence of vancomycin resistant enterococci is less than 10% in the majority of the countries, but the incidence increases dramatically up to 25% in Ireland, Luxembourg and

Greece.[10] In Germany the fraction of vancomycin resistant *Enterococcus faecium* (*E. faecium*) of all enterococci is reported to be between 6.1% and 13.5% and hence presents a serious problem with a tendency to rise. [9, 10]

Enterococci are Gram-positive diplococci, which appear as single cells or (up to) small chains.[11] Their treatment is problematic, since they are tenacious and grow also under for bacteria usually unfavourable environments such as extreme pH (4-9.6),[11, 12] at high temperatures (up to 60 °C) and in saline solution (NaCl 6.5%).[10, 11] Enterococci belong to the natural habitat of the human gut and are normally not pathogenic.[11] Only after invasion into an existing wound, that means as secondary invaders, they provoke infections.[2, 11] This is even more problematic for immunocompromised patients, because of changed physiological properties and missing immune defence, which might deteriorate the patient's condition.

Several subspecies of enterococci exist, but only two of them cause the majority of enterococcal infections: *Enterococcus faecalis* (*E. faecalis*) and *Enterococcus faecium*.[13] A biochemical differentiation of both strains is recommended for some infections, because of the naturally occurring differences in the susceptibility of the strains. Among them *E. faecium* provokes the more complicated infections.[11]

Enterococci are involved in enterococcal endocarditis, urinary tract and intraabdominal wound infections and purulent abdominal infections after damage of the gastrointestinal tract. Bacteraemia very often originates from enterococci and might lead to sepsis and septic shock with a high mortality.[11, 14, 15] In Germany, enterococci cause 11% of the catheter-associated sepsis;[8] in the US are even three of four bloodstream infections caused by enterococci.[10] The increasing number of superinfections caused by enterococci is also based on the misuse of antibiotics for the species lacking the respective indication.[11]

Enterococci have a natural, high potential of resistance. Intrinsic resistance against penicillase resistant penicillins, cephalosporins, clindamycin and aminoglycosides (low level resistance) is resided on the chromosomes as a species characteristic. Acquired resistance caused by mutation in the DNA or acquisition of new DNA (e.g. by plasmids) was found for enterococci against chloramphenicol, fluorquinolones, aminoglycosides (high level resistance) and others. Also the glycopeptide vancomycin, which is a commonly used drug in antimicrobial therapy, can be passed by enterococci. Five different types of vancomycin resistance in enterococci exist categorised by the resistance profile to vancomycin and teicoplanin and the modification of cell wall proteins: VanA (in 80% of all VRE), VanB, VanC, VanD and VanE resistance.[13]

E. faecium exhibits resistance mutations more frequently than *E. faecalis*.[11] It is more often involved in nosocomial infections – with tendency to rise – and therefore of higher importance for supervision.[9, 10, 16] The inappropriate handling of VRE infections, the overuse of antibiotics, but also better methods of detection of VRE, lead to an increasing number of registered VRE infections.[17]

1.3 Linezolid

Linezolid (LZD, Figure 1) is the first agent of the class of oxazolidinones, which inhibit the protein biosynthesis. It was released to the US and German market in 2000 and in 2001, respectively;[18, 19] other oxazolidinones, such as eperezolid, ranbezolid or torezolid, are still in development.[20-23]
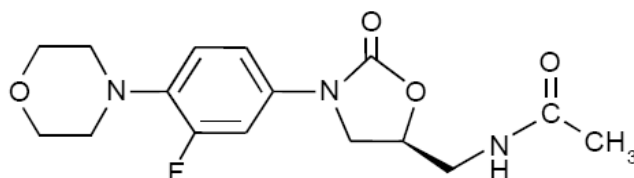
Figure 1 Chemical structure of linezolid.

LZD inhibits the bacterial protein biosynthesis by binding to the 23S site of the bacterial 50S subunit of the ribosomes. Thus, the formation of a functional 70S initiation complex, which is an essential component of the bacterial translation process, is prevented. Since this mechanism of action is not used by other antibacterial agents, no resistances to other antibiotics are expected, so far none have been observed.[18]

The bacterial targets of LZD are aerobic Gram-positive bacteria, but it also exhibits activity against certain Gram-negative bacteria and anaerobic bacteria *in vitro*.[18] LZD is bacteriostatic against enterococci and staphylococci and it is bactericidal for the majority of streptococci strains.[18] The drug is one of the most active agents against *E. faecium* including VRE.[24] The minimum inhibitory concentration (MIC, see 1.6.1), which is regarded as a clinical breakpoint for bacterial strains, ranges between 0.5-4 µg/mL, at which 4 µg/mL is the MIC for strains resistant to other antibiotics such as VRE or MRSA.[18, 25, 26]

LZD is available as oral and intravenous formulation. The intravenous formulation has to be given as short-term infusion ($\geq$ 30 min), by reason of the volume needed to dissolve the drug (600 mg/300 mL). The drug is administered as 600 mg dose every 12 h for uncomplicated and complicated skin and skin structure infections and pneumonia (community acquired or nosocomial origin) over 10 to 14 days. For infections with VRE the drug therapy can be prolonged up to 28 days.[18] The oral formulation has a bioavailability compared to intravenous administration of 100% (complete absorption). This simplifies a sequential intravenous-to-oral therapy, and therewith lowering costs.[27] Maximum plasma concentrations are reached 1-2 h after intake. The parallel intake of LZD and meals delays the time to the maximum concentration but has no influence on the extent of drug absorption.[18]

The plasma protein binding of LZD is about 31% and concentration independent. The drug distributes properly into well-perfused tissue,[18] so that after equilibration the drug

concentrations in interstitial fluids are close to those in plasma.[28, 29] The volume of distribution at steady state is 40-50 L, which approximates the total body water.[19, 30]

LZD is metabolised by oxidation of the morpholine ring, resulting in two inactive carboxylic acid derivates with open ring structure: the aminoethoxyacetic acid metabolite (A), and the hydroxyethyl glycine metabolite (B).[18] Metabolite A is presumed to be formed by an enzymatic pathway, whereas metabolite B should originate from a non-enzymatic pathway. Discussed pathways for B are an uncharacterised cytochrome P450 enzyme and an alternative microsomally mediated oxidation,[31] which might be by nicotine adenine dinucleotide phosphate (NADPH).[32] The nonrenal clearance eliminates 65% of LZD, 30% of the drug appears unchanged in urine and virtually nothing in faeces. The metabolites A and B are excreted to high degree with the urine (10% and 40%, respectively) and less with the faeces (3% and 6%).[18]

Beside the antimicrobial activity, LZD often leads to gastrointestinal adverse effects and headaches. More serious adverse drug reactions are thrombocytopenia and myelosuppression, which appear even under the standard dosing regimen of 600 mg every 12 h.[18, 33] Nevertheless, it is well tolerated *in vivo*.[34]

Resistance towards LZD has already been observed and is most often caused by a point mutation in domain V of the 23S RNA of the 50S ribosomal subunit.[18, 35] LZD resistance occurs *in vitro* at a frequency of 1x 10^{-9} to 1x 10^{-11}.[18] Long-term therapies have been identified as a risk factor for clinical resistance development.[35] Especially VRE became resistant to LZD during antimicrobial therapy,[18, 36] but also cases of LZD resistant *S. aureus* are known.[37] Reasons for the increasing LZD resistance might be the ascending use of LZD and the resulting selection pressure on the treated pathogens. But also the appropriate use of LZD has to be reassessed. Therefore, LZD has to be rationally used especially in treatment of these problematic pathogens and the dosing regimen has to be optimised to preserve the antibiotic for severe infections.

1.4   Demand for *in vitro* models

Due to the low number of newly developed antibiotics, the demand of rational dosing of the existing antibiotics increases. The dose-response relationships of antibiotics are often not well known and therewith also the dosing regimens are improvable.[38] A reason for this shortcoming can be found in the site of measurement. On one hand, the pure antibiotic effect in the patient, which stands for the pharmacodynamics (PD) of the drug,[39] cannot be exactly separated from other factors influencing the infection such as the immune system. On the other hand, also the physiological properties of the patient, which enable the drug to reach its target, have to be considered. The resulting progress of the drug in the body - the pharmacokinetics (PK) - can be described by parameters such as the clearance or the bioavailability of the drug.[39] Since PK and PD are characteristics of an antibacterial agent, they should both be considered in the

development and the assessment of efficacy of the antibiotic therapy.[40, 41] The systematic study of the concentration-time course of the drug (at the site of action) and its linking to the drug effect enables investigations of various dosing regimens. Such PK/PD investigations allow the identification of potentially effective dosing regimens.[40, 42] Moreover, also hypotheses for enhanced therapies can be tested.[41]

So far, no standardised processes for the conduction of PK/PD investigations for antibiotics exist, although they are recommended for new compounds by both the European Medicines Agency (EMA) [38] and the Food and Drug Administration (FDA). [40, 43] Ongoing debates discuss optimal experimental design, the definitions of outcomes and methods of analysis, as well the integration of PK/PD investigations into drug discovery and genomics programs.[41]

The PD of an antibiotic can be characterised by studies of bacterial growth and death under antibiotic exposure.[40] Since these measurements are difficult to conduct in human tissue, animal and *in vitro* models have been utilised. The main advantage of animal models is the human-like growing conditions for bacteria. The human infection can closely be imitated and the outcome of the therapy is clearly defined as cure or death, comparable to humans.[44, 45] The disadvantages are found in PK properties such as the different elimination,[38, 45] which limits the transferability of the data or necessitates sophisticated scaling methods of data from animals to humans.[40, 45]

Contrary to this, *in vitro* models do not need scaling methods, since they can imitate human PK[38] and thus, they are better suited for investigations of the antibiotic activity.[46] Furthermore resistance analyses,[47, 48] determination of the time-kill behaviour (see 1.6.3),[49] and the identification and optimisation of relevant PK/PD indices and breakpoints can be performed within *in vitro* models.[50-54] *In vitro* models are highly flexible and adaptable to different conditions and beside this technical appropriateness, they are also less cost- and resource-intensive.[40] The PK properties of a drug can be directly mimicked in *in vitro* models and exactly monitored. A drawback is their need for special conditions, such as a temperature-controlled environment, and the increasing risk of contamination, the longer the experiment lasts.[40, 55] Furthermore, *in vitro* models cannot mimic immunological factors, the pathology of the infection and the virulence and metabolic behaviour of pathogens.[38, 56] Thus, the *in vitro* derived PD parameters cannot be directly transferred to *in vivo*.[40] Considerations on the different growth environment *in vivo* and *in vitro* have to be made. *In vitro* growth is faster than *in vivo*,[57-59] and the stronger competition for nutrition *in vitro* can lead to a higher expression of drug targets and result in a higher susceptibility of bacteria.[57, 60] Additionally, changes of the phenotype of bacteria may also appear *in vitro*.[61]

However, the bacterial growth *in vivo* can be acceptably predicted by *in vitro* models and different dosing regimens of one or more drugs can easily be compared.[40] Altogether, *in vitro* models give significant contribution to dose optimisation.[56, 62-64]

1.5 Types of *in vitro* models

1.5.1 Static *in vitro* models

Different types of *in vitro* models have been developed to investigate the effect of a drug on bacteria over time. Static *in vitro* models can be used to quantify the effect of a constant drug concentration in a constant environment on a pathogen.[40] The determination of the effect over time by time-kill curves (see 1.6.3) [65, 66] is a recommended,[38, 43] and often used methodology to obtain basic information of the antibacterial effect.

Static *in vitro* models consist of a closed culture vessel, such as a cell culture flask, where the bacteria are suspended in growth medium (Figure 2) and antibiotics can be added. To study the antibiotic effect at predefined time points, bacteria and drug samples can be taken. In general, all growing conditions as well as the drug concentration remain the same over the whole observation period, because of the closed system. But this is also the shortcoming of static models compared to *in vivo* conditions, where the drug concentration declines over time and the surrounding medium is continuously renewed. The depletion of nutrients, space limitations and expansion of toxic metabolites lead to growth restrictions,[58] which advise static models to be adequate for shorter observations of about 24 h only. The favourable economic aspects of static models and the easy handling made them an extensively used tool. The quick-and-easy findings bring useful preliminary knowledge for further dynamic investigations (see 1.5.2). [40]

Figure 2 Schematic depiction of a static in vitro model; the closed culture vessel contains drug and bacteria.

1.5.2 Dynamic *in vitro* models

Drug concentrations *in vivo* are not constant but change over time, therefore the effect of antibiotics on bacteria should also be related to changing (dynamic) drug concentrations.[65] Dynamic *in vitro* models reflect the *in vivo* conditions of changing drug concentrations and medium (nutrition) much closer than static models.[65, 67] The PK at the target site such as tissue or bone concentrations can be applied to the bacteria.[40] The idea of dynamic models is to change the drug concentrations *in vitro* to mimic the *in vivo* elimination capacity (clearance).[65] For this purpose, two different operation principles for declining drug concentrations have been used: dilution and diffusion.[40, 67] Dilution means to change the drug concentration directly in the

culture vessel by the incoming fresh, drug-free medium; whereas in a diffusion (or dialysis) model, the drug has to pass a membrane to reach the bacteria. Another distinction in dynamic models concerns the bacterial concentration. The bacterial concentration can be reduced by dilution in new, incoming medium without outflow. Or incoming medium leads to an overflow of medium (constant total volume) and hence bacteria are lost by flushing out with the outgoing medium. Alternatively, the bacterial loss can also be prevented by technical barriers (filters), when the total volume is kept constant.[40] Figure 3 displays a schematic depiction of a dynamic dilution model without bacteria loss as it is representative for this thesis. Fresh medium is pumped from a reservoir into the culture vessel, which contains the bacteria, and from there into the waste. So the drug concentration in the culture vessel declines by the incoming (and outgoing) volume of medium. In- and outflow are controlled and the volume in the culture vessel remains constant.[40] The filter in front of the waste allows the passage of drug molecules, but retains bacteria. Different routes of drug administration can be simulated in dilution models: For imitation of an intravenous (i.v.) bolus administration (no absorption), the drug can be directly added to the culture vessel. An intravenous infusion (zero-order absorption) can be mimicked by addition of the drug to the reservoir. So the drug-containing medium is transported into the culture vessel and from there into the waste. The end of the infusion can be realised by exchange of the drug-containing medium to drug-free medium. Also an extravascular administration (first-order absorption) could be realised.[40, 68]
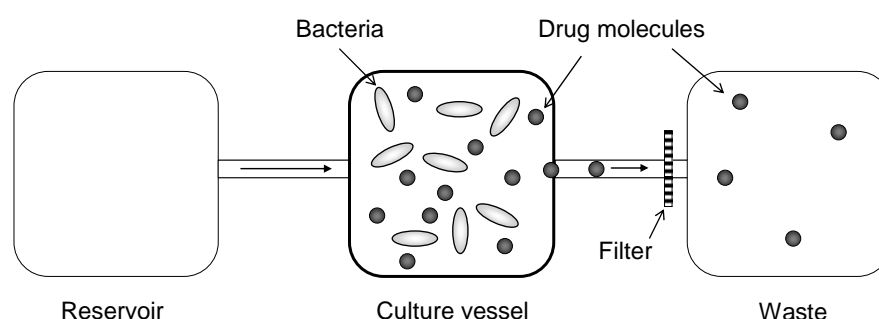
Figure 3 Schematic depiction of a dynamic dilution model with continuous dilution and bacteria retain; adapted from Gloede et al. [40]. The setting would be suitable for simulations of i.v. bolus administration or i.v. infusion.

In diffusion models bacteria are captured behind a barrier, such as a dialysis membrane, in a peripheral compartment. The drug is added to the central compartment and reaches the bacteria by passive diffusion through the membrane. The concentration gradient between central and peripheral compartment is the driving force. Not all PK profiles can be directly applied in diffusion models, because of the time the drug needs to diffuse to the peripheral compartment (time delay). Thus, the actual drug exposure to bacteria need not be the intended one. In contrast

to this, dilution models unite drug and bacteria in the same compartment, so that the bacteria are directly exposed to the designated drug concentration.[40] By this reason, the present work used a dilution model without bacterial loss for investigations of the effect of continuously changing drug concentrations on bacteria, which allows imitation of virtually all relevant *in vivo* PK profiles. More information on the mechanism and use of diffusion models can be found in the literature.[40, 67, 69-73]

Compared to static *in vitro* models, dynamic models have several advantages: They allow investigations of antibiotic effects under *in vivo* like drug concentrations and enable prolonged treatment studies,[74-78] where multiple dosing can be performed.[70, 79] However, blockage of the filtering membrane in dilution and diffusion models,[80, 81] and bacteria adhering to the vessel wall leading to artefacts in cell counts, are serious experimental problems.[82] The large volumes, which are needed to change the drug concentration according to the half-life, might be cost-intensive. For antibiotics with a long half-life a low flow rate and a low volume of medium replacement have to be applied. As a consequence the nutrition may be depleted and toxic metabolites might increase. Due to the slow flow rate bacteria might grow back into the medium reservoir. Even though dynamic models yield more realistic results than static models.[40]

1.6 Evaluation of the antibacterial effect

1.6.1 Minimum inhibitory concentration

The minimum inhibitory concentration (MIC) is defined as the lowest concentration of a drug that inhibits visible growth of bacteria after overnight incubation (18 or 24 h).[83, 84] Based on the applied drug concentration, pathogens are divided in susceptible, intermediate and resistant to the drug.[3] The MIC can be determined by diffusion or turbidity measurement.[85] In the first case, the drug diffuses into the bacteria inoculated agar and the effect is measured (growth or no growth).[85] The diffusion measurement is used for the disc diffusion method [86] and the E-test.[87] In the second case, the turbidity of a drug and bacteria containing medium is visually assessed (cloudy or clear).[85] Methods with turbidity measurement are: micro broth dilution, macro broth dilution [88] and agar dilution method.[84] The different measurements for MIC determination may lead to different results,[89] which necessitates standard drugs and bacteria to compare the results from both measurements. Geometric rows of drug dilutions are commonly used to investigate a wide range of drug concentrations.[83, 85]

Decisions for a suitable drug and an optimised therapy are mostly based on the MIC of the bacteria.[90] Furthermore, related PK/PD indices (see 1.6.2) such as the time above the MIC are used for dose optimisation and require a reliable MIC value.[89] The advantage of the MIC as an effect measurement rests in its routine determination.[91] On the contrary variations in the MIC results appear due to inconsistent methodologies concerning the unbound drug concentration,

the bacterial inoculum size, the growth medium and the incubation period (time of reading).[89, 92] Variations in the MIC results up to factor eight may follow.[89] The MIC does also not reflect the needed time to reach a bactericidal or bacteriostatic effect.[92] Slow and fast acting agents cannot be differentiated by reading once after 24 h. Finally, the MIC is identified under constant drug concentrations whereas they change *in vivo*.[91] Despite the MIC has limitations, it is still used and considered as important breakpoint in clinical practice and should therefore be determined as advised in general instructions.[85, 93]

1.6.2 Pharmacokinetic/pharmacodynamic indices

PK/PD indices were composed to quantify the relationship between PD parameters (e.g. MIC) and PK parameters (e.g. clearance).[50] They are determined in animal or *in vitro* studies for special doses and pathogens,[53] and should be related to unbound drug concentrations. They depend on the frequency of dosing (single vs. multiple dosing) and the linearity of drug decline.[50]

The most frequently used PK/PD indices are the area under the concentration-time curve divided by the MIC (AUC/MIC), the time with drug concentration above the MIC ($T_{C>MIC}$) and the ratio of maximum concentration to MIC (C_{max}/MIC).[41] PK/PD breakpoints are claimed to predict with a high probability the success of a therapy in patients.[53] They can be used to find more reliable clinical MIC breakpoints differing between susceptible and resistant pathogens.[53] By adaptation of the PK/PD indices to the conditions of the patient and the MIC of the pathogen, appropriate dosages could be calculated and administered *in vivo*.[53] Although PK/PD indices include more factors influencing the clinical therapy, they are still based on the MIC with its inherent drawbacks (see 1.6.1) and are thus also highly variable.[53, 63, 91] Thus, further efforts for the interpretation and correct application of PK/PD indices have to be made.[53]

1.6.3 Time-kill curve investigations

Time-kill curves are PK/PD investigations of the antibacterial effect, where the bacterial concentration-time course is followed by monitoring the number of viable bacterial cells (PD) [40] at predefined time points under consideration of the drug concentration (PK).[65, 91] This can be achieved *in vivo*[45, 94] and *in vitro*. *In vitro* time-kill studies can be performed under constant (static model, see 1.5.1) or changing drug concentrations (dynamic model, see 1.5.2). Thus, more detailed information on the bacterial concentration-time course can be revealed, such as the time to reach a bactericidal or bacteriostatic effect.[65]

When mathematical models are applied to time-kill curves, the bacterial growth/death over time as effect of the drug (killing of bacteria) can be related to a dosing regimen and several potential dosing regimens can be investigated in silico.[49] Generally, an E_{max} model is utilised, whereupon

at least three single PD parameters can mathematically describe the effect (over time) instead of using MIC threshold values: the growth rate constant (k_0), the maximum effect rate constant (E_{max}) and the drug concentration provoking the half-maximum effect (EC_{50}).[91] Various models have been developed for single drugs or groups of drugs.[95-97] Thereby they enable further insights into the mechanism of drug effect such as time- or concentration-dependent killing,[91] and they allow simulations and effect predictions, which can improve study designs.[95, 98]

Because time-kill curve studies are time-consuming, resource-intensive and laborious they are not always favoured. As mentioned for the MIC and PK/PD indices, they do not consider the influence of the immune system and the protein binding *in vivo*, except when the applied drug concentrations are related to unbound *in vivo* concentrations.[91] However, the ability to follow the bacterial survival (or dying) offers chances for dose optimisation based on a rational, scientific approach.[65]

1.7   Objectives

Based on the desribed problematic of quantification antibacterial effects to improve dosing regimens, the following objectives should have been prepared and are described in the present thesis:

PART I   Experimental work

a) Bioanalytics of LZD – Reliable and reproducible drug concentrations are a requirement for reliable conditions in the *in vitro* experiments and for the correct determination of the antibiotic effect. To determined actual drug concentrations applied in the *in vitro* experiments, a validated analysis of LZD in bacterial growth medium had to be generated.

b) Analytics for bacterial determinations – Also the determination of bacteria should be reliable, thus reproducible methods for bacterial dilution, bacterial purification and bacterial quantification had to be developed.

c) Dynamic in vitro model - For investigations of the effect of *in vivo*-like changing LZD concentrations on VRE, an efficient dynamic *in vitro* model, working on the principle of drug dilution, should be developed. Known problems of filter blockage and bacterial backgrowth should be considered and improved. The dynamic model should be qualified concerning provision of recurring, robust conditions for a high reproducibility of experiments, but it should still be flexible enough to adapt it to other imitated PK properties and new drugs.

d) In vitro models – 1. A static *in vitro* model should be established under use of vancomycin resistant *E. faecium*, a serious pathogen causing nosocomial infections and with a high resistance potential. The effect and benefit of a wide range of LZD should be studied over time resulting in time-kill curves, which allow more sophisticated analyses. *2.* The developed

dynamic *in vitro* model should be utilised to investigate the effect of LZD on VRE under *in vivo*-like PK conditions. Different doses, routes of administration and rates of elimination should be considered.

PART II   Modelling and simulation

a) PK/PD modelling – The experimentally derived time-kill curves of VRE (PD) under constant and changing LZD exposure (PK) should be subject to mathematical descriptions of the bacterial concentration-time course (PK/PD models). Different modelling approaches, including time-kill curve modelling and relative bacterial reduction, should be persuited, whereupon the models should be as general as possible with a good representation of the bacterial situation.

b) Assessment of LZD dosing regimens – Based on the descriptive analyses of bacterial concentration-time courses, the present dosing regimen of LZD should be assessed and options for rational dosing suggested.

c) Simulations – The developed PK/PD models could serve for computational simulations, which could be *1.* deterministic to investigate the effect-time courses resulting from different dosing regimens in patients with typical PK properties, and *2.* stochastic to determine the range of the effect size of the same dosing regimens for a patient population (healthy and criticall-ill).

d) Worst-case scenario - The antibacterial effect-time course of the standard dosing regimen should be evaluated in patients with worst assumable PK conditions and an alternative optimised dosing regimens for these patients should be suggested.

2 Materials and methods

2.1 Chemicals

Acetonitrile, HPLC gradient grade	Carl Roth GmbH, Karlsruhe, Germany
Bacillol® AF	Bode Chemie GmbH, Hamburg, Germany
Columbia agar plates with 5% sheep blood	Oxoid GmbH, Wesel, Germany
Densichek calibration standard	BioMerieux, Nuertingen, Germany
Disodium hydrogen phosphate (purity > 99.5%)	Laborchemie Apolda GmbH, Apolda, Germany
Ethanol, 96%, denatured with methylethyleketone	Carl Roth GmbH, Karlsruhe, Germany
Linezolid (purity > 99.8%)	Pfizer, Groton, Connecticut, USA
Methanol, HPLC gradient grade	Carl Roth GmbH, Karlsruhe, Germany
Mueller-Hinton agar plates with 5% sheep blood	Oxoid GmbH, Wesel, Germany
Mueller-Hinton broth dry powder	Oxoid GmbH, Wesel, Germany
Neodisher A8	Chemische Fabrik Dr. Weigert GmbH & Co.KG, Hamburg, Germany
Peptone from casein, pancreatic digested	Merck KGaA, Darmstadt, Germany
Potassium dihydrogen phosphate (purity > 99%)	Merck KGaA, Darmstadt, Germany
Sekusept® Plus	Ecolab GmbH und Co. OHG, Duesseldorf, Germany
Sodium chloride (purity > 99.5%)	Carl Roth GmbH, Karlsruhe, Germany
Sodium chloride (purity > 99.5%)	AppliChem GmbH, Darmstadt, Germany
Water, purified	Elect 80, Elga Berkefeld GmbH, Celle, Germany
Water, distilled	Purelab Plus, Elga Berkefeld GmbH, Celle, Germany

2.2 Bacterial strain

The microbiological experiments were carried out with a vancomycin resistant *Enterococcus faecium* (VRE) strain received from the American Type Culture Collection, Rockville, MD, USA (ATCC 700221). For long-term availability, aliquots of the strain were stored at -30 °C in cryo tubes. For short-term availability, stock cultures were grown on Columbia agar plates with 5% sheep blood (Col-SB agar plates) for 24 h at 37 °C and subsequently stored at 4 °C. Fresh cultures for experiments were prepared on the day before each experiment by cultivation on Col-SB agar plates at 37 °C over night.

2.3   Consumables

Brown tubes, G1	CS Chromatographie Service GmbH, Langerwehe, Germany
Cannulae, BD Microlance™ 3	Becton Dickinson, Fraga, Spain
Cannulae, sterile, 0.70 x 80 mm	Ehrhardt Medizinprodukte GmbH, Geislingen, Germany
Cannulae, Sterican, sterile, 0.90 x 70 mm	B. Braun Melsungen AG, Melsungen, Germany
Canted neck culture flasks with vented caps Nunclon®, 70 mL	Nunc, Roskilde, Denmark
Centrifuge tubes (15, 50 mL)	BD, Franklin Lakes, NJ, USA
Combitips® Plus	Eppendorf, Hamburg, Germany
Cover disks, G 8-PTFE	CS Chromatographie Service GmbH, Langerwehe, Germany
Cryo tubes	Carl Roth GmbH, Karlsruhe, Germany
Discofix two-way cock, blue	B. Braun Melsungen AG, Melsungen, Germany
Drigalski spreaders, glass	Carl Roth GmbH, Karlsruhe, Germany
HPLC vials	CS Chromatographie Service GmbH, Langerwehe, Germany
Inoculating loops	Copan, Brescia, Italy
Kapsenberg caps, Ø 16 mm	KMF Laborchemie Handels GmbH, Leipzig, Germany
Laboratory bottles, Duran® (100, 500, 1000 mL)	Schott AG, Mainz, Germany
Membrane filter units, minisart® NML, Ø 0.2 μm	Sartorius, Goettingen, Germany
Membrane filter, 0.45 μm, ø 47 mm, white plain	Millipore, Carrigtwohill, Ireland
Prefilter, glass fibre, 0.2-0.6 μm, ø 47 mm	Millipore, Carrigtwohill, Ireland
Pipettes, disposable, Cellstar®	Greiner Bio-One, Kremsmuenster, Austria
Screw caps	CS Chromatographie Service GmbH, Langerwehe, Germany
Silicone gaskets for caps, GL 14, piercable for sampling	Bohlender GmbH, Gruensfeld, Germany
Syringes, disposable, BD Plastipak™ with Luer conus (1 mL)	Becton Dickinson, Madrid, Spain
Syringes, disposable, Omnifix 50 mL (60 mL)	B. Braun Melsungen AG, Melsungen, Germany
Test tubes, DURAN®	Schott AG, Mainz, Germany
Pipette tips (10, 100, 1000, 5000 μL)	Eppendorf, Hamburg, Germany
Safe lock tubes (0.5, 1.5 mL)	Eppendorf, Hamburg, Germany

Tubes (0.5, 1.5 mL)	Brand, Wertheim, Germany
Tubes 2 mL	Brand, Wertheim, Germany
Tubes for Densichek®, PP, 5 mL, 75 x 12 mm	Sarstedt, Nuernbrecht, Germany

2.4   Solutions

Mueller-Hinton broth

Mueller-Hinton (MH) broth was prepared as described by the manufacturer: 21 g Mueller-Hinton broth dry powder were dissolved in 1000 mL distilled water and autoclaved for 20 min at 121 °C to prepare a nutrient solution (pH = 7.4 ± 0.2).

Phosphate-buffered saline solution with peptone

The phosphate-buffered saline solution with peptone (PBSP) for bacterial suspension was prepared as suggested by Bast.[99] It consisted of:

Potassium dihydrogen phosphate (KH_2PO_4)	0.3 g
Disodium hydrogen phosphate (Na_2HPO_4 x 2 H_2O)	0.6 g
Sodium chloride (NaCl; AppliChem GmbH)	8.5 g
Peptone from casein, pancreatic digested	1.0 g
Distilled water	ad 1000 mL
pH = 7.0	

Saline solutions

Saline solutions of 0.45% and 0.9% sodium chloride were produced by dissolving 4.5 g and 9.0 g sodium chloride (Roth GmbH), respectively, in 1000 mL purified water, followed by autoclaving at 121 °C for 20 min.

Linezolid solutions for HPLC calibration

The LZD stock solution for the calibration of the HPLC analysis was prepared by dissolving 10 mg of LZD in 10 mL purified and tempered (20 °C) water, resulting in a concentration of 1 mg/mL. The stock solution was stored at -80 °C. LZD working solutions for the calibration with concentrations of 2, 5, 10, 50, 200, 300 and 350 µg/mL were obtained by dilution of various volumes of the stock solution ad 5 mL MH broth. The working solutions were divided into 15 µL aliquots and stored at -30 °C. Fresh calibrators were prepared before each run by tenfold dilution of 10 µL working solutions with 90 µL MH broth. This resulted in calibrator concentrations of 0.2, 0.5, 1, 2, 5, 30 and 35 µg/mL.

Solutions

Linezolid solutions for HPLC quality control

The LZD stock solution for quality control of the HPLC assay was made of 10 mg LZD and 10 mL purified, tempered (20 °C) water. Quality control working solutions were obtained by dilution of various volumes of the stock solution with MH broth ad 5 mL, leading to concentrations of 2, 20, 100 and 290 µg/mL. Stock and working solution were stored at -80 °C. For quality control samples the working solutions were tenfold diluted with MH broth to 0.2, 2, 10 and 29 µg/mL. The quality controls were divided into 70 µL aliquots and stored at -30 °C until use.

Linezolid solutions for *in vitro* PK simulations

For the *in vitro* PK simulations, 20 mg LZD were dissolved ad 10 mL purified, tempered (20 °C) water. The administered drug amounts and calculated dilutions for each simulated compartmental model and administration route are described in 2.9.3.

Linezolid solutions for microbiological use

LZD solutions for microbiological use in the static model were prepared from a 1 mg/mL stock solution. For this stock solution 10 mg LZD were diluted ad 10 mL of tempered (20 °C) and purified water. The stock solution was stored at -80 °C.

For the dynamic *in vitro* model a 2 mg/mL LZD stock solution was prepared by dilution of 200 mg LZD in 100 mL purified, tempered (20 °C) water.

Table 1 Experimental implementation of LZD doses for microbiological investigations in the dynamic *in vitro* model.

Parameter	Unit	No. of compartments in the PK model			
		1	1	1	2
Administration route		Bolus	Infusion[*]	Infusion[*]	Infusion[*]
PK conditions					
Drug half-life ($t_{1/2}$)	h	3.54	3.54	5.00	3.22[**]
C_{max} (LZD) *in vitro*	µg/mL	20.13	38.36	19.45	15.94
Technical implementation					
Drug amount	mg	2.01	4.02	2.04	2.57
Type of diluent		Distilled water	MH broth	MH broth	MH broth
Volume of diluent	mL	1.00	7.70	5.91	103.93
Total volume of working solution	mL	2.00	9.78	6.93	105.21
Flow rate	mL/min	0.326	0.326	0.231	0.359[**]

[*]for 30 min; [**]related to the terminal phase

Different working solutions varying in volume and concentration depending on the imitated administration routes and compartments were produced. For bolus administration of LZD, the stock solution was diluted with purified water, and for administration as 30 min infusion it was diluted with MH broth (Table 1). All working solutions for microbiological investigations in the dynamic *in vitro* model were freshly prepared or maximum one day before the experiment.

Linezolid solutions for resistance analysis

The LZD stock solution ($C_{nom}=2$ mg/mL) for resistance analysis consisted of 200 mg LZD diluted in 100 mL purified, tempered (20 °C) water. A working solution of 1.6 mg/mL was prepared by dilution of 8 mL stock solution ad 10 mL purified water. The stock solution was stored at -80 °C; the working solution was freshly prepared one day before use.

Mobile phase for HPLC analysis

The mobile phase for the HPLC analysis consisted of acetonitrile and purified water at the ratio of 20 to 80 (V/V). The mobile phase was mixed, filtered via a glass drip by a water jet pump and degassed by ultrasound for 10 min. The completed solution continuously circulated in the HPLC system; renewal was carried out after analysis of 300 samples or after two months of use.

2.5 Devices and equipment

General devices

Digital analytical balance, Sartorius Analytic A200S	Sartorius, Goettingen, Germany
Pipettes, single channel, Research (1-5000 μL)	Eppendorf, Hamburg, Germany
Pipettes, Reference®, 0.5-1000 μL	Eppendorf, Hamburg, Germany
Eppendorf Centrifuge 5417 R	Eppendorf, Hamburg, Germany
Colony counter, ColonyQuant®, digital automated	Schuett-biotec, Goettingen, Germany
Cooling incubator	Binder, Tuttlingen, Germany
Laminar air flow box, LaminAir® HB 2436	Heraeus, Hanau, Germany
Multipette® (5-1000 μL)	Eppendorf, Hamburg, Germany
Pipette controller, Accu-Jet®	Brand, Wertheim, Germany
Shaking incubator	Gesellschaft für Labortechnik, Burgwedel, Germany
Speed-Vac® Savant-AES1010	Savant, Farmingdale, NY, USA
Turbidity meter, Densichek®	BioMerieux, Nuertingen, Germany
Vortexer	IKA, Staufen, Germany
Ultrasonic bath	Bandelin electronic, Berlin, Germany

HPLC-system

All HPLC components were manufactured by Jasco GmbH Deutschland, Gross-Umstadt, Germany. For validation the HPLC system consisted of:

- o Pump PU 980
- o Autosampler AS 1555
- o UV detector UV-975
- o Net box LC-Net II/ADC
- o Degasser DG-980-50
- o LG-980-02.

For further analysis

- o Pump PU-2080 Plus
- o UV detector UV-2075

were additionally used.

The HPLC separating column (125 x 4 mm, Sphere-Image 80-5 ODS 2 with integrated pre-column) was from Knauer, Berlin, Germany.

Dynamic *in vitro* model

3-stop tube, silicone, $\varnothing = 1.3$ mm, 0.90 mm wall	Ismatec, Glattbrugg, Switzerland
BOLA multiple distributors for bottles, Teflon	Bohlender GmbH, Gruensfeld, Germany
BOLA Screw Caps, closed, red, GL 14	Bohlender GmbH, Gruensfeld, Germany
BOLA Screw Caps, with aperture, red, GL 14	Bohlender GmbH, Gruensfeld, Germany
Circulating thermostat, TopTech MV-4	Julabo Labortechnik GmbH, Seelbach, Germany
Culture vessel of dynamic *in vitro* model 1 (see 3.5.1)	constructed by F. Leinung, Humbold-Universitaet Berlin, Germany
Culture vessel of dynamic *in vitro* model 2 (see 3.5.2)	constructed by D. Reese, Martin-Luther Universitaet Halle-Wittenberg, Germany
GL screw joint system GL 14 for tubes with $\varnothing = 1.6$ mm	Bohlender GmbH, Gruensfeld, Germany
GL screw joint system GL 14 for tubes with $\varnothing = 0.8$ mm	Bohlender GmbH, Gruensfeld, Germany
Perforated strainer, Teflon-coated, GV 050/1/03	Whatman GmbH, Dassel, Germany
Peristaltic pump, MCP Process	Ismatec, Glattbrugg, Switzerland
Plug Luer Lock male, for LL female, PP	Ismatec, Glattbrugg, Switzerland
Plug Luer Lock female, for LL male, PP	Ismatec, Glattbrugg, Switzerland
Rubber band (0-ring), external $\varnothing$ 39 mm, internal $\varnothing$ 35.5 mm	Reiff Technische Produkte GmbH, Reutlingen, Germany
Screw cap with internal cone, red, GL 14	Bohlender GmbH, Gruensfeld, Germany
Silicone tube, $\varnothing = 1.3$ mm, 0.90 mm wall	Ismatec, Glattbrugg, Switzerland

Teflon tube, 0.8 x 1.6 mm, $\emptyset=0.40$ mm	Schuett24, Goettingen, Germany
Teflon tube, 1.6 x 3.2 mm, $\emptyset=0.80$ mm	Schuett24, Goettingen, Germany
Tube connection Luer-Lock, male, PP, for tubes $\emptyset=1.6$ mm	Ismatec, Glattbrugg, Switzerland
Tube connection Luer-Lock, female, PP, for tubes $\emptyset=1.6$ mm	Ismatec, Glattbrugg, Switzerland
Water bath, TW 20	Julabo Labortechnik GmbH, Seelbach, Germany

2.6 Linezolid quantification

2.6.1 HPLC method and sample preparation

LZD concentrations in MH broth could be quantified by a recently published, valid HPLC method.[100] Since the method was transferred from the Department of Clinical Pharmacy of Prof. Dr. Charlotte Kloft in Berlin to Halle, it necessitated a short validation (see 2.6.2), which was performed according to FDA guidelines.[101]

At the HPLC system a flow of 1 mL/min and a detection wavelength of 251 nm were applied. The HPLC analysis was performed as sample loss mode, which means that additional mobile phase (60 µL) was drawn after the uptake of the low sample volume (30 µL). So the injection loop was filled and the whole sample volume could be analysed. LZD was eluted approximately 4.5 min after injection, a whole run lasted 7 min. The signals of the UV detector were recorded and integrated by the Chrompass HPLC software (see 2.12). Before each run, 80 µL aqueous LZD tests of 1 µg/mL spiked with 20 µL acetonitrile were used to test the system. Peak form and retention time were examined and mean and standard deviation of peak area calculated (n=5). If the findings were in accordance with prior experiments and the standard deviation was lower than 5%, the analysis of samples including calibration and quality control samples was started.

For the analysis of LZD in MH broth a 50 µL sample (from static or dynamic investigations, see 2.8 and 2.9) was spiked with 200 µL acetonitrile in a 1 mL Eppendorf tube for protein precipitation, rested at room temperature for 10 min and centrifuged at 10.000 g for 10 min. The supernatant was transferred to a 0.5 mL Eppendorf tube and vacuum vaporised in the speed vac at medium temperature (=45 °C) for 1 h. The evaporated sample was resolved with 50 µL acetonitrile/water (20/80 V/V) and transferred to an HPLC vial including a glass insert. The vial was closed with a Teflon disk and a screw cap.

LZD samples diluted in water were only spiked with acetonitrile (80 µL sample + 20 µL acetonitrile), to reach a ratio of acetonitrile/water (20/80 V/V) as in the mobile phase. They were injected twice and the signals compared to each other without extra calibration samples.

2.6.2 Short validation of the HPLC method

The short validation of LZD in MH broth was performed on three separate days according to FDA criteria.[101] The evaluation considered imprecision, inaccuracy, reproducibility and linearity of the method. Seven different calibration solutions were freshly prepared before each run. The concentrations ranged from 0.2-35 µg/mL (see 2.4). Aliquots of all four quality control solutions were thawed and prepared before each run. The concentrations of quality controls ranged from 0.2-30 µg/mL (see 2.4).

At day one and three, one aliquot of each concentration of calibration solutions and three aliquots of each concentration of quality controls were processed. At day two, three aliquots of each concentration of calibration solutions (total: 21) and three aliquots of each concentration of quality controls (total: 12) were processed. Reproducibility was tested by measuring six separately prepared samples with a nominal concentration of 1 µg/mL.

2.7 Preliminary microbiological investigations

2.7.1 Assessment of inoculum size

To achieve a bacterial concentration of 10^6 cfu/mL as it is recommended in the literature,[83, 84] an appropriate dilution of bacteria had to be found. Therefore bacteria were suspended in 0.45% NaCl solution in a 5 mL PP tube until a density of McFarland 0.5 was obtained.[88] This suspension was tenfold diluted with PBSP several times. Six aliquots of 100 µL of $1:10^3$, $1:10^4$, $1:10^5$ and $1:10^6$ dilutions were plated on MH agar plates and incubated at 37 °C for 24 h. Bacterial counting was performed manually. The experiment was repeated three times.

2.7.2 Determination of the lag-time of *Enterococcus faecium*

The lag-time is the required time of a culture to change from no bacterial growth (growth rate zero) to exponential growth (constant growth rate).[102] The lag-time of *E. faecium* should be determined, to assure a sufficiently long preincubation period. For this purpose, a bacterial suspension with McFarland 0.5 was 60-fold diluted with MH broth (= bacterial working suspension). 2 mL of the working suspension were added to 18 mL MH broth in a cell culture flask, incubated at 37 °C and shaken with 62 rounds per minute (rpm). Bacterial samples of 100 µL were taken from the cell culture flask at 0, 20, 40, 60, 80, 90, 100, 120, 140, 160, 180 and 240 min, plated on MH agar plates and incubated at 37 °C for 24 h. Colonies were digitally counted (see 2.7.5). The experiment was repeated three times on separate days.

2.7.3   Implementation of bacterial sample preparation

PBSP is regarded as gentle dilution medium, whereas 0.9% NaCl solution is typically used.[99] Hence, the suitability of these two dilution media together with a 0.45% NaCl solution (used for density adjustment) was investigated. The feasibility of sample preparation with respect to duration of preparation and type of dilution medium was studied. For that reason, three tubes with 10 mL dilution medium were spiked with appropriate bacterial volumes. Bacterial samples were taken every 10 min over 1 h and plated on MH agar for viable cell counting. After 24 h of incubation at 37 °C the plates were digitally counted (see 2.7.5). The experiment was repeated for each dilution medium. A Kruskal-Wallis test (H test) was performed to detect differences between bacterial survival in the different media and the duration of sampling. The level of statistical significance α was set to 0.05.

2.7.4   Bacteria purification

The antibiotic carry-over effect is a serious problem in antibacterial *in vitro* investigations.[103-105] Undiluted bacterial samples may contain so high antibacterial drug concentrations, that the drug still affects the bacterial growth on agar plates. This results in too few colony forming units per plate and therewith to an overestimation of the drug effect. Therefore appropriate purification methods have to be applied. One way to avoid the antibiotic carry over effect is the dilution of the bacterial samples and therewith of the drug. In the present work serial tenfold dilution was applied, whereby dilutions of at least 200-fold were plated.

Another way of bacteria purification is a washing and centrifugation procedure as described by Scheerans.[100] For bacteria washing, 100 µL of the bacterial suspension were spiked with 1.4 mL PBSP in a 2 mL tube and vortexed for 10 s. Afterwards the tube was centrifuged at 650 g for 10 min. 1.3 mL of the supernatant were discarded and the remaining 200 µL reintroduced to the washing process. The washing process started again with addition of 1.3 mL PBSP. The whole procedure included three washing and centrifugation cycles. At the end of the third centrifugation cycle, 1.3 mL supernatant were discarded, the remaining 200 µL could be used for plating on agar (see 2.7.5).

2.7.5   Bacteria quantification

2.7.5.1   Method of quantification

Viable cell counting is one of several methods to determine either the growth of bacteria or indirectly the antibacterial effect of a drug.[40] It can be performed manually or computer based. For the present work, a computer-based digital automated colony counter – the ColonyQuant® – was used. The system consisted of a colony counter with a camera and of the computer

software. The digital picture of an agar plate was analysed by the software with regard to differences in colour and size. Differences in colour allowed distinguishing between colony and agar. It could also discriminate between different strains on agar, which could be useful for investigating more strains parallel or for detection of contamination. Differences in size allowed discrimination between one or more colonies. As a consequence, different counting methods associated with the size and colour of *E. faecium* had to be developed.

2.7.5.2 Qualification of the colony counter and system suitability

The colony counter (Figure 4) was qualified for *E. faecium* on MH agar plates with 5% sheep blood with respect to FDA criteria for bioanalytical methods[101] with manual counting as reference method.
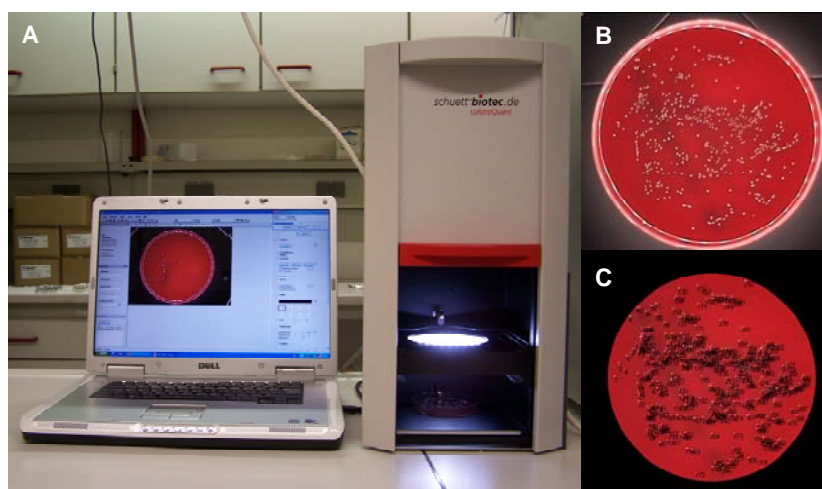
Figure 4: Colony counter (A) with a raw (B) and the computer processed (C) picture of a MH agar plate.

Four dilutions of different bacterial concentrations (2×10^0, 2×10^1, 2×10^2, 2×10^3 cfu/mL) were prepared from one start inoculum (see 2.7.1). Each dilution was plated six times. The first plate of each dilution was counted six times manually and also six times by the colony counter. Each of the following plates was once counted manually and by the colony counter. Depending on the approximated number of colonies per plate, one of the previous developed counting methods (see 3.3) was applied. The experiment was repeated three times (n = 3).

For the data interpretation, the detection reliability (one plate counted six times), the preparation variability (within-day, one bacterial concentration on six plates) and the system variability (between-day) were determined for manual and computer based counting. Variability below 15%, and below 20% for the lowest bacterial concentrations, was aspired.

2.8   Static *in vitro* model

A static *in vitro* model (see 1.5.1) was used to attain basic knowledge about the effect of LZD on VRE. The bacteria were exposed to constant LZD concentrations and observed over time by viable cell counting.

Time-kill investigations (see 1.6.3) with static drug concentrations were carried out with an overnight culture of VRE. 1.5 mL of the start inoculum with McFarland 0.5 (=stock suspension, see 2.7.1) were suspended in 18.5 mL MH broth (=working suspension). 2 mL of the working suspension were added to 17 mL MH broth in a cell culture flask and pre-incubated at 37 °C and 62 rpm (shaking). After 2 h of pre-incubation the experiment started with bacterial concentrations of 10^6 cfu/mL (t=0 h). For this purpose 1 mL of the LZD working solutions (see 2.4) or 1 mL MH broth for growth control experiments were given to each cell culture flask. Eight cell culture flasks were incubated in parallel, one always as growth control. Bacterial samples were taken at the beginning (t=0 h) and 1, 2, 4, 6, 8, 10, 12, 16, 20 and 24 h after the experimental start. Volumes of 10 or 50 µL were collected depending on the expected higher or lower bacterial concentrations, respectively. Samples were prepared by bacteria purification (see 2.7.4) and counted after 24 h of incubation at 37 °C by the colony counter (see 2.7.5). LZD samples were taken at the beginning (0 h) and the end of experiments (24 h) and were stored at -80 °C until HPLC determination (see 2.6.1). The whole experiment was repeated in triplicate.

LZD working solutions (see 2.4) for the static *in vitro* model were prepared in geometric rows based on the minimum inhibitory concentration (MIC) of LZD against VRE, which is specified with 2-4 µg/mL.[18] After addition of LZD working solutions to the bacterial suspension LZD concentrations of 0.5, 1, 2, 4, 8, 16 and 32 µg/mL were anticipated.

2.9   Dynamic *in vitro* model

2.9.1   Basic idea for the model setting

A dynamic *in vitro* model (see 1.5.2) should be used to investigate the effect of LZD on VRE under *in vivo* like conditions. This means fluctuating drug concentrations. Therefore a suitable *in vitro* model had to be developed. The model development was based on the dynamic dilution model without bacterial loss by Löwdin et al.,[106] which seemed flexible and most suitable to simulate all relevant PK profiles appearing *in vivo*. Compared to the model by Löwdin improvements concerning the filter blockage and the bacterial backgrowth were intended. Additionally, the model body should be easy to manage. This led to the development of two different shapes of the culture vessel with different experimental setting and their investigation.

2.9.2   Preliminary investigations on equipment and settings

2.9.2.1   Type of pump

A convenient pump should be able to generate low flow rates as they were needed to simulate LZD PK profiles, that means flow rates between 0.1 and 1 mL/min. Two types of pumps were compared: a perfusor pump and a peristaltic pump. In the perfusor, the plunger of a syringe is continuously pushed in by a screw. Thus, the medium in the syringe is continuously pushed out. In the peristaltic pump, the silicone tube is fixed over a roller. When the roller presses the tube, the medium in the tube is transported. Thus, the movement of medium happens in intervals.

The suitability of both pumps to transport designated volumes of water per time with respect to imprecision and inaccuracy was investigated. Flow rates of 0.1, 0.2, 0.3, 0.4 and 0.5 mL/min over 2 min and 1, 2 and 5 mL/min over 1 min were applied. Samples were collected in tubes and controlled by weighing. Analysis of linearity was performed by linear weighted ($1/y^2$) regression (n=8).

2.9.2.2   Mode of pumping

The peristaltic pump offers two special pump settings; one is pumping according to flow rate, where the transported volume per minute is constant. The other setting is pumping a specific volume per time. This setting is recommended by the manufacturer Ismatec for precise pumping, accepting that a higher volume is pumped at the beginning and a lower at the end of time to meet the designated total volume. The two possible pump settings were compared in model 1 (see 3.5.1), simulating a one-compartment model with bolus injection of LZD in distilled water. LZD samples were taken at 0, 0.5, 1, 2 and 5 h and analysed by HPLC (n=10, see 2.6.1).

2.9.2.3   Choice of bacteria retaining filter

The membrane filter should retain bacteria, while blockage by bacteria should be avoided. Therefore a single membrane filter (Millipore), membrane filter plus a prefilter (Millipore) and a syringe filter (membrane filter units, Sartorius) were compared. Prefilters hold back the main part of bacteria, and thus were assumed to keep the membrane filter clean. Syringe filters are easy to change also during an experiment, which could be a possibility to avoid membrane blockage. The suitability of a single membrane versus a membrane filter plus prefilter was investigated in model 1 (see 3.5.1) using water. The suitability of a single membrane versus a syringe filter was compared in model 2 (variant A and B, see 3.5.2) using water and broth including bacteria (as for growth control experiments).

2.9.3 *In vitro* simulation of pharmacokinetic profiles

In vitro simulated PK profiles should be founded on the *in vivo* profiles of LZD. Since LZD concentrations at the infection site (interstitial fluid) are close to those in plasma at steady state,[28] the applied PK conditions were based on steady state LZD plasma concentrations. Thus, simulations were based on the *in vivo* clearance. PK studies of LZD proposed either a one-compartment model,[107] or a two-compartment model.[32, 108] A one-compartment model is easier to imitate *in vitro* and commonly used, whereas a two-compartment model might better reflect the *in vivo* situation.

The simulation of a bolus administration of LZD can be easily applied *in vitro* (see 1.5.2), but *in vivo* LZD is administered as infusion. Based on the administration of 600 mg LZD as single dose *in vivo* the pharmacokinetics of LZD were investigated assuming a

a) one-compartment model, bolus administration

b) one-compartment model, 30 min infusion

c) two-compartment model, bolus administration

d) two-compartment model, 30 min infusion.

The idea of the underlying compartmental models and the drug administration is illustrated in Figure 5. Table 2 shows the practical implementation of LZD doses for each investigated profile and the applied PK conditions. The experimental PK simulations a) and b) were carried out in model 1 (see 3.5.1), the simulations of c), d) and also a) were performed in model 2 (see 3.5.2). The drug working solutions were administered in purified water as dilution medium (Table 2).
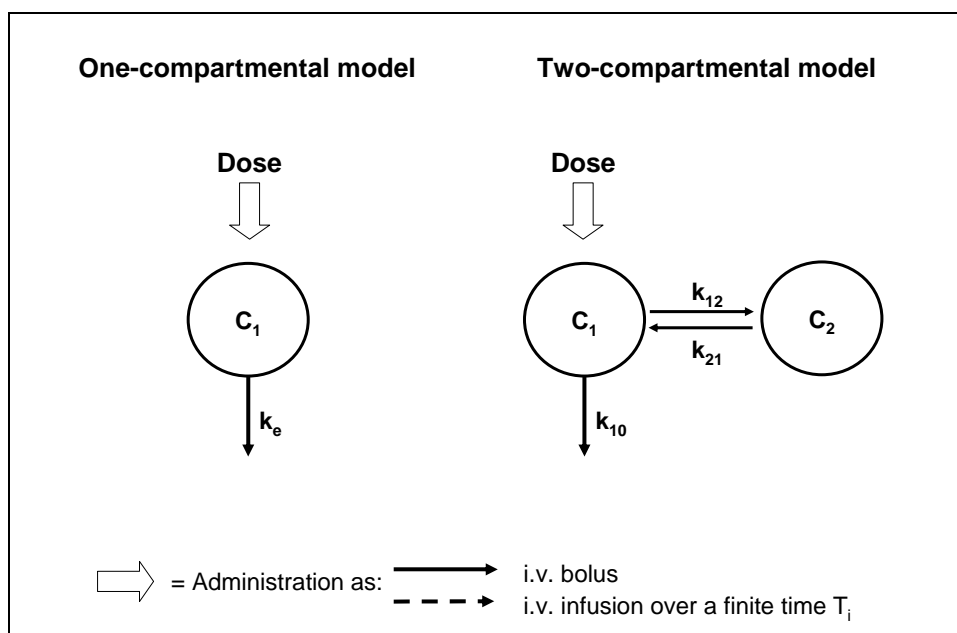
Figure 5 Scheme of applied compartmental models and administration routes. C_1 – concentration in the central (first) compartment, C_2 - concentration in the peripheral (second) compartment, k_e and k_{10} - elimination rate constants, k_{12} and k_{21} - distribution rate constants.

Table 2 Experimental implementation of LZD profiles for *in vitro* PK simulations.

Parameter	Unit	No. of compartments in the PK model			
		1		**2**	
		a)	**b)**	**c)**	**d)**
Administration route		Bolus	Infusion[*]	Bolus	Infusion[*]
PK conditions					
Drug half-life ($t_{1/2}$)	h	3.54	3.54	3.22[**]	3.22[**]
C_{max} (LZD) *in vitro*	µg/mL	20.13	17.35	30.00	15.94
Clearance	L/h	5.8		11.1 (CL) 75 (Q)	
Volume of distribution	L	29.8		20.0 (V2) 28.9 (V3)	
Distribution rate constants	h^{-1}			k_{12} = 3.750 k_{21} = 2.595	
Elimination rate constants	h^{-1}	k_e = 0.196		k_{10} = 0.555	
Technical implementation					
Drug amount	mg	2.01	1.82	3.00	2.57
Applied volume of stock solution	mL	1.00	0.91	1.50	1.29
Type of diluent		Distilled water	Distilled water	Distilled water	Distilled water
Volume of diluent	mL	-	8.87	-	103.93
Total volume of working solution	mL	1.00	9.78	1.50	105.21
Flow rate	mL/min	0.326	0.326	0.359[*]	0.359[*]

[*]for 30 min; [**]related to the terminal phase; CL - clearance of the central compartment, V2 – volume of distribution in the central compartment, Q – inter-compartmental clearance, V3 – volume of distribution in the peripheral compartment, k_e and k_{10} - elimination rate constants, k_{12} and k_{21} – distribution rate constants.

To imitate a bolus administration, the aqueous drug solution (low volume) was given at once by a syringe via the sampling port of the model. Infusion was imitated by pumping the drug working solution from a tube into the bacterial vessel. After the end of infusion, the input source was changed from the drug-containing tube to the reservoir with fresh, drug-free medium. Drug samples were taken by a syringe with a 80 mm long cannulae from the centre of the culture vessel and were immediately analysed by HPLC (see 2.6.1). The observation of PK *in vitro* simulations lasted about 5 h.

2.9.4 Reproducibility of the dynamic *in vitro* model

2.9.4.1 Pharmacokinetic variability

The PK variability was determined from the *in vitro* PK simulations in model 2 (see 3.5.2) and later as a matter of routine during the time-kill investigations, to confirm the designated PK

profiles. To determine PK variability, LZD was administered as 2 mL bolus injection in 98 mL purified water simulating a one-compartment model (see 2.9.3). Samples of 0.5 mL were taken at 0, 0.25, 0.5, 1, 2 and 5 h after injection. The aqueous samples were immediately double-analysed by HPLC (see 2.6.1). The sample signals were compared concerning imprecision and inaccuracy. The experiment was conducted in triplicate.

2.9.4.2   Pharmacodynamic variability

For investigations of the PD variability in the dynamic model four separate growth control experiments under continuously renewing medium and stirring were performed (model 2, see 3.5.2). The dynamic model was aseptically assembled. 10 mL of the bacterial inoculum were added to 90 mL MH broth in the culture vessel, stirred and preincubated at 37 °C for 2 h. One peristaltic pump was used for one culture vessel controlling in- and outlet tubes. For pump calibration before the experiments, the tubes were handled separate from the culture vessel. The tubes were flushed with distilled water at a flow rate of 1 mL/min for approximately 1 h to expand and equilibrate. Then calibration of the pumps was performed according to the instruction manual with a flow rate of 1 mL/min at the inlet tube. Afterwards the tube was connected to the reservoir, the culture vessel and the waste container (without pumping). When the experimental observation period began (t=0 h) the pumps were started with the designated flow rate. Fresh medium was continuously pumped from the reservoir into the culture vessel. The clearance of MH broth, implemented by the flow rate, was chosen as in a one-compartment model (Table 2). The same volume of used medium left the culture vessel by the outlet tube over the pump. Bacterial samples of 100 µL were taken by a syringe at 0, 1, 2, 3, 4, 6, 12, 20 and 24 h at the sampling port and prepared for viable cell counting (see 2.7.5). The experiment was repeated in triplicate. The logarithmic data were explored concerning mean, standard deviation and imprecision.

2.9.5   Time-kill investigations

Before the experiment started, the dynamic *in vitro* model had to be set up free from contamination and the pumps had to be calibrated (see 2.9.4.2). The culture vessel was filled with 90 mL (88 mL for bolus experiments) MH broth. 10 mL of the bacterial working suspension (see 2.7.2) were added to each vessel and subsequently mixed. Afterwards the preincubation phase started. At the beginning of the experimental observation period (t=0 h) the pumps were started with the designated flow rate and drug administration could start.

In experiments simulating bolus administration, 2 mL working solution of the drug were injected by a syringe through the sampling port directly into the culture vessel. Fresh medium was transported from the reservoir into the culture vessel and diluted the present drug concentration. To simulate an infusion, a two-way cock was embedded into the inlet tube

previous to the pump. An additional tube led from a vessel with the drug working solution to the two-way cock. The cock was set in such a way, that the drug working solution was pumped during the time of infusion, afterwards it was set back to enable the transport of fresh medium from the reservoir. Samples of 200 µL were taken with a syringe via the sampling port at predefined times. 50 µL of the samples were transferred with Eppendorf pipettes in PBSP for bacterial determination (see 2.7.5); the residual 150 µL were prepared and used for LZD analysis (see 2.6.1). So the applied PK profiles could be validated by the drug samples.

The time-kill investigations started with the simplest type of simulation: a bolus administration of LZD in a one-compartment model with a dose corresponding to the *in vivo* approved dose of 600 mg (Table 3, see also Table 1).

In addition, a more physiology-like simulation with an infusion (30 min) and a longer LZD half-life ($t_{1/2} = 5$ h) was applied.[18] Another experiment was performed to demonstrate the influence of dose. Therefore an infusion in a one-compartment model with the doubled *in vivo* dose (1200 mg) was chosen. The fourth time-kill experiment investigated the bacterial concentration-time behaviour under the *in vivo* PK conditions of unbound LZD in plasma, which were a two-compartment model with infusion (30 min) and a dose according to 600 mg *in vivo*.[32]

Table 3 PK profiles for time-kill investigations in the dynamic model.

Administration route	No. of cmts	k_e [h^{-1}]	$CL_{(in\,vivo)}$* [L/h]	$t_{1/2}$ [h]	Dose$_{(in\,vivo)}$ [mg]	T_i [h]	C_{max} [µg/mL]	Flow rate [mL/min]
- (Growth Control)	1	0.196	5.835	3.54	0	-	0	0.326
Bolus	1	0.196	5.835	3.54	600	-	20.13	0.326
Infusion	1	0.196	5.835	3.54	1200	0.5	36.68	0.326
Infusion	1	0.139	4.131	5.00	600	0.5	19.45	0.231
Infusion	2	0.216**	4.310	3.22	600	0.5	15.94	0.359**

* 1-cmt: V = 29.8 L; 2-cmt V = 20 L, ** parameters related to the terminal phase, Cmts – compartments, k_e – elimination rate constant, $CL_{(in\,vivo)}$ – *in vivo* clearance, $t_{1/2}$ – half-life of the drug, T_i – duration of infusion, C_{max} – maximum concentration

2.9.6 Investigations on linezolid resistance

The resistance analysis was performed as part of the investigations in the one-compartment model with bolus administration ($C_{max} = 20.13$ µg/mL). Prior to the experiment, MH agar plates were impregnated with LZD working solutions for resistance analysis (see 2.4) resulting in 8 or 12 µg/mL LZD per plate. For this purpose, 100 µL of the LZD working solution ($C_{nom} = 1.6$ mg/mL) and 120 µL of the stock solution for resistance analysis ($C_{nom} = 2.0$ mg/mL) were plated on MH agar plates (volume: 20 mL), respectively. Bacterial samples (50 µL) – generally taken during the experiment for viable cell counting over 24 h – were additionally plated undilutedly on the drug-containing plates. These bacterial samples were taken from three

separate culture vessels (n=3) and plated in duplets. Drug-containing plates were incubated for up to 160 h at 37 °C before viable cell counts were carried out.

Resistant subpopulations of VRE should be detected at a concentration equivalent to threefold the MIC, i.e. 12 µg/mL.[109] Other sources reported twice the MIC, i.e. 8 µg/mL as breakpoint concentration.[110] Since susceptibility testing is normally performed in twofold dilutions, 8 µg/mL (2x MIC) might be inappropriate to detect a difference in susceptibility. However, both concentrations, 8 and 12 µg/mL, were used for resistance observations.

2.10 Comparison of *in vitro* models

The growth control experiments of the static, the dynamic and a previously investigated semi-dynamic *in vitro* model[111] were compared, whether they provide equal or different results concerning the bacterial concentration after 24 h of growth. For this purpose the raw bacterial concentrations of the growth controls (see Appendix, Table 29) derived in each model were analysed for the variance of medians per investigated time point. The Mann-Whitney-Wilcoxon test (U-test) was performed to compare a) if the models led to different bacterial concentrations at different time points and b) at which time the maximum bacterial concentration was reached in each model. The U-test was non-parametric and independent from the sample size. It was carried out as two-tailed test with a level of statistical significance α of 0.05. The null hypothesis read as no difference (=equivalence) between means of two samples.

The growth rate constants represent the slope in bacterial concentration. They were calculated over the first 6 h by linear regression of the logarithmic bacterial concentrations and compared.

2.11 Pharmacokinetic/pharmacodynamic analyses

2.11.1 Characteristic concentrations

2.11.1.1 Minimum inhibitory concentration

The determination of the MIC in the experiments of the static *in vitro* model in MH broth under doubling dilution steps of LZD is comparable to the macro broth dilution method. The bacteria were incubated with the drug at 37 °C. The MIC was visually determined after the generally recommended 18 h [83] and after 24 h as proposed for glycopeptide resistant enterococci [93].

2.11.1.2 Stationary concentration

Because the MIC does not necessarily need to indicate the concentration, where no bacterial growth occurs, the stationary concentration - describing the stasis of bacterial growth - was introduced and calculated as a more precise PK/PD index.[52, 112] The stationary concentration is

the drug concentration C, at which the extent of killing is equal to the amount of growing bacteria and thus the bacterial concentration N over time t does not change ($\frac{dN(C,t)}{dt} = 0$).

The stationary concentration was calculated with the basic time-kill curve model with Excel using the Solver function. The concentration of bacteria after 24 h was assumed to be the same as at the beginning (t=0 h).

2.11.2 Pharmacokinetic/pharmacodynamic indices

The area under the LZD concentration-time curve over 24 h divided by the MIC (AUC/MIC) and the time above the MIC ($T_{C>MIC}$) were calculated.[50] The AUC was calculated by the trapezoidal rule.

2.11.3 Relative bacterial reduction

The relative bacterial reduction (*RBR*) was previously developed in the group of Prof. Dr. Charlotte Kloft to reveal the drug effect over time with regard to the respective basal bacterial growth,[100] graphically analysed as area between the curves. It could be calculated, relating the difference between the logarithmic concentrations of untreated bacteria (basal bacterial growth/baseline effect E_B) and the bacteria growing under LZD exposure (drug effect E_D) to the basal bacterial growth E_B, expressed as percentage ratio (Eq. 1). Medians of bootstrapped geometric means (see 7.4.2) of logarithmic bacterial concentrations served for the calculations.

$$RBR(C,t) = \frac{E_B(t) - E_D(C,t)}{|E_B(t)|} \cdot 100\%$$

Eq. 1 Definition of the relative bacterial reduction, from Scheerans [100].

2.11.4 Modelling the relative bacterial reduction

A mathematical model describing the RBR data should be developed. As basis served a typically used maximum effect model (E_{max} model; Eq. 2). The shape of the curve could be easily adapted by insertion of an exponent, which is called the Hill coefficient (*H*). This results in a sigmoidal E_{max} model (Eq. 3). Prior investigations have shown, that a modified sigmoidal E_{max} model (Eq. 4) has been appropriate to describe data from static investigations.[100]

$$E(C) = \frac{E_{max} \cdot C}{EC_{50} + C}$$

Eq. 2 General maximum effect model (E$_{max}$ model).

$$E(C) = \frac{E_{max} \cdot C^H}{EC_{50}{}^H + C^H}$$

Eq. 3 Sigmoidal maximum effect model (including the Hill coefficient *H*).

$$E(C,t) = \frac{E_{max}(t) \cdot C^{H(t)}}{EC_{50}(t)^{H(t)} + C^{H(t)}}$$

Eq. 4 Modified sigmoidal E$_{max}$ model applied on RBR, from Scheerans [100].

In Eq. 2 to Eq. 4, E_{max} is the maximum kill rate constant (in h^{-1}) and a measure of the maximum effect. *C* is the drug concentration, which is time invariant for the data from static experiments. EC_{50} is the drug concentration, provoking half of the maximum effect and *H* is the Hill coefficient. The modification of the sigmoidal E$_{max}$ model consisted of introducing a time-delay term (1-e^{-xt}) to E_{max}, EC_{50} and *H* (Eq. 4) with a delay rate constant *a*, *b* or *z*, respectively, which accounted for the time-dependencies of the parameters (Eq. 5).

$$E_{max}(t) = E_{max,0} \cdot (1 - e^{-a \cdot t}) ; \qquad EC_{50}(t) = EC_{50,0} \cdot (1 - e^{-b \cdot t}) ; \qquad H(t) = H_0 \cdot (1 - e^{-z \cdot t})$$

Eq. 5 Time dependence of E$_{max}$, of EC$_{50}$ and of H used for the sigmoidal E$_{max}$ model.

A basic RBR model with mean RBR data derived from the static *in vitro* model (see Appendix, Table 30) was developed exercising Eq. 4. The final modelling was based on single RBR data from the static and the dynamic *in vitro* model. Therefore, a modelling data set with 517 records was created (see Appendix, Table 31). Based on prior findings a modified sigmoidal E$_{max}$ model (Eq. 4) and an indirect link model were used to describe the data from static and dynamic experiments.[100] An indirect link model can be used, when time shifts between maximum drug concentration and maximum effect are observed. Time shifts can be caused pharmacodynamically, when the mechanism of effect is time-consuming. It is indicated by an anti-clockwise hysteresis loop in effect-concentration plots.[113] The time shifts can be modelled by implementation of a hypothetical effect compartment (Figure 6). The drug concentration C_e in the effect compartment can be described with Eq. 6.
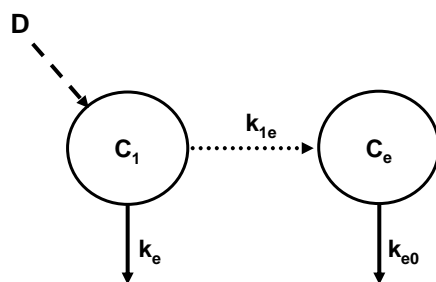
Figure 6 Compartmental model including a hypothetical effect compartment; D - drug dose, C_1 – drug concentration in the central compartment, C_e – drug concentration in the hypothetical effect compartment, k_{1e} – drug transfer rate constant between central and effect compartment, k_e – elimination rate constant from the central compartment, k_{e0} – elimination rate constant from the effect compartment.

$$\frac{dC_e}{dt} = k_{e0} \cdot (C_1(t) - C_e(t))$$

Eq. 6 Concentration at the effect site, adapted from Scheerans [100].

The change of drug concentration at the effect site is determined by the elimination rate constant of the drug from the effect compartment k_{e0} and the difference between drug concentration in the central and the effect compartment, C_1 and C_e, respectively. Incorporating the concentration in the effect compartment into the sigmoidal E_{max} model enables the description of the time shift and leads to Eq. 7 – the indirect link model applied for RBR modelling of all data.

$$E(C,t) = \frac{E_{max}(t) \cdot C_e(t)^{H(t)}}{EC_{50}{}^{H(t)} + C_e(t)^{H(t)}}$$

Eq. 7 Indirect link model based on the modified sigmoidal E_{max} model with drug concentration C_e at the effect site.

The fitting of parameters to the data was performed in Scientist 3.0. The Scientist model files for RBR modelling with the sigmoidal E_{max} model (static model data) and with the indirect link model (static and dynamic model data) can be found in the Appendix, Figure 50 and Figure 51. All data were simultaneously fitted using the Simplex fit algorithm and afterwards the least square algorithm in Scientist. The lower limits of model parameters were set to zero. All parameters were simultaneously estimated. The maximum kill rate constant could be reliably determined only in the static model (basic modelling) due to the wide range of investigated LZD concentrations. Therewith the half-maximum effect and its corresponding concentration could

also be reliably estimated by this fitting. So, EC_{50} was fixed for final modelling to the value found in basic investigations.

To evaluate the developed model and its estimates, the RBR was predicted for all data (n = 1324, modelling + evaluation data set, Table 31). Residuals were calculated as difference between observed and predicted RBR values per time without weighting. Observed and predicted RBR values were directly compared; the residual plots (residuals versus drug concentration, versus time and versus RBR values) served for the evaluation of the goodness of model fit.

2.11.5   Time-kill curve modelling

The principle of time-kill curve modelling is the mathematical description of bacterial growth/kill over time. The model structure incorporates natural, continuous growth of bacteria. The concentration of growing bacteria is reduced by the antibiotic. Hence, changes in bacterial concentrations over time *dN/dt* can be described by differential equations as the difference between natural bacterial growth and changes in bacterial concentration due to the drug effect *E* (=kill, Eq. 8). In other words, the bacterial concentration under drug exposure is the sum of growth and death processes, which makes the model structure partly mechanistic (semi-mechanistic).[95, 114]

$$\frac{dN(C,t)}{dt} = \left(k_0 - E(C)\right) \cdot N(t)$$

Eq. 8 General approach of time-kill curve modelling

In Eq. 8, *N* is the bacterial concentration at a specific time and k_0 is the natural bacterial growth rate constant. The effect *E* of the drug can be expressed by an E_{max} model (Eq. 2), which incorporates the drug concentration into the model (*E(C)*) and thus links the bacterial concentration (PD) to the drug concentration (PK of the drug).

The PK/PD modelling of time-kill curves was performed with Scientist 3.0 using the simplex fit algorithm for primary estimations and following the least square fit for precisioning of the results. During the model development the model selection criterion (MSC), the Akaike`s information criterion (AIC), the coefficient of determination (R^2), the coefficient of correlation (R) and the standard deviation (SD) of the estimated values (see Appendix, 7.4.2) served for comparison of results. Furthermore graphical inspection of semilog arithmetic-scaled plots for bacterial concentrations over time of predicted and observed data were carried out.

A basic time-kill curve model was developed with data from the static *in vitro* model, which were expressed as bootstrapped geometric means. The growth control bacterial concentrations (n = 11) from static experiments were used for the description of natural bacterial growth. The

bacterial concentrations under 32 µg/mL LZD exposure (n=11, see Appendix, Table 32) were taken to describe the kill process, which was the effect (*E(C)*). The other bacterial concentrations under constant LZD exposure (N for C = 0.5, 1, 2, 4, 8, 16 µg/mL) were used to evaluate the model (n=66, see Appendix, Table 32).

The basic model was built up in a stepwise manner, starting with the description of the growth process. The growth rate constant k_0 was estimated and fixed for modelling of the effect. The initial bacterial concentrations were taken from mean experimentally determined bacterial concentrations. The actually determined constant LZD concentrations (PK) were incorporated into the E_{max} model for each respective bacterial concentration-time course (PD, see Appendix, Figure 52). For evaluation of the basic model, each bacterial concentration-time course was simulated using the respective actual LZD concentrations and observed initial bacterial concentrations and analysed with regard to goodness of fit and graphical criteria.

Based on the obtained basic model and the respective parameter estimates, a final model was set up, which used the dynamic *in vitro* data (single values per time point). The dynamic *in vitro* data were splitted in a model data set (n=188 records) for estimation of parameters and an evaluation data set (n=153 records; see Appendix, Table 33) for determination of the model quality. Changing LZD concentrations were included in the final model by equations accounting for compartments, routes of administration and doses (see Appendix, Figure 53). The final model was evaluated using all data of the dynamic *in vitro* model (n=341) with analyses of the goodness of fit and graphical criteria.

2.11.6 Effect at different time points

The knowledge of the relationship between drug concentration and effect (killing) can help to find effective drug concentrations and thus to optimise the doses.[40] The concentration-killing profiles of the static *in vitro* model were explored regarding different time points, which might aid in the optimisation of the times of drug administration.[115, 116]

For this reason an inhibitory effect model in WinNonlin with sigmoidal maximum effect was used (see Eq. 9). The observed effect $E_{I,tx}$, the killing of bacteria (or inhibition of bacterial growth), was calculated as difference between maximum bacterial concentration N_{max} and a term, which describes the difference between N_{max} and the minimum observed bacterial concentration N_0, depending on the drug concentration C and the drug concentration with half-maximum effect EC_{50}. To account for the sigmoidal curve shape the shape factor H (Hill coefficient) was introduced. The drug concentrations were assumed to be zero at N_{max} and infinite at N_0. Bacterial concentrations were expressed as logarithmic values.

$$E_I(C) = N_{max} - \frac{(N_{max} - N_0) \cdot C^H}{C^H + EC_{50}{}^H}$$

Eq. 9 Equation for the inhibitory effect model used to describe the effect at different time points.

The initial parameter based on logarithmic bacterial concentrations from the time-kill curve experiments in the static model, their values were set to N_{max}=8.536, N_0=4.813, EC_{50}=1.553 µg/mL, H=1. The estimation was carried out with the Gauss-Newton method.

The effect, where 90% of the maximum effect (i.e. kill) $E_{I,90}$ could be described by Eq. 10. To obtain the corresponding the drug concentration, Eq. 10 could be set equal to Eq. 9 and solved for C, which results in Eq. 11. Figure 54 in the Appendix locates the different parameters and characteristic concentrations of the inhibitory effect model on a bacterial concentration-drug concentration curve.

$$E_{I,90} = N_{max} - (N_{max} - N_0) \cdot 0.9$$

Eq. 10 Equation to calculate 90% of the maximum inhibitory effect ($E_{I,90}$) of the effect at different time points.

$$EC_{I,90} = \sqrt[H]{9 \cdot EC_{50}^H}$$

Eq. 11 Drug concentration corresponding to $E_{I,90}$.

2.11.7   Simulations

2.11.7.1   Population pharmacokinetic model

For dose optimisation, the final RBR model should be related to *in vivo* PK characteristics of LZD. For this purpose, a previously developed *in vivo* population PK model for unbound plasma concentrations in the treatment of 10 healthy volunteers and 24 critically ill patients with LZD was utilised.[32] The studied individuals received 600 mg LZD orally or as short-term infusion (30 min). A two-compartment model with linear clearance, which was partially inhibited over time by LZD itself, was found (Figure 7).[32]

The figure expresses the intravenous administration of LZD with a specific infusion rate (R_0) over a finite time (T_i). The drug appears in the central compartment (central CMT, plasma) with the concentration Cp (plasma concentration, not shown in figure) and is distributed to the peripheral compartment (periph. CMT) by the inter-compartmental clearance Q. $V2$ and $V3$ (not shown in figure) are the respective volumes of distribution for the central and peripheral compartment. The distribution of LZD from the central to the hypothetical inhibition

compartment (inhib. CMT) is determined by the transfer rate constant k_{1i}. From the inhibition compartment LZD is eliminated in a linear way determined by the elimination rate constant k_{i0}. The inhibition function *INH* influences the elimination from the central compartment. It incorporates a non-inhibitable clearance fraction *RCLF* and an inhibitable fraction dependent on the concentration in the inhibition compartment. IC_{50} is the LZD concentration in the inhibition compartment, which produces the half-maximum effect of clearance inhibition (Eq. 12).

$$INH(X4) = RCLF + (1 - RCLF) \cdot \left[1 - X4(t)/(IC_{50} + X4(t)) \right]$$

Eq. 12 Inhibition function for the clearance in the population PK model for LZD, adapted from Plock[32].
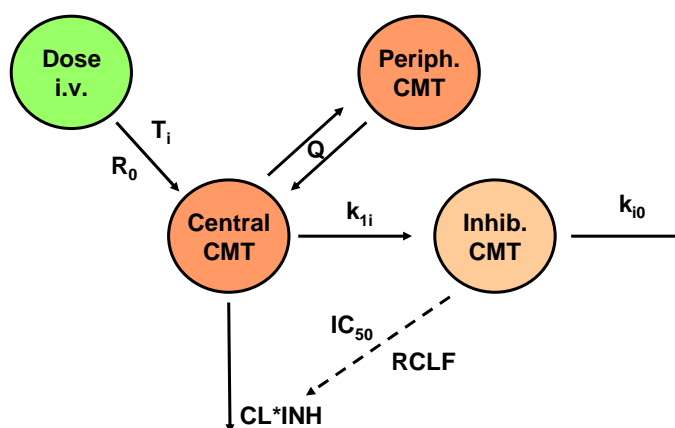
Figure 7 Two compartment PK model with i.v. infusion for unbound plasma concentrations of LZD in healthy volunteers and critically ill patients; adapted from Plock[32] and Scheerans[100].

Table 4 Model parameter of the PK model of unbound LZD concentrations in plasma, adapted from Plock[32].

Model parameters	Unit	Population estimate	Inter-individual variability (ω; CV, %)
CL	[L/h]	11.1	41.7
Q	[L/h]	75.0	-
V2	[L]	20.0	40.1
V3	[L]	28.9	34.8
RCLF		0.764	-
IC_{50}	[μg/mL]	0.0019	-
k_{i0}	[h^{-1}]	0.1	-

X4(t) is the drug concentration in the inhibition compartment depending on time t (see Appendix, Eq. 18). The clearance *CL* of LZD from the central compartment is partially

inhibited over time, which is expressed by multiplication (CL*INH). For the inter-individual variability (IIV) of LZD on *CL*, *V2* and *V3* was accounted in PK/PD simulations as specified in Table 4.

2.11.7.2 Effect simulations of various dosing regimens

The dose optimisation of LZD against VRE was based on simulations with the final RBR model. By combining the *in vivo* PK and the *in vitro* PD model a final PK/PD model as shown as in Figure 8 was formed,[100] and used for further simulations.
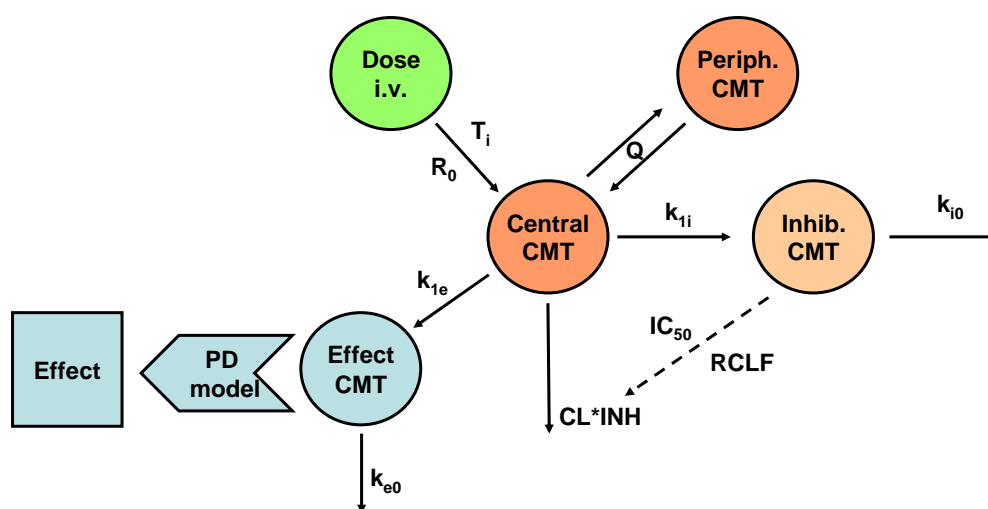
Figure 8 *In vivo/in vitro* **PK/PD model used for simulations; additionally to the PK components, a hypothetical effect compartment was introduced in the PD part, from Scheerans [100].**

Twelve dosing regimens, based on multiples of daily doses (DD), and one standard dosing regimen (600 mg twice a day) were simulated (Table 5). Simulations of the dosing regimens were performed as administration over 14 days for (i) one typical patient as deterministic simulations using population estimates (= typical patient, Table 4) and for (ii) 1000 in silico patients each with individual values of CL, V2 and V3 based on the inter-individual population estimates (computer generated) as stochastic simulations. The stochastic simulations were considered as Monte Carlo simulations (based on the Monte Carlo method).[100] The IIV on Cl, V2 and V3 was applied on each patient as normally distributed exponential variability model.[100] So, inter-individual differences on the dosing regimen could be investigated.

All simulations were carried out in Excel using a previously developed visual basic for applications (VBA) script (see Appendix, Figure 55).[100] The differential equations were numerically solved using the fourth-order Runge-Kutta method with a step size of 1 min (dt = 1 min). Multiple dosing was realised by implementing the principle of superposition.

Table 5 LZD dosing regimens applied for simulations; standard dosing regimen in grey.

Daily dose	Dosing regimen	R_0	T_i	No. of total doses
[mg/day]		[mg/h]	[h]	
600	1 × 600 mg	1200	0.5	14
1200	1 × 1200 mg	1200	1.0	14
1200	2 × 600 mg	1200	0.5	28
1200	3 × 400 mg	1200	0.333	42
1200	4 × 300 mg	1200	0.25	56
1800	1 × 1800 mg	1200	1.5	14
1800	2 × 900 mg	1200	0.75	28
1800	3 × 600 mg	1200	0.5	42
1800	4 × 450 mg	1200	0.375	56
2400	1 × 2400 mg	1200	2.0	14
2400	2 × 1200 mg	1200	2.0	28
2400	3 × 800 mg	1200	0.666	42
2400	4 × 600 mg	1200	0.5	56

R_0 – infusion rate, T_i – duration of infusion,

As effect measure, the area under the effect-time curve over 14 days ($AUC_{E(14\ days)}$) was chosen (Eq. 13). It incorporated the drug effect E, which was calculated by the trapezoidal rule with a step size (Δt) of 1 min. The distribution of the measured AUC_E values for different LZD dosing regimens was analysed by the effect size ES (Eq. 14).

$$AUC_E(t) = \int_{t_0}^{t_n} E \cdot dt \approx \sum_{i=0}^{n-1} \frac{E_i + E_{i+1}}{2} \cdot \Delta t$$

Eq. 13 Calculation of the area under the effect-time curve (AUC_E), adapted from Scheerans[100].

$$ES = \frac{M_I - M_{II}}{R}$$

Eq. 14 Calculation of the effect size.

The parameters M_I and M_{II} were the respective median values of $AUC_{E(14\ days)}$ of LZD doses, which should be compared. The parameter R was the median of the inter-quartile ranges of all investigated dosing regimens (= average box size). One box size reflected 50% of the underlying population. That means, if ES would be larger or equal to 0.6 a relevant difference between compared dosing regimens existed. If ES would be smaller than 0.6, the probable difference was considered to be not relevant.

2.11.7.3   Simulations of worst-case patients

The final *in vivo/in vitro* PK/PD model (see 0) was used with worst possible PK conditions of a patient to simulate the worst-case of efficacy of antibacterial therapy, i.e. underdosing. For this purpose the clearance, the volume of distribution in the central compartment and the volume of distribution in the peripheral compartment were varied with respect to the upper and lower limits found in the stochastic simulation for standard dosing regimen (see 3.8.5.2). All combinations were incorporated in the final RBR model and investigated on standard dosing of LZD (2x 600 mg/day over 14 days). The worst-case of PK combinations was identified and the dosing regimen optimised based on results of stochastic simulations (see 3.8.5.2).

2.12 Computational software

Microsoft® Office Excel 2003	Version 11.0, Microsoft Corporation, Redmond, USA
Chrompass	Version 1.8.6.1, Jasco GmbH Deutschland, Gross-Umstadt, Germany
Scientist	Version 3.0, Micromath, Saint Louis, Missouri USA
SPSS	Version 17, IBM, Chicago, Illinois, USA
WinNonlin®	Version 5.2, Pharsight, Mountain View, CA, USA

3 Results

3.1 Validation of the HPLC method for linezolid in Mueller-Hinton broth

The HPLC determination of LZD in MH broth was validated according to the FDA guideline for bioanalytical method validation.[101] The lower limit of quantification (LLOQ) was found with 0.204 µg/mL, the upper limit of quantification was 35.7 µg/mL. In reproducibility measures, a mean concentration of 0.939 ± 0.084 µg/mL (C_{nom} = 1.02 µg/mL) was found, which means an imprecision of 9.0% CV and an inaccuracy of -7.9% RE. Both parameters characterise the errors by preparation and HPLC system. Within one day imprecision ranged from +3.2 to +6.9% CV, inaccuracy ranged from +0.01 to +0.05% RE (Table 6). The total variability of the assay, expressed as between-day variability, ranged from +4.7 to +13.6% CV concerning imprecision and from -1.8 to +2.5% RE concerning inaccuracy.

Table 6 Variability of quality control samples during validation of LZD in MH broth with respect to mean estimated concentrations (C_{est}), imprecision and inaccuracy.

C_{nom} [µg/mL]	C_{est} mean ± S.D. [µg/mL]	Imprecision CV, %	Inaccuracy RE, %
Within-day variability (n = 3)			
0.204	0.215 ± 0.009	4.1	+ 0.04
2.04	2.152 ± 0.069	3.2	+ 0.05
10.2	10.248 ± 0.660	6.4	+ 0.01
29.6	30.524 ± 2.117	6.9	+ 0.03
Between-day variability (n = 9)			
0.204	0.201 ± 0.027	13.6	- 1.47
2.04	2.091 ± 0.174	8.3	+ 2.50
10.2	10.016 ± 0.488	4.9	- 1.80
29.6	29.774 ± 1.388	4.7	+ 0.66

For the assessment of the calibration function of all 3 days correlation coefficient (R), mean, standard deviation and imprecision of the intercept and the slope of the calibration line were taken into account (Table 7). A graphical analysis of all calibration samples with respect to the overall calibration line can be found in Figure 9. The high correlation between calibration samples and measured peak area supported the validity of the assay. The summarised results in respect of imprecision, inaccuracy and mean values for the calibration samples can be found in the Appendix, Table 34.

In conclusion, the assay results were conform with the specifications of the FDA guideline, where imprecision and inaccuracy were demanded to be below ±15% (LLOQ <±20%). Thus, the analysis of LZD in MH broth by HPLC was valid and could be applied for further LZD determinations.

Table 7 Validation parameters for the HPLC analysis of LZD in MH broth.

Attribute	Intercept [mV*min]	Slope [mV*min*µg/mL]	R
Day 1	0.0222	0.608	0.994
Day 2	0.0329	0.646	0.993
Day 3	0.0620	0.657	0.998
Mean ± SD	0.0390 ± 0.0206	0.637 ± 0.0253	0.995 ± 0.0030
CV	52.8%	4.0%	0.3%
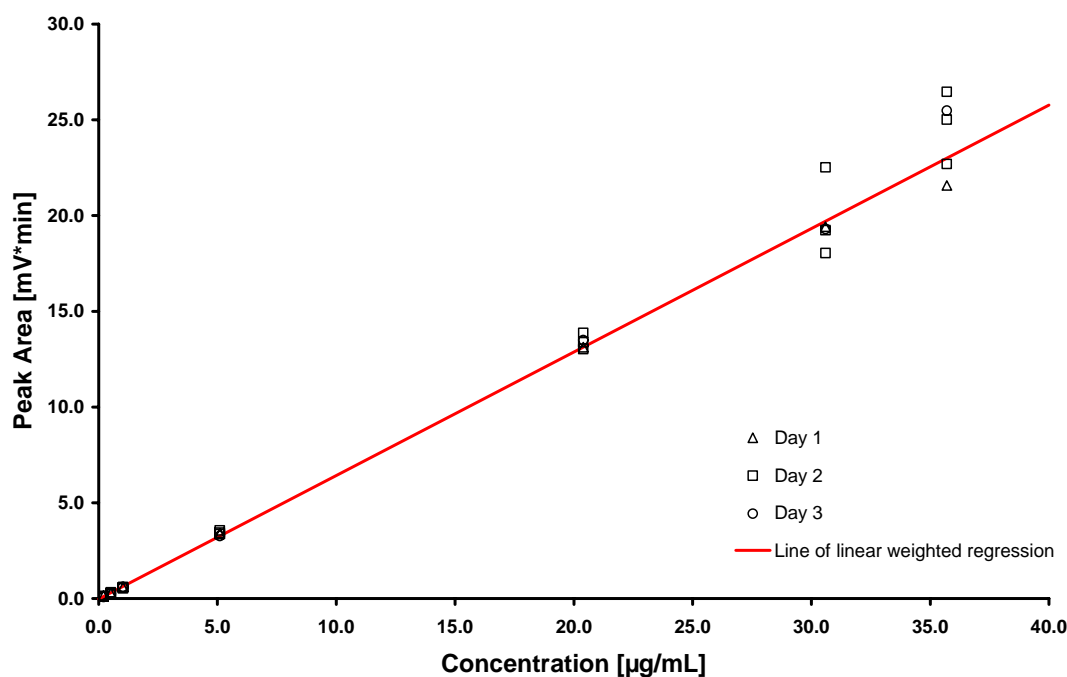
Figure 9 Overall calibration line of LZD in MH broth by HPLC analysis.

3.2   Preliminary microbiological investigations

The preliminary microbiological investigations should ascertain suitable and constant conditions for bacteria quantification in the *in vitro* models.

The McFarland index of 0.5 was conforming to 2×10^6 cfu/mL of *E. faecium*, whereby the bacterial dilutions had to be adapted. The data can be found in the Appendix, Table 35. The

bacterial concentrations increased linearly up to 90 min and then the bacteria passed over to exponential growth (see Appendix, Table 36 and Figure 56). Thus, the usual preincubation period of 2 h was sufficient for *E. faecium* to reach the exponential growth phase and it was applied in further experiments.

The comparison of dilution media did not show a significant difference between bacteria diluted in NaCl 0.45%, NaCl 0.9% and PBSP after 60 min (test 2.49 < quantil 5.99); see also Appendix, Figure 57. So the three dilution media NaCl 0.45%, 0.9% and PBSP were equivalent regarding bacterial viability. The differences of bacterial concentrations at the beginning of the experiment and after 60 minutes were also statistically not significant in all dilution media (test 7.595 > quantil 3.84; see also Appendix, Table 37). This allowed bacterial sample preparation over a length of 60 min. An advantage of PBSP was its ability to separate bacteria from each other, which facilitated viable cell counting. So, PBSP was taken for further experiments as dilution medium.

A centrifugation and a dilution procedure for bacteria purification were tested and compared. The methods did not show a difference in bacterial counts (Appendix Figure 58, for raw data see Appendix, Table 38). For higher bacterial concentrations, the dilution method was applied due to its countable results. For low bacterial concentrations the centrifugation method was more appropriate, since bacterial samples could be transferred on agar nearly without dilution. Thus, both methods could be used parallel in experimental settings. The centrifugation method determined the lower limit of bacteria quantification (LLOQ), which was 2×10^2 cfu/mL.

3.3 Qualification of the colony counter for bacterial counts

To count *E. faecium* on MH agar, three different digital counting methods depending on the number of bacterial colonies per plate were developed (see Appendix, Table 39). The numbers of colonies per plate were <100 (low No. of bacterial colonies), >100 (intermediate No. of bacterial colonies) and between 1000 and 2000 (high No. of bacterial colonies; Figure 10). Plates with >100 colonies per plate were most appropriate for further experiments, since colonies were clearly separated from each other and the number was high enough to confirm variability.

The results of the colony counting by the digital automated colony counter were compared to manual counts (see Appendix, Table 35). One- and two-digit bacterial concentrations ($<2 \times 10^1$ cfu/mL) were counted with the method for low number of bacterial colonies and served as control of the inaccuracy of the colony counter. Two-digit and three-digit bacterial concentrations (2×10^2 cfu/mL and 2×10^3 cfu/mL, respectively) were counted with the method for intermediate and high number of bacterial colonies, respectively. For the developed counting

methods, the reliability of the colony counter, the variability of the preparation and of the whole system were calculated (Table 8).
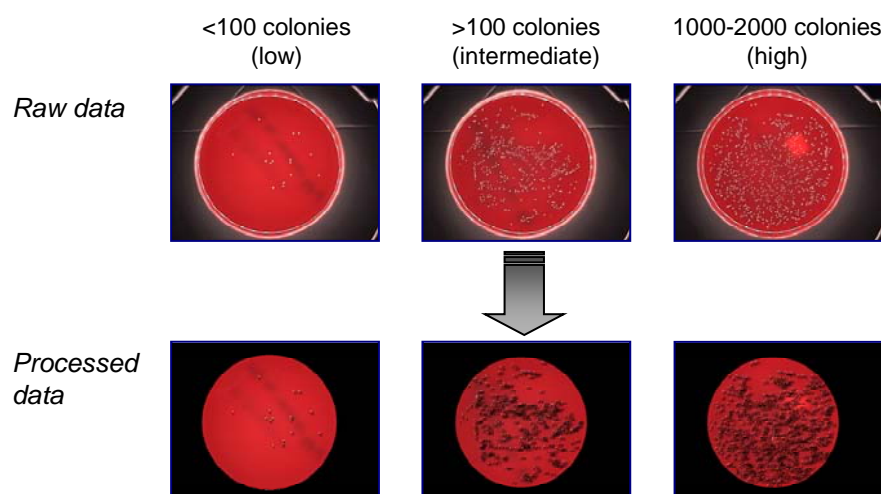
Figure 10 Data processed by the colony counter: raw data were analysed with respect to the number of bacterial colonies per plate using different counting methods; in processed pictures counted bacterial colonies were each indicated with a number.

Table 8 Variability of the digital automated colony counter (reference: manual counting).

Counting method	Parameter	Reliability of CQ (n=6)	Preparation variability (n=6)	System variability (n=18)
<100 colonies (low)	Mean±S.D. [cfu/mL]	15 ± 1	16 ± 1	19 ± 1
	Imprecision, % CV	6.7	9.0	6.9
	Inaccuracy, % RE	-1.1	6.9	24.9
>100 colonies (intermediate)	Mean±S.D. [cfu/mL]	177 ± 1	175 ± 1	200 ± 1
	Imprecision, % CV	0.6	0.6	0.6
	Inaccuracy, % RE	-3.9	-5.0	9.0
1000 – 2000 colonies (high)	Mean±S.D. [cfu/mL]	1844 ± 1	1826 ± 1	1815 ± 1
	Imprecision, % CV	0.1	0.1	0.1
	Inaccuracy, % RE	1.6	0.6	0.0

The reliability of the colony counter was maximum 6.7% CV imprecision and -3.9% RE inaccuracy, which meant for all counting methods a variation of only 1 colony as standard deviation. The variability between differently prepared plates showed maximum 9.0% CV imprecision and 6.9% RE inaccuracy. These qualification results were within the limits of ±15% imprecision and inaccuracy of the FDA guidance for bioanalytical methods.[101] For the system variability, which includes variance in preparation on different days and variance in counting, a maximum imprecision of 6.9% CV was found. This was in accordance with the FDA guideline,

whereas the maximum inaccuracy of 24.9% RE was not within the limits. Nonetheless the result was accepted, since the amount of inaccuracy was highly affected by the low number of colonies. Thus, the digital automated colony counter was qualified with respect to FDA guidance. For further experiments a short visual inspection of all processed plates was suggested.

3.4 Investigations in the static *in vitro* model

3.4.1 Reproducibility of experiments in the static *in vitro* model (pharmacodynamic variability)

The characterisation of the static *in vitro* model was based on growth control experiments. Therefore logarithmic bacterial concentrations from 13 experiments were analysed per time point (Table 9). Shown are the mean of logarithmic bacterial concentrations, the standard deviation (SD), imprecision (CV) of data, median bacterial concentration, range of observed bacterial concentrations and the number of bacterial determinations (n) underlying the calculations.

Table 9 Variability in the static *in vitro* model derived as logarithmic bacterial concentrations from the 13 growth control experiments.

Time	Mean	SD	CV	Median	Range	n
[h]	[lg cfu/mL]	[lg cfu/mL]	%	[lg cfu/mL]	[lg cfu/mL]	
0	5.885	0.305	5.2	5.866	5.204 - 6.580	50
1	6.384	0.377	5.9	6.365	5.447 - 7.274	64
2	7.094	0.617	8.7	6.987	6.170 - 8.519	59
4	8.023	0.436	5.4	8.070	6.748 - 8.700	55
6	8.440	0.157	1.9	8.497	7.820 - 8.681	52
8	8.501	0.127	1.5	8.524	8.126 - 8.771	55
10	8.511	0.166	2.0	8.519	8.041 - 8.934	42
12	8.547	0.139	1.6	8.505	8.332 - 8.924	34
16	8.593	0.109	1.3	8.580	8.415 - 8.799	24
20	8.613	0.159	1.9	8.577	8.301 - 8.934	22
24	8.622	0.369	4.3	8.541	7.602 - 9.580	38

The imprecision in the static model varied between 1.3% CV (at 16 h) and 8.7% CV (at 2 h). This was also found by a graphical analysis, where mean and maximum/minimum bacterial concentrations were depicted over time (Figure 11). The data were highly reliable, since they were based on at least 22 data points from 13 different experiments. From the graphical and

descriptive analysis could be concluded, that the static *in vitro* model produced precise and robust results (imprecision <10% CV).
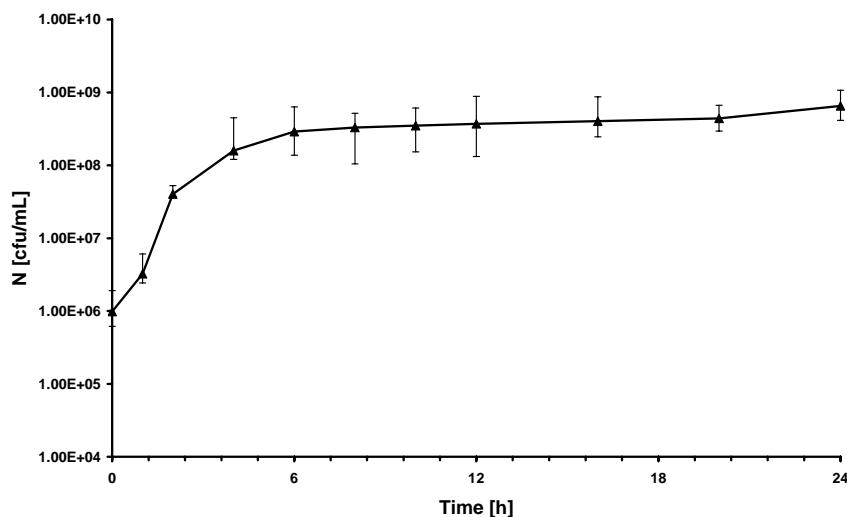
Figure 11 Bacterial concentration-time curve for growth controls in the static *in vitro* model (n=13 experiments); data points represent means of bacterial concentrations (n=22-64); bars indicate minimum and maximum bacterial concentrations.

3.4.2 Time-kill investigations

All time-kill experiments started with the same required bacterial concentration of 10^6 cfu/mL (at 0 h; Figure 12). In growth control experiments, exponential growth lasted at least from 0 to 4 h (see also 3.7). This part could be used to determine the growth rate constant of VRE. After 6 h bacterial growth became slower. At 24 h maximum bacterial growth of ~4×10^8 cfu/mL was reached, which was comparable to bacterial concentrations at 12 h and later. Hence, after 12 h growth and death were balanced; bacteria were in a persistence phase.

Under LZD concentration of 0.5 μg/mL bacterial growth was slower than in the untreated growth control, but after 12 h maximum bacterial concentrations reached the same extent as in growth control experiments. Also under 1 μg/mL LZD, bacteria grew and reached maximum concentrations (at 24 h) slightly below that in growth control experiments. Under 2 μg/mL LZD exposure the amount of growing and dying bacteria seemed to be at the same rate. The calculated difference of initial and final bacterial concentrations (Table 10), displayed an increase of bacteria at 24 h and thus a slight bacterial growth. Starting from a constant LZD concentration of ~4 μg/mL, there was no bacterial growth detectable. This LZD concentration can be assumed to be bacteriostatic.
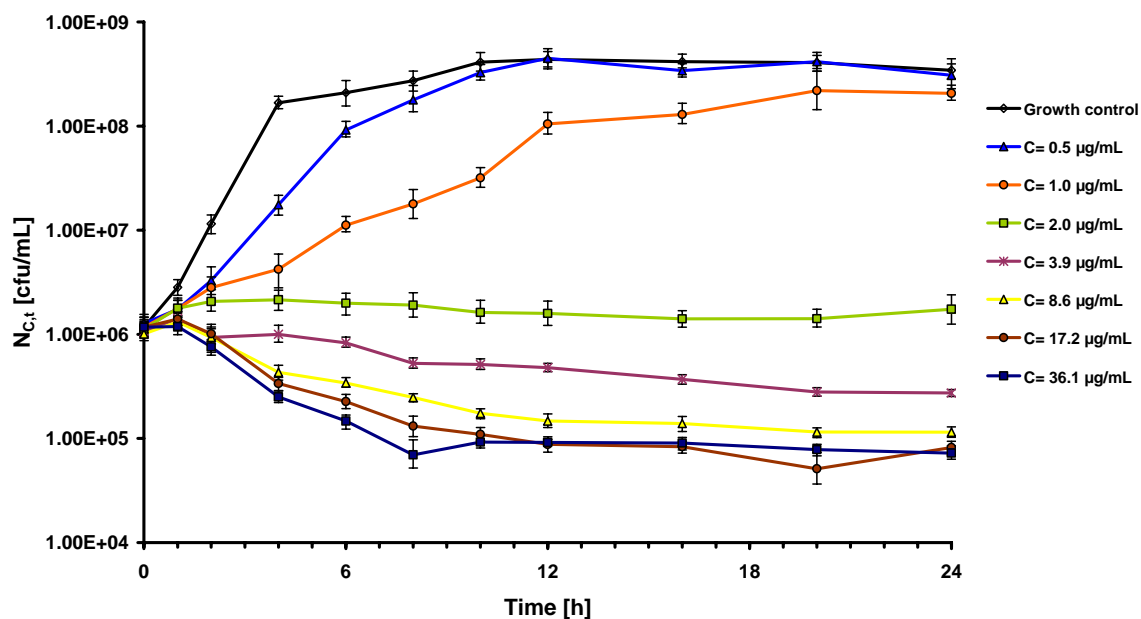
Figure 12 Time-kill curves of VRE under constant LZD exposure (static model); shown are median bacterial concentrations of bootstrapped geometric means (n = 1000) over time, error bars indicate 95% confidence interval.

Bacterial killing was observed for 3.9, 8.6, 17.2 and 36.1 µg/mL LZD (Table 10). The lowest effect was observed for 3.9 µg/mL (0.6 $\log_{10}$ bacterial reduction). Higher killing was seen for 8.6 µg/mL (~1 $\log_{10}$ unit) – the doubled concentration. The highest killing (1.2 $\log_{10}$ units) was found for 17.2 and 36.1 µg/mL. Both concentrations led to the same reduction of bacteria, which implies reaching the maximum effect. Bacteria could be reduced to a minimum of 6×10^4 cfu/mL.

For all data series a time delay of the effect was visible: No dying occurred within 1 h of LZD exposure, but first after 2 h. That means, the effect (killing of bacteria) was delayed towards the administration of the drug for approximately 1 h. A further characteristic of all data series was the constant bacterial concentration between 12 and 24 h. The maximum effect was nearly always reached after 12 h, except for bacterial concentrations under 1 µg/mL LZD. The effect of LZD might significantly increase between 1 und 2 µg/mL LZD, since the bacterial concentration-time courses caused by this drug concentrations revealed a strong difference ("gap" between the curves).

The LZD concentrations did not change significantly during the experiments (see Appendix, Table 40). Generally, a trend to lower drug concentrations at 24 h was found. Changes in concentrations might be due to drug degradation, errors in sample taking, in preparation as well as in measurement.

Table 10 Bacterial reduction in the static model after 24 h.

C_{LZD} [µg/mL]	log_{10} bacterial reduction (Δ)*	Nomination
0 (GC)	-2.470	
0.53	-2.383	Regrowth
1.0	-2.250	($\Delta<0$)
2.0	-0.191	
3.9	0.588	
8.6	0.943	Bacteriostatic
17.2	1.156	($0<\Delta<3$)
36.1	1.209	

* log bacterial reduction $\Delta = lg(N_{0h}) - lg(N_{24h})$
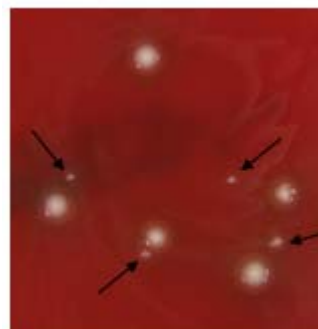
Figure 13 Small colony variants indicated by arrows developed under constant LZD exposure in the static in vitro model.

During all experiments with LZD small colony variants (SCV)[117] were developed in all cell culture flasks (Figure 13). The first occurred after 24 h of incubation at 37 °C and were better visible after a prolonged incubation of 48 h.

In conclusion, LZD was found to have no bactericidal (reduction of 3 log_{10} units), only a bacteriostatic effect on VRE. The effect was time-delayed and could not be increased by LZD concentrations higher than 8 µg/mL. The raw data of time-kill experiments in the static model are listed in the Appendix, Table 29 and Table 33.

3.4.3 Descriptive analysis of relative bacterial reduction

The relative bacterial reduction of VRE under constant LZD exposure in the static model was analysed with respect to time (Figure 14) and LZD concentration (Figure 15). A fast bacterial reduction was found until 4 h (steep slope in Figure 14). This means, the major part of the bacteria in a normal growing phase, was affected by the drug in that time. After this extensive killing, the remaining bacteria were also sensitive to the drug, but due to less growth, they were less affected. Thus, a slower killing per time was observed.[118] For 0.53 and 1.0 µg/mL LZD even a regrowth (RBR decline) was observed. Between 12 and 24 h, all RBR curves passed over in a constant phase (compare Figure 12). The maximum effect of approximately 45% RBR was reached at 8 h and continued up to 24 h. This means a log_{10} reduction of VRE of 45% compared to the growth control. It also expresses, that LZD could not eradicate VRE. The maximum effect was obtained by 8.6, 17.2 and 36.1 µg/mL LZD. The time delay of the effect (see 3.4.2) is here also visible as slow slope in RBR at the beginning (0 – 1 h).

Figure 15 A underlines the time dependence of the effect by reason of the abrupt rise in RBR between 2 and 4 h for all LZD concentrations. A detailed analysis of the lower LZD

concentrations led to Figure 15 B. An intersection for nearly all time points at 1.7 µg/mL LZD and 22% relative bacterial reduction became obvious. This concentration is in accordance with the abrupt change in bacterial growth observed in the time-kill curve analysis (see 3.4.2) at 1.0 and 2.0 µg/mL.[35]
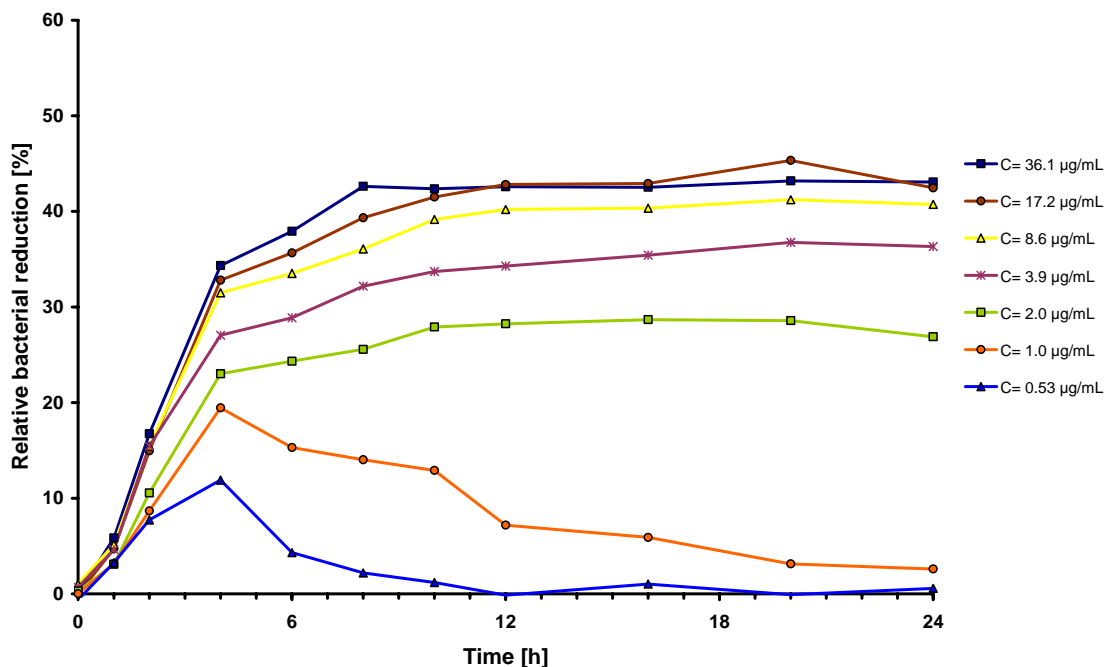
Figure 14 Relative bacterial reduction over time under constant LZD exposure.
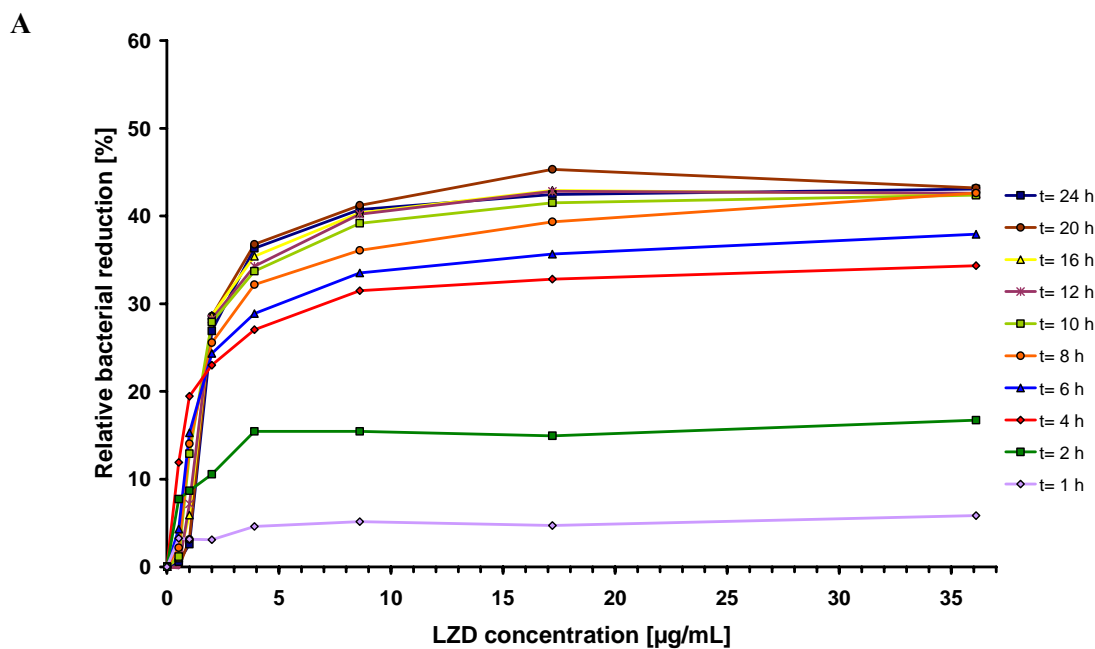
Figure 15 Relative bacterial reduction versus LZD concentration (static model), part A shows the complete LZD concentration range, part B enlarges the intersection of the hysteresis loop.

B
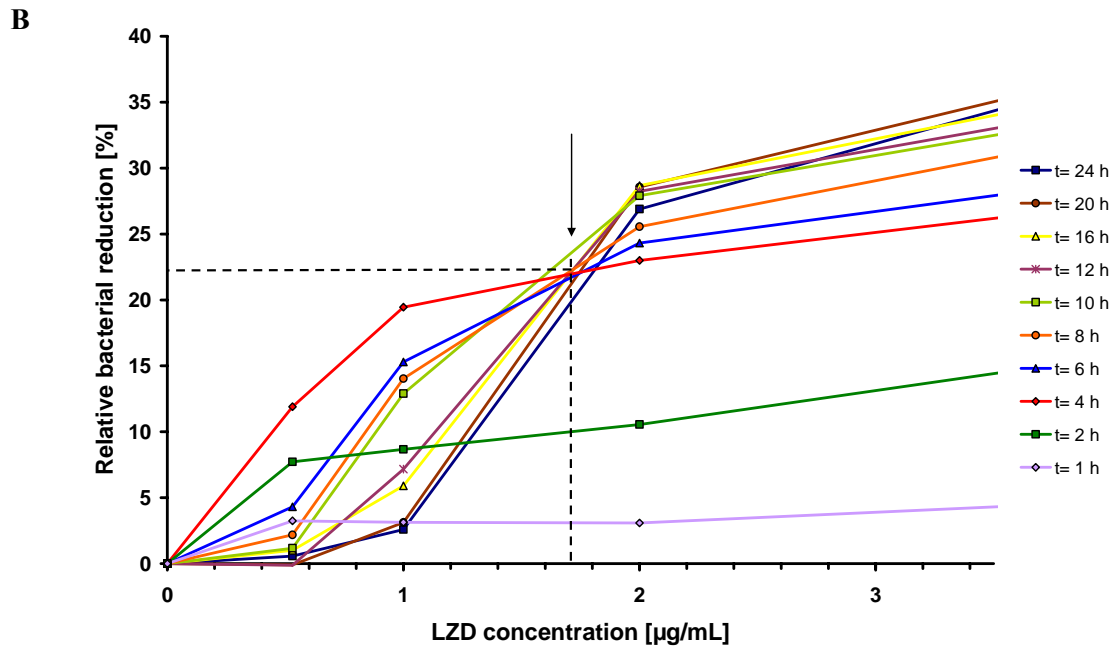
Figure 15 Relative bacterial reduction versus LZD concentration (static model), part A shows the complete LZD concentration range, part B enlarges the intersection of the hysteresis loop (continued).

Considering the effect over time in Figure 15 B, a hysteresis loop appeared,[100] which underlined again the time delay of the effect. For lower concentrations the RBR was highest at 4 h. Longer interaction of VRE and low LZD concentrations did not enhance the relative bacterial reduction. At 1.7 µg/mL LZD this relationship changed. The higher the time of the drug interaction with bacteria, the higher the RBR increased. Thus, the time of interaction should be at least 4 h to enable a sufficient bacterial reduction.

3.4.4   Minimum inhibitory concentration

The MIC was determined within the static model after 18 h with 2 µg/mL and after 24 h with 4 µg/mL. This is in accordance with the producer's information,[18] where VRE were described to be susceptible to 4 µg/mL, whereas non vancomycin resistant Enterococci were susceptible to 2 µg/mL.

3.5   Development of the dynamic *in vitro* model

3.5.1   Model 1

Model 1 had previously been constructed at the Department of Clinical Pharmacy of Prof. Kloft by Christian Scheerans and Fred Leinung (Figure 16). The main component, the bacterial vessel, consisted of a glass cylinder surrounded by a water jacket (Figure 17).
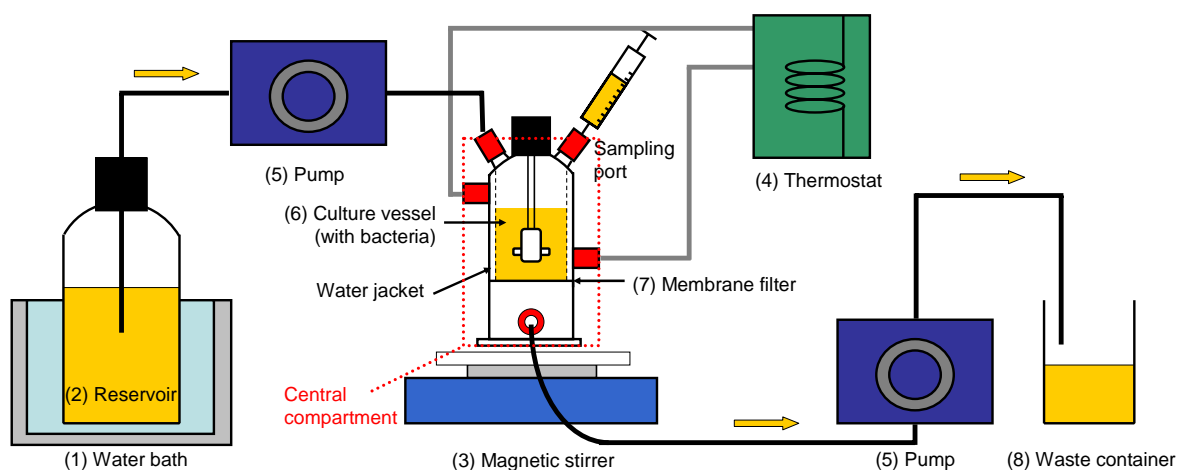
Figure 16 Schematic depiction of model 1, arrows represent the direction of medium flow; the central compartment is marked with a dotted box.
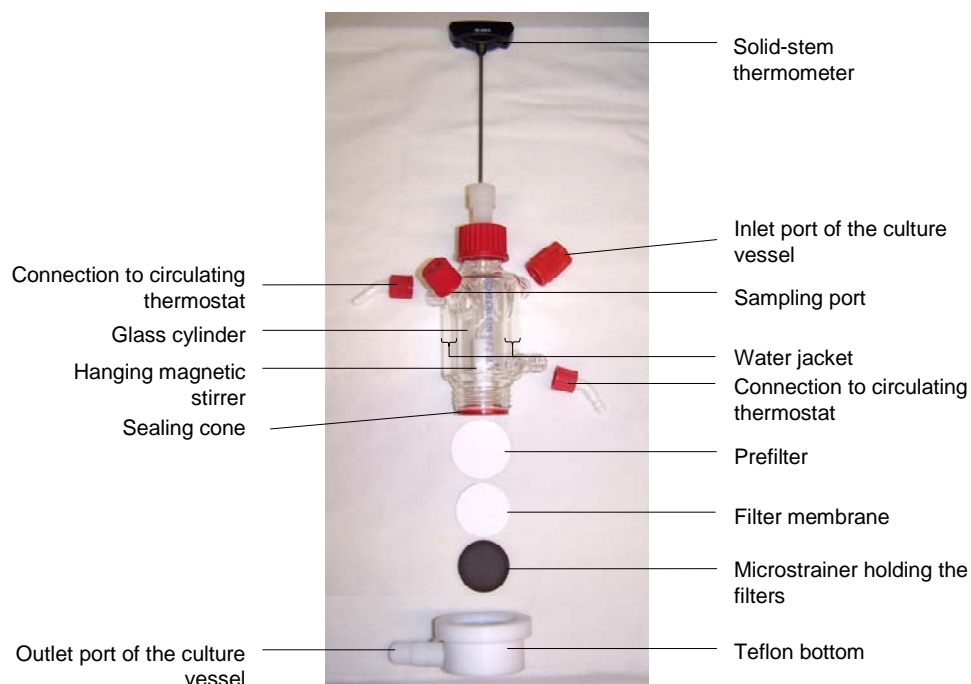
Figure 17 Central compartment of model 1.

The Teflon bottom of the bacterial vessel was prepared to hold a Teflon coated microstrainer with the bacteria retaining filter and was fixed by screwing on the glass vessel.[119] A specially constructed hanging magnetic stirrer at the end of a glass pipe was implemented in the culture vessel. Since the glass pipe was surrounded by medium, it could be used to measure the temperature of the medium without direct contact. The further components of model 1 are explained in Table 11.

The constancy of temperature was a particular issue for model 1, where the culture vessel was tempered by a thermostat. The intended temperature of 37 °C was reached 30 min after experimental start. The measurement in the glass cylinder of the hanging magnetic stick and inside the culture vessel showed the same temperature. Hence, a preliminary lead time would be needed for this setting before each experiment, but a water jacket around the culture flask was suitable for bacteria cultivation. The temperature could be measured correctly in the glass cylinder of the hanging magnetic stick, where it had no contact to bacteria (see Appendix, Figure 59).

Table 11 Components of the dynamic *in vitro* model.

Component	Function
(1) Water bath	Tempering the fresh medium in the reservoir
(2) Reservoir	Containing fresh sterile medium
(3) Magnetic stirrer	Providing even distribution and avoiding membrane blockage by stirring the medium
(4) Circulating thermostat	Tempering the water in the water jacket of the culture vessel
(5) Peristaltic pump	Pumping fresh medium from the reservoir into the culture vessel and used medium from the culture vessel to the waste container
(6) Culture vessel	Containing bacteria and drug
(7) Membrane filter with prefilter	Retaining bacteria, avoiding bacterial loss to the waste
(8) Waste container	Carrying the used, drug-containing medium

3.5.2   Model 2

Since model 1 showed static instability, when thermostat and tubes for dilution of growth medium were connected, another approach for the experimental setting based on the principle of continuous dilution was further developed resulting in model 2. Model 2 was designed within this PhD thesis by Dieter Reese and Julia Michael (Figure 18). The culture vessel was composed as glass cylinder with a Teflon ring at the bottom end (variant A, Figure 19).
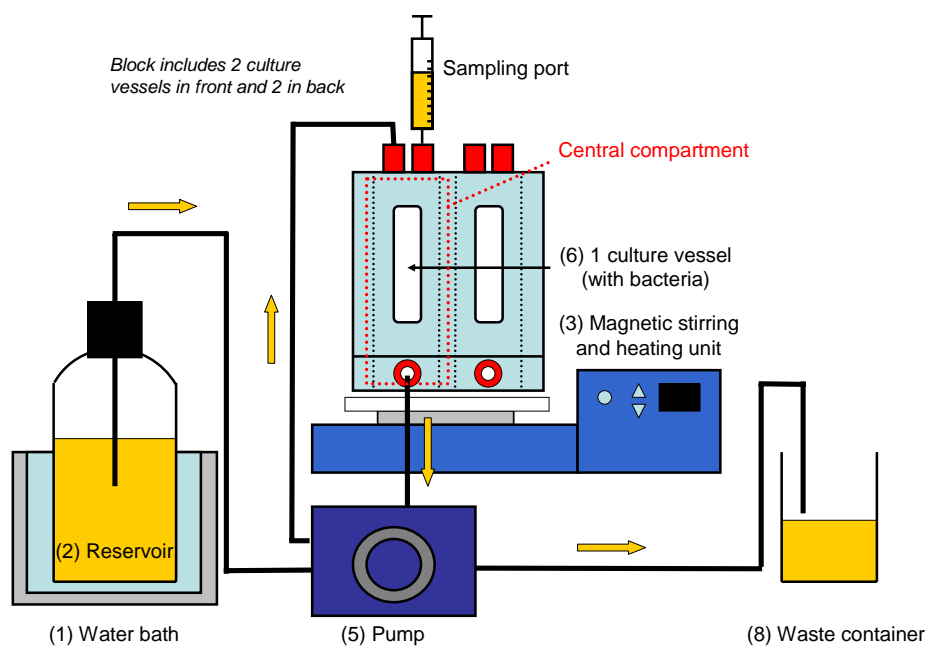
Figure 18 Schematic depiction of model 2 (variant A), arrows present the direction of medium flow and the dotted box the central compartment that means, one of four culture vessels.
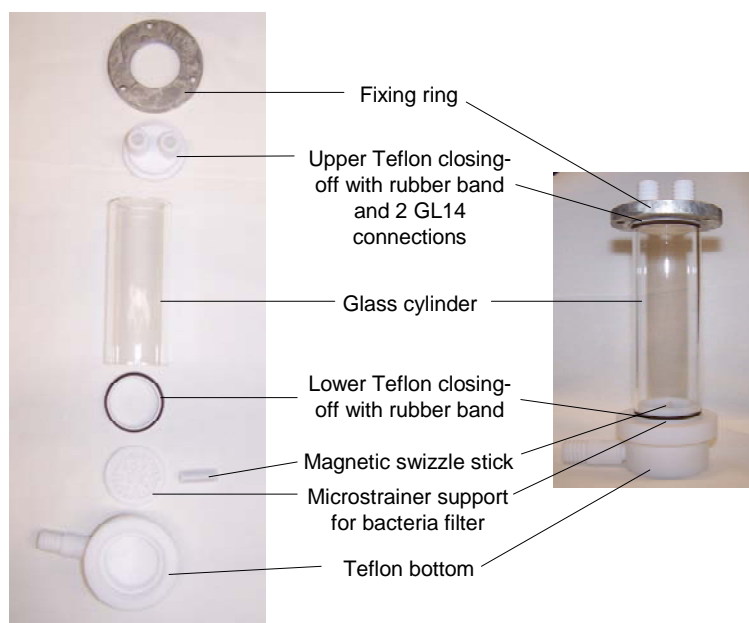
Figure 19 Single components of the culture vessel in model 2.

The glass cylinder could be plugged in an aluminium block. At the bottom end of the glass cylinder, a Teflon base held a Teflon strainer with the membrane filter. The upper end of the glass cylinder was covered by a modified multiple distributor for bottles. The lower part of the

distributor was straightened to close leak-proof with the glass cylinder. When all components were pieced together to the central compartment, a magnetic swizzle stick was put on the membrane filter to ensure homogenous distribution and keep the membrane filter clean. The central compartment was fixed and closed through pressure by pulling on screws on the top. The aluminium block could keep several culture vessels parallel. It was constructed to temper the culture vessel and facilitate magnetic stirring (fixed to 650 rpm) inside the vessels.

The further components of model 2 are the same as in model 1 (Table 11) except for the circulating thermostat. The function of this device (tempering) was adopted by the aluminium heating block.

In another variant (variant B) a syringe filter was installed instead of the membrane filter. This required a change of the position of the outflow (Figure 20). This variant was only used to investigate the suitability of the syringe filter. The further called model 2 is always variant A.
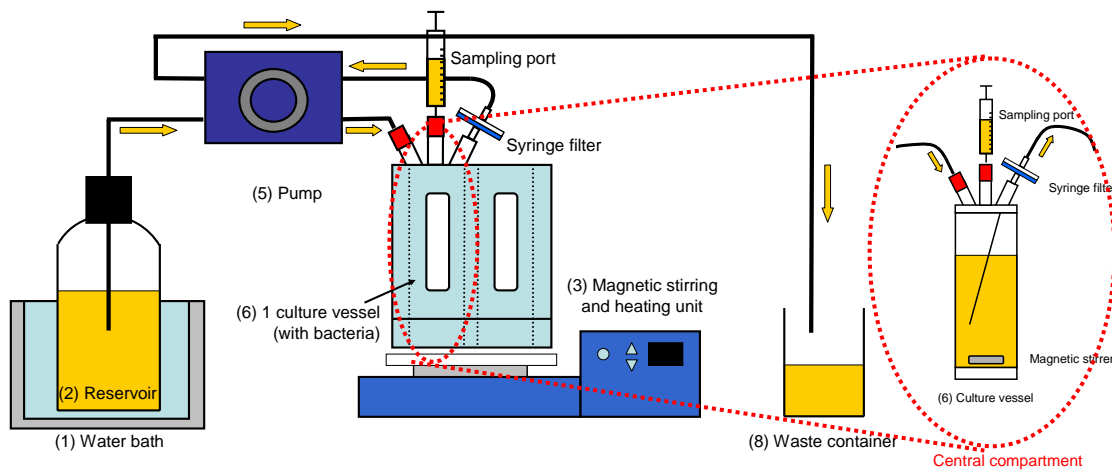
Figure 20 Schematic depiction of model 2 with syringe filter (variant B), arrows present the direction of medium flow.

3.5.3 Finalisation of the dynamic *in vitro* model

The finalisation of the dynamic *in vitro* model was based on model 2 (Figure 21). The aluminium block of model 2 provided static stability, tempering and stirring of culture vessels all in one. Model 2 was equipped with four culture vessels. Three vessels were intended for conduction of experiments with dynamic drug concentrations in parallel, one vessel could be used for growth control. The growth control vessel was constructed as static model, which was less resource- and cost-intensive, but provided reliable data to detect problems during experimental conduction. Since the commercial Teflon coated microstrainer from model 1 showed unevenness resulting in leakage, a plain, full-Teflon microstrainer was constructed by the section of scientific instrumentation of the Martin-Luther-Universitaet.
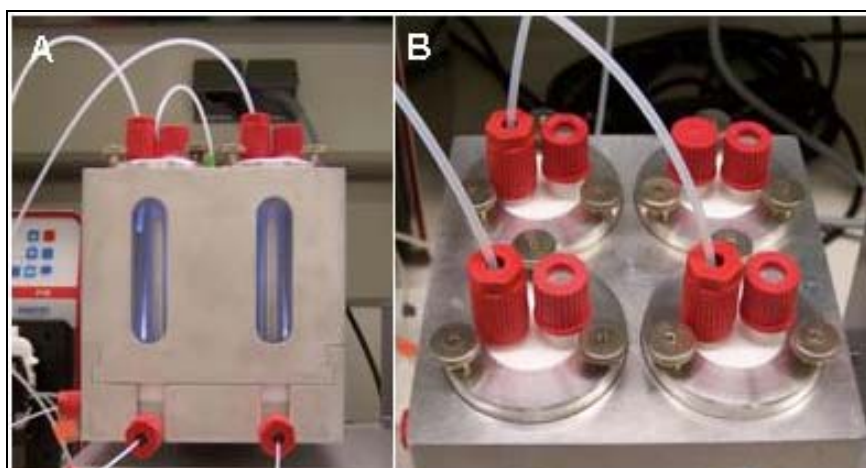
Figure 21 Aluminium block of the final dynamic *in vitro* model with 4 culture vessels in front (A) and top view (B).

In the final model the prefilter was omitted, only a single membrane filter was inserted to avoid bacterial loss. A magnetic swizzle stick on a safety strainer (above the membrane) was tested to retain bacteria and prevent injuries of the membrane filter by the swizzle stick. The safety strainer led to membrane blockage and was therefore removed. The function of retaining the major part of bacteria and cleaning the membrane filter was instead realised only by the magnetic swizzle stick directly placed on the membrane filter. The magnetic swizzle stick did not damage the membrane filter over 26 h.
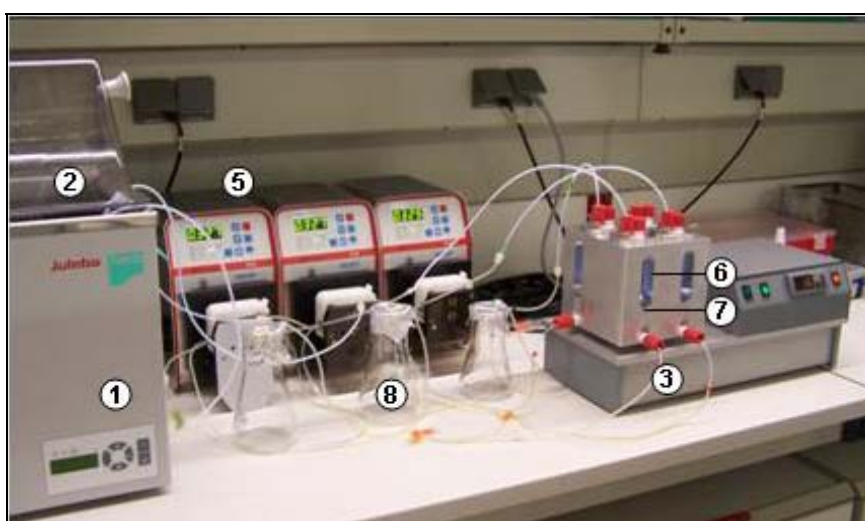
Figure 22 The final dynamic *in vitro* model with all components: (1) water bath, (2) reservoir, (3) magnetic stirrer and heating unit, (5) peristaltic pumps, (6) culture vessel, (7) membrane filter and (8) waste container (without (4) circulatingthermostat).

For cleaning and disinfection, the final dynamic *in vitro* model (Figure 22) could be completely decomposed. All parts could be disinfected with Sekusept® Plus, washed and autoclaved after use. The sterilisation of Teflon units by autoclave could not be recommended, since they are high precision products and might shift in form due to the properties of Teflon. For them the preparation with ethanol 70% after washing as sterilisation would be suitable. The aluminium block was also only disinfected with Bacillol® and ethanol 70% and cleaned with water. The final model is recommended for future experiments with dynamic drug concentrations.

3.5.4   Settings and devices for the final dynamic model

3.5.4.1   Constancy of temperature

The temperature in the final model was regulated by the aluminium block. No time delay between the temperature in the culture vessel and in the aluminium block occurred. The desired 37 °C were reached 15 min after the experiment started.

3.5.4.2   Type of pump

The suitability of a perfusor and a peristaltic pump concerning transport of designated volumes of water per time was investigated. Figure 23 shows the relation between nominal and estimated volumes transported per time by both pump types. The estimated volumes per time were close to or exactly on the line of identity, so the highly precise pumping of designated volumes became obvious for both pump types. The correlation was determined by a weighted linear regression (Table 12).
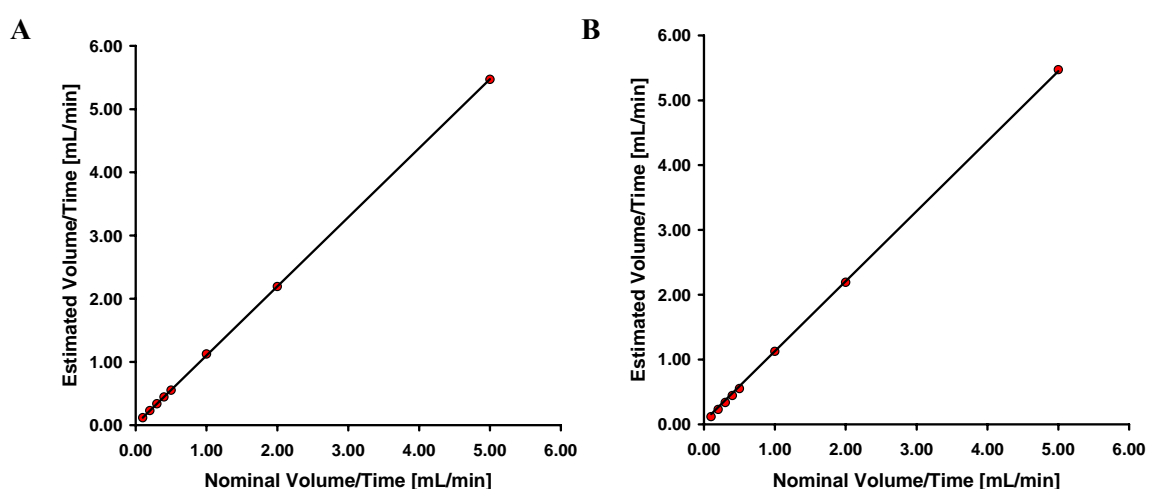
Figure 23 Relation between nominal and estimated volumes transported per time by the perfusor (A) and the peristaltic pump (B); the red symbols mark the measurements, the black line presents the line of regression.

The perfusor had an extremely high linearity (R=0.99993) and precision of pumping in the investigated calibration range. Precise setting of designated flow rates was possible, which would be necessary for exact drug concentration-time profiles. By continuous pushing the plunger of the syringe continuous pumping was possible.

Slight differences in linearity and precision of pumping existed within perfusor and peristaltic pump, but they were too marginal to be relevant. Precise setting of flow rates was only possible by computational programming of the peristaltic pump. Using the manual setting, possible flow rates were dependent on the prior calibration. Thus, jerky leaps in setting the designated flow rate appeared. Also the way of pumping by the peristaltic pump was not optimal, since intervals of flow appeared by the mechanism of pumping. This was especially important at low flow rates, whereby times of flow and times of no flow appeared. Another disadvantage presented the silicone tubes inserted in the peristaltic pump (see 3.5.4.4).

On the other hand, in the peristaltic pump the required dilution medium could be kept in a huge bottle (e.g. 1 L) as reservoir, which could be tempered in a water bath. Using a perfusor, only a small syringe of 60 mL contained the medium reserve. Assuming an *in vitro* flow rate of 0.326 mL/min (see 2.9.3), this would mean exchange of the reservoir in the perfusor every 2 h, whereas it needed to be changed only after 48 h in the peristaltic pump. In addition, since the syringe with the medium reserve was installed in the perfusor, the syringe could not be tempered except when the whole pump was tempered.

Hence, the peristaltic pump was chosen for PK and PK/PD experiments, since it enabled a huge reserve volume and tempering of broth. A huge reservoir containing tempered broth reduced the experimental efforts. Furthermore, linearity and precision of the peristaltic pump were sufficient.

Table 12 Comparison of perfusor and peristaltic pump.

Attribute	Perfusor	Peristaltic pump
Regression		
Intercept	0.00806	0.00606
Slope	1.0974	1.0024
Correlation R	0.99993	0.99961
Max. difference from regression line	-0.020 mL/min / -1.8%	0.167 mL/min / 3.3%
Use within the calibration range possible	yes	yes
Reproducibility *(n = 5)*		
$V/t_{theoretical}$ [mL/min]	0.326	0.325
$V/t_{estimated}$, mean [mL/min]	0.359 ± 0.004	0.333 ± 0.005
Imprecision (CV, %)	1.05	1.42
Inaccuracy (RE, %)	10.02	2.06

3.5.4.3 Mode of pumping

Comparing the determined percentage concentrations of dispensing volume per time or pumping a flow rate facilitated by the peristaltic pump, a slight difference became visible (Figure 24). LZD concentrations sampled from volume per time pumping were further away from the nominal concentration-time curve than samples of dispensing flow rates. The highest differences were found at 0.5 and 2 h. Thus, in PK and PK/PD investigations pumping of flow rate was applied.
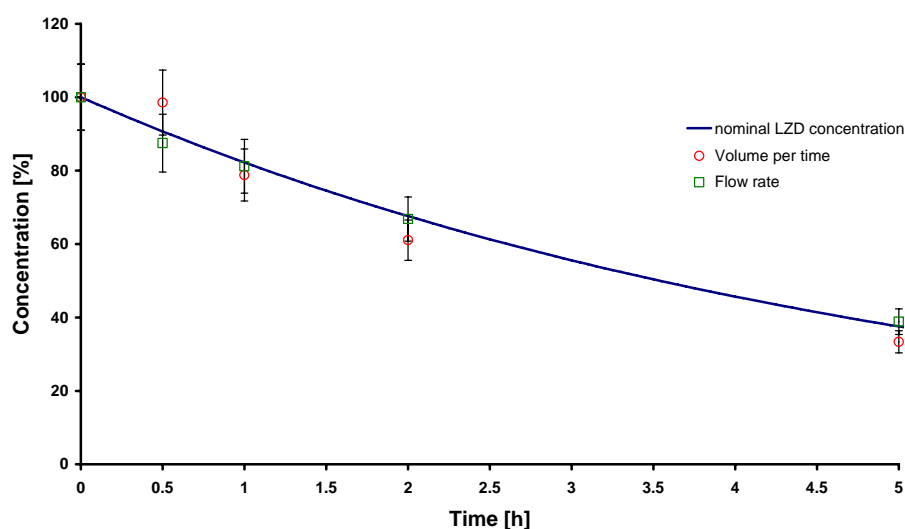
Figure 24 Comparison of determined drug concentrations by pumping volume per time or flow rate; shown are means of double injections, error bars indicate 9% imprecision of the HPLC assay.

3.5.4.4 Types of tubes

During the experimental conduction, silicone and Teflon tubes were used as connection between pumps and other devices (e.g. reservoir). MH broth adhered stronger to the silicone tube, thereby it became brown. The silicone tubes could be easily cleaned by pumping soap water (Neodisher A8) though it. Decontamination of both types of tubes with standard desinfective Sekusept® Plus was not possible. Ingredients of Sekusept® Plus adhered to the tube wall, were released by MH broth and could kill bacteria during PK/PD investigations. Thus, after each experiment, the tubes had to be cleaned by rinsing the tubes with clear water and autoclave them afterwards at 121 °C for 20 min.

The tubes in the peristaltic pump always had to be silicone tubes (3-stop tubes), otherwise they would not be squeezable and medium could not be transported. Under pressure, as it may appear in the dynamic model, 3-stop tubes had only a limited life-time (100 h). Their technical qualification is dependent on the saturation with medium and the hours of applied service life. Due to these incessant changes, calibration of tubes was necessary before each experiment.

3.5.4.5 Choice of filter

The inserted prefilter was supposed to retain most of the bacteria and thus avoid blockage of the membrane filter. The culture vessel was constructed in a way that the prefilter (and also the membrane filter) was inserted and fixed between glass vessel and Teflon bottom, such that bacteria could not pass around it. The utilised glass fibre prefilters expanded in water and so the thickness of the prefilter increased and the tightness of the culture vessel was interrupted. Thus, the prefilter was omitted in the final model.

A syringe filter was investigated in model 2 (variant B). It was supposed to be an alternative to the combination of prefilter + membrane filter, since it could be easily exchanged. Model 2 with the syringe filter produced the same results in PK investigations as the model with the membrane filter (Appendix, Table 41 and Figure 60). That meant, LZD did not adhere stronger to one of the membrane materials than to the other. The decisive unsuitability of the syringe filter was found in growth control experiments. Within 3 h the syringe filter was blocked by bacteria, which made it improper for further investigations. So, variant B of model 2 was completely rejected.

In conclusion, only the single membrane filter suited the model requirements. A pore size of 0.45 µm was sufficient to prevent *E. faecium* from outflow and was used in the final model.

3.6 Investigations in the dynamic *in vitro* model

3.6.1 Ability of application of different pharmacokinetic profiles

The dynamic *in vitro* models 1 and 2 were exercised to demonstrate the general application of different PK profiles of LZD (or other drugs) to the *in vitro* model and therewith to microbiological time-kill investigations. Both, one-compartmental and two-compartmental drug decline, were simulated in the dynamic *in vitro* model (Figure 25). Simple bolus administration as well as a short-term continuous infusion could be applied as administration routes. The relative errors between nominal and *in vitro* simulated LZD concentrations were randomly scattered around zero. Nevertheless a trend to exceed the nominal concentrations at later times was visible (compare Appendix, Table 42). The relative errors did not exceed 15%, except for the two-compartment model with continuous infusion with one deviation of 22% after 5 h.

Errors might be due to the experimental conduction, to the HPLC analysis and to the LLOQ (0.2 µg/mL), especially when sample concentrations were lower than the LLOQ in some cases.

The investigations point out the ability of the developed dynamic *in vitro* model to imitate one and two compartmental models (different drug dispositions) and bolus and infusion administration. Thus, the model offers various drug applications resulting in more realistic, *in vivo* like conditions, which might lead to a higher predictability of the derived bacterial data.
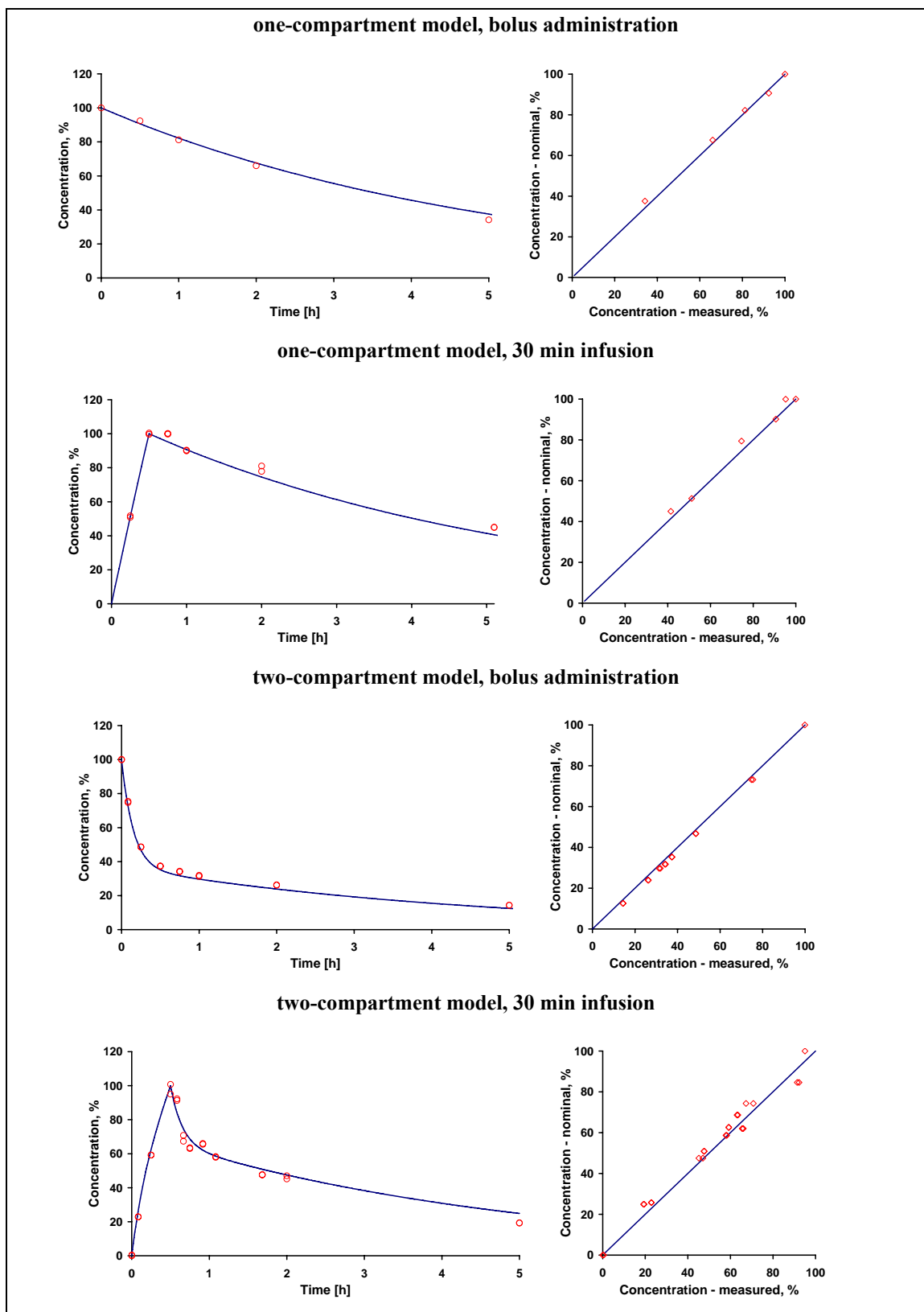
Figure 25 Ability of application of different administration routes and compartments in the dynamic *in vitro* model. Left panel: LZD concentration-time profiles with nominal concentration-time course (blue line) and measured concentrations (red symbols); right panel: the respective goodness of experimental application between nominal and measured concentrations (red symbols) and the line of identity (blue line).

3.6.2 Reproducibility

3.6.2.1 Pharmacokinetic variability

The general determination of the PK variability (see 2.9.4.1) resulted from a bolus administration of LZD simulating a one-compartment model in the dynamic *in vitro* model (see 3.5.2). The overall variability was below 15% CV, which is the limit recommended by the FDA for bioanalytical methods and is appropriate for bioanalytical experiments (Table 13).

The imprecision was mostly below 6% CV, but increased up to 11% CV after 5 h of experimental duration. The inaccuracy was found to be between -4% and 2% RE. It also increased, the longer the experiment lasted. The graphical evaluation (Figure 26) of the determined drug concentrations per culture vessel showed a random scatter of the data around the nominal curve. This means errors were random, potentially due to the HPLC assay and the experimental conduction. Decreasing imitated drug concentrations might be due to saturation and aging of the tubes (see 3.5.4.4), which led to more flexible and soft tubes and so to higher volumes transported per time.

Table 13 General PK variability in the dynamic in vitro model given as percentage variances depending on the nominal percentage LZD concentration, n=3 culture vessels; the maximum LZD concentrations at t=0 h were set to be 100%.

Time	C_{nom}	C_{est} (mean ± SD)	CV	RE
[h]	%	%	%	%
0	100.0	100.0 ± 2.4	2.4	0.0
0.25	95.2	97.3 ± 5.6	5.7	2.1
0.5	90.7	90.0 ± 1.8	2.0	-0.8
1	82.2	81.7 ± 4.2	5.1	-0.6
2	67.6	65.1 ± 2.5	3.8	-3.7
5	37.6	36.1 ± 3.9	10.9	-3.9

C_{nom} – nominal LZD concentration; C_{est} – estimated LZD concentration
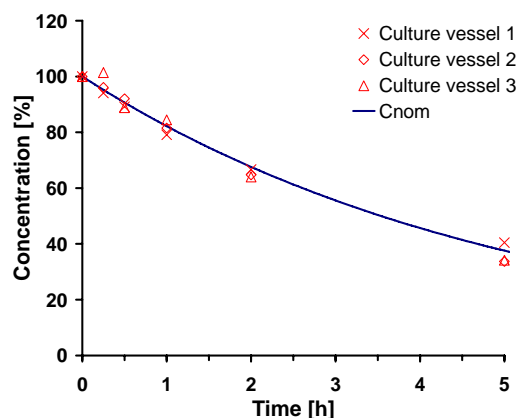
Figure 26 General PK variability in the dynamic in vitro model after bolus administration with first-order drug decline (one-compartment model); red symbols measured concentrations, blue line – nominal concentration.

3.6.2.2 Pharmacodynamic variability

Growth control experiments served for the determination of PD variability (see 2.9.4.2) in the final dynamic *in vitro* model. Mean, standard deviation and the coefficient of variation were calculated from the logarithmic bacterial concentrations (Table 14).

Table 14 Variability in the dynamic *in vitro* model derived as logarithmic bacterial concentrations from 3 growth control experiments.

Time	Mean	SD	CV	Median	Range	N
[h]	[lg cfu/mL]	[lg cfu/mL]	%	[lg cfu/mL]	[lg cfu/mL]	
0	6.087	0.163	2.7	6.093	5.892 - 6.418	11
1	6.551	0.109	1.7	6.584	6.287 - 6.656	12
2	7.382	0.217	2.9	7.367	7.009 - 7.667	12
3	7.723	0.122	1.6	7.732	7.477 - 7.924	12
4	8.187	0.190	2.3	8.250	7.787 - 8.387	12
6	8.672	0.160	1.8	8.711	8.465 - 8.931	12
12	8.980	0.414	4.6	9.009	8.121 - 9.826	12
20	9.059	0.181	2.0	9.077	8.892 - 9.238	4
24	9.205	0.253	2.8	9.178	8.795 - 9.772	12
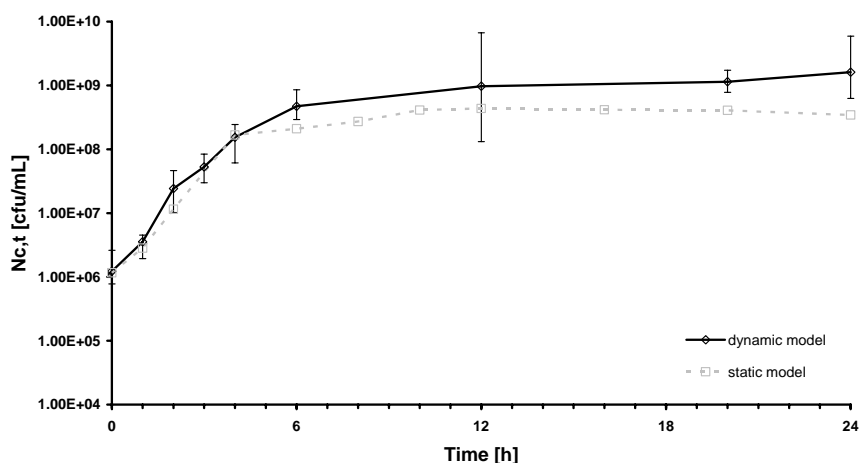
Figure 27 Bacterial concentration-time curve of growth controls in the dynamic *in vitro* model, data points represent geometric means of bacterial concentrations and bars indicate minimum and maximum bacterial concentrations; the growth control of the static model is presented as reference.

The location of bacterial counts was characterised by median and range of logarithmic bacterial concentrations. The imprecision (CV) varied between 1.6 and 4.6% CV. The highest imprecision was observed at 12 h. After 24 h the imprecision was again as low as at the

beginning of the experiment. Hence, even if the experimental setting was kept constant, which was confirmed by low imprecision of bacterial concentrations at 0 and 24 h, the bacterial concentration-time curve had a high variability during the experiment. So, high variability in bacterial concentrations between 0 and 24 h, especially at 12 h, had to be taken as acceptable in other experiments. The low number of observations at 20 h was caused by missing sampling and contamination of agar plates. The four existing observations were reliable, but should cautiously be interpreted. The graphical depiction of the normal data on a log-scale underlined the high variability within 24 h (Figure 27).

3.6.3 Time-kill investigations

The effect of changing LZD concentrations on VRE was investigated in the final dynamic *in vitro* model. To validate the conditions and correctness of the PK profiles during the PK/PD experiments, drug concentrations were routinely taken, determined by HPLC and compared to the nominal drug concentrations. Figure 28 opposes the nominal applied LZD PK profiles to the experimentally obtained concentrations. Overall, the applied PK profiles were adequately simulated *in vitro*. For the LZD concentrations in each single experiment see Appendix, Table 43 and Figure 61.
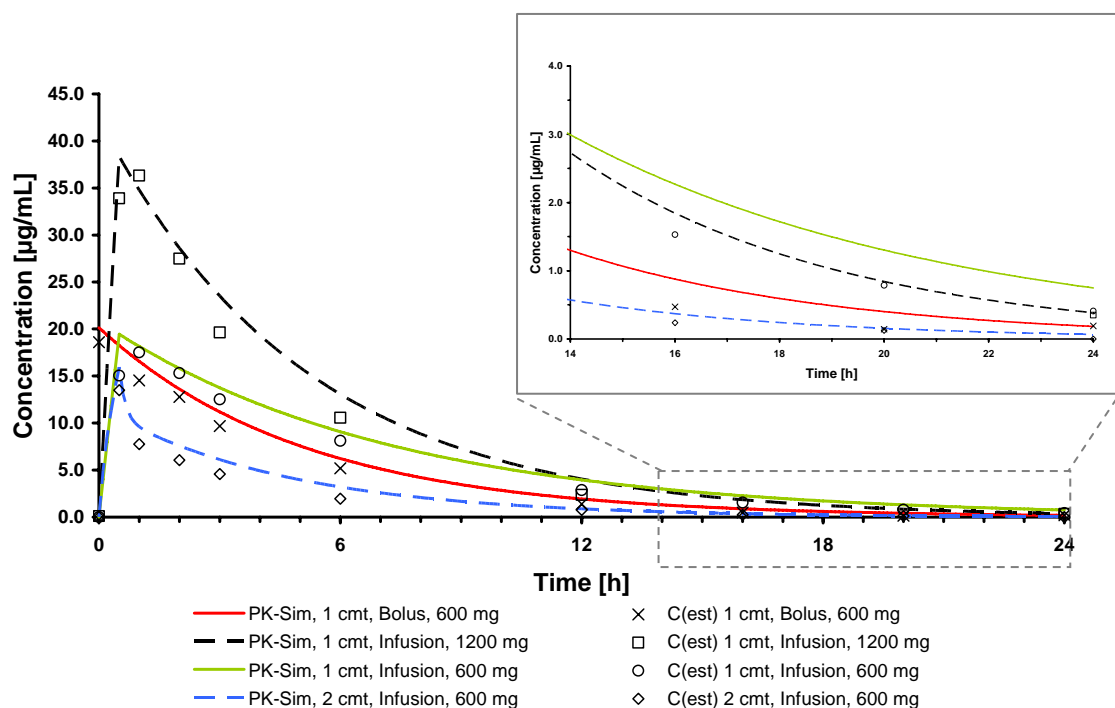
Figure 28 Nominal LZD concentrations (solid lines) and *in vitro* determined mean LZD concentrations (symbols) applied in time-kill experiments in the dynamic *in vitro* model.

Table 15 shows the resulting PK profiles and PK parameters. The elimination rate constant k_e (two compartment model: hybrid constants α and β), the volume of the central compartment V (two compartment model: $V2$ and $V3$, see 2.9.3 and Figure 7) and the AUC were calculated by a compartmental analysis in Winnonlin based on the determined LZD concentrations.

Table 15 Actual LZD concentration-time-profiles and resulting PK/PD indices determined from time-kill-experiments in the dynamic *in vitro* model.

Parameter	Unit	Bolus administration	Infusion	Infusion	Infusion
Preset parameter					
No. of compartments		1	1	1	2
$D_{(in\ vivo)}$	[mg]	600	1200	600	600
T_i	[h]	-	0.5	0.5	0.5
$t_{1/2,\ nominal}$	[h]	3.54	3.54	5.00	3.22[*]
Obtained parameters					
$k_{e,\ estimated}$	[h^{-1}]	0.211	0.224	0.140	$\alpha = 6.140$ $\beta = 0.240$
$V_{estimated}$	[L]	32.362	31.018	33.424	V2 = 19.538 V3 = 35.743
$AUC_{0-24\ h}$	[mg*h/L]	87.18	171.63	123.816	41.37
AUC_{0-12h}	[mg*h/L]	80.86	160.24	103.76	39.27
$t_{1/2,\ estimated}$	[h]	3.28	3.09	4.96	2.89[*]
$C_{max,\ estimated}$	[μg/mL]	18.540	36.597	17.338	15.303
$CL_{(in\ vivo),\ estimated}$	[L/h]	6.839	6.962	4.670	Q = 14.458 CL = 71.255
PK/PD indices (24 h)					
$AUC_{0-24\ h}/MIC_{2\ μg/mL}$	[h]	43.59	85.81	61.90	20.69
$AUC_{0-24\ h}/MIC_{4\ μg/mL}$	[h]	21.80	42.91	30.95	9.82
$T_{C>MIC,\ 2\ μg/mL}$	%	44	56	66	33
$T_{C>MIC,\ 4\ μg/mL}$	%	30	43	46	20
PK/PD indices (12 h)					
$AUC_{0-12\ h}/MIC_{2\ μg/mL}$	[h]	40.43	80.12	51.88	19.63
$AUC_{0-12\ h}/MIC_{4\ μg/mL}$	[h]	20.21	40.06	25.94	9.82
$T_{C>MIC,\ 2\ μg/mL}$	%	88	100	100	66
$T_{C>MIC,\ 4\ μg/mL}$	%	60	86	91	40

[*] related to terminal phase; D = dose, T_i = time of infusion, $t_{1/2}$=half-life of the drug, k_e = elimination rate constant, α and β = elimination rate constants in the two compartment model, V = volume of distribution, V2 and V3 volumes of distribution in the central and peripheral compartment, respectively, C_{max} = maximum concentration, CL = clearance of the drug.

Elimination rate constant and volume of distribution served for further calculations of the half-life $t_{1/2}$, the drug clearance *CL* (two-compartmental model: *Q* and *CL*). The PK/PD indices AUC/MIC(x) base on the AUC.

The obtained bacterial concentrations per experiment and the geometric means after bootstrapping are shown in the Appendix, Table 33 and Table 44, respectively. The initial bacterial concentrations (t=0 h) of the different experiments were comparable and as requested at 10^6 cfu/mL for all investigated PK profiles (Figure 29). The variability of bacterial concentrations increased for all experiments after 12 h.

The investigations of changing LZD concentrations comprised the administration of 600 mg LZD as bolus, the administration of 1200 mg as infusion, the administration of 600 mg as infusion, all with one-compartmental kinetics, and the administration of 600 mg as infusion with two-compartmental kinetics (drug amount reflects the *in vivo* condition). For none of the four PK profiles, a bactericidal effect was observed (reduction of 3 $\log_{10}$ units). Instead, all administered doses and PK profiles were found to be bacteriostatic at least at 12 h. The maximum bacterial reduction was less than 1.6 $\log_{10}$ units for all investigated PK profiles (Table 16).

Table 16 Maximum bacterial reduction in the dynamic *in vitro* model.

PK profile	Max. $\log_{10}$ reduction	Time point of max. reduction
1 cmt, bolus, 600 mg	1.581	12 h
1 cmt, infusion, 1200 mg	1.101	12 h
1 cmt, infusion, 600 mg	1.356	20 h
2 cmt, infusion, 600 mg	0.951	16 h

Only under LZD treatment with a long drug half-life, that would mean reduced clearance *in vivo* and thus longer availability in the body, the bacteriostatic effect was continued until 24 h and a bacterial regrowth prevented. After bolus administration (comparable to 600 mg *in vivo*) bacterial concentrations decreased until 12 h about 1.5 decimal power. Subsequently, regrowth of bacteria was visible. After 24 h, the initial bacterial concentration of 10^6 cfu/mL was reached again. Since 600 mg LZD cannot be administered as bolus *in vivo* due to its low solubility (~2 mg/mL), it is given as time-finite infusion (600 mg/300 mL)[19] and was therefore investigated *in vitro* also as infusion. The decline of bacterial concentration over 6 h is nearly the same in all imitated PK profiles and dosing regimens. For all others than the bolus administration, the bacterial concentration was maximal reduced about 1 decimal power.
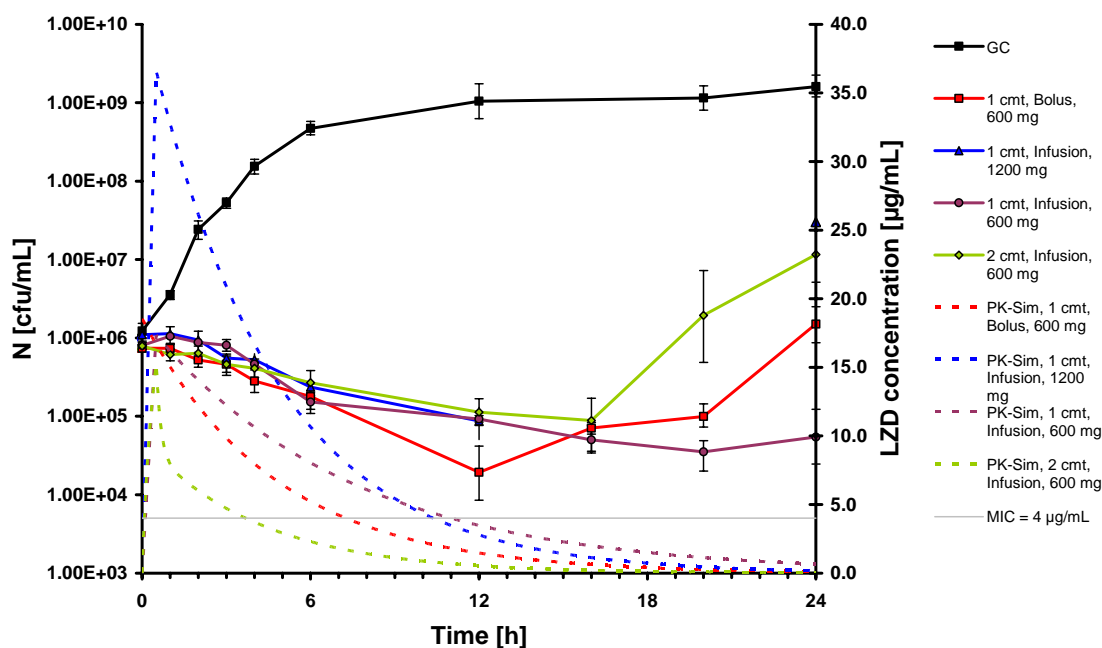
Figure 29 Time-kill curves of VRE under changing LZD exposure (dynamic model); solid lines present median bacterial concentrations of bootstrapped geometric means (n=1000) over time, error bars indicate 95% confidence interval; dashed lines present respective *in vitro* determined LZD profiles.

Under the doubled dose of LZD (1200 mg) in a one-compartment model with 30 min infusion, the lowest bacterial concentrations were found. At 24 h higher bacterial concentrations (3×10^7 cfu/mL, compared to 12 h value) can be reported, which meant bacterial regrowth also under doubled dose treatment. For the most physiology-like simulated profile (two-compartment model, infusion) regrowth was found after 16 h.

Regarding the PD data (bacterial concentrations) with the PK data (LZD concentrations) the time delay of the effect of approximately 1 h could be confirmed (compare 3.4.2). The LZD concentration in the culture vessel had been fallen below the MIC (4 µg/mL) for 1 h (up to 8 h), when bacterial regrowth started. From the similar bacterial decline at the beginning of all experiments and the higher bacterial concentrations after 24 h could be inferred, that the route of administration had only a minor influence on bacterial killing (due to the similar decline). A dose escalation from 600 to 1200 mg did not enhance the effect, bacterial regrowth was also visible at high LZD concentrations. Furthermore, a delay in the drug effect was found, which could possibly explain the delayed resulting bacterial regrowth.

The development of SCV was observed under changing LZD concentrations for all investigated drug profiles.

3.6.4   Descriptive analysis of relative bacterial reduction

The descriptive RBR analysis of the different, simulated PK profiles and dosing regimens pointed out the same increase of RBR over time for all dosing regimens and PK profiles up to 6 h (Figure 30). The highest overall bacterial reduction (RBR ~55%) was obtained by bolus administration at 12 h. This result cannot be achieved *in vivo*, since bolus injection of LZD is impeded due to its low solubility.

All other simulated PK profiles and dosing regimens, demonstrated the same height of effect (RBR ~45%) at 12 h. Only the effect by the time-finite infusion with a long half-life (one-compartmental model, 600 mg) increased longer than 12 h up to a RBR of 50 %. The RBR analysis showed no significant difference between one- or two-compartment models, between bolus administration and time-finite infusion or between short (3.2 h) and long (5 h) half-life of the drug for the first 12 h. It could be concluded, that in case of physiology-like short half-lives a dose escalation did not result in a gain of effect – not even at the beginning of treatment.

A difference between the effects resulting from the different simulated PK profiles and dosing regimens was clearly visible 20 h after the experiment started. Thus, first at this time, different dosing, half-lives and compartmental distribution might be relevant.
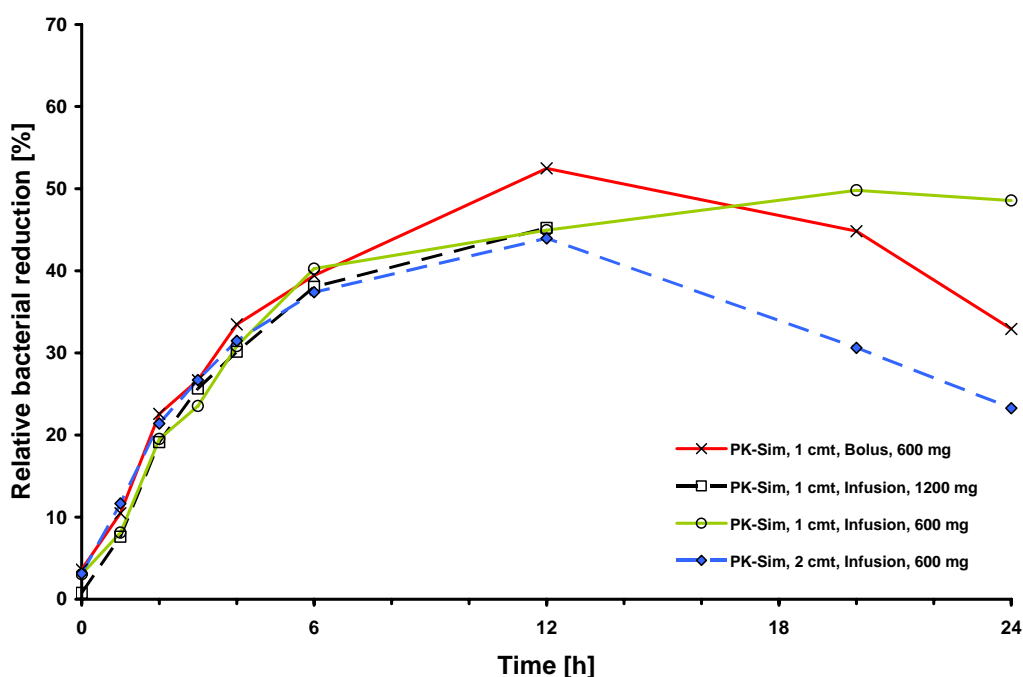
Figure 30 Relative bacterial reduction over time under changing LZD exposure (dynamic model).

The bolus administration, which had the highest RBR at 12 h, showed a bacterial reduction of only ~35% at 24 h, this means bacterial regrowth. The lowest relative bacterial reduction was obtained by infusion combined with two-compartmental kinetics (RBR ~23%) at the same time,

whereas this PK profile led to a maximum effect of 45% at 12 h, too. This might be due to the fast decrease in drug concentration, which was simulated to account for the rapid distribution and elimination (α-phase). So the most physiology-like drug administration showed the lowest relative bacterial reduction *in vitro*. A maximal difference in RBR of nearly 30% was found between the different PK profiles and dosing regimens at 24 h.

When analysing the RBR versus LZD concentration, a hysteresis (indicated by arrows in Figure 31) was noteworthy: The RBR rised with increasing drug concentration, but it did not fall with declining drug concentrations. With decreasing drug concentrations, the RBR still increased, until it reached its maximum of 45 – 55% at approximately 2 µg/mL. This is also the lower limit of the MIC for VRE. The highest RBR and the corresponding concentration (2 – 4 µg/mL) were nearly the same for all PK profiles and dosing regimens, although the slopes of the curves were not equal. Thus, 2 - 4 µg/mL LZD seemed to be a breakpoint of the effect. The maxima of LZD concentrations of infusion experiments could not be included in Figure 31, because the corresponding bacterial concentrations were not counted at 0.5 h. Different maximum LZD concentrations led to slightly different RBRs. The figure shows, that physiologically tolerable concentrations, such as in the two-compartment model, led to the same bacterial reduction as less likely LZD concentrations. All RBR data can be found in the Appendix, Table 45.
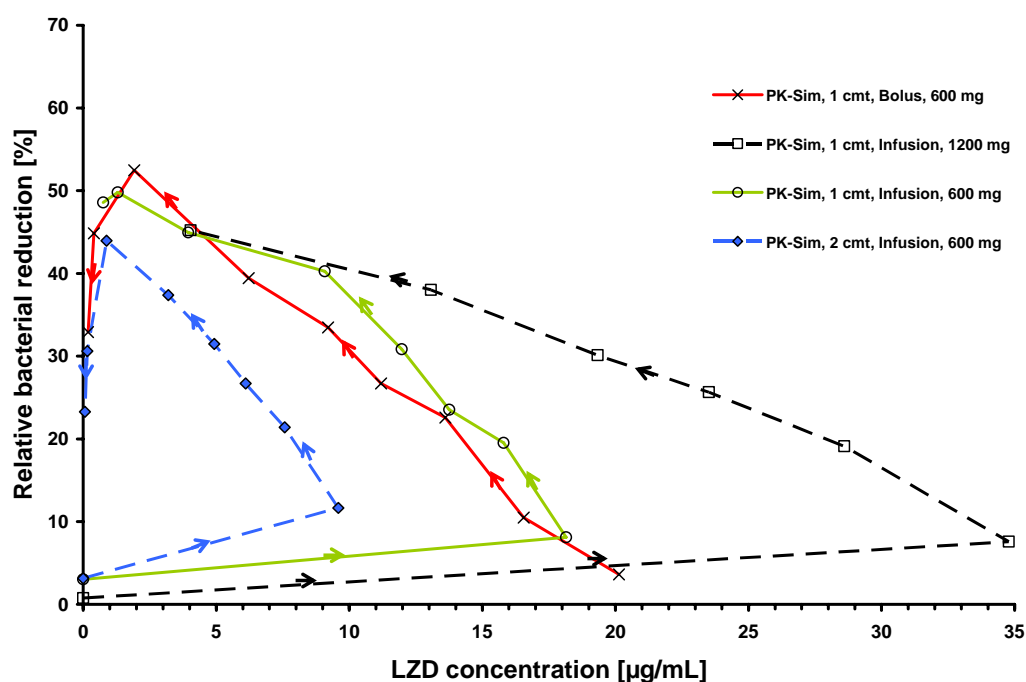
Figure 31 Relative bacterial reduction versus estimated LZD concentration (dynamic model); arrows indicate direction of concentration change.

3.6.5   Investigations on linezolid resistance

The observation of SCV (Figure 13) in the static and dynamic model suggested the development of less susceptible cells either as persisters or resistant bacteria during exposition to antibiotic drugs. The latter hypothesis should be supported by the detection of LZD resistant VRE, derived from experiments in the dynamic model under one-compartmental conditions with bolus administration of LZD. The bacterial samples were plated on LZD containing agar plates. In resistance investigations with 8 µg/mL LZD on agar (2x MIC)[110], a first inspection after 48 h of incubation showed also no visible growth of bacteria. After 160 h small colony variants of VRE were detectable. At the beginning of the experiment, the less susceptible cells were not detectable in one of the remaining two culture vessels (t=0 h; Figure 32). Over time, the concentration of less susceptible cells increased suggesting an exponential growth phase - unaffected by LZD. The concentration of less susceptible bacteria was very low towards normally susceptible bacteria during the complete observation period. The increase of less susceptible bacteria starting at 6 h precedes the increase of the total bacterial concentration after 12 h treatment.
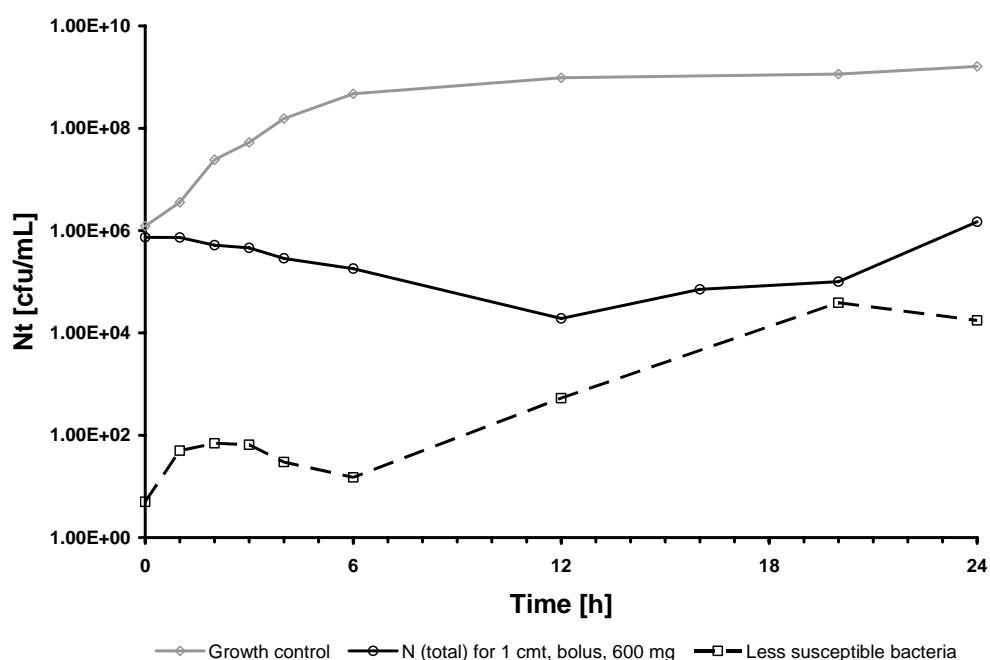
Figure 32 Bacterial concentration-time course with less susceptible bacteria after exposure to 600 mg LZD (bolus, one-compartmental model). Detection of less susceptible bacteria was performed on 8 µg/mL LZD MH agar plates after 160 h of incubation; dotted lines – mean of less susceptible bacteria (n=2 culture vessels), grey line – growth control, black line – total bacterial concentration.

The plates with 12 µg/mL LZD concentration (3x MIC)[109] showed no visible growth after 96 h of incubation over the complete observation period. That means, under changing LZD concentrations and with an initial bacterial concentration of 10^6 cfu/mL, a LZD resistance was not developed.

3.7 Comparison of *in vitro* models

In this work investigated three different *in vitro* models: a static, a dynamic and a previously investigated semi-dynamic[111] *in vitro* model. To compare whether the model conditions influence the bacterial growth, the growth control experiments were explored concerning mean bacterial concentrations and the respective variability (see Appendix, Table 29).

All growth curves (Figure 33) had a similar shape. Their growth rate constants seemed to be similar and they exhibited exponential growth during the first 6 h, afterwards a plateau was reached. After 6 h until the end of the experiment the bacterial concentrations from the different model driffed apart. In the static model, the imprecision ranged from 1.3% to 8.6% CV (n=13 experiments; Table 9). In the semi-dynamic model, the imprecision ranged from 0.6% to 2% CV (n=3 experiments; see Appendix, Table 46) and in the dynamic model was an imprecision between 1.6% and 4.6% CV found (n=3 experiments; Table 14). So for all *in vitro* models the imprecision was below 10% CV, which included inter-experimental, analyst and counting variability. Thus, all three models produced reliable results.
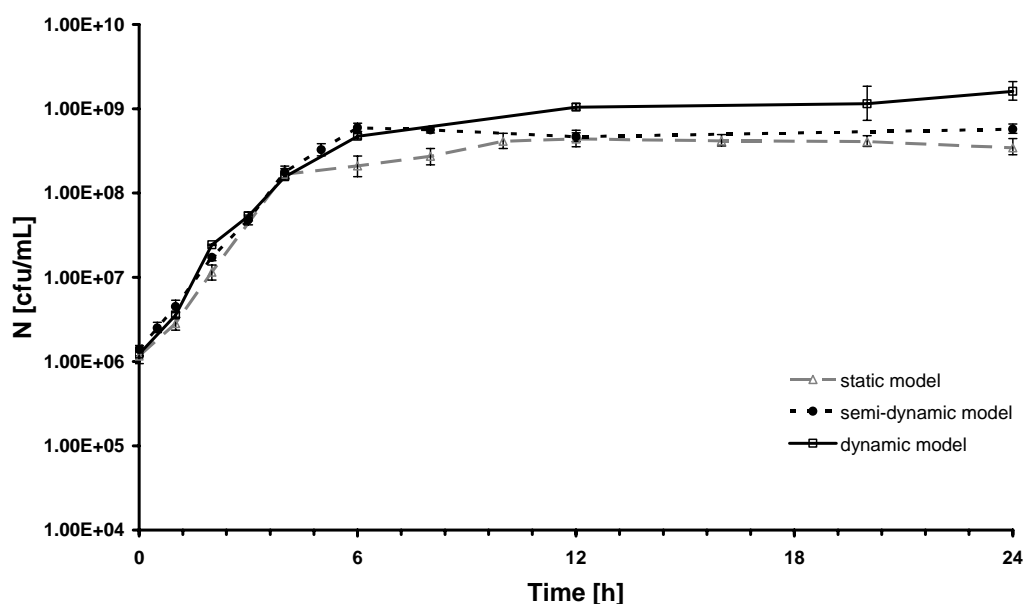
Figure 33 Comparison of growth controls of the static, semi-dynamic and dynamic *in vitro* model; data present medians of bootstrapped geometric means (n=1000), error bars show the 95% confidence intervals.

To control the comparability of the growth controls in the different *in vitro* models, the start conditions, that means initial bacterial concentrations (t=0 h), were analysed by the Mann-Whitney-Wilcoxon test. The test found no significant differences (p > 0.05) between growth controls in the different model types (see Appendix, Figure 62). Hence, only the bacterial treatment after experimental start could be responsible for changes in bacterial growth.

The differences between the growth rate constants from the three models were minimal. The growth rate constants of the semi-dynamic and the dynamic model were equivalent ($k_{0,\text{semi-dynamic}} = k_{0,\text{dynamic}} = 0.445$ h^{-1}). The growth in the static *in vitro* model seemed to be the fastest ($k_{0,\text{static}} = 0.481$ h^{-1}).

In the next step, the beginning of the plateau phase was determined. Therefore, bacterial concentrations at 6, 12 and 24 h were analysed for their difference by the Mann-Whitney-Wilcoxon test for each model type (see Appendix, Figure 63). In all model types, a significant difference between 6 and 12 h was found. Thus, bacterial growth (changes in bacterial concentration) took place until 12 h. In the static and the dynamic model, no changes in bacterial concentration between 12 and 24 h could be found. That means, a plateau phase of (exponential) bacterial growth was reached after 12 h. In contrast, in the semi-dynamic model changes in bacterial concentrations between 12 and 24 h were found. This might be due to the different analysts or to the fewer data for the semi-dynamic model, pretending higher bacterial concentrations. Differences derived from the bacterial treatment could be neglected, since on one hand the semi-dynamic model was changed to static conditions after 12 h and on the other hand the treatment of bacteria in the dynamic model is rougher than in the semi-dynamic model.

At last, the outcome (bacterial concentrations) after 24 h was compared. The test detected significantly different bacterial concentrations (p < 0.05) after 24 h treatment between the three models (see Appendix, Figure 64). Bacterial concentrations in the static *in vitro* model were the lowest, the dynamic *in vitro* model led to highest bacterial concentrations.

It can be concluded, that the three investigated *in vitro* models showed the same variability (< 10%) on determined bacterial concentrations. But although the same start conditions were applied, different bacterial growth rate constants as well as different final bacterial concentrations were found. The plateau phase was reached after 12 h in the static and dynamic, but first after 24 h in the semi-dynamic model.

3.8 Pharmacokinetic/pharmacodynamic modelling and simulation

3.8.1 Stationary concentration

Using the basic time-kill curve model, the stationary concentration of LZD on VRE was calculated to be 2.25 µg/mL LZD. This means, to achieve no bacterial net growth (bacteriostasis) at 24 h, a constant LZD concentration of 2.25 µg/mL would be needed. The expected bacterial concentration-time course under this concentration and the respective experimental data from the static model were shown in the Appendix, Figure 65. The value of the stationary concentration was between the two MIC values determined at 18 h and 24 h with 2 and 4 µg/mL, respectively, thus the MIC can be assumed as reliable bacteriostatic concentration in case of VRE and LZD. The stationary concentration was suggested to be achieved *in vivo* at the least, so that under assistance of the immune system, the antibiotic therapy would be successful.

3.8.2 Modelling of relative bacterial reduction

3.8.2.1 Model development

RBR data from the **static** *in vitro* model for *E. faecium* were successfully fitted by a sigmoidal modified E_{max} model (**basic** model, Table 17 and Appendix, Figure 66) as described previously for *S. aureus*.[100] The integration of RBR data determined under changing LZD concentration (**dynamic + static** data) should enable a more general description of the bacterial concentration-time course (**final** model). The developed modified sigmoidal E_{max} model was not adequate to fit all data from both models correctly, which led to termination of the model run in Scientist. The incorporation of an effect compartment in the E_{max} model – an indirect link model – enabled adequate fitting of all data. Since the data from the static model represent a systematic investigation of the concentration-effect dependence, the concentration of the half-maximum effect EC_{50} was adopted from the basic modelling and fixed for the final modelling parameters. The value of the LZD concentration provoking the half-maximum effect of 1.765 µg/mL was in accordance with the findings from the static model (3.4.2), where the half-maximum effect was located between time-kill curves by 1 and 2 µg/mL. The comparison of parameter estimates derived from the modified sigmoidal E_{max} model (basic model) and of the parameter estimates from the indirect link model (final model), showed nearly the same estimates for E_{max} and the time-delay constant a (Table 17). The parameter H was more precisely determined in the indirect link model. The value decreased with incorporation of dynamic data from 6.108 to 3.167. The time-delay constants b and z varied slightly between the modified sigmoidal E_{max} and the indirect link model. The reduced value of b in the final model, led to a higher total EC_{50} over time (compared to the basic model), that means a reduced susceptibility of bacteria, which must

result from the dynamic data. Since the value of z was higher in the final than in the basic model, the total value of H decreased, which would also decrease the steepness of the curves (more flat). The elimination rate constant from the effect compartment k_{e0} was estimated with 0.054 h^{-1}. Thus, the drug half-life in the effect compartment was 12.8 h and the time to reach steady state concentrations in the effect compartment would take 63.8 h (5x $t_{1/2}$). All parameters of the basic model were estimated with an imprecision below 10% CV (except b, CV = 18%); in the final model imprecision of parameter estimates ranged from 1.6% to 26% CV.

Table 17 Estimated parameters for the RBR model; the basic model incorporates data from the static model, the final model incorporates data from the static and dynamic model.

Parameter	Unit	Basic model (static data)		Final model (static + dynamic data)	
		Value	95% CI	Value	95% CI
E_{max}	%	42.274	41.063 - 43.484	42.733	41.408 - 44.058
EC_{50}	µg/mL	1.765	1.621 - 1.909	1.765[*]	
H		6.108	0.452 - 11.765	3.167	2.192 - 4.142
a	h^{-1}	0.321	0.270 - 0.371	0.379	0.339 - 0.420
b	h^{-1}	0.206	0.131 - 0.281	0.042	0.033 - 0.051
z	h^{-1}	0.047	-0.011 - 0.106	0.120	0.059 - 0.181
k_{e0}	h^{-1}	-	-	0.054	0.041 - 0.068

*fixed value

The suitability of the model and the goodness of parameter estimates were evaluated by calculation of AIC and MSC for all data (Table 18). By integration of an effect compartment in the final model, the data from the static (Figure 34) as well as from the dynamic *in vitro* model (Figure 35) were overall well described by the indirect link model.

The final RBR model overestimated the effect of 1 and 4 µg/mL LZD in the static model at late time points, but the effect of the critical concentration of 2 µg/mL (MIC) was well predicted over the whole time. The RBR data from the dynamic model were overall well predicted, although they were lower in number than the data from the static model and thus had less influence on the parameter estimation.

The decrease of RBR under changing LZD concentrations at 24 h was well described by the final RBR model. The similarities in the RBR for different dynamic LZD concentration-time profiles could be explained by examination of the effective LZD concentrations over time (Figure 36). Though the LZD concentrations in the different investigated concentration-time profiles varied strongly in the central compartment, they spread less widely in the effect compartment. Thus, the similar effect site concentrations caused only slightly different RBR over time for the different PK profiles as it was already found in the descriptive RBR analysis

(Figure 30). For LZD in the static model and respective modelled concentrations in the effect compartment consult Appendix, Figure 67. The final RBR model served for the computational simulations (see 3.8.5).

Table 18 Goodness of RBR model estimates.

Parameter	Modified sigmoidal E_{max} model (static data)	Indirect link model (static + dynamic data)
n	906	1324
SSR	14428	27769
AIC	2524	4045
AICc	2524	4045
MSC	3.9051	2.5008
Correlation	0.9916	0.9591
R^2	0.9933	0.9662

n = number of observed medians used for model evaluation, SSR = sum of squared residuals, AIC = Akaike's information criterion, AICc = corrected Akaike's information criterion, MSC = model selection criterion given by Scientist 3.0, R^2 = coefficient of determination.
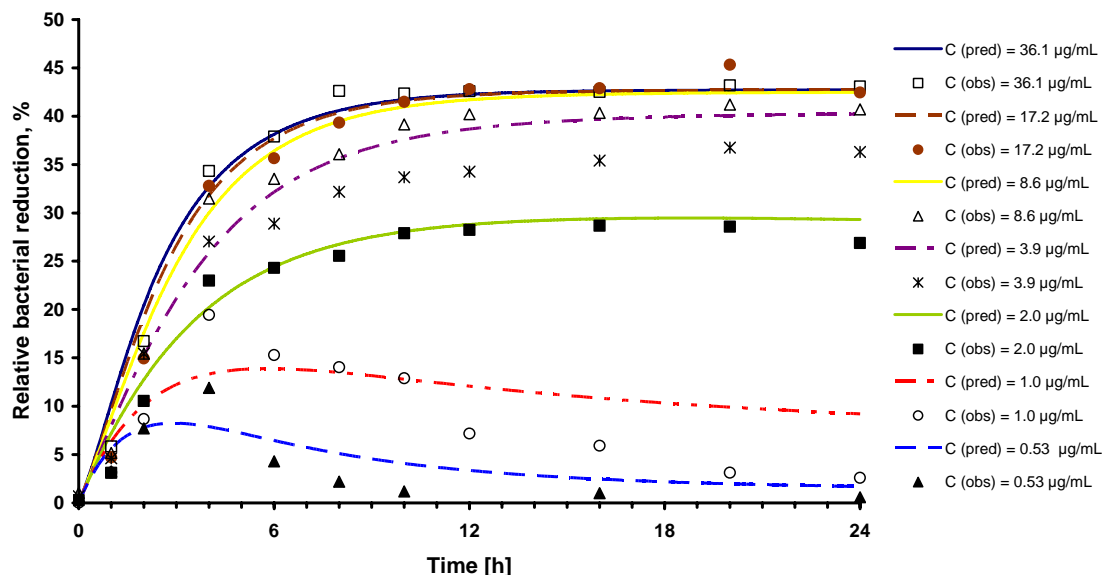
Figure 34 RBR data versus time in the static model, shown are RBR data predicted by the final RBR (indirect link) model for constant LZD concentrations and respective observed median RBR data (from bootstrapped geometric means).
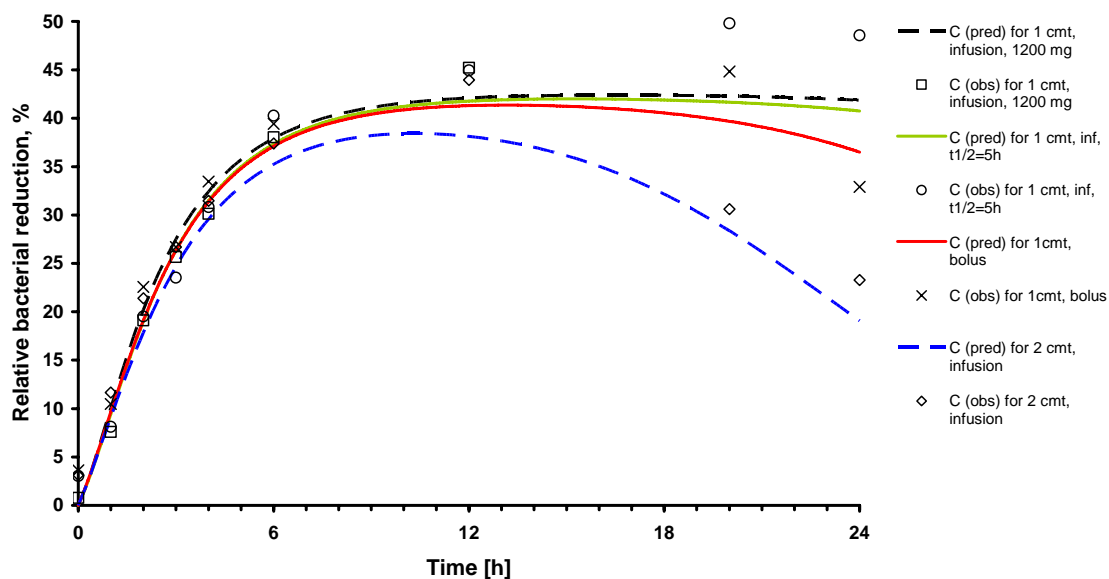
Figure 35 RBR data versus time for the dynamic model, shown are RBR data predicted by the final RBR model (indirect link) for changing LZD concentrations and respective observed median RBR data (calculated from bootstrapped geometric means).
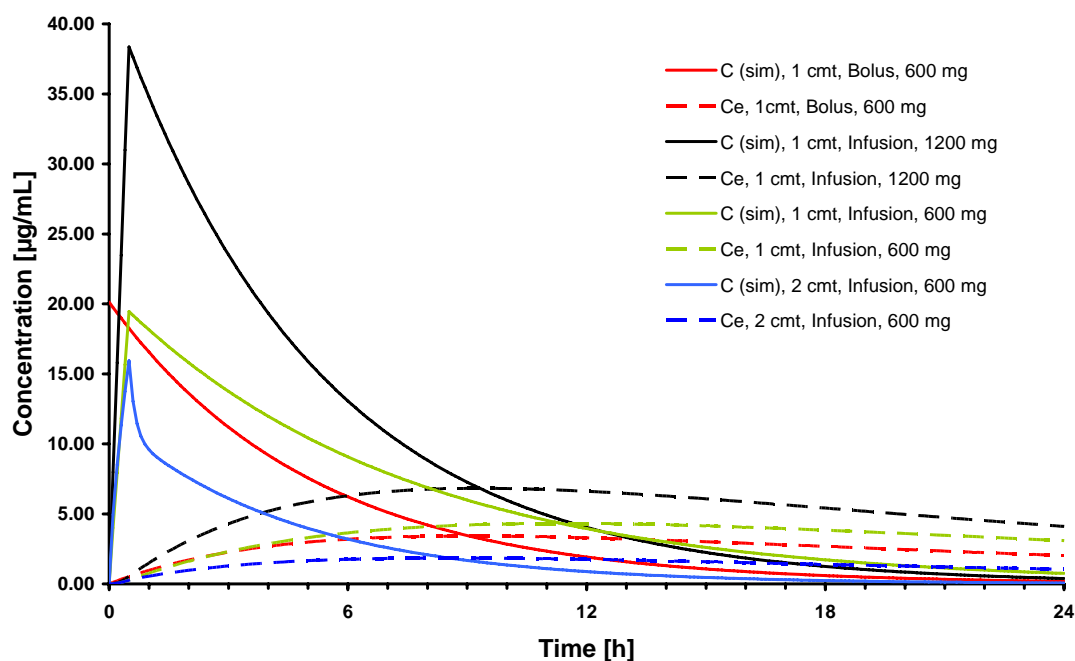
Figure 36 Simulated LZD concentrations in the central (solid lines) and in the effect compartment (dashed lines) under dynamic conditions.

3.8.2.2 Model evaluation

Under consideration of the modelling and evaluation data set, the goodness of fit of the indirect link model and its parameters was determined. Analysis of residuals over LZD concentration, over time and residuals over predicted RBR showed even distribution around zero (see Appendix, Figure 68). Modelling and evaluation data set were distributed in the same extent. The analysis of residuals over observed RBR data showed outliers at low RBR values for the modelling data set and an increase of residuals for high RBR values in the evaluation data set. Thus, some low RBR values in the modelling data set were overestimated and high RBR values of the evaluation data set were underestimated. A detailed analysis showed, that the outliers were mainly RBR data from the dynamic *in vitro* model at maximum drug concentrations. The underestimated RBR values from the evaluation data set were especially high RBR values at the end of observation (20 or 24 h). In both cases this could mean, that the effect of LZD is more strongly delayed than it could be expressed by an effect compartment.

The comparison of model-predicted and observed RBR data, indicated a good prediction of RBR values higher than 10 for the model and the evaluation data set and an acceptable prediction for RBR values lower than 10 (Figure 37). The figure shows also a concentration of points on the axis of observed RBR, where the RBR was predicted with zero. This resulted from the slightly different single bacterial determinations at the beginning of experiments.
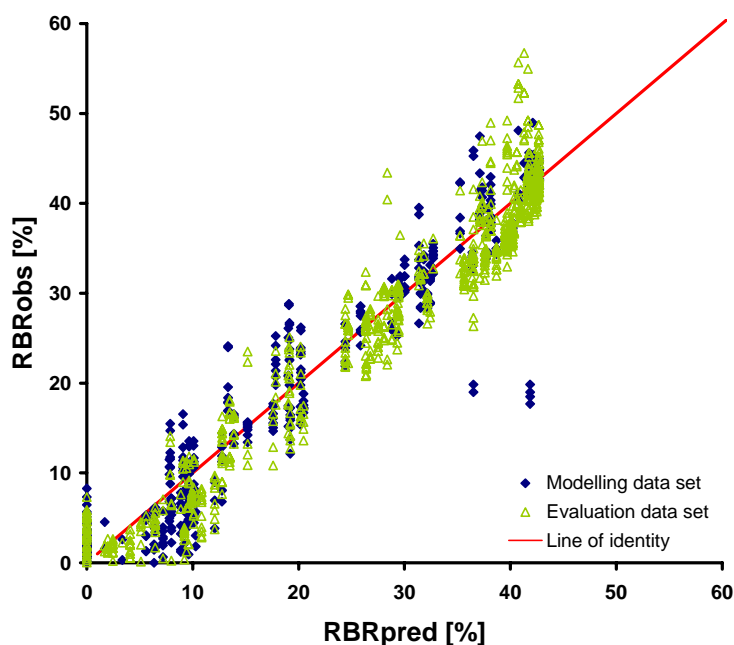
Figure 37 Goodness of fit plot for the final RBR (indirect link) model comparing mean observed with model-predicted RBR values.

The RBR was predicted to be zero, that means no difference in bacterial concentration between growth control and bacteria exposed to drug would appear. Actually, the bacterial concentration varied about 2.7 % at the beginning of experiments (see 3.6.2.2), which led to different RBR by calculation of each bacterial concentration. Altogether, the estimation of the parameters and the suitability of the applied model were accepted.

3.8.3   Time-kill curve modelling

3.8.3.1   Model development

The **basic** time-kill curve model (Eq. 15), which described the **static** *in vitro* data, incorporates a limitation of the bacterial growth with a maximum value GC_{max} (Table 19). An additional term was inserted to account for the limitation of bacterial killing. Different variations of the killing limitation were assessed and the term $\dfrac{N_C(t)}{N_{min} + N_C(t)}$ was most suitable. Therein, N_{min} is the lowest observed bacterial concentration and N_C is the current bacterial concentration at time t. The model also accounted for the delay in killing (dk; see 3.4.2) towards the effect by the term $\left(1 - e^{-dk*t}\right)$.

$$\frac{dN_C}{dt} = \left[k_0 \cdot \left(1 - \frac{N_C}{GC_{max}}\right) - \frac{E_{max} \cdot C(t)}{EC_{50} + C(t)} \cdot \frac{N_C}{N_{min} + N_C} \cdot \left(1 - e^{-dk \cdot t}\right) \right] \cdot N_C$$

Eq. 15 Time-kill curve model.

The addition of a Hill coefficient ($H \neq 1$) on EC_{50} and C did not optimise the fitting to the data. The **final** model describing the **dynamic** bacterial concentrations over time was built up on the basic model. Due to the higher maximal growth of bacteria in the dynamic model (see 3.7), the maximal bacterial concentration GC_{max} had to be adapted for the dynamic data. The maximum effect rate constant E_{max} and the minimum bacterial concentration N_{min} were adopted from the basic model, because they could only be reliably determined in the static model. The bacterial growth rate constant k_0 was the same for static and dynamic data (see 3.7) and therefore adopted. While fitting the model to the data, the delay in kill dk always approximated the same value as in the basic model. So it was finally kept constant, which improved the precision of the other parameters. The basic time-kill curve model describes the observed data well as visible in Figure 38, where the experimentally observed bacterial concentrations from the static experiments were contrasted towards the model-predicted values. Figure 39 shows the model fit

(observed and predicted (simulated) bacterial concentrations over time) for the dynamic experiments, whereby the model predicted values are close to the observed.

Table 19 Estimated model parameters of the basic and final time-kill curve model with 95% confidence interval (95% CI).

Parameters	Unit	Basic model Estimate (95% CI)	Final model Estimate (95% CI)
Deduced parameters*			
GC_{max}	cfu/mL	3.44×10^8	1.62×10^9
N_{min}	cfu/mL	6.50×10^4	
Estimated parameters			
k_0	h^{-1}	1.139 (0.976 – 1.301)	
E_{max}	h^{-1}	2.024 (-8.206 – 12.254)	
EC_{50}	µg/mL	1.553 (-164.530 – 167.640)	0.347 (-0.101 - 0.795)
Dk	h^{-1}	2.067 (-3.123 – 7.258)	

*based on the highest bacterial concentration (geometric mean) of the growth control and on the lowest bacterial concentration (geometric mean) of the bacteria exposed to 36.1 µg/mL LZD
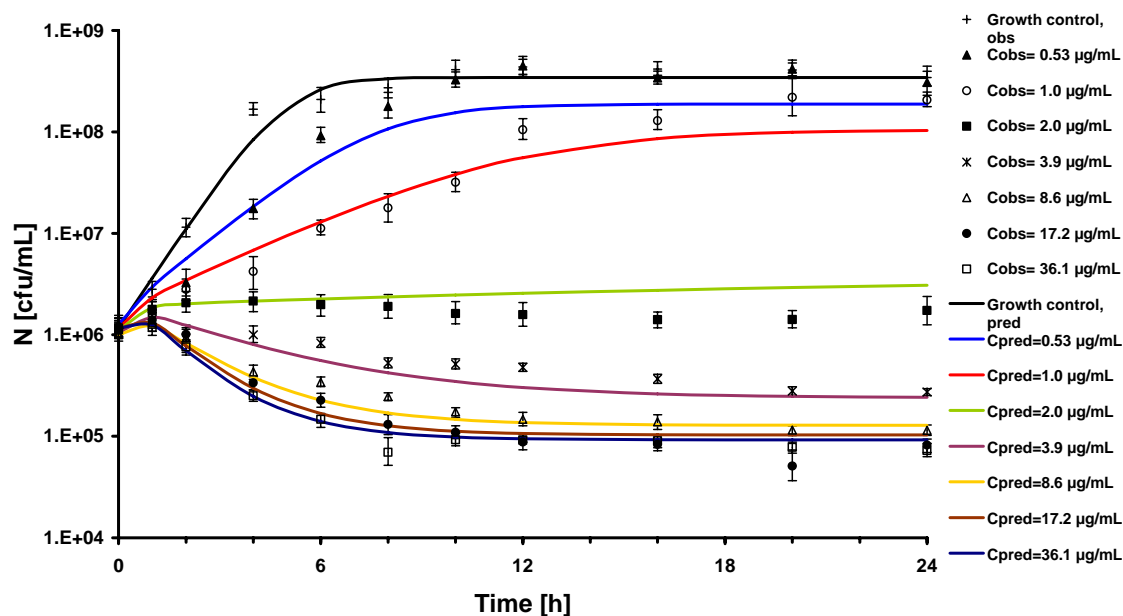
Figure 38 Description of the static *in vitro* data with the basic time-kill curve model; solid lines present the model-predicted curve progression, symbols are geometric means of observed data, error bars are the 95% confidence intervals for observed data.
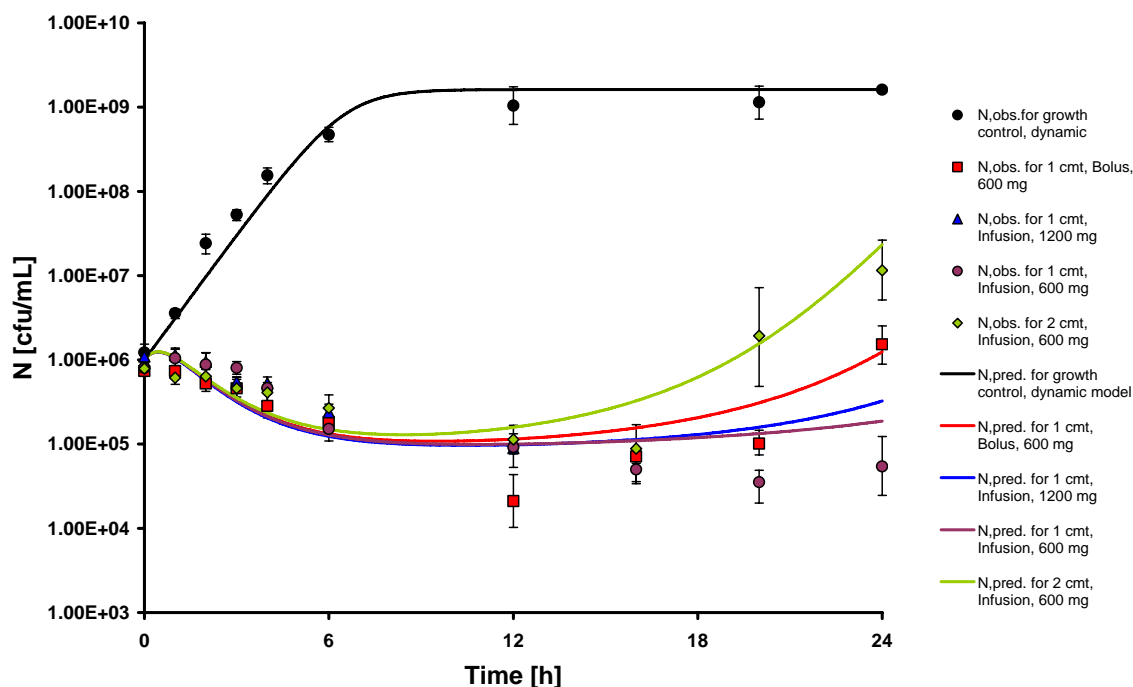
Figure 39 Description of the dynamic *in vitro* data with the final time-kill curve model; solid lines present the model-predicted curve progression, symbols are geometric means of observed data, error bars are 95% confidence intervals for observed data.

Variations in the model structure were made by insertion of a Hill coefficient and/or an effect compartment (see Appendix, Figure 69 and Figure 70).[98] Both terms did not improve the predictions by the model (see Appendix, Figure 71). The insertion of an effect compartment might be mechanistically correct (see also 3.8.2), but in favour of the principle of parsimony disregarded. In summary, the same structural model (Eq. 15) was used to describe static and dynamic data, but different EC_{50} values were estimated.

3.8.3.2   Model evaluation

The basic time-kill curve model was evaluated under use of all geometric mean bacterial concentrations per LZD concentration and time. Figure 40 relates the observed and model-predicted values for the basic model. The formation of groups at low and high bacterial concentrations, below and above the line of identity, respectively, advised further improvements of the model. Despite this, the correlation was high (R=0.9931). Figure 41 relates the values predicted by the final model to the experimentally observed bacterial concentrations. The predictions were randomly scattered around the line of identity. A tendency to overestimate low bacterial concentrations could be assumed by the grouping of data points in the lower left corner. This concerned the bacterial concentrations after 12 h, where the samples of bacterial concentrations were widely scattered, even if they originated from one experiment. A high

correlation was found between observed and predicted values (R = 0.9463). Residuals were calculated as difference between logarithmic observed and logarithmic predicted values (see Appendix, Figure 72). The analysis of residuals over LZD concentrations indicated a low predictability of the model for low LZD concentrations resulting in an underestimation of the effect at late time points. The analysis of residuals over time and the plot of residuals over observed logarithmic bacterial concentrations underlined the underestimation of the effect at 12 h and later times.
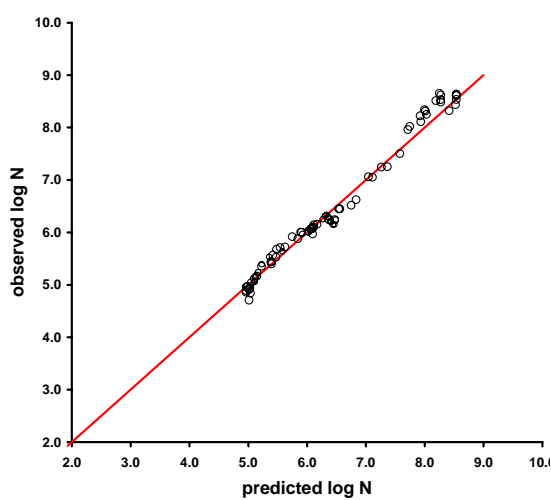
Figure 40 Goodness of fit plot for the basic time-kill-curve model comparing observed geometric means towards predicted logarithmic bacterial concentrations; line of identity in red.
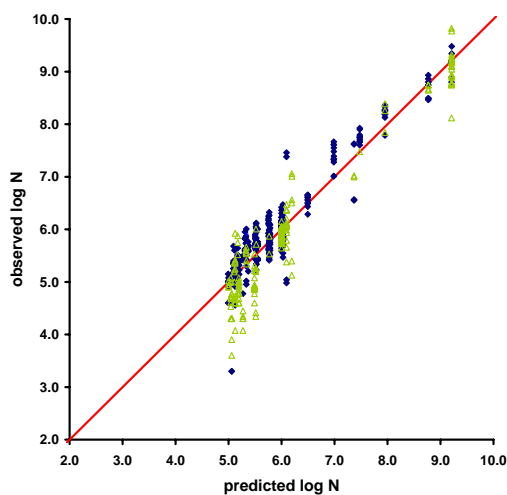
Figure 41 Goodness of fit plot for the final time-kill curve model comparing observed to predicted logarithmic bacterial concentrations; line of identity in red; blue diamonds represent data for modelling, green triangles stand for validation data.

3.8.4   Effect at different time points

The inhibitory effect model with sigmoidal maximum effect was appropriate to describe the observed bacterial concentrations from the static model over time. The model was not applicable to data at 0 and 1 h due to indiscriminate data values (see Appendix, Figure 73). Despite this, the model was regarded as adequate, since deviations of the model predictions for 2-24 h were minor. The model has a high predictability for the data, as seen in Figure 42, where the model-predicted versus observed data and the correlation of observed and predicted values (goodness of fit) for 24 h exemplarily are shown. All other data can be found in the Appendix, Figure 74. The estimated model parameters at time points 2-24 h can be found in Table 20.
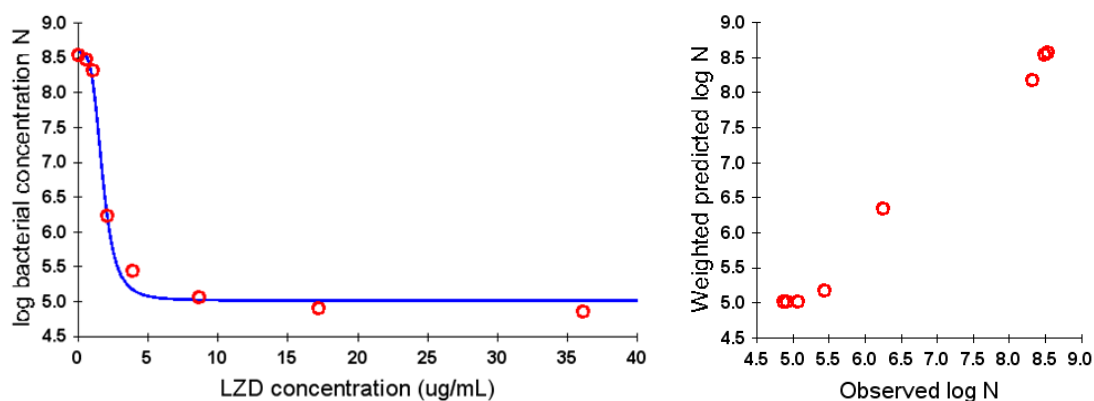
Figure 42 Modelling of the effect at different time points for 24 h, left panel: bacterial concentration versus LZD concentration with model-predicted effect as blue line and observed effect as red circles; right panel: goodness of fit plot for observed versus predicted bacterial concentrations.

After 24 h the bacterial concentrations decreased asymptotically towards 10^5 cfu/mL, while LZD concentrations increased. This was a minimum bacterial concentrations, where bacterial concentrations could not fall below for the investigated LZD exposure (see also N_{min} in time-kill curve modelling; 3.8.3). This would suggest a combination of LZD with other antibiotics to further reduce the bacterial concentration.

The $EC_{I,90}$ was suggested as LZD concentration, which should be at least achieved at steady state, and enable assumptions about steady state efficacy. With progression in time, $EC_{I,90}$ decreased from 10.6 to approximately 3 µg/mL (Table 20). This supported the assumption of time-dependent killing. The convergence at 24 h to 3 µg/mL might be asymptotical, but it could not be concluded, that further increases in effect were impossible. Rather it seemed that the conditions in the static model restrict the bacterial growth at the $EC_{I,90}$ of ~3 µg/mL.

Table 20 Estimated parameters of the inhibitory E_{max} model describing the effect at different time points.

Parameter	Unit	Observation time [h]								
		2	**4**	**6**	**8**	**10**	**12**	**16**	**20**	**24**
N_{max}		7.056	8.230	8.382	8.535	8.721	8.743	8.655	8.676	8.571
$EC_{I,50}$	[µg/mL]	0.797	0.954	1.345	1.509	1.458	1.610	1.622	1.695	1.745
N_0		5.849	5.306	5.268	5.025	5.068	5.060	5.060	4.965	5.009
H		0.848	0.895	1.485	1.641	2.001	2.618	3.070	3.714	3.799
$EC_{I,90}$	[µg/mL]	10.639	11.115	5.910	5.755	4.371	3.727	3.318	3.064	3.110
EC_{inf}	[µg/mL]	*1	*1	0.447	0.637	0.842	1.184	1.301	1.461	1.514

* no inflexion points available

Since sigmoidal curves were mostly seen, the inflexion points of the curves were calculated as characteristic points. At the inflexion point of the effect-drug concentration curve the second derivative (Eq. 16) of the inhibitory effect model was assumed to be zero and solved in Excel via the Solver function. The derivation of this equation can be found in the Appendix, Figure 75. The estimated effect at inflexion point (E_{inf}) was used to calculate the drug concentration (EC_{inf}) at inflexion point by Eq. 9.

$$E_I''(C) = (N_o - N_{max}) \cdot EC_{50}{}^H \cdot H \cdot \frac{(H-1) \cdot C^{H-2} \cdot (C^H + EC_{50}{}^H)^2 - 2H \cdot C^{H-1} \cdot (C^{2H-1} + EC_{50}{}^H \cdot C^{H-1})}{(C^H + EC_{50}{}^H)^4}$$

Eq. 16 Equation for calculation of the inflexion point of the inhibitory effect model.

The inflexion point is a new characteristic concentration (EC_{inf} in Table 20) depending on the time of observation. When the EC_{inf} was exceeded, the effect changed significantly. Concentrations above the inflexion point led to a disproportionately high increase of the effect. The inflexion point could also be seen as breakpoint concentration, where bacterial net growth changes into bacterial net kill. Since growth and kill always appear together, the term "net" describes the dominating process which leads to increase or decrease of the bacterial concentration. Until 12 h the inflexion concentration is relatively low (<1 µg/mL). After 12 h, more than 1 µg/mL would be needed to obtain sufficient bacterial killing. The highest concentration for inflexion (1.5 µg/mL) was reached at 24 h. Thus, concentrations below 1.5 µg/mL led to bacterial growth, concentrations higher than 1.5 µg/mL enabled killing. For dosing LZD every 24 h, at least 1.5 µg/mL LZD would be needed to obtain bacterial killing. The bacterial concentrations corresponding to LZD concentrations at the values of $EC_{I,50}$, $EC_{I,90}$ and EC_{inf} are illustrated in the Appendix, Figure 76.

3.8.5 Simulations

3.8.5.1 Deterministic simulations

Deterministic simulations were carried out with typical patient PK parameters (see Table 4) for 13 dosing regimens and model parameter estimates of the final RBR model (see Table 17). Table 21 shows the maximum obtained plasma ($Cp_{ss,max}$) and effect compartment concentrations ($Ce_{ss,max}$) of LZD at steady state and the resulting maximum ($E_{ss,max}$) and minimum RBR effect ($E_{ss,min}$). The simulated concentration in the effect compartment reached steady state after ~64 h (time to steady state = 5×ln2/k_{e0}; ~2.7 days), which suggests that also the maximum effect could first be reached after this time. All dosing regimens led to relatively constant drug effects, despite fluctuating concentrations in the effect compartment (see Appendix, Figure 77). Only

the dosing of 600 mg once a day (1x 600 mg) led to high fluctuations of the effect, which would be inappropriate for therapeutic use. As effect related parameter, the area under the effect-time curve over 14 days was calculated ($AUC_{E(14\ days)}$).

Table 21 Overview on determined effects and concentrations by simulation of various dosing regimens for a typical patient; standard dosing is underlined in grey.

Daily dose [mg/day]	Dosing regimen	$Cp_{ss,max}$ [µg/mL]	$Ce_{ss,max}$ [µg/mL]	$E_{ss,max}$ %	$E_{ss,min}$ %	$AUC_{E(14\ days)}$ [%*h]
600	1× 600 mg	16.84	3.59	37.7	26.1	11615
1200	1× 1200 mg	27.16	7.13	42.2	40.0	13863
1200	2× 600 mg	18.38	6.35	42.0	41.5	13910
1200	3× 400 mg	14.94	5.97	41.9	41.6	13859
1200	4× 300 mg	13.96	6.31	42.0	41.9	13911
1800	1× 1800 mg	36.50	10.66	42.6	42.0	14130
1800	2× 900 mg	24.41	9.45	42.5	42.4	14137
1800	3× 600 mg	20.63	9.29	42.5	42.5	14130
1800	4× 450 mg	18.44	9.10	42.5	42.5	14117
2400	1× 2400 mg	45.09	14.19	42.7	42.4	14193
2400	2× 1200 mg	30.08	12.56	42.7	42.6	14193
2400	3× 800 mg	24.92	12.01	42.6	42.6	14182
2400	4× 600 mg	23.14	12.29	42.6	42.6	14184

3.8.5.2 Stochastic simulations

Stochastic simulations were based on CL, V2 and V3 values with inter-individual disposition derived from the population PK model.[32] The simulated PK parameter values were normally distributed and comparable for all simulated dosing regimens (see Appendix, Figure 78).

Figure 43 shows the location and distribution of AUC_E for each dosing regimen over a 14 days therapy of LZD. The administration of 600 mg once a day (green box) had the widest distribution of effect in the population. For all dosing regimens within the same DD, the location of AUC_E was relatively similar (red, blue and black boxes, respectively).

The distribution of the AUC_E decreased with increasing daily dose, thus the effect for each patient in the population became virtually identical and the influence of inter-individual PK parameters decreased. A maximum AUC_E would be reached with the suggested dosing regimens. The analysis of the differences in effect size between the different DDs showed, that the effect of 1800 mg LZD per day was similar to the effect of 2400 mg LZD per day (Figure 44). So, achieving the maximum effect was possible with 1800 mg LZD per day.
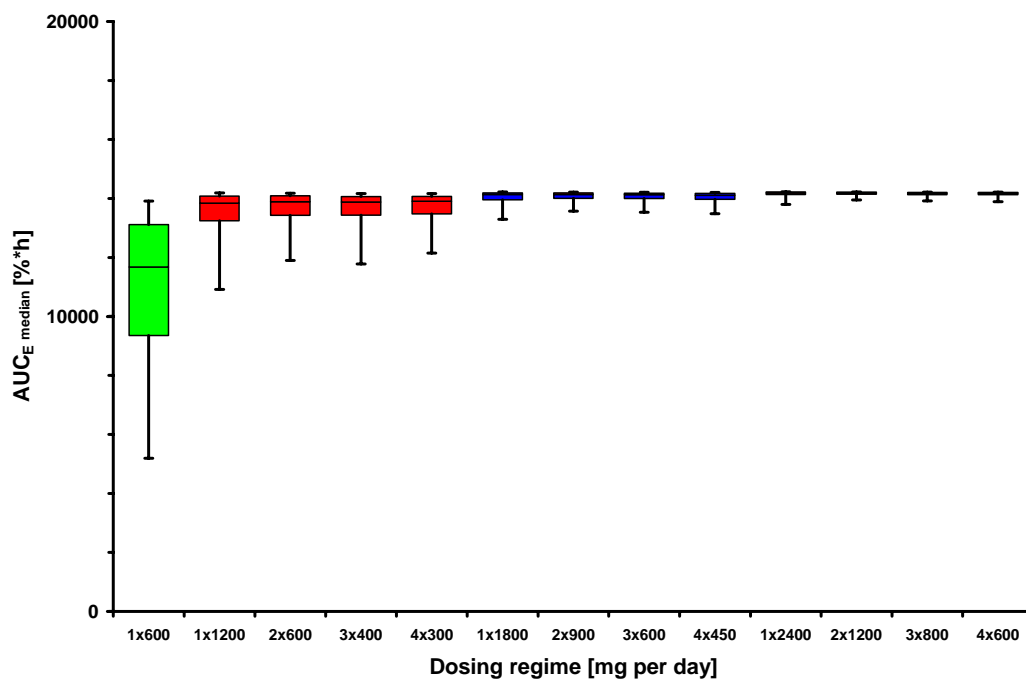
Figure 43 Median AUC$_E$ values of various dosing regimens simulated for 1000 in silico patients with population estimates of CL, V2 and V3 and their respective IIV; boxes present 25th to 75th percentiles, horizontal lines show medians, error bars indicate the respective 5th and 95th percentile.
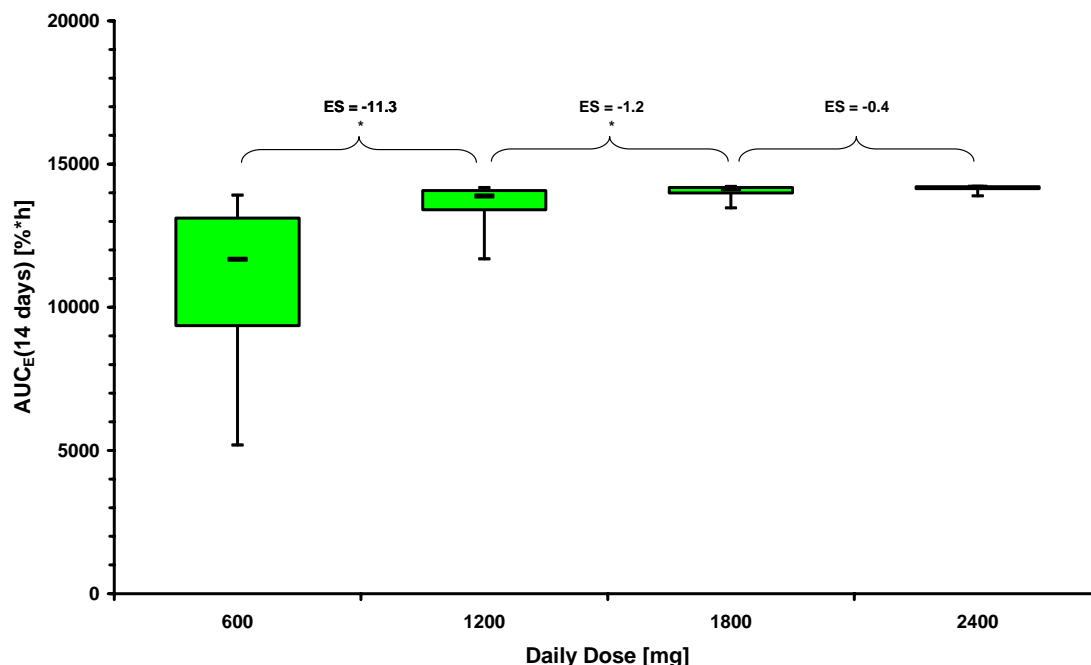
Figure 44 Median AUC$_E$ values per daily dose of LZD; differences are indicated by the effect size (ES), which might be considered significant (*) or not. Boxes present the 25th to 75th percentiles of distribution, horizontal lines show medians, error bars indicate the 5th and 95th percentiles.

The results advise that even 1200 mg LZD per day might be sufficient to reach the maximum effect. The effect of 1200 mg per day seemed to be comparable to the effect of 1800 mg per day, but due to higher variability in the concentration in the effect compartment, the effect size was slightly different. A marginal pharmacodynamic difference between the effects of 1200 and 1800 mg LZD per day exists. The difference between AUC_E values might be due to different distributions; the distribution of AUC_E for 1200 mg DD was wider, thus not all patients achieve the maximum effect of LZD. The closer distribution of AUC_E for 1800 mg per day, suggested that a therapy with 1800 mg per day would bring more patients to the maximum effect and thus probably to cure. Concerning the pharmacokinetics, the different daily doses led to high differences in maximal plasma concentrations and thus in tolerance and adverse drug effects (see 1.3). So the safety of LZD administration should determine the splitting of the daily dose, i.e. dosing interval.

The relationship between stochastically simulated $AUC_{E(14\ days)}$ values and the daily doses could be expressed by a sigmoidal E_{max} model (Eq. 17), where $AUC_{E,max}$ is the maximum reachable area under the effect time curve over 14 days, DD is the daily dose, H is the Hill coefficient and DD_{50} is the daily dose producing the half maximum $AUC_{E(14\ days)}$.

$$AUC_{E(14days)} = \frac{AUC_{E,\max} \cdot DD^H}{DD_{50}{}^H + DD^H}$$

Eq. 17 Sigmoidal E_{max} model to describe the relationship between $AUC_{E(14\ days)}$ and daily dose (DD).

The model described the simulated $AUC_{E(14\ days)}$ corresponding to the DD with a high correlation (R = 0.9999). Figure 45 shows the model-predicted median of $AUC_{E(14\ days)}$ as well as its 90% distribution interval. The calculated model parameters can be found in Table 22.

Table 22 Parameters describing the relationship between AUC_E and daily dose.

Parameter	Unit	5th percentile	Median	95th percentile
$AUC_{E,max}$	[%*h]	14314	14228	14234
H		2.980	3.152	2.509
DD_{50}	[mg]	725	374	133

The maximum reachable $AUC_{E(14\ days)}$ values were comparable for the median, upper and lower $AUC_{E(14\ days)}$-DD curves. The Hill coefficient indicated the steepest curve slope for the median $AUC_{E(14\ days)}$-DD course (H = 3.152), but in total the coefficients were comparable. The main differences in curve shapes result from different doses provoking the half-maximum effect (DD_{50}). For an $AUC_{E(14\ days)}$ at the upper range of the distribution (95th percentile), a DD of

133 mg would be sufficient to reach the half-maximum effect, whereas at the lower $AUC_{E(14\ days)}$ limit 725 mg DD would be needed. Using the model, every daily dose of interest can be analysed on its efficacy ($AUC_{E(14days)}$). So the dose, which is needed to reach 90% of the maximum effect (median $AUC_{E(14days)}$) over 14 days (DD_{90}) was calculated as 750 mg. This suggests a sufficient effect by 750 mg LZD per day in patients with population PK parameters, whereby this DD was also linked with a wide distribution of $AUC_{E(14days)}$ values (different effect size). The model-predicted plasma and effect compartment concentration-time profiles for 750 mg DD as well as the corresponding RBR-time profiles are demonstrated in Figure 46 with regard to the standard dosing regimen, both for a typical patient.
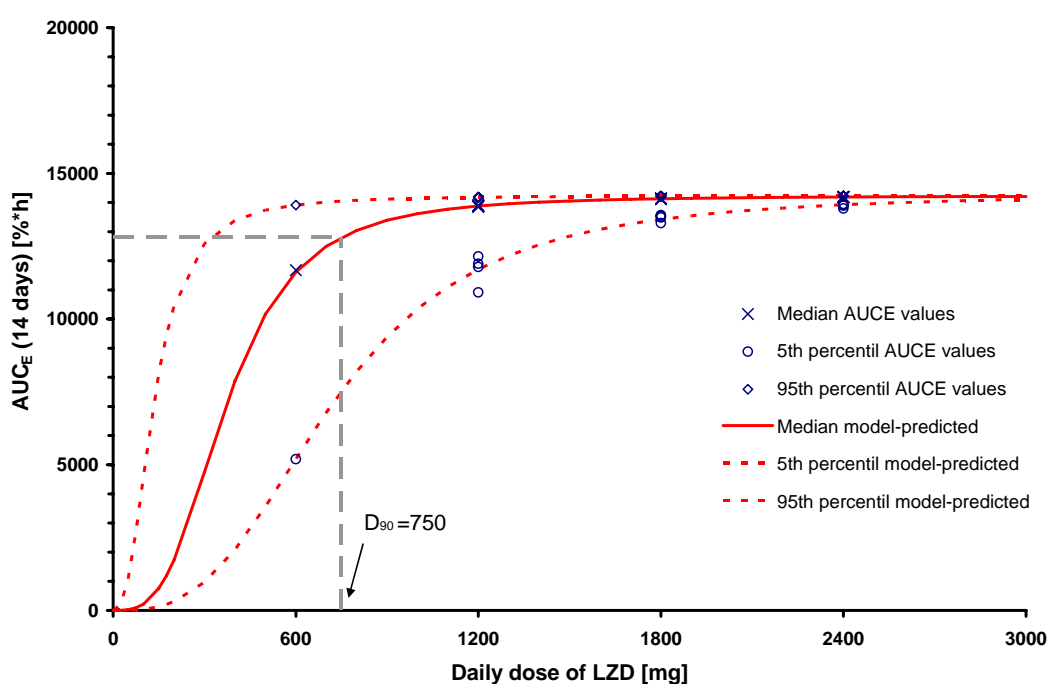
Figure 45 Relationship between AUC_E and daily dose of LZD correlated to a sigmoidal E_{max} model; the arrow indicates the necessary dose to reach 90% of the maximum AUC_E.
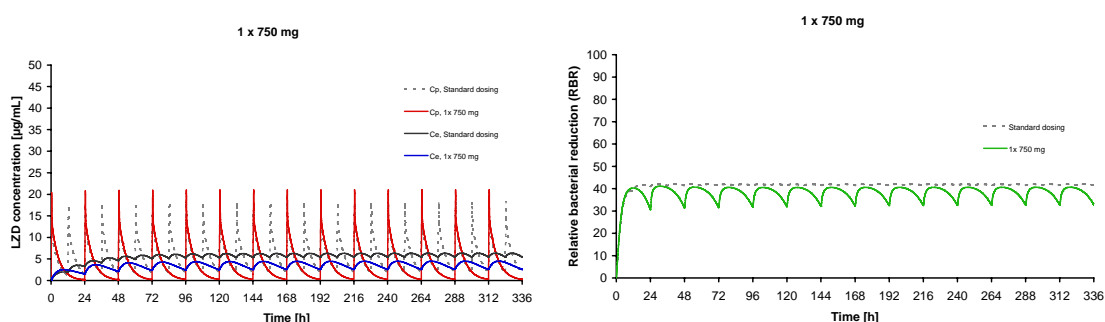
Figure 46 Concentration-time profiles of 1x 750 mg in plasma and effect compartment (left panel) and the corresponding effect (right panel); both compared to the standard dosing of 2x 600 mg.

3.8.5.3   Simulation of worst-case patients and their dosing optimisation

The following simulations should predict the therapeutic efficacy of LZD against a VRE infection for a patient with worst physiological and PK conditions resulting in the worst assumable antibiotic effect. Four different cases of worst-case PK were identified; a high drug clearance (CL=21.9 L/h) always resulted in worst-case conditions, whereas the size of the volume of distribution in the central and peripheral compartment did not influence the result (V2=10.3 or 38.1 L, V3=16.6 L or 50.2 L). Table 23 summarises the PK parameters for simulations of worst-cases and the respective obtained concentrations and PD effects after standard therapy (2x 600 mg). The LZD concentrations in plasma and in the effect compartment for case 2 are exemplarily presented in Figure 47. The drug concentrations in plasma were much higher than for the typical patient, which would probably lead *in vivo* to adverse drug effects. In contrast, the LZD concentrations in the effect compartment achieved only about half of the concentration of a typical patient, because of the fast fluctuations of concentrations in plasma. The cases 1, 3 and 4 can be found in the Appendix, Figure 79 and Table 47.

Table 23 PK parameters for simulations of worst-case patients and the respective LZD concentrations and PD effects after standard therapy.

Parameter	Typical patient	Case 1	Case 2	Case 3	Case 4
Simulated PK parameters					
CL [L/h]	11.1	21.9	21.9	21.9	21.9
V2 [L]	20.0	38.1	10.3	38.1	10.3
V3 [L]	28.9	16.6	16.6	50.2	50.2
Obtained LZD concentration					
$C_{p,max}$ [µg/mL]	18.38	11.83	22.83	11.06	17.47
$C_{e,max}$ [µg/mL]	6.35	3.31	3.48	3.21	3.27
Obtained PD parameters					
$AUC_{E,max}/AUC_{E,max\ (typical)}$, %	100	84	83	84	84
$E_{(ss,\ max)}$, %	42.0	37.6	38.3	37.1	37.4
$E_{(ss,\ min)}$, %	41.5	32.7	30.8	33.8	32.9

The effect of antibacterial standard therapy expressed as RBR was clearly lower for all worst-cases than for a typical patient. The high concentration fluctuation influenced also the effect, which fluctuated stronger than in the typical patient. The steady state of the effect was reached after 24 h. The area under the effect-time curve was only 83% of the possible maximum area for a typical patient. This means, in a worst-case situation such as the simulated one, the patient would not achieve the maximum therapeutic efficacy, and so the bacteriostatic effect of LZD on VRE could not be guaranteed.
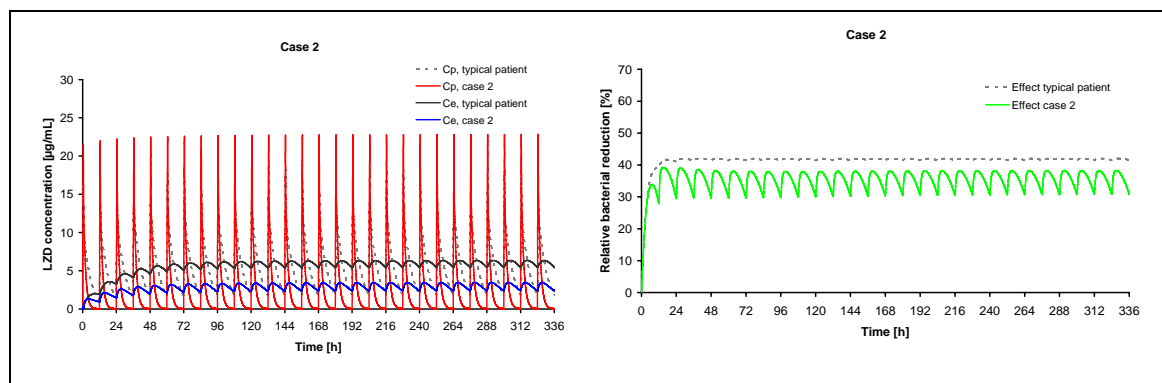
Figure 47 Simulation of the efficacy of standard LZD therapy against VRE for a worst-case patient (case 2) compared to the typical patient receiving standard therapy; LZD concentrations in the central and effect compartment are shown on the left, the resulting effect-time course is revealed on the right side.

Based on the stochastic simulations, 1800 mg DD were taken as basis for the dosing optimisation. Dosing regimens of 1x 1800 mg, 2x 900 mg, 3x 600 mg and 4x 450 mg administered over 14 days were investigated on their suitability. Table 24 presents characteristic parameters of these dosing regimens, which are the maximum plasma ($C_{p,\,max}$) and effect compartmental concentrations ($C_{e,\,max}$), the ratio of the area under the effect-time curve between worst-case and typical patient ($AUC_{E,max}/AUC_{E,max\,(typical)}$) and the maximum ($E_{max,\,ss}$) and minimum effects at steady state ($E_{min,\,ss}$). Figure 48 illustrates the modified concentration-time course of plasma and effect compartment on the left side and the resulting effect time course on the right side. For a better comparison, the diagrams include the time-courses for the standard dosing regimen of case 2. Table 24 and Figure 48 underline the increase of the relative bacterial reduction – the effect – by an enhanced daily dose of 1800 mg. Minimum and maximum effects at steady state were increased towards standard dosing (2x 600 mg) of the worst-case patient (case 2). By enhancing the daily dose to 1800 mg more than 90% of the AUC_E at steady state (as observed for typical patients) can be reached by the worst-case patient.

The dosing of 1x 1800 mg showed 92% of the maximum AUC_E, whereas for 2x 900 mg, 3x 600 mg and 4x 450 mg the AUC_E increased to 95% and the effect varied only marginally between these dosing regimens. This means also, that a splitting of the daily dose in several single doses is superior to a once-a-day administration, but a portioning on more two doses does not necessarily increase the effect. Furthermore, 1x 1800 mg led to high LZD concentrations in plasma, whereas the concentrations were decreased with the higher frequency of administration. The dose optimisation for case 1, 3 and 4 is shown in the Appendix, Figure 80, Figure 81 and Figure 82.
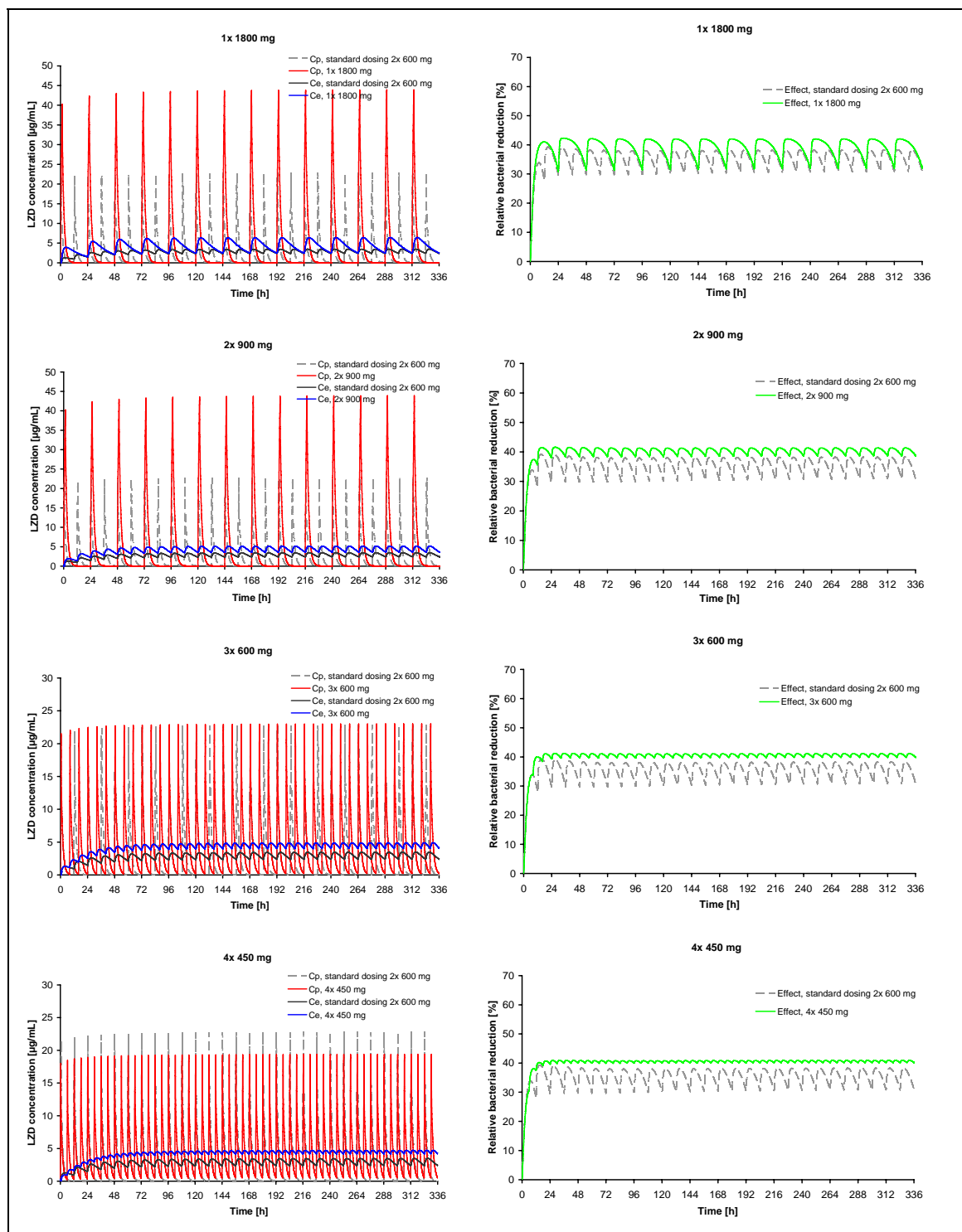
Figure 48 Simulations of plasma and effect concentrations (left) and the resulting effect (right) of the worst-case patient (case 2) after increase of DD to 1800mg, administered in different dosing regimens. The graphs are compared to standard dosing regimen.

Table 24 Overview on obtained effects by simulated dosing optimisation for case 1; the standard dosing is underlined in grey.

Dosing regimen	$C_{p, max}$ [µg/mL]	$C_{e, max}$ [µg/mL]	$AUC_{E,max}/AUC_{E,max\ (typical)}$, %	$E_{max, ss}$, %	$E_{min, ss}$, %
2x 600 mg	22.831	3.481	83	38.3	30.8
1x 1800 mg	43.922	6.447	92	41.0	32.0
2x 900 mg	29.340	5.195	95	41.4	38.6
3x 600 mg	23.016	4.911	95	41.1	39.8
4x 450 mg	19.380	4.722	95	40.9	40.1

4 Discussion

4.1 Preliminary microbiological investigations

Several preliminary investigations for microbiological experiments were necessary, to ensure stable conditions during the *in vitro* experiments and facilitate standard procedures. The dilution and centrifugation procedure for bacteria purification were adapted from a previous work.[100] The procedures led to equivalent results for *E. faecium* as previously also described for *S. aureus*.[100] The three investigated dilution media (NaCl 0.45%, NaCl 0.9% and PBSP) have different properties regarding the bacterial separation, but would all be suitable for the preparation of *E. faecium* over 60 min. A slight difference was seen for *S. aureus*. The strain seemed to be more sensitive to the kind of dilution media concerning the viability over 60 min, stable results could be only obtained with PBSP.[100] The bacteria specific methods, which were inoculum preparation and digital colony counting, brought different or new results and will be discussed more detailed in the following.

The preparation of the start inoculum is generally carried out by tenfold dilution of a bacterial suspension with McFarland index 0.5, because an initial bacterial concentration of 10^8 cfu/mL is mostly assumed to correspond to this index.[25, 120-123] Since different strains vary in their optical density,[84] the dilution of the initial bacterial suspension was adapted in this work to ensure constant procedures. A McFarland index of 0.5 was provoked by an *E. faecium* concentration of 2×10^6 cfu/mL and not by 10^8 cfu/mL. More attention to the inoculum preparation of the investigated strains is therefore recommended, to ensure the comparability of experiments.

In the present work, the growth of bacteria was detected by viable cell counting, which is relatively laborious, but still presents the gold standard of bacterial quantification. It has two advantages: Firstly, only living cells are detected, dead bacterial cells do not affect the result. Secondly, phenotypic changes due to drug exposure can be detected.[40, 102] Digital automated colony counters have been sparsely used yet for viable cell counting; manual counting is still the typical way of analysis, which might be due to the low investment costs. The quality of digital viable cell counting depends on the method of plating (spread plate (see 2.7.3),[124] spiral plate[125] or droplet plate method,[124, 126]), the arrangement of bacteria (single cocci, diplococci or streptococci)[126, 127] and of the system of reading (photographical analysis or laser scanning[128]). For a laser colony scanner, a difference of one logarithmic cycle was found for the normal spread plating and spiral plating methods (10^6 cfu/mL ± 10^5 cfu/mL) compared towards manual reading.[128] This error is much higher than achieved with the present dilution and consecutive spread plating method (10^6 cfu/mL ± 10^2 cfu/mL). Sharpe et al. developed a counting method for *S. aureus* on a standard agar, whereupon a good contrast between bacteria and agar existed, but also some very small colonies appeared.[127] Those conditions, and so also

the qualification, were comparable to the results of the present work. In this work, the bacteria could be counted with 0.6% CV imprecision and 9% RE inaccuracy towards manual counting in the same range of bacterial concentration (intermediate).The imprecision of the method by Sharpe was at 1.5% CV, the inaccuracy compared to manual counting was 2.5% RE. Thus, the methods for bacterial quantification found in this work were less accurate than in the comparable method[127], but even more suitable for the digital analysis of viable cells than others[128].

4.2 Comparison of *in vitro* models

The use of different *in vitro* models in this work and in the literature led to the question of the comparability of the obtained results. Therefore, the growth controls of the static, a semi-dynamic[111] and the dynamic *in vitro* model were compared. Obvious differences were the exchange of medium in the semi-dynamic and dynamic models and no exchange in the static model, and the size of the culture vessel, which was 20 mL in the static and semi-dynamic versus 100 mL the dynamic model. The supply of bacteria with fresh nutrition and the evacuation of toxic metabolites, led to higher bacterial concentrations in the dynamic model.[58, 61, 102] Nevertheless, the maximum growth was reached at the same time as in the static model (compare 3.7, Figure 33). The space in the semi-dynamic model was the same as in the static model (V = 20 mL), but bacteria in the semi-dynamic model were exposed to fresh medium (nutrition) and toxic metabolites were removed. Thus, they could continue growing. This emphasises that bacterial growth is limited by nutrition and toxic metabolites.[61, 129] The high difference of one decimal power of the maximum bacterial concentration between static and dynamic and a half decimal power between semi-dynamic and dynamic *in vitro* model might be explained by nutrition and metabolites. The space might be less important, since the initial bacterial concentrations were comparable. The difference between maximum bacterial growth in the semi-dynamic and dynamic model could be caused by omitting medium exchange in the semi-dynamic model after 12 h. Thus,changing the experimental setting in composition and the supply of nutrition[58, 61, 102] as well as removal of metabolites might lead to different results.

Concerning the bacterial concentration-time course under LZD exposure in the semi-dynamic and the dynamic *in vitro* model, a similar time course until 12 h appeared (Figure 49). The bacterial killing under two-compartmental LZD kinetics with 30 minutes infusion and a maximum LZD concentration of ~15 µg/mL (see Appendix, Figure 83) was investigated in the semi-dynamic and the dynamic *in vitro* model. The exchange of medium happened continuously in the dynamic model and in uniform intervals of 15 min in the semi-dynamic model. Despite the slightly different initial bacterial inoculum, the same bacterial concentration time course appeared until 12 h (after experimental start). Afterwards the LZD concentration was kept

constant in the semi-dynamic model, which led to different final LZD concentrations and thus also to different bacterial concentrations.

In summary, the results from the dynamic model were confirmed by those from the semi-dynamic model. The models were comparable and could be regarded as interchangeable. The influence of fresh nutrition and removal of metabolites suggests, that static and dynamic models are not comparable. By this reason, extrapolation from results determined under static conditions to *in vitro* dynamic conditions should only be carried out with caution.
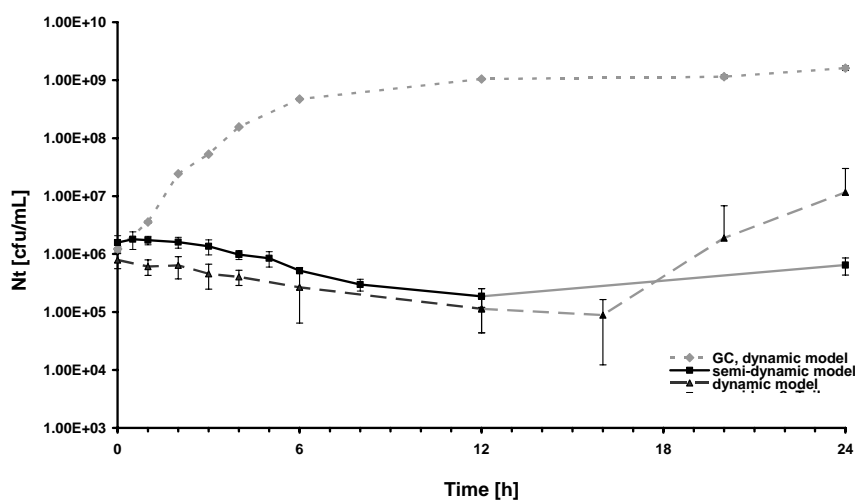
Figure 49 Bacterial concentration-time course derived with imitation of a two-compartmental model with $C_{max}=15\mu g/mL$ in the dynamic *in vitro* (dashed line) and a semi-dynamic[111] (solid line) model; the growth control (GC) was taken from the dynamic model.

4.3   Enterococcus faecium under constant linezolid concentrations

Although LZD is a valuable antibiotic against VRE infections, it had so far not systematically been investigated in time-kill studies. In the present work a commercially available *Enterococcus faecium* strain with vancomycin resistance was studied at close time intervals under a wide range of constant LZD concentrations (0.53 – 36.1 μg/mL). The experimental conduction led to precise and reliable results.[126] The examined bacterial strain had formerly been investigated on its MIC[130] and in dynamic studies[35]. Studies with other VRE strains investigated only one to three LZD concentrations and used only a few observations of the bacterial growth (3-6 observation points) to generate time kill curves (Table 25).

The growth control of *E. faecium* of this work was in good accordance with those of other studies.[131, 132] The same maximal bacterial concentration of $\sim 8\times 10^8$ cfu/mL was reached in other studies, although they used different *E. faecium* strains and a slightly different experimental

setting (use of microtiter plates[131]) from the present work. So, comparable conditions, also for experiments with LZD, should be expected. In the present work, 8 µg/mL LZD reduced the bacterial concentration over 24 h about 0.9 $\log_{10}$ units (see Table 10). The extent of the LZD effect in the present work is confirmed by others,[131-133] where bacterial concentrations under 8 µg/mL declined slower than in the present work, but reached the same final value of 10^5 cfu/mL after 24 h. Investigations with 8 µg/mL LZD by Zurenko et al. found a maxium bacterial reduction of 0.2 - 0.6 $\log_{10}$ units.[25] Also the time-kill assays performed by Wise et al. found lower LZD effects.[134] A possible reason for the discrepancy might be due to the higher start inoculum in the studies by Zurenko et al.[25] and Wise et al.[134], which determines the antibacterial activity of a drug.[135, 136] Higher start inocula lead to lower antibiotic effects regarding bacterial concentrations. The findings by Jones et al. for 4 µg/mL were in accordance with the present work.[137] They found only a minor change in the bacterial concentration of 0.3 $\log_{10}$ units after 24 h (present work ~0.6 $\log_{10}$ units).

Table 25 Studies on the *in vitro* activity of constant LZD concentrations on VRE.

Study	Strain	LZD concentrations	Observation time points	Start inoculum
Present study	ATCC 700221	0.53, 1, 2, 3.9, 8.6, 17.2, 36.1 µg/mL	10 (0, 2, 4, 6, 8, 10, 12, 16, 20, 24 h)	10^6 cfu/mL
Bostic [133]	69 clinical isolates of *E. faecium*	4, 8, 16 µg/mL	5 (0, 3, 4, 5, 24 h)	10^6 cfu/mL
Jones [137]	15 clinical isolates of *E. faecium*	4 µg/mL	4 (0, 6, 24 h)	10^6 cfu/mL
McKay [131]	ATCC 51559	8 µg/mL	6 (0, 1, 3, 6, 10, 24 h)	10^6 cfu/mL
Rybak [132]	R20	8 µg/mL	5 (0, 2, 4, 8, 24 h)	10^6 cfu/mL
Wise [134]	50 clinical isolates of *E. faecium*	2 and 10 µg/mL	5 (0, 2, 4, 6, 24 h)	10^8 cfu/mL
Zurenko [25]	UC 12712	8 µg/mL	3 (0, 6, 24 h)	10^6-10^7 cfu/mL

Figure 12 and Figure 14 (see 3.4.2 and 3.4.3) show a decline of the bacterial concentrations (killing) in two steps. The cause of this behaviour might be attributed to the growth phase of the bacteria. Only growing bacteria (log phase) can be influenced by LZD,[138] which leads to a rapid bacterial killing at the beginning (0-6 h). In contrast, in persisting bacteria the protein biosynthesis is reduced and as a consequence not affected by the drug (lag phase). When the persisters change to normally growing organisms again, they could be killed by LZD and the determined bacterial killing is slower. The appearance of small colony variants might support this assumption: SCV might be part of the persisting subpopulation, not affected by the drug, but when more suitable growing conditions such as on a drug-free agar appear, SCV adapt their

growth (to normal growth) again. Generally, the phenotypic switch was probably formed due to stress (drug exposure), but SCV were still sensitive to the antibiotic after regrowth.[61, 118, 139]

Comparing the present time-kill curves for VRE treated with constant LZD concentrations with those of *S. aureus* (same conduction),[100] it becomes obvious, that LZD does not achieve the same high extent of killing for VRE. This means although the strains have the same MIC,[18] LZD does not execute the same killing behaviour on them. The slope of bacterial decline, the maximum effect and the time to the maximum effect vary between the strain (Table 26).[100] Killing as well as growing of *E. faecium* are slower and less extensive than for *S. aureus*. The shallow slope of the killing curve of *E. faecium* and the lower maximum effect result in different shapes of the killing curves and mean an unequal effect of LZD (bacteriostatic and bactericidal, respectively) on *E. faecium* and *S. aureus*.[140] This strain dependent effect was also described in the literature.[25]

In the static *in vitro* model, LZD concentrations of 2-4 µg/mL have been bacteriostatic on VRE. This is equivalent to the visually determined MIC, which was determined with 2 or 4 µg/mL LZD depending on the time of reading (18 or 24 h, respectively). Other studies found congruent results for VRE strains.[25, 131, 132, 134, 137, 138] The investigated conditions of constant drug concentrations are comparable to a continuous infusion *in vivo*. The results would suggest a LZD concentration of 2-4 µg/mL to obtain a bacteriostatic effect and therewith a successful treatment. The highest change of the effect size was found for LZD concentrations between 1 and 1.5 µg/mL, which is confirmed by others.[35] The depletion of nutrition and lower growth *in vivo* resulting in lower susceptibility were not considered here, chapters 4.2 and 4.4 will elucidate this aspect.

Table 26 Comparison of the bacterial concentration-time course of *E. faecium* and *S. aureus* in the static *in vitro* model. Data of *S. aureus* from Scheerans[100].

Attribute	*E. faecium*	*S. aureus*
Slope of growth curve	0.5 lg(cfu/mL) /h	0.6 lg(cfu/mL) /h
Maximum growth*	3×10^8 cfu/mL	1×10^{10} cfu/mL
Time to maximum growth	12 h	10 h
Slope of max. killing curve	-0.2 lg(cfu/mL) /h	-0.6 lg(cfu/mL) /h
Maximum effect**	1.3 lg(cfu/mL)	3.5 lg(cfu/mL)
Time to maximum effect	8 h	24 h

*start inoculum: 10^6 cfu/mL; **log(start inoculum)-log(lowest bacterial concentration)

4.4   Development of the dynamic *in vitro* model of infection

A dynamic *in vitro* model was successfully developed and used for first investigations within this thesis. The conception of the dynamic *in vitro* model was based on the models by Löwdin et al.[106] and Barger et al.[119], whereupon for model 1 even the model body was captured from these prior studies. During first experiments model 1 showed static instability and tilted to turn over. The experiments should be composed in triplicate (3 culture vessels) with a growth control (+1 culture vessel), but the required equipment, especially the tubes for the thermostat and the medium, became too space intensive. The main improvement of model 2 compared to model 1 were the four culture vessels in one metal heating block. Due to this, the model body was more stable and the tubes were reduced to the medium transporting tube only. The glass vessel was no longer fixed, but consisted of single parts, which were assembled to one vessel. Thereby it was more laborious to build up, but much easier to clean and sterilise and so the risk of contamination declined.

The blockage of the membrane filter was one problem of former dynamic *in vitro* models, which should be overcome. During 24 h experiments, the membrane filter was not blocked by *E. faecium*, which is an advantage in comparison to other models and strains.[70, 81] Presumably the magnetic stirrer carried out the function of cleaning. This way of cleaning is possibly not sufficient for long-term experiments (> 48 h), and suitable prefilters or changeable syringe filters should be tested. Prefilters or syringe filters with other materials and following other properties and bacterial adherence, than the here investigated, could help. In some experiments quick membrane blockage (<6 h) occurred due to an external contamination with a bacillus strain. In the following the medium increased in the culture vessels until the filling level caught the inlet tube. This led to bacterial backgrowth into the reservoir and thus abandoned the experiments. Bacterial backgrowth was not observed in other cases, for this purpose high attention should be given to the material and personal hygiene. Furthermore, the pumping of very low flow rates might also be a reason for bacterial backgrowth.

The pumps of the final dynamic model were also challenging. They should operate with four tubes each, but calibration can only be carried out for one tube. Thus, tubes have to have the same abrasion and service life to carry equal volumes. Otherwise the variation in transported medium increases extremely. Furthermore, the silicone tubes showed a fast abrasion in the peristaltic pumps. Due to the material properties and the temperature of the medium, the service life of the tubes was limited to 100 h.

4.5 Experimental conduction in the dynamic model

The imitation of different drug administrations and PK drug declines (see 3.6.1) is a remarkable property of the developed final dynamic *in vitro* model. Dynamic *in vitro* investigations usually perform one-compartmental drug decline and bolus administration; seldom, infusion is mimicked. Two-compartmental drug decline was previously only seen in dialysis models.[40] The here developed pharmacodynamic *in vitro* model offers a wide range of drug reproducible administration and drug decline.

The studies in the dynamic *in vitro* model used the *in vivo* observed drug clearance and half-life, respectively, to describe the drug decline. The advantage of this approach is the description of the real drug decline in a patient, which could also follow a biphasic pattern (two-compartmental disposition kinetics). In a previous clinical study,[141, 142] different PK parameters of LZD, such as the *in vivo* drug half-life, were determined in critically ill patients and healthy volunteers. The LZD half-life of 3.5-5 h applied in this thesis is within the range of the half-life of unbound plasma concentrations in healthy volunteers, septic shock and severe sepsis patients and so the determined PK/PD correlation of LZD and VRE might be relevant for them. Since the LZD concentrations in plasma are close to those in interstitial fluid,[28] the here presented bacterial concentration-time courses - based on plasma PK of LZD – might be transferrable to tissue conditions.

From the time-kill curves it can be concluded, that the route of administration as well as the number of simulated compartments have only a minor influence on the bacterial killing of VRE by LZD due to the similar slope of bacterial concentrations (see 3.6.4). This is more important for the simplification of the *in vitro* setting of experiments than for *in vivo* administration, since the administration as bolus is unfeasible *in vivo*.

4.6 Enterococcus faecium under changing linezolid concentrations

The present work investigated also the effect of physiology-like changing LZD concentrations on VRE. The bacteria were exposed to four different LZD PK profiles and dosing regimens: one-compartmental kinetics with 600 mg bolus administration, 1200 mg infusion and 600 mg infusion (long half-life) were mimicked. *In vivo* plasma concentrations with two-compartmental kinetics and 600 mg LZD were also applied.

Comparing the present time-kill studies to others, the lack of standardised conditions in general such as the initial bacterial inoculum, the use of a commercially available strain or different types of dynamic *in vitro* model becomes obvious (Table 27). The obtained maximum growth and the growth control curve under dynamic conditions were comparable to others [110, 138, 143, 144] and [114], respectively. The maximum effect of physiology-like changing LZD concentrations was reached after 12 h, afterwards bacterial regrowth occured. Regrowth could be suppressed by

consequent re-dosing every 12 h as done in other studies.[35, 110, 138] For other strains treated with LZD, such as *S. aureus* under 16 µg/mL initial LZD concentration, bacterial regrowth was found too.[145] If MRSA was treated with LZD every 12 h, no regrowth occured.[138]

The time of maximum LZD effect recommends the next administration time. Thus, after 12 h re-dosing of LZD should be considered in VRE infections (compare RBR analysis, 3.4.3), which was also found to be an effective dosing interval by others.[35, 110, 138] For clinical therapy of VRE infections with LZD this would mean an administration twice a day. A more frequent administration for the given PK characteristics would not be required, since the maximum antibacterial effect is not reached before 12 h. Furthermore, the higher drug concentrations resulting from more frequent administration would not lead to a higher effect. Further experiments with multiple dosing could give more insights into the antibacterial effect or bacterial regrowth. Most studies in dynamic models found in the literature were carried out longer than in the present study and with multiple dosing. Such studies, but with reproducible conditions as in the present work, should be performed in the future. The design of the time-kill studies of this work was based on LZD concentration-time profiles as they appear *in vivo* and not on PK/PD indices. For a successful antibiotic therapy, the AUC/MIC of LZD should be >100 h and the time above the MIC ($T_{C>MIC}$) over 85%.[146] The here investigated concentration-time profiles did not achieve these breakpoints due to administration once over 24 h and – in accordance with the literature – the bacterial growth could not be successfully suppressed. The exception is the trial mimicking one-compartmental kinetics with infusion of 600 mg and a half-life of 5 h. Under these conditions, no bacterial regrowth occurred and the PK/PD indices were closest to the breakpoints. An administration twice a day would lead to other experimental PK/PD indices. By assumption of linear PK the $AUC_{0-12\,h}$ would double and the $AUC_{0-24\,h}$/MIC ratio would thus exceed the breakpoint of 100 h for all investigated profiles and MIC values. Thus, the maximum effect could be reached by all profiles and regrowth could be suppressed, when administering LZD twice a day. Concerning only the $T_{C>MIC}$ in a 12 h dosing intervall, the most *in vivo*-like profile (two compartmentanl kinetics) would not lead to a successful therapy.

When thinking about the bacterial regrowth in the time-kill studies after 12 h, it should also be considered, that bacterial growth *in vivo* is slower than *in vitro*,[61] and the immune system also influences the bacterial growth. This means on one hand disease progression does not necessarily worsen *in vivo* as proposed for *in vitro*, on the other hand the bacteria might not expose the same susceptibility to the drug *in vivo* as *in vitro*. Furthermore, a change of LZD susceptibility of *E. faecium* might appear *in vivo* during drug therapy and should be considered.[147]

Table 27 Studies on the activity of LZD on *E. faecium* under changing LZD concentrations.

Study	Type of dynamic model [40]	Strain	Imitated LZD dose	C_{max}	Administration	Duration of experiment	Start inoculum
Present study	Dilution model with continuous dilution and filters	E. faecium ATCC 700221	600 mg, 1200 mg	20.13, 36.68, 19.45, 15.94 µg/mL	1 cmt - bolus, infusion, $t_{1/2}$= 3.54, 5.00 h 2 cmt – infusion $t_{1/2}$= 3.22 h (beta phase)	24 h	10^6 cfu/mL
Allen [110]	Dilution model with continuous simple dilution	Clinical isolate of *E. faecium*	600 mg	10.4 µg/mL	1 cmt, 600 mg BID, $t_{1/2}$= 4.8 h	72 h	10^{10} cfu/mL
Boak [35]	Dilution model with continuous simple dilution	VRE. *faecium* ATCC 700221	600 mg; 120 mg, 120 mg, 30 mg	20 µg/mL; 2.0 µg/mL 4.0 µg/mL 0.5 µg/mL	1 cmt, 600 mg BID, loading dose + maintenance dose (bolus); 120 mg/24 h continuous infusion 120 mg BID, loading dose + maintenance dose (bolus); 30 mg/24 h continuous infusion	72 h	10^6 cfu/mL
Gunderson [138]	Dialysis model	Clinical isolate of VRE *faecium*	600 mg	20 µg/mL	Bolus, BID	24 h	10^6 cfu/mL
LaPlante [148]	Dilution model with continuous simple dilution	Clinical isolates of *E. faecalis* + *S. aureus*	600 mg	21.9 µg/mL	1 cmt, 600 mg BID, $t_{1/2}$= 5.5 h	48 h	$5×10^6$ cfu/mL
Wiederhold [143]	Dialysis model	Clinical isolate of *E. faecium*	600 mg	13.3 µg/mL	600 mg, BID	48 h	10^4 cfu/mL
Zinner [144]	Dialysis model	Clinical isolate of VRE *faecium*		6 – 11 µg/mL	BID with 60 min infusion	72 h	10^8 cfu/mL

4.7 Investigations on linezolid resistance

The described investigations on LZD resistance were exploratory studies to determine wether the resistance and/or a possible correlation with the experimentally developed SCV. The number of SCVs of *E. faecium* was not related to the number of colonies growing on LZD containing agar (assumed as resistant bacteria). The results of the resistance investigations in the dynamic model showed, that LZD concentrations of 12 µg/mL did not allow growth of VRE. Thus, the developed colonies on 8 µg/mL LZD agar plates might be handled as intermediate susceptible.[3] Furthermore, a differentiation between persistent and resistant bacteria was not pursued. For sole resistance investigations, the start inoculum should exceed the spontaneous mutation frequency (inoculum: 10^9-10^{11} cfu/mL)[18] and a long-term treatment (e.g. 96 h) with LZD should be build up, to permit resistance mutations. The extended time of incubation (160 h) might have enabled bacterial growth with slow biosynthesis. Reliable detection of resistant subpopulations can only be suggested by the relatively high LZD concentration of 12 µg/mL, because already one dilution difference is a usual experimental variability. A clear distinction could only be made by a PCR analysis of resistance genes in the colonies growing on LZD agar.[149, 150]

4.8 Bacteriostatic versus bactericidal effect

The results from the static *in vitro* model demonstrated, that 4 µg/mL LZD have a bacteriostatic effect on VRE after 24 h, which is in good accordance with the MIC in the literature.[18, 25, 26] Furthermore, LZD showed no concentration-dependent effect on VRE in static experiments. An increase of the dose did not necessarily lead to an increased effect. This was also found in the dynamic *in vitro* model, where the doubled dose (1200 mg) did not decrease the bacterial concentration more than the standard dose. Results by Jones et al.[137] approved this, whereas the study by Zinner et al. [144] found a concentration-dependent effect of LZD.

The maximum bacterial reduction was less than 3 $\log_{10}$ units in both types of *in vitro* models, thus the effect of LZD was bacteriostatic but not bactericidal for *E. faecium*,[18, 133, 138, 143] which was also confirmed by an *in vivo* rat intra-abdominal abscess model.[151] The bacteriostatic effect can be explained by the mechanism of action: LZD does not directly damage the bacteria, but inhibits the assembling of the ribosomal subunits.[18] Thereby, the translation of protein coding t-RNA becomes impossible and in the following necessary proteins cannot be produced, disrupting the bacterial cell functions (with time delay).

While the bacteriostatic effect seems consistent, it remains unclear, why changing concentrations of LZD were also found to be bactericidal against *E. faecium.*[35] Different results concerning the extent of the effect also exist for *S. aureus*. The effect of LZD against this strain was determined as bacteriostatic [145] and bactericidal [100] in both, static and dynamic *in vitro*

models. Nevertheless, *in vivo* the time for bacterial eradication in MRSA infections lasts in mean 9 days,[152] whereby the whole therapy takes 14 up to 28 days.[18]

The minimum bacterial concentrations of ~5×10^4 cfu/mL of VRE should be interpreted with caution and further investigations are suggested to evaluate its relevance in clinical therapy. *In vitro*, the bacterial killing did not fall below this minimum bacterial concentration (compare 3.4.2 and 3.8.4). Other studies also found residues of *E. faecium*.[110, 143, 148] Complete eradication of VRE by LZD seems to be impossible in clinical therapy, the assistance of the immune system would always be needed in the cure of these infections.

4.9 Pharmacokinetic/pharmacodynamic analyses

Generally, the strain to strain variability is considered to be relatively high,[153] and so all critical concentrations found in this work are limited to *E. faecium*. All suggested concentrations should be regarded to the unbound LZD concentrations.[91] The here determined plasma concentrations are comparable to the interstitial concentrations in steady state.[28] By this reason the determined effects are proposed to appear at the site of infection in the same way as described here.

4.9.1 Stationary and minimum inhibitory concentration

To the author's knowledge, the stationary concentration,[112] which was also named "critical concentration"[154] or "pharmacodynamic minimum inhibitory concentration"[155], has not been published for LZD on VRE yet. Because LZD is a drug with a concentration-independent effect, the MIC would be a reasonable estimate of the *in vivo* stationary concentration.[112] Since the MIC was determined with 2-4 µg/mL, this would also count for the stationary concentration. Based on the assumption, that lower growth *in vivo* results also in a lower stationary concentration *in vivo* and the stationary concentration *in vitro* approximates the *in vivo* one,[112] a concentration of 2 µg/mL (calculated as 2.25 µg/mL, see 3.8.3) could be assumed as stationary concentration *in vivo*. In other words, 2.25 µg/mL LZD were presumed to inhibit the growth of VRE *in vivo* and maintain no net growth, so that under assistance of the immune system, the antibiotic therapy would be successful. The inconsistence of the method of MIC determination disburdens comparison of MIC results and the resulting range of determination appears as crude estimate compared to the stationary concentration.

4.9.2 Analysis and modelling of relative bacterial reduction

The RBR analysis approach has been developed by C. Scheerans,[100] whereupon related analysis methods of the antibacterial effect exist.[62, 91] Firsov et al. for example described the intensity of the effect (I_E) expressed as area between the bacterial concentration curve under antibiotic

influence and the growth control curve.[156] In contrast to the RBR it was expressed as absolute value and not related to the growth control curve (in percent). The same relationship was described by the area between the growth control and antibiotic effect curves (AUBC).[41, 157]

The final RBR model was based on an indirect link model. This model structure could still be improved by inclusion of mechanistic processes, since high RBR values at late time points were underestimated with the current model. However, 1300 single values of the bacterial concentration with a high variability were included in the analysis, whereupon the model quality is always related to the data. Hence, the RBR model exerted a high descriptive performance of the antibacterial effect.

For comparing the RBR analysis of *E. faecium*, the results of a *S. aureus* strain, previously investigated under the same conditions with LZD in the group of Prof. Kloft, were used.[100] The shape of the effect-time curves and the effect-concentration curves were the same for both strains. For *E. faecium* the maximum effect of 45% was reached by 8.6 µg/mL, whereas the maximum effect of *S. aureus* was higher (78%), but also obtained by a higher LZD concentration (17.1 µg/mL). The plateau of the effect was reached for *E. faecium* after 8 h, whereas it appeared for *S. aureus* after 6 h. The killing behaviour of LZD in extent and time to maximum effect differs between the strains; despite they exhibit the same MIC (see 4.3). The difference in killing of the two strains became also obvious in the parameters of the RBR models (Table 28).

Table 28 Comparison of parameters for the RBR model estimated for *E. faecium* in this work and for *S. aureus* in a previous work[100].

Parameter	Unit	Estimates for *E. faecium*	Estimates for *S. aureus*
E_{max}	%	43	74
EC_{50}	µg/mL	1.765*	5.994
H		3.167	1.975
a	h^{-1}	0.379	0.113
b	h^{-1}	0.042	0.430
z	h^{-1}	0.120	0.026
k_{e0}	h^{-1}	0.054	0.131

*fixed value, based on basic modelling

The RBR model for *E. faecium* was based on the model for *S. aureus*. The highest variations in the parameter values appeared for E_{max}, EC_{50}, H and k_{e0}. E_{max} corresponds to the maximum obtainable effect, which was for *E. faecium* nearly only the half as that for *S. aureus*. The different EC_{50} values indicated a higher intrinsic activity of *E. faecium* towards LZD. The steeper slope of the killing curves of *E. faecium* was expressed by the Hill coefficient H. The

parameter k_{e0} characterises the equilibrium time between the simulated plasma and effect compartment concentrations.[158] The lower value of k_{e0} for *E. faecium* correlated with the steeper slope of the killing curve, but not with the shorter time to the maximum effect.

The differences in the killing behaviour of *E. faecium* and *S. aureus* might be attributed to differences in growth, protein biosynthesis and cellular structures. The killing behaviour could be relevant for the course of disease and dose adjustments, e.g. the amount of dose and the time of re-dosing.

4.9.3   Time-kill curve modelling

The bacterial concentration-time courses (time-kill curves) determined under constant and changing LZD concentrations were described by a semi-mechanistic model of growth and death.[95] The same structural model could describe the data from the static and dynamic models. The basic time-kill curve model permitted only inadequate predictions for the dynamic bacterial concentration time course (see Appendix, Figure 84). The effect under changing conditions was underestimated by the basic model especially for late time points and low drug concentrations. Also the final time-kill curve model for the dynamic data could not describe conditions with constant LZD concentrations.

Only the change in the EC_{50} value adjusted the time-kill curve model to the data of the two different origins (static/dynamic *in vitro* model). EC_{50} is as measure of the susceptibility of the bacteria towards the drug.[66, 95] Hence a higher EC_{50} value for the data from the static *in vitro* models meant higher drug concentrations would be needed to achieve the maximum effect. The lower EC_{50} for the dynamic data indicated that lower drug concentrations under changing conditions might be sufficient to obtain the maximum effect. In other words, the bacteria seemed to be more sensitive to LZD, if the drug concentrations changed, whereby the extent of the maximum effect as reached under constant concentrations might not be obtained. A solution to model static and dynamic data together would be the adaptation of the EC_{50} value. Tam et al. found an adaptation function for EC_{50} depending on time and drug concentration.[116] With increasing time and decreasing drug concentration, the adaptation function approximated zero, so EC_{50} was lowered and thus the whole time-kill curve function might have been more suitable to reflect the lower intrinsic activity of the bacteria resulting in a longer lasting effect and a slower incline of bacterial growth.

Beside this, the model parameters were compared to antibiotics with time-dependent killing reported by Czock and Keller.[95] Amongst them, k_0 is in good accordance with the median growth rate constant ($k_{0,median} = 1\ h^{-1}$) for time-dependent drugs (with $H = 1$). H was not estimated in the present work and so it takes a value of one, which is also in good accordance with the authors. The other parameters E_{max}, EC_{50} and the MIC are within the range of time-dependent

killing agents and close to the median values ($E_{max,median}$=2.4 h^{-1} [range: 1.5-4.8 h^{-1}]; $EC_{50,median}$=0.04 µg/mL [range: 0.004–31.7 µg/mL]; MIC_{median}=0.1 µg/mL [range: 0.012–8 µg/mL]).

The introduction of a minimum bacterial concentration N_{min} is a concept to account for the observed bacteria, [140, 157, 159] which appear despite high drug concentrations. The fact, that a minimum bacterial concentration exists, militates in favour of an equilibrium state between bacterial growth and kill, thus an "intermediate" kill and not an absolutely bactericidal effect exists.[157] The terms $\left(1 - \dfrac{N_{min}}{N_C(t)}\right)$, $\left(\dfrac{N_C(t)}{1 + N_C(t)}\right)$ and $\left(\dfrac{N_C(t)}{N_{min} + N_C(t)}\right)$ were explored for the description of the limited bacterial killing over time, but only the last term was found adequate. To the author's knowledge, the term was not used for antimicrobial PK/PD modelling before. Other groups used different methods (and models) to account for the incomplete bacteria eradication. Regoes et al. introduced a separate minimum bacterial net growth rate.[160] Other ideas are based on the reduced susceptibility of a bacterial subpopulation, which is in a persistence stage (persisters).[114, 145, 161, 162] These persisters shall also be responsible for the bacterial killing in two phases.[118] In the beginning, mainly the growing bacteria would be killed; later the killing of less sensitive persisters would result in a slower killing rate. The killing in two steps was modelled by Schuck et al. with two killing rates.[163] The assumption of resistant subpopulations of bacteria (two-population model) impedes also the complete decline of bacteria.[76, 96, 154, 164-166]

In the present work, the minimum bacterial concentration was favoured, since resistant subpopulations could not reliably be detected and small number of parameters (principle of parsimony) was favoured due to the low number of data points. In future experiments, the capture of small colony variants might be useful to quantify the less susceptible subpopulations and utilise them for a more mechanistic model approach. The value of the minimum bacterial concentration seems to depend on the initial inoculum size.[135, 136] This would mean, only standardised experiments with the same conditions are generally comparable.

Nevertheless, the final time-kill curve model enables first suitable predictions of the bacterial concentration-time course under changing drug concentrations. For low drug concentrations the model still underestimates the effect, and the bacterial growth is slower than predicted by the model. Further model adaptations should be carried out to improve the model and enhance more reliable predictions. The seldom incorporation of data from static and dynamic experiments suggests general problems in modelling or no accordance of data.[116, 145]

One application of the time-kill curve model could be the combination with a bacterial surrogate, which can be monitored *in vivo*, and would allow a therapeutic drug monitoring of LZD in VRE infections. Such a surrogate might be bacteriocin (=enterocin), where a growth model already exists.[167]

4.9.4 Dose optimisation

The dose optimisation of LZD should result in a decrease of the bacterial burden, avoid the amplification of resistant subpopulations and show as few as possible adverse drug effects.

The results of descriptive time-kill curves and RBR analyses were consulted for the dose optimisation. They indicated that a dose escalation did not necessarily lead to a higher antibacterial effect. The effect of LZD is time-dependent as demonstrated by the time-kill curves (see 3.4.2). So, not the extent of the drug exposure, but its duration ($\geq$12 h) seems to be important for the effectiveness. Additionally, a re-dosing of LZD in VRE infections after 12 h is recommended to capture the maximum drug effect and avoid bacterial regrowth. Also the experimental breakpoint concentration of 1.5 – 1.7 µg/mL ($EC_{I,50}$, EC_{inf}) might be relevant *in vivo* and should therefore be further investigated.

Other resources for dose optimisation than time-kill studies or RBR analysis are PK/PD indices. The AUC/MIC ratio was found to be an important hint for dose optimisation.[35, 146, 168] In the present work, the AUC/MIC ratios were not the basis for dose optimisation. They were determined from the *in vitro* LZD concentration-time profiles and were mainly related to bacterial regrowth. This might be a hint, that the imitated dosing regimens would probably fail in clinical therapy due to administration only once every 24 h. An AUC/MIC ratio of 70 – 100 h, which is related to 600 mg twice a day, should be achieved at least, but still enables mutations of resistant enterococci.[144] The experiments indicate $AUC_{0\text{-}12\,h}$/MIC ratios higher than 100 h, when given twice a day. The most in vivo-like with two-compartmental kinetics would not achieve this breakpoint for VRE with 4 µg/mL MIC susceptibility. In combination with doxycycline, AUC/MIC ratios of LZD of >200 h could prevent LZD-resistant enterococci and thus be successful in clinical therapy.[144] This would enhance the administration of higher LZD doses. The other important PK/PD index for LZD is the time above the MIC, which should exceed 82% for clinical cure.[146] In the present work, the $T_{C>MIC}$ of 66% (over 24 h) correlated with a bacteriostatic effect on *E. faecium*. Ba et al. found a $T_{C>MIC}$ of 70%, which was realised by 600 mg every 12 h, to be without significant effect against *E. faecalis* and *S. aureus*.[169]

Based on the descriptive RBR analysis and the *in vivo/in vitro* PK/PD model, computer simulations for typical patients and worst-case patients were carried out. Dosing regimens as investigated in deterministic simulations for the typical patient (see 3.8.5.1) of 1x 1800 mg, 1x 2400 mg and 2x 1200 mg might cause severe adverse drug effects, because of high maximum plasma concentrations and so were considered less suitable for clinical use. Also dosing regimens of 4x 300 mg, 4x 450 mg and 4x 600 mg could be inappropriate in practise due to highly necessitated adherence to therapy. Thus, only dosing regimens of 2x 600 mg (standard dosing), 3x 400 mg, 3x 600 mg and 3x 800 mg can be recommended for therapeutic use based on PK/PD simulations for typical patients. The deterministic simulation indicated also that the maximum effect could already be reached and kept constant by a DD of 1200 mg. Hence, the

standard dosing (2x 600 mg) seemed sufficient for these patients for an effective antibacterial therapy and a further dose adjustment would not necessarily be needed.[170] The modelling of the correlation between stochastical simulated $AUC_{E(14\ days)}$ and the DD found a DD of 750 mg LZD to be sufficient to reach 90% of the maximum effect in a typical patient (see 3.8.5.2). Comparable results were experimentally shown for LZD against *Bacillus anthracis* in a dialysis model, where 700 mg every 24 h permitted optimal kill without resistance selection.[78] However, a DD of 750 mg LZD would result in an AUC/MIC ratio of only 38 h, which might be insufficient.[35, 146] Furthermore, the range of the effect of 750 mg DD was so huge, that success and non-success could be reached at the same rate.

On the other hand possibly not all patients were cured with the standard dosing due to their physiological and PK conditions. For this purpose, an increase of the dose up to 1800 mg DD might advance the likelihood of reaching the maximum effect (Figure 43) as advised by stochastical simulations (see 3.8.5.2). For a worst-case patient, the dose optimisation would bring a higher benefit concerning antibacterial therapy. The clearance used for simulations of a worst-case patient, was based on the LZD clearances of patients with severe sepsis.[142] Such patients urgently need a well-dosed and successful therapy. Despite this, the adverse effects of high LZD concentrations in plasma (e.g. thrombocytopenia) should also be considered. They might appear even under a dose of 600 mg every 12 h given over more than 14 days, should be considered when adjusting the dose.[18] A splitting of the DD might not necessarily lead to a higher effect, but it could reduce the drug peaks in plasma. With regard towards the clinical administration and the compliance, a splitting of the DD in more than 3 parts could not be recommended. Both, increased (1800 mg) and reduced daily doses (750 mg) are required to be investigated in a clinical study before applied to routine use.

5 Conclusions and perspectives

Linezolid, a valuable antibiotic in severe infections, was investigated on its antibacterial effect on a commercially available vancomycin-resistant *Enterococcus faecium* strain. The strain was systematically investigated under a wide range of LZD concentrations over 24 h. Therefore a static *in vitro* model was established, ensuring stable conditions by preliminary microbiological studies, a qualified method for bacterial quantification and a valid method for drug determination.

To estimate the drug effect on VRE under *in vivo*-like changing drug concentrations, an *in vitro* dynamic dilution model without bacterial loss was developed. The former problems of bacterial loss, filter blockage and bacterial backgrowth were conveniently solved. The model enabled the application of different PK profiles with different drug administrations and drug declines. VRE were investigated under four LZD concentration-time profiles in the dynamic model. Further studies in the future should exercise the dynamic *in vitro* model for multiple dosing studies and long term treatment of bacteria.[95] By use of both *in vitro* models, the effect of LZD was shown to be time-dependent and thus, a dose escalation does not lead to an enhanced effect. The maximum effect of LZD was obtained after 12 h, which advises this time as meaningful time for re-dosing. The MIC of 2-4 µg/mL was confirmed, and a growth inhibition within this concentration range, which was also found by the stationary concentration, can be assumed. LZD concentrations of 1.5-1.7 µg/mL were identified by all modelling approaches as breakpoint concentrations for a disproportionately high increase of effect against VRE and should therefore be tested on their relevance in practise.

The different modelling approaches offer different applications: The RBR analysis and the RBR model are suitable tools for detection and comparison of the efficacy of a drug on a percentage scale. The time-kill curve model offers a rational approach describing the actual bacterial concentration. The combination of this model with a model for an *in vivo* surrogate marker, such as bacteriocin (enterocin),[167] could be a step towards therapeutic drug monitoring of LZD in VRE infections. Therewith in future, the current *in vivo* bacterial concentration might be calculated and an appropriate LZD dose administered. However, further developments of the model structure should incorporate static and dynamic data in one model. Also data of the effect of repeated LZD dosing on VRE could extend the model. The multiple dosing data could reflect more realistic *in vivo* conditions and ameliorate the developed models for time-kill curves and RBR. In addition, the influence of the body temperature, such as fever or coolness in extremities, as co-factor of antimicrobial therapy could be investigated.[171]

In computational simulations based on the final RBR model, the effect of different daily doses on patients with typical PK parameters and those with worst PK conditions was simulated over 14 days of therapy. The standard dosing (2x 600 mg) of LZD on VRE infections were advised

as suitable for patients exhibiting the typical PK properties. For patients with a higher drug clearance as formed during sepsis or septic shock, a higher daily dose of LZD of 1800 mg might be more effective. However, the simulated dosing regimens should be tested on their suitability and safety in clinical trials. The dose optimisation performed in this work does not incorporate the natural host defence mechanisms (immune system). So the findings might be more applicable to immunocompromised patients. Since complete bacteria eradication was not found in this work (RBR maximally 42%) immunocompromised patients would need the synergistic effect of an additional drug (combination therapy) to reach complete VRE eradication.

The comparison of VRE data with those of *S. aureus* showed differences in sensitivity towards LZD, despite the exhibition of the same MIC, which might be relevant for differences in disease and cure progression. VRE are less sensitive towards LZD, thus a LZD-resistance mutation becomes more likely. To avoid the progression of LZD resistance in enterococci, further investigations should be made on resistance development. The present exploratory investigations of LZD resistance are a good basis for future studies to understand and reduce resistance development.Here, the already described small colony variants (SCV) of VRE should be in focus. The detection of their origin, thus a distinction between persistence and resistance by PCR analysis of resistance genes, could be useful.[149, 150] Their quantification could be valuable additional knowledge for the effect modelling and thus also for predictions and optimisation of the drug effect in patients.

The here presented results of the antibacterial effect of LZD in VRE infections should be incorporated in future clinical (*in vivo*) studies, to substantiate the proposals of dose optimisation and transfer them to the patients.

6   References

1.   WHO 2004. The World health report 2004 - Changing history. http://www.who.int/entity/whr/2004/en/report04_en.pdf (18 July 2008, date last accessed).

2.   Hellenbrand W. Neu und vermehrt auftretende Infektionskrankheiten. *Gesundheitsberichterstattung des Bundes*; **18**: 1-35 (2003).

3.   EUCAST 2000. Terminology relating to methods for the determination of susceptibility of bacteria to antimicrobial agents - EUCAST Definitve Document E.Def 1.2. http://eucast.www137.server1.mensemedia.net/fileadmin/src/media/PDFs/4ESCMID_Library/3Publications/EUCAST_Documents/Publications/E_Def_1_2_03_2000.pdf (18 June 2009, date last accessed).

4.   Spellberg B, Powers JH, Brass EP *et al.* Trends in antimicrobial drug development: implications for the future. *Clin Infect Dis*; **38**: 1279-86 (2004).

5.   ECDC, EMEA 2009. The bacterial challenge: time to react. http://www.ema.europa.eu/docs/en_GB/document_library/Report/2009/11/WC500008770.pdf (01 February 2011, date last accessed).

6.   Lesko LJ. Personalized Medicine: Elusive Dream or Imminent Reality? *Clin Pharmacol Ther*; **81**: 807-16 (2007).

7.   Shah VP, Besancon LJ, Stolk P *et al.* The pharmaceutical sciences in 2020--report of a conference organized by the Board of Pharmaceutical Sciences of the International Pharmaceutical Federation (FIP). *Eur J Pharm Sci*; **38**: 419-25 (2009).

8.   Geffers C, Gastmeier P, Rüden H. Nosokomiale Infektionen. *Gesundheitsberichterstattung des Bundes*; **8**: 1-18 (2002).

9.   Kresken M, Hafner D, Schmitz F *et al.* PEG-Resistenzstudie 2004. Rheinbach: Antiinfectives Intelligence, Gesellschaft für klinisch-mikrobiologische Forschung und Kommunikation mbH, (2006).

10.   ECDC 2010. Antimicrobial resistance surveillance in Europe 2009. Annual Report of the European Antimicrobial Resistance Surveillance Network (EARS-Net). http://www.ecdc.europa.eu/en/publications/Publications/1011_SUR_annual_EARS_Net_2009.pdf (26 January 2011, date last accessed).

11.   Murray BE. The life and times of the Enterococcus. *Clin Microbiol Rev*; **3**: 46-65 (1990).

12.   Boehner JS. Untersuchung des Wachstumsverhaltens von E. faecium unter sauren pH-Bedingungen und unter Linezolidexposition. Diploma thesis - in preparation, Martin-Luther-Universitaet Halle-Wittenberg, Halle, (2011).

13.   Linden PK. Treatment options for vancomycin-resistant enterococcal infections. *Drugs*; **62**: 425-41 (2002).

14.   Karchmer AW. Nosocomial bloodstream infections: organisms, risk factors, and implications. *Clin Infect Dis*; **31 Suppl 4**: S139-43 (2000).

15.   Theilacker C, Jonas D, Huebner J *et al.* Outcomes of invasive infection due to vancomycin-resistant Enterococcus faecium during a recent outbreak. *Infection*; **37**: 540-3 (2009).

16.   Klare I, Werner G, Witte W *et al.* Vancomycin-resistente Enterokokken in deutschen Krankenhäusern 2006/2007. *Epidemiologisches Bulletin*; **23**: 179-89 (2008).

17.   Tacconelli E, Cataldo MA. Vancomycin-resistant enterococci (VRE): transmission and control. *Int J Antimicrob Agents*; **31**: 99-106 (2008).

18.   Pfizer 2010. Zyvox U.S. Physician Prescribing Information. http://media.pfizer.com/files/products/uspi_zyvox.pdf (05 January 2011, date last accessed).

19.   Pfizer. Fachinformation Zyvoxid.   1-7 (2007).

20.   Vara Prasad JV. New oxazolidinones. *Curr Opin Microbiol*; **10**: 454-60 (2007).

21.   Yong D, Yum JH, Lee K *et al.* In vitro activities of DA-7867, a novel oxazolidinone, against recent clinical isolates of aerobic and anaerobic bacteria. *Antimicrob Agents Chemother*; **48**: 352-7 (2004).

22.   Skripkin E, McConnell TS, DeVito J *et al.* R chi-01, a new family of oxazolidinones that overcome ribosome-based linezolid resistance. *Antimicrob Agents Chemother*; **52**: 3550-7 (2008).

23.   Im WB, Choi SH, Park JY *et al.* Discovery of torezolid as a novel 5-hydroxymethyl-oxazolidinone antibacterial agent. *Eur J Med Chem*;   (2011).

24.   Noskin GA, Siddiqui F, Stosor V *et al.* In vitro activities of linezolid against important gram-positive bacterial pathogens including vancomycin-resistant enterococci. *Antimicrob Agents Chemother*; **43**: 2059-62 (1999).

25.   Zurenko GE, Yagi BH, Schaadt RD *et al.* In vitro activities of U-100592 and U-100766, novel oxazolidinone antibacterial agents. *Antimicrob Agents Chemother*; **40**: 839-45 (1996).

26.   EUCAST 2006. EUCAST Technical Note on linezolid. http://eucast.www137.server1.mensemedia.net/fileadmin/src/media/PDFs/4ESCMID_Library/3Publicatio

ns/EUCAST_Documents/Technical_Notes/EUCAST_Tech_Note_linezolid_CMI_2006_v12.pdf (18 June 2009, date last accessed).

27.   Plosker GL, Figgitt DP. Linezolid: a pharmacoeconomic review of its use in serious Gram-positive infections. *Pharmacoeconomics*; **23**: 945-64 (2005).

28.   Dehghanyar P, Burger C, Zeitlinger M *et al.* Penetration of linezolid into soft tissues of healthy volunteers after single and multiple doses. *Antimicrob Agents Chemother*; **49**: 2367-71 (2005).

29.   Bouza E, Munoz P. Linezolid: pharmacokinetic characteristics and clinical studies. *Clin Microbiol Infect*; **7 Suppl 4**: 75-82 (2001).

30.   Diekema DI, Jones RN. Oxazolidinones: a review. *Drugs*; **59**: 7-16 (2000).

31.   Wynalda MA, Hauer MJ, Wienkers LC. Oxidation of the novel oxazolidinone antibiotic linezolid in human liver microsomes. *Drug Metab Dispos*; **28**: 1014-7 (2000).

32.   Plock N, Buerger C, Joukhadar C *et al.* Does linezolid inhibit its own metabolism? Population pharmacokinetics as a tool to explain the observed nonlinearity in both healthy volunteers and septic patients. *Drug Metab Dispos*; **35**: 1816-23 (2007).

33.   Birmingham MC, Rayner CR, Meagher AK *et al.* Linezolid for the treatment of multidrug-resistant, gram-positive infections: experience from a compassionate-use program. *Clin Infect Dis*; **36**: 159-68 (2003).

34.   Halle E, Majcher-Peszynska J, Drewelow B. Linezolid: das erste Antibiotikum aus der Klasse der Oxazolidinone. *Chemotherapie Journal*; **11**: 1-11 (2002).

35.   Boak LM, Li J, Rayner CR *et al.* Pharmacokinetic/pharmacodynamic factors influencing emergence of resistance to linezolid in an in vitro model. *Antimicrob Agents Chemother*; **51**: 1287-92 (2007).

36.   Gonzales RD, Schreckenberger PC, Graham MB *et al.* Infections due to vancomycin-resistant Enterococcus faecium resistant to linezolid. *Lancet*; **357**: 1179 (2001).

37.   Tsiodras S, Gold HS, Sakoulas G *et al.* Linezolid resistance in a clinical isolate of Staphylococcus aureus. *Lancet*; **358**: 207-8 (2001).

38.   EMEA 2000. CPMP/EWP/2655/99 - Points to consider on pharmacokinetics and pharmacodynamics in the development of antibacterial medicinal products. http://www.emea.europa.eu/pdfs/human/ewp/265599en.pdf (4 March 2008, date last accessed).

39.   Holford NH, Sheiner LB. Kinetics of pharmacologic response. *Pharmacol Ther*; **16**: 143-66 (1982).

40.   Gloede J, Scheerans C, Derendorf H *et al.* In vitro pharmacodynamic models to determine the effect of antibacterial drugs. *J Antimicrob Chemother*; **65**: 186-201 (2010).

41.   MacGowan A, Rogers C, Bowker K. In vitro models, in vivo models, and pharmacokinetics: what can we learn from in vitro models? *Clin Infect Dis*; **33 Suppl 3**: 214-20 (2001).

42.   Delacher S, Derendorf H, Hollenstein U *et al.* A combined in vivo pharmacokinetic-in vitro pharmacodynamic approach to simulate target site pharmacodynamics of antibiotics in humans. *J Antimicrob Chemother*; **46**: 733-9 (2000).

43.   FDA 1998. Developing Antimicrobial Drugs - General Considerations for Clinical Trials (Draft Guidance). http://www.fda.gov/downloads/Drugs/GuidanceComplianceRegulatoryInformation/Guidances/ucm070983.pdf (19 May 2009, date last accessed).

44.   Fantin B, Carbon C. In vivo antibiotic synergism: contribution of animal models. *Antimicrob Agents Chemother*; **36**: 907-12 (1992).

45.   Dudley MN, Griffith D. Animal Models of Infection for the Study of Antibiotic Pharmacodynamics. In: Nightingale, CH, Murakawa, T, Ambrose, PG, eds. *Antimicrobial Pharmacodynamics in Theory and Clinical Practice.* New York: Marcel Dekker, Inc., pp. 67-98; (2002).

46.   Craig WA. Pharmacokinetic/pharmacodynamic parameters: rationale for antibacterial dosing of mice and men. *Clin Infect Dis*; **26**: 1-10 (1998).

47.   Hickey E. Tools to define the relevance of PK/PD parameters to the efficacy, toxicity and emergence of resistance of antimicrobials. *Curr Opin Drug Discov Devel*; **10**: 49-52 (2007).

48.   Drusano GL, Louie A, Deziel M *et al.* The crisis of resistance: identifying drug exposures to suppress amplification of resistant mutant subpopulations. *Clin Infect Dis*; **42**: 525-32 (2006).

49.   Derendorf H, Meibohm B. Modeling of pharmacokinetic/pharmacodynamic (PK/PD) relationships: concepts and perspectives. *Pharm Res*; **16**: 176-85 (1999).

50.   Mouton JW, Dudley MN, Cars O *et al.* Standardization of pharmacokinetic/pharmacodynamic (PK/PD) terminology for anti-infective drugs. *Int J Antimicrob Agents*; **19**: 355-8 (2002).

51.   Mouton JW, Dudley MN, Cars O *et al.* Standardization of pharmacokinetic/pharmacodynamic (PK/PD) terminology for anti-infective drugs: an update. *J Antimicrob Chemother*; **55**: 601-7 (2005).

52.   Mouton JW, Vinks AA. Relationship between minimum inhibitory concentration and stationary concentration revisited: growth rates and minimum bactericidal concentrations. *Clin Pharmacokinet*; **44**: 767-8 (2005).

53.   Barger A, Fuhst C, Wiedemann B. Pharmacological indices in antibiotic therapy. *J Antimicrob Chemother*; **52**: 893-8 (2003).

54.   Blondeau JM, Hansen G, Metzler K *et al.* The role of PK/PD parameters to avoid selection and increase of resistance: mutant prevention concentration. *J Chemother*; **16 Suppl 3**: 1-19 (2004).

55.   Wang L, Wismer MK, Racine F *et al.* Development of an integrated semi-automated system for in vitro pharmacodynamic modelling. *J Antimicrob Chemother*; **62**: 1070-7 (2008).

56.   Lorian V. In vitro simulation of in vivo conditions: physical state of the culture medium. *J Clin Microbiol*; **27**: 2403-6 (1989).

57.   Brown MR, Collier PJ, Gilbert P. Influence of growth rate on susceptibility to antimicrobial agents: modification of the cell envelope and batch and continuous culture studies. *Antimicrob Agents Chemother*; **34**: 1623-8 (1990).

58.   Gilbert P. The theory and relevance of continuous culture. *J Antimicrob Chemother*; **15 Suppl A**: 1-6 (1985).

59.   Lorian V. Differences between in vitro and in vivo studies. *Antimicrob Agents Chemother*; **32**: 1600-1 (1988).

60.   Garrett ER, Miller GH, Brown MR. Kinetics and mechanisms of action of antibiotics on microorganisms. V. Chloramphenicol and tetracycline affected Escherichia coli generation rates. *J Pharm Sci*; **55**: 593-600 (1966).

61.   Dalhoff A. Differences between bacteria grown in vitro and in vivo. *J Antimicrob Chemother*; **15 Suppl A**: 175-95 (1985).

62.   MacGowan A, Bowker K. Developments in PK/PD: optimising efficacy and prevention of resistance. A critical review of PK/PD in in vitro models. *Int J Antimicrob Agents*; **19**: 291-8 (2002).

63.   Frimodt-Moller N. How predictive is PK/PD for antibacterial agents? *Int J Antimicrob Agents*; **19**: 333-9 (2002).

64.   Blaser J, Vergeres P, Widmer AF *et al.* In vivo verification of in vitro model of antibiotic treatment of device-related infection. *Antimicrob Agents Chemother*; **39**: 1134-9 (1995).

65.   Mueller M, de la Pena A, Derendorf H. Issues in pharmacokinetics and pharmacodynamics of anti-infective agents: kill curves versus MIC. *Antimicrob Agents Chemother*; **48**: 369-77 (2004).

66.   Nolting A, Derendorf H. Pharmacokinetic/Pharmacodynamic Modelling of Antibiotics. In: Derendorf, H, Hochhaus, G, eds. *Handbook of pharmacokinetic/pharmacodynamic correlation.* Boca Raton: CRC Press Inc., pp. 363-288; (1995).

67.   Grasso S. Historical review of in-vitro models. *J Antimicrob Chemother*; **15 Suppl A**: 99-102 (1985).

68.   Grasso S, Meinardi G, de Carneri I *et al.* New in vitro model to study the effect of antibiotic concentration and rate of elimination on antibacterial activity. *Antimicrob Agents Chemother*; **13**: 570-6 (1978).

69.   Li RC, Zhu ZY. In vitro models for prediction of antimicrobial activity: a pharmacokinetic and pharmacodynamic perspective. *J Chemother*; **9 Suppl 1**: 55-63 (1997).

70.   Blaser J, Stone BB, Zinner SH. Two compartment kinetic model with multiple artificial capillary units. *J Antimicrob Chemother*; **15 Suppl A**: 131-7 (1985).

71.   Zinner SH, Husson M, Klastersky J. An artificial capillary in vitro kinetic model of antibiotic bactericidal activity. *J Infect Dis*; **144**: 583-7 (1981).

72.   Mouton JW, den Hollander JG. Killing of Pseudomonas aeruginosa during continuous and intermittent infusion of ceftazidime in an in vitro pharmacokinetic model. *Antimicrob Agents Chemother*; **38**: 931-6 (1994).

73.   Rybak MJ, Allen GP, Hershberger E. In Vitro Antibiotic Pharmacodynamic Models. In: Nightingale, CH, Murakawa, T, Ambrose, PG, eds. *Antimicrobial Pharmacodynamics in Theory and Clinical Practice.* New York: Marcel Dekker, Inc., pp. 41-66; (2002).

74.   Tam VH, Kabbara S, Vo G *et al.* Comparative pharmacodynamics of gentamicin against Staphylococcus aureus and Pseudomonas aeruginosa. *Antimicrob Agents Chemother*; **50**: 2626-31 (2006).

75.   Tam VH, Schilling AN, Neshat S *et al.* Optimization of meropenem minimum concentration/MIC ratio to suppress in vitro resistance of Pseudomonas aeruginosa. *Antimicrob Agents Chemother*; **49**: 4920-7 (2005).

76.   Gumbo T, Louie A, Deziel MR *et al.* Selection of a moxifloxacin dose that suppresses drug resistance in Mycobacterium tuberculosis, by use of an in vitro pharmacodynamic infection model and mathematical modeling. *J Infect Dis*; **190**: 1642-51 (2004).

77.　　Louie A, Brown DL, Liu W *et al.* In vitro infection model characterizing the effect of efflux pump inhibition on prevention of resistance to levofloxacin and ciprofloxacin in Streptococcus pneumoniae. *Antimicrob Agents Chemother*; **51**: 3988-4000 (2007).

78.　　Louie A, Heine HS, Kim K *et al.* Use of an in vitro pharmacodynamic model to derive a linezolid regimen that optimizes bacterial kill and prevents emergence of resistance in Bacillus anthracis. *Antimicrob Agents Chemother*; **52**: 2486-96 (2008).

79.　　Ledergerber B, Blaser J, Luthy R. Computer-controlled in-vitro simulation of multiple dosing regimens. *J Antimicrob Chemother*; **15 Suppl A**: 169-73 (1985).

80.　　Al-Asadi MJ, Greenwood D, O'Grady F. In vitro model simulating the form of exposure of bacteria to antimicrobial drugs encountered in infection. *Antimicrob Agents Chemother*; **16**: 77-80 (1979).

81.　　Venisse N, Gregoire N, Marliat M *et al.* Mechanism-based pharmacokinetic-pharmacodynamic models of in vitro fungistatic and fungicidal effects against Candida albicans. *Antimicrob Agents Chemother*; **52**: 937-43 (2008).

82.　　Haag R, Lexa P, Werkhauser I. Artifacts in dilution pharmacokinetic models caused by adherent bacteria. *Antimicrob Agents Chemother*; **29**: 765-8 (1986).

83.　　Andrews JM. Determination of minimum inhibitory concentrations. *J Antimicrob Chemother*; **48 Suppl 1**: 5-16 (2001).

84.　　Turnidge JD, Bell JM. Antimicrobial Susceptibility on Solid Media. In: Lorian, V, ed *Antibiotics in Laboratory Medicine.* Philadelphia: Lippincott Williams & Wilkins, pp. 8-60; (2005).

85.　　Microbiological Assay of Antibiotics. *European Pharmacopoeia 5.0.* Deutscher Apotheker Verlag, pp. 188-94; (2005).

86.　　EUCAST 2009. Antimicrobial susceptibility testing EUCAST disk diffusion method. (04.02.2011, date last accessed).

87.　　Smaill F. Antibiotic susceptibility and resistance testing: an overview. *Can J Gastroenterol*; **14**: 871-5 (2000).

88.　　Amsterdam D. Susceptibility Testing of Antmicrobials in Liquid Media. In: Lorian, V, ed *Antibiotics in Laboratory Medicine.* Philadelphia: Lippincott Williams & Wilkins, pp. 8-60; (2005).

89.　　Schuurmans JM, Nuri Hayali AS, Koenders BB *et al.* Variations in MIC value caused by differences in experimental protocol. *Journal of Microbiological Methods*; **79**: 44-7 (2009).

90.　　Saravolatz LD, Pea F, Viale P. The Antimicrobial Therapy Puzzle: Could Pharmacokinetic-Pharmacodynamic Relationships Be Helpful in Addressing the Issue of Appropriate Pneumonia Treatment in Critically Ill Patients? *Clinical Infectious Diseases*; **42**: 1764-71 (2006).

91.　　Schuck EL, Derendorf H. Pharmacokinetic/pharmacodynamic evaluation of anti-infective agents. *Expert Rev Anti Infect Ther*; **3**: 361-73 (2005).

92.　　Greenwood D. Unrealistic nature of the 'MIC'. *J Antimicrob Chemother*; **2**: 312-3 (1976).

93.　　EUCAST 2003. Determination of minimum inhibitory concentrations (MICs) of antibacterial agents by broth dilution - Eucast Discussion Document E.Dis 5.1. http://eucast.www137.server1.mensemedia.net/fileadmin/src/media/PDFs/2News_Discussions/3Discussion_Documents/E_Def_5_1_03_2003.pdf (18 June 2009, date last accessed).

94.　　Craig WA, Andes DR. In Vivo Pharmacodynamics of Ceftobiprole against Multiple Bacterial Pathogens in Murine Thigh and Lung Infection Models. *Antimicrob. Agents Chemother.*; **52**: 3492-6 (2008).

95.　　Czock D, Keller F. Mechanism-based pharmacokinetic-pharmacodynamic modeling of antimicrobial drug effects. *J Pharmacokinet Pharmacodyn*; **34**: 727-51 (2007).

96.　　Nikolaou M, Tam VH. A new modeling approach to the effect of antimicrobial agents on heterogeneous microbial populations. *J Math Biol*; **52**: 154-82 (2006).

97.　　Garrett ER, Wright OK, Miller GH *et al.* Quantification and prediction of the biological activities of chloramphenicol analogs by microbial kinetics. *J Med Chem*; **9**: 203-8 (1966).

98.　　Meibohm B, Derendorf H. Basic concepts of pharmacokinetic/pharmacodynamic (PK/PD) modelling. *Int J Clin Pharmacol Ther*; **35**: 401-13 (1997).

99.　　Bast E. Mikrobiologische Methoden - Eine Einführung in grundlegende Arbeitstechniken. Heidelberg, Berlin: Spektrum Akademischer Verlag GmbH, (2001).

100.　　Scheerans C. In vitro pharmacodynamics, pharmacokinetic/pharmacodynamic modelling, and in silico simulation & analysis for the evaluation of dosing regimens for linezolid. Doctoral thesis, Martin-Luther-Universitaet Halle-Wittenberg, Halle, (2010).

101.　　FDA 2001. Guidance for Industry - Bioanalytical Method Validation. http://www.fda.gov/downloads/Drugs/GuidanceComplianceRegulatoryInformation/Guidances/UCM070107.pdf (02 March 2010, date last accessed).

102.　　Monod J. The growth of bacterial cultures. *Annual Review of Microbiology*; **3**: 371-94 (1949).

103.　　Eng RH, Smith SM, Cherubin CE *et al.* Evaluation of two methods for overcoming the antibiotic carry-over effect. *Eur J Clin Microbiol Infect Dis*; **10**: 34-8 (1991).

104.   den Hollander JG, Mouton JW, Bakker-Woudenberg IA *et al.* Enzymatic method for inactivation of aminoglycosides during measurement of postantibiotic effect. *Antimicrob Agents Chemother*; **40**: 488-90 (1996).

105.   den Hollander JG, Mouton JW, van Goor MP *et al.* Alteration of postantibiotic effect during one dosing interval of tobramycin, simulated in an in vitro pharmacokinetic model. *Antimicrob Agents Chemother*; **40**: 784-6 (1996).

106.   Lowdin E, Odenholt I, Bengtsson S *et al.* Pharmacodynamic effects of sub-MICs of benzylpenicillin against Streptococcus pyogenes in a newly developed in vitro kinetic model. *Antimicrob Agents Chemother*; **40**: 2478-82 (1996).

107.   Slatter JG, Stalker DJ, Feenstra KL *et al.* Pharmacokinetics, metabolism, and excretion of linezolid following an oral dose of [(14)C]linezolid to healthy human subjects. *Drug Metab Dispos*; **29**: 1136-45 (2001).

108.   Meagher AK, Forrest A, Rayner CR *et al.* Population pharmacokinetics of linezolid in patients treated in a compassionate-use program. *Antimicrob Agents Chemother*; **47**: 548-53 (2003).

109.   Tam VH, Ledesma KR, Vo G *et al.* Pharmacodynamic modeling of aminoglycosides against Pseudomonas aeruginosa and Acinetobacter baumannii: identifying dosing regimens to suppress resistance development. *Antimicrob Agents Chemother*; **52**: 3987-93 (2008).

110.   Allen GP, Bierman BC. In vitro analysis of resistance selection by linezolid in vancomycin-susceptible and -resistant Enterococcus faecalis and Enterococcus faecium. *Int J Antimicrob Agents*; **34**: 21-4 (2009).

111.   Binner F. Entwicklung und Validierung eines dynamischen In-vitro-Infektionsmodells: Untersuchung des Absterbeverhaltens von Enterokokken durch Linezolid und der pharmakokinetisch-pharmakodynamischen Zusammenhänge. Diploma thesis, Martin-Luther-Universitaet Halle-Wittenberg, Halle, (2010).

112.   Mouton JW, Vinks AA. Pharmacokinetic/pharmacodynamic modelling of antibacterials in vitro and in vivo using bacterial growth and kill kinetics: the minimum inhibitory concentration versus stationary concentration. *Clin Pharmacokinet*; **44**: 201-10 (2005).

113.   Derendorf H. Pharmakokinetik und Pharmakodynamik. In: Derendorf, H, Gramatté, T, Schäfer, H-G, eds. *Pharmakokinetik, Einführung in die Theorie und Relevanz für die Arzneimitteltherapie.* Stuttgart Wissenschaftliche Verlagsgesellschaft mbH, pp. 277-96; (2002).

114.   Nielsen EI, Viberg A, Lowdin E *et al.* Semimechanistic pharmacokinetic/pharmacodynamic model for assessment of activity of antibacterial agents from time-kill curve experiments. *Antimicrob Agents Chemother*; **51**: 128-36 (2007).

115.   Tam VH, Schilling AN, Lewis RE *et al.* Novel approach to characterization of combined pharmacodynamic effects of antimicrobial agents. *Antimicrob Agents Chemother*; **48**: 4315-21 (2004).

116.   Tam VH, Schilling AN, Nikolaou M. Modelling time-kill studies to discern the pharmacodynamics of meropenem. *J Antimicrob Chemother*; **55**: 699-706 (2005).

117.   Proctor RA, von Eiff C, Kahl BC *et al.* Small colony variants: a pathogenic form of bacteria that facilitates persistent and recurrent infections. *Nat Rev Microbiol*; **4**: 295-305 (2006).

118.   Balaban NQ, Merrin J, Chait R *et al.* Bacterial persistence as a phenotypic switch. *Science*; **305**: 1622-5 (2004).

119.   Barger A. Entwicklung eines mathematischen Modells zur Vorhersage der Wirkung von Antibiotika. Doctoral thesis, Rheinische Friedrich-Wilhelms-Universitaet Bonn, Bonn, (2003).

120.   Dalla Costa T, Nolting A, Rand K *et al.* Pharmacokinetic-pharmacodynamic modelling of the in vitro antiinfective effect of piperacillin-tazobactam combinations. *Int J Clin Pharmacol Ther*; **35**: 426-33 (1997).

121.   Schmidt S, Rock K, Sahre M *et al.* Effect of protein binding on the pharmacological activity of highly bound antibiotics. *Antimicrob Agents Chemother*; **52**: 3994-4000 (2008).

122.   Sahm DF, Olsen L. In vitro detection of enterococcal vancomycin resistance. *Antimicrob Agents Chemother*; **34**: 1846-8 (1990).

123.   Rybak MJ, Hershberger E, Moldovan T *et al.* In vitro activities of daptomycin, vancomycin, linezolid, and quinupristin-dalfopristin against Staphylococci and Enterococci, including vancomycin-intermediate and -resistant strains. *Antimicrob Agents Chemother*; **44**: 1062-6 (2000).

124.   Herigstad B, Hamilton M, Heersink J. How to optimize the drop plate method for enumerating bacteria. *Journal of Microbiological Methods*; **44**: 121-9 (2001).

125.   Hedges AJ, Shannon R, Hobbs RP. Comparison of the Precision Obtained in Counting Viable Bacteria by the Spiral Plate Maker, the Droplette and the Miles & Misra Methods. *Journal of Applied Microbiology*; **45**: 57-65 (1978).

126.   Barbosa HR, Rodrigues MFA, Campos CC *et al.* Counting of viable cluster-forming and non cluster-forming bacteria: A comparison between the drop and the spread methods. *Journal of Microbiological Methods*; **22**: 39-50 (1995).

127.   Sharpe AN, Diotte MP, Peterkin PI *et al.* Towards the truly automated colony counter. *Food Microbiology*; **3**: 161-84 (1986).

128.   Manninen MT, Fung DYC, Hart RA. SPIRAL SYSTEM AND LASER COLONY SCANNER FOR ENUMERATION OF MICROORGANISMS. *Journal of Food Safety*; **11**: 177-87 (1990).

129.   Zinn M, Witholt B, Egli T. Dual nutrient limited growth: models, experimental observations, and applications. *J Biotechnol*; **113**: 263-79 (2004).

130.   Ryge TS, Frimodt-Moller N, Hansen PR. Antimicrobial activities of twenty lysine-peptoid hybrids against clinically relevant bacteria and fungi. *Chemotherapy*; **54**: 152-6 (2008).

131.   McKay GA, Beaulieu S, Arhin FF *et al.* Time-kill kinetics of oritavancin and comparator agents against Staphylococcus aureus, Enterococcus faecalis and Enterococcus faecium. *J Antimicrob Chemother*; **63**: 1191-9 (2009).

132.   Rybak MJ, Cappelletty DM, Moldovan T *et al.* Comparative in vitro activities and postantibiotic effects of the oxazolidinone compounds eperezolid (PNU-100592) and linezolid (PNU-100766) versus vancomycin against Staphylococcus aureus, coagulase-negative staphylococci, Enterococcus faecalis, and Enterococcus faecium. *Antimicrob Agents Chemother*; **42**: 721-4 (1998).

133.   Bostic GD, Perri MB, Thal LA *et al.* Comparative in vitro and bactericidal activity of oxazolidinone antibiotics against multidrug-resistant enterococci. *Diagn Microbiol Infect Dis*; **30**: 109-12 (1998).

134.   Wise R, Andrews JM, Boswell FJ *et al.* The in-vitro activity of linezolid (U-100766) and tentative breakpoints. *J Antimicrob Chemother*; **42**: 721-8 (1998).

135.   Bulitta JB, Ly NS, Yang JC *et al.* Development and qualification of a pharmacodynamic model for the pronounced inoculum effect of ceftazidime against Pseudomonas aeruginosa. *Antimicrob Agents Chemother*; **53**: 46-56 (2009).

136.   Slee AM, Wuonola MA, McRipley RJ *et al.* Oxazolidinones, a new class of synthetic antibacterial agents: in vitro and in vivo activities of DuP 105 and DuP 721. *Antimicrob Agents Chemother*; **31**: 1791-7 (1987).

137.   Jones RN, Johnson DM, Erwin ME. In vitro antimicrobial activities and spectra of U-100592 and U-100766, two novel fluorinated oxazolidinones. *Antimicrob Agents Chemother*; **40**: 720-6 (1996).

138.   Gunderson BW, Ibrahim KH, Peloquin CA *et al.* Comparison of linezolid activities under aerobic and anaerobic conditions against methicillin-resistant Staphylococcus aureus and vancomycin-resistant Enterococcus faecium. *Antimicrob Agents Chemother*; **47**: 398-9 (2003).

139.   Petersen A, Chadfield MS, Christensen JP *et al.* Characterization of small-colony variants of Enterococcus faecalis isolated from chickens with amyloid arthropathy. *J Clin Microbiol*; **46**: 2686-91 (2008).

140.   Guerillot F, Carret G, Flandrois JP (1993). Mathematical model for comparison of time-killing curves. pp. 1685-9.

141.   Buerger C, Plock N, Dehghanyar P *et al.* Pharmacokinetics of unbound linezolid in plasma and tissue interstitium of critically ill patients after multiple dosing using microdialysis. *Antimicrob Agents Chemother*; **50**: 2455-63 (2006).

142.   Thallinger C, Buerger C, Plock N *et al.* Effect of severity of sepsis on tissue concentrations of linezolid. *J Antimicrob Chemother*; **61**: 173-6 (2008).

143.   Wiederhold NP, Coyle EA, Raad, II *et al.* Antibacterial activity of linezolid and vancomycin in an in vitro pharmacodynamic model of gram-positive catheter-related bacteraemia. *J Antimicrob Chemother*; **55**: 792-5 (2005).

144.   Zinner SH, Gilbert D, Lubenko IY *et al.* Selection of linezolid-resistant Enterococcus faecium in an in vitro dynamic model: protective effect of doxycycline. *J Antimicrob Chemother*; **61**: 629-35 (2008).

145.   Schmidt S, Sabarinath SN, Barbour A *et al.* (2009). Pharmacokinetic/Pharmacodynamic Modeling of the In Vitro Activity of Oxazolidinone Antimicobial Agents Against Methicillin-Resistant Staphylococcus aureus. pp. AAC.00633-09.

146.   Rayner CR, Forrest A, Meagher AK *et al.* Clinical pharmacodynamics of linezolid in seriously ill patients treated in a compassionate use programme. *Clin Pharmacokinet*; **42**: 1411-23 (2003).

147.   Swoboda S, Fritz S, Martignoni ME *et al.* Varying linezolid susceptibility of vancomycin-resistant Enterococcus faecium isolates during therapy: a case report. *J Antimicrob Chemother*; **56**: 787-9 (2005).

148.   LaPlante KL, Rybak MJ, Leuthner KD *et al.* Impact of Enterococcus faecalis on the bactericidal activities of arbekacin, daptomycin, linezolid, and tigecycline against methicillin-resistant Staphylococcus aureus in a mixed-pathogen pharmacodynamic model. *Antimicrob Agents Chemother*; **50**: 1298-303 (2006).

149.   Morales G, Picazo JJ, Baos E *et al.* Resistance to Linezolid Is Mediated by the cfr Gene in the First Report of an Outbreak of Linezolid-Resistant Staphylococcus aureus. *Clinical Infectious Diseases*; **50**: 821-5 (2010).

150.	Bourgeois-Nicolaos N, Massias L, Couson B *et al.* Dose dependence of emergence of resistance to linezolid in Enterococcus faecalis in vivo. *J Infect Dis*; **195**: 1480-8 (2007).

151.	Schulin T, Thauvin-Eliopoulos C, Moellering RC, Jr. *et al.* Activities of the oxazolidinones linezolid and eperezolid in experimental intra-abdominal abscess due to Enterococcus faecalis or vancomycin-resistant Enterococcus faecium. *Antimicrob Agents Chemother*; **43**: 2873-6 (1999).

152.	Moise PA, Castro RS, Sul C *et al.* Relationship of linezolid minimum inhibitory concentration and time to bacterial eradication in treatment for methicillin-resistant Staphylococcus aureus infection. *Ann Pharmacother*; **42**: 592-3 (2008).

153.	MacGowan AP, Reynolds R, Noel AR *et al.* Bacterial Strain-to-Strain Variation in Pharmacodynamic Index Magnitude, a Hitherto Unconsidered Factor in Establishing Antibiotic Clinical Breakpoints. *Antimicrob. Agents Chemother.*; **53**: 5181-4 (2009).

154.	Nikolaou M, Schilling AN, Vo G *et al.* Modeling of microbial population responses to time-periodic concentrations of antimicrobial agents. *Ann Biomed Eng*; **35**: 1458-70 (2007).

155.	dYvoire H, Maire PH. Dosage regimens of antibacterials - Implications of a pharmacokinetic pharmacodynamic model. *Clinical Drug Investigation*; **11**: 229-39 (1996).

156.	Firsov AA, Chernykh VM, Navashin SM. Quantitative analysis of antimicrobial effect kinetics in an in vitro dynamic model. *Antimicrob Agents Chemother*; **34**: 1312-7 (1990).

157.	Firsov AA, Vostrov SN, Shevchenko AA *et al.* Parameters of bacterial killing and regrowth kinetics and antimicrobial effect examined in terms of area under the concentration-time curve relationships: action of ciprofloxacin against Escherichia coli in an in vitro dynamic model. *Antimicrob Agents Chemother*; **41**: 1281-7 (1997).

158.	Lalonde RL. Pharmacokinetic-Pharmacodynamic Relationships of Cardiovascular Drugs. In: Derendorf, H, Hochhaus, G, eds. *Pharmacokinetic/Pharmacodynamic Correlation.* Boca Raton: CRC Press Inc., pp. 197-226; (1995).

159.	Shah PM (1981). Bactericidal activity of ceftazidime against Pseudomonas aeruginosa under conditions simulating serum pharmacokinetic. pp. 135-40.

160.	Regoes RR, Wiuff C, Zappala RM *et al.* Pharmacodynamic functions: a multiparameter approach to the design of antibiotic treatment regimens. *Antimicrob Agents Chemother*; **48**: 3670-6 (2004).

161.	Yano Y, Oguma T, Nagata H *et al.* Application of logistic growth model to pharmacodynamic analysis of in vitro bactericidal kinetics. *J Pharm Sci*; **87**: 1177-83 (1998).

162.	Katsube T, Yano Y, Yamano Y *et al.* Pharmacokinetic-pharmacodynamic modeling and simulation for bactericidal effect in an in vitro dynamic model. *J Pharm Sci*; **97**: 4108-17 (2008).

163.	Schuck EL, Dalhoff A, Stass H *et al.* Pharmacokinetic/pharmacodynamic (PK/PD) evaluation of a once-daily treatment using ciprofloxacin in an extended-release dosage form. *Infection*; **33 Suppl 2**: 22-8 (2005).

164.	Mouton JW, Vinks AA, Punt NC. Pharmacokinetic-pharmacodynamic modeling of activity of ceftazidime during continuous and intermittent infusion. *Antimicrob Agents Chemother*; **41**: 733-8 (1997).

165.	Chung P, McNamara PJ, Campion JJ *et al.* Mechanism-based pharmacodynamic models of fluoroquinolone resistance in Staphylococcus aureus. *Antimicrob Agents Chemother*; **50**: 2957-65 (2006).

166.	Campion JJ, Chung P, McNamara PJ *et al.* Pharmacodynamic modeling of the evolution of levofloxacin resistance in Staphylococcus aureus. *Antimicrob Agents Chemother*; **49**: 2189-99 (2005).

167.	Parente E, Brienza C, Ricciardi A *et al.* Growth and bacteriocin production by Enterococcus faecium DPC1146 in batch and continuous culture. *J Ind Microbiol Biotechnol*; **18**: 62-7 (1997).

168.	Rello J, Restrepo MI, Udy A *et al.* Dose Adjustment and Pharmacodynamic Considerations for Antibiotics in Severe Sepsis and Septic Shock. *Sepsis.* Springer Berlin Heidelberg, pp. 97-136; (2008).

169.	Ba BB, Arpin C, Bikie Bi Nso B *et al.* Activity of linezolid in an in vitro pharmacokinetic-pharmacodynamic model using different dosages and Staphylococcus aureus and Enterococcus faecalis strains with either a hypermutator phenotype or not. *Antimicrob Agents Chemother*; (2010).

170.	Whitehouse T, Cepeda JA, Shulman R *et al.* Pharmacokinetic studies of linezolid and teicoplanin in the critically ill. *J Antimicrob Chemother*; **55**: 333-40 (2005).

171.	Martinez S, Lopez M, Bernardo A. Thermal inactivation of Enterococcus faecium: effect of growth temperature and physiological state of microbial cells. *Lett Appl Microbiol*; **37**: 475-81 (2003).

172.	Micromath. Scientist for experimental data fitting, Scientist Handbook. Salt Lake City: (2005).

173.	Barrett JS. Population Pharmacokinetics. In: Schoenwald, RD, ed *Pharmacokinetics in drug discovery and development.* Boca Raton: CRC Press, pp. 315-56; (2002).

174.	Christie D. Resampling with Excel. *Teaching Statistics*; **26**: 9-14 (2004).

7 Appendix

7.1 Figures

// RBR modelling of static data

IndVars: C
DepVars: E2, E3, E4, E5, E6, E7, E8, E9, E10, E11
Params: Emax0, EC500, H0, a, b, z

//E is the effect at a specific time point (e.g. 2 h) over the range of LZD concentration 0.5-36.1 μg/mL

//Emax Model Coding:

E2=Emax2*C^h2/(EC502^h2+C^h2)
Emax2=Emax0*(1-exp(-a*t2))
EC502=EC500*(1-exp(-b*t2))
H2=H0*(1-exp(-z*t2))

E3=Emax3*C^h3/(EC503^h3+C^h3)
Emax3=Emax0*(1-exp(-a*t3))
EC503=EC500*(1-exp(-b*t3))
H3=H0*(1-exp(-z*t3))

E4=Emax4*C^h4/(EC504^h4+C^h4)
Emax4=Emax0*(1-exp(-a*t4))
EC504=EC500*(1-exp(-b*t4))
H4=H0*(1-exp(-z*t4))

E5=Emax5*C^h5/(EC505^h5+C^h5)
Emax5=Emax0*(1-exp(-a*t5))
EC505=EC500*(1-exp(-b*t5))
H5=H0*(1-exp(-z*t5))

E6=Emax6*C^h6/(EC506^h6+C^h6)
Emax6=Emax0*(1-exp(-a*t6))
EC506=EC500*(1-exp(-b*t6))
H6=H0*(1-exp(-z*t6))

E7=Emax7*C^h7/(EC507^h7+C^h7)
Emax7=Emax0*(1-exp(-a*t7))
EC507=EC500*(1-exp(-b*t7))
H7=H0*(1-exp(-z*t7))

E8=Emax8*C^h8/(EC508^h8+C^h8)
Emax8=Emax0*(1-exp(-a*t8))
EC508=EC500*(1-exp(-b*t8))
H8=H0*(1-exp(-z*t8))

E9=Emax9*C^h9/(EC509^h9+C^h9)
Emax9=Emax0*(1-exp(-a*t9))
EC509=EC500*(1-exp(-b*t9))
H9=H0*(1-exp(-z*t9))

E10=Emax10*C^h10/(EC5010^h10+C^h10)
Emax10=Emax0*(1-exp(-a*t10))
EC5010=EC500*(1-exp(-b*t10))
H10=H0*(1-exp(-z*t10))

```
E11=Emax11*C^h11/(EC5011^h11+C^h11)
Emax11=Emax0*(1-exp(-a*t11))
EC5011=EC500*(1-exp(-b*t11))
H11=H0*(1-exp(-z*t11))




//Initial Estimates and Conditions
t1=0.02
t2=1
t3=2
t4=4
t5=6
t6=8
t7=10
t8=12
t9=16
t10=20
t11=24
Emax0=43
EC500=2
a=0.1986
b=1.0707
H0=1.6711
z=1
```

Figure 50 Model script for RBR modelling of data from the static *in vitro* model (Emax model).

```
//RBR Modelling of static and dynamic bacterial concentrations including time variance of effect

IndVars: t
LaplaceVar: S
DepVars: E2, E3, E4, E5, E6, E7, E8, E9, E10, E11, E12
Params: Emax0, EC500, H0, a, b, z, keo

//Definition of C, static model

Ce2=0.53*(1-exp(-keo*t))
Ce3=1*(1-exp(-keo*t))
Ce4=2*(1-exp(-keo*t))
Ce5=3.9*(1-exp(-keo*t))
Ce6=8.6*(1-exp(-keo*t))
Ce7=17.2*(1-exp(-keo*t))
Ce8=36.1*(1-exp(-keo*t))

//Definition C, dynamic model

C9=Dose/V1*exp(-CL1/V1*t)
Ce9'=keo*(C9-Ce9)

INPUT10=(2*Dose/Tau)*(1-EXP((-TAU)*S))/S
DIST10=(1/(S+(CL1/V1))/V1)
CTRAN10=INPUT10*DIST10
C10=LAPLACEINVERSE(T, CTRAN10, S)
Ce10'=keo*(C10-Ce10)

INPUT11=(Dose/Tau)/S*(1-EXP((-TAU)*S))
DIST11=(1/(S+(CL2/V1))/V1)
CTRAN11=INPUT11*DIST11
```

```
C11=LAPLACEINVERSE(T, CTRAN11, S)
Ce11'= keo*(C11-Ce11)

INPUT12=(Dose/Tau)/S*(1-EXP((-TAU)*S))
DIST12=(A12/(S+ALPHA)+B12/(S+BETA))/DOSE
CTRAN12=INPUT12*DIST12
C12=LAPLACEINVERSE(T, CTRAN12, S)
Ce12'= keo*(C12-Ce12)


//Emax Model

Emax2=Emax0*(1-exp(-a*t))
H2=H0*(1-exp(-z*t))
EC502=EC500*(1-exp(-b*t))
E2=Emax2*(Ce2^h2)/(EC502^h2+Ce2^h2)

Emax3=Emax0*(1-exp(-a*t))
H3=H0*(1-exp(-z*t))
EC503=EC500*(1-exp(-b*t))
E3=Emax3*Ce3^h3/(EC503^h3+Ce3^h3)

Emax4=Emax0*(1-exp(-a*t))
H4=H0*(1-exp(-z*t))
EC504=EC500*(1-exp(-b*t))
E4=Emax4*Ce4^h4/(EC504^h4+Ce4^h4)

Emax5=Emax0*(1-exp(-a*t))
EC505=EC500*(1-exp(-b*t))
H5=H0*(1-exp(-z*t))
E5=Emax5*Ce5^h5/(EC505^h5+Ce5^h5)

Emax6=Emax0*(1-exp(-a*t))
EC506=EC500*(1-exp(-b*t))
H6=H0*(1-exp(-z*t))
E6=Emax6*Ce6^h6/(EC506^h6+Ce6^h6)

Emax7=Emax0*(1-exp(-a*t))
EC507=EC500*(1-exp(-b*t))
H7=H0*(1-exp(-z*t))
E7=Emax7*Ce7^h7/(EC507^h7+Ce7^h7)

Emax8=Emax0*(1-exp(-a*t))
EC508=EC500*(1-exp(-b*t))
H8=H0*(1-exp(-z*t))
E8=Emax8*Ce8^h8/(EC508^h8+Ce8^h8)

Emax9=Emax0*(1-exp(-a*t))
EC509=EC500*(1-exp(-b*t))
H9=H0*(1-exp(-z*t))
E9=Emax9*Ce9^h9/(EC509^h9+Ce9^h9)

Emax10=Emax0*(1-exp(-a*t))
EC5010=EC500*(1-exp(-b*t))
H10=H0*(1-exp(-z*t))
E10=Emax10*Ce10^h10/(EC5010^h10+Ce10^h10)

Emax11=Emax0*(1-exp(-a*t))
EC5011=EC500*(1-exp(-b*t))
H11=H0*(1-exp(-z*t))
E11=Emax11*Ce11^h11/(EC5011^h11+Ce11^h11)
```

```
Emax12=Emax0*(1-exp(-a*t))
EC5012=EC500*(1-exp(-b*t))
H12=H0*(1-exp(-z*t))
E12=Emax12*Ce12^h12/(EC5012^h12+Ce12^h12)


//Initial Estimates and Conditions
t=0
keo=0.2
Dose=600
Tau=0.5
V1=29.8
Ce9=0

// for t1/2=3.54 h
CL1=5.835
Ce10=0

// for t1/2=5
CL2=4.131
Ce11=0

A12=18.965
B12=11.035
Alpha=6.685
Beta=0.2155
Ce12=0

Emax0=43
EC500=1
a=0.3
b=0.2
H0=6
z=0.05
```

Figure 51 Model script for RBR modelling of data from the static and dynamic data together (indirect link model).

```
// Time-kill curve model for static data (basic model)
IndVars: T
DepVars: GC, N1, N2, N3, N4, N5, N6, N7
Params:  k0, GCmax, Emax, EC50, dk

//PK

C1=0.5
C2=1
C3=2
C4=4
C5=8
C6=16
C7=32


//PD

GC'=k0*(1-GC/GCmax)*GC
```

```
//PK-PD
// N is the bacterial concentration under different LZD concentrations

N1'=(k0*(1-N1/GCmax)-(Emax*C1/(EC50+C1))*(N1/(Nmin+N1))*(1-exp(-dk*T)))*N1
N2'=(k0*(1-N2/GCmax)-(Emax*C2/(EC50+C2))*(N2/(Nmin+N2))*(1-exp(-dk*T)))*N2
N3'=(k0*(1-N3/GCmax)-(Emax*C3/(EC50+C3))*(N3/(Nmin+N3))*(1-exp(-dk*T)))*N3
N4'=(k0*(1-N4/GCmax)-(Emax*C4/(EC50+C4))*(N4/(Nmin+N4))*(1-exp(-dk*T)))*N4
N5'=(k0*(1-N5/GCmax)-(Emax*C5/(EC50+C5))*(N5/(Nmin+N5))*(1-exp(-dk*T)))*N5
N6'=(k0*(1-N6/GCmax)-(Emax*C6/(EC50+C6))*(N6/(Nmin+N6))*(1-exp(-dk*T)))*N6
N7'=(k0*(1-N7/GCmax)-(Emax*C7/(EC50+C7))*(N7/(Nmin+N7))*(1-exp(-dk*T)))*N7



//Initial estimates and conditions

T=0
k0=1.1386
GC=1.165E006
GCmax=3.439E008
N1=1.271E006
N2=1.162E006
N3=1.121E006
N4=1.058E006
N5=1.008E006
N6=1.17E006
N7=1.17E006
Nmin=65000
Emax=2.0241
EC50=1.553
dk=2.0674
```

Figure 52 Model script for the basic time-kill curve model.

```
// Time-kill curve modelling of dynamic data
IndVars: T
LaplaceVar: S
DepVars: GC, N8, N9, N10, N11, C8, C9, C10, C11
Params:  k0, Emax, EC50, dk

//dynamic Model
//N8 – 1cmt, bolus, N9 – 1 cmt, infusion mit t=3.54 h D=1200mg, N10 – 1 cmt, infusion, t=5h, N11 -
2cmt, infusion


//PK - dynamic

C8=Dose/V1*exp(-CL1/V1*t)

INPUT9=(2*Dose/Tau)*(1-EXP((-TAU)*S))/S
DIST9=(1/(S+(CL1/V1))/V1)
CTRAN9=INPUT9*DIST9
C9=LAPLACEINVERSE(T, CTRAN9, S)

INPUT10=(Dose/Tau)/S*(1-EXP((-TAU)*S))
DIST10=(1/(S+(CL2/V1))/V1)
CTRAN10=INPUT10*DIST10
C10=LAPLACEINVERSE(T, CTRAN10, S)
```

```
INPUT11=(Dose/Tau)/S*(1-EXP((-TAU)*S))
DIST11=(A11/(S+ALPHA)+B11/(S+BETA))/DOSE
CTRAN11=INPUT11*DIST11
C11=LAPLACEINVERSE(T, CTRAN11, S)


//PD part

GC'=k0*(1-GC/GCmax)*GC


//PK-PD combination

N8'=(k0*(1-N8/GCmax)-(Emax*C8/(EC50+C8))*(N8/(Nmin+N8))*(1-exp(-dk*T)))*N8
N9'=(k0*(1-N9/GCmax)-(Emax*C9/(EC50+C9))*(N9/(Nmin+N9))*(1-exp(-dk*T)))*N9
N10'=(k0*(1-N10/GCmax)-(Emax*C10/(EC50+C10))*(N10/(Nmin+N10))*(1-exp(-dk*T)))*N10
N11'=(k0*(1-N11/GCmax)-(Emax*C11/(EC50+C11))*(N11/(Nmin+N11))*(1-exp(-dk*T)))*N11


//Initial estimates and conditions

T=0

Dose=600
Tau=0.5
V1=29.8

// for 1cmt, infusion and bolus with t1/2=3.54 h
CL1=5.835

// for 1cmt, infusion with t1/2=5 h
CL2=4.131

// for 2 cmt, infusion
A11=18.965
B11=11.035
Alpha=6.685
Beta=0.2155

//fixed values underlined in yellow

k0=1.1386
GC=1.23E006
GCmax=1.62E009

N8=7.37E005
N9=1.28E006
N10=0.802E006
N11=0.79E006

Nmin=65000
Emax=2.0241
EC50=0.347
dk=2.0674
```

**Figure 53 Model script for the final time-kill curve model.**
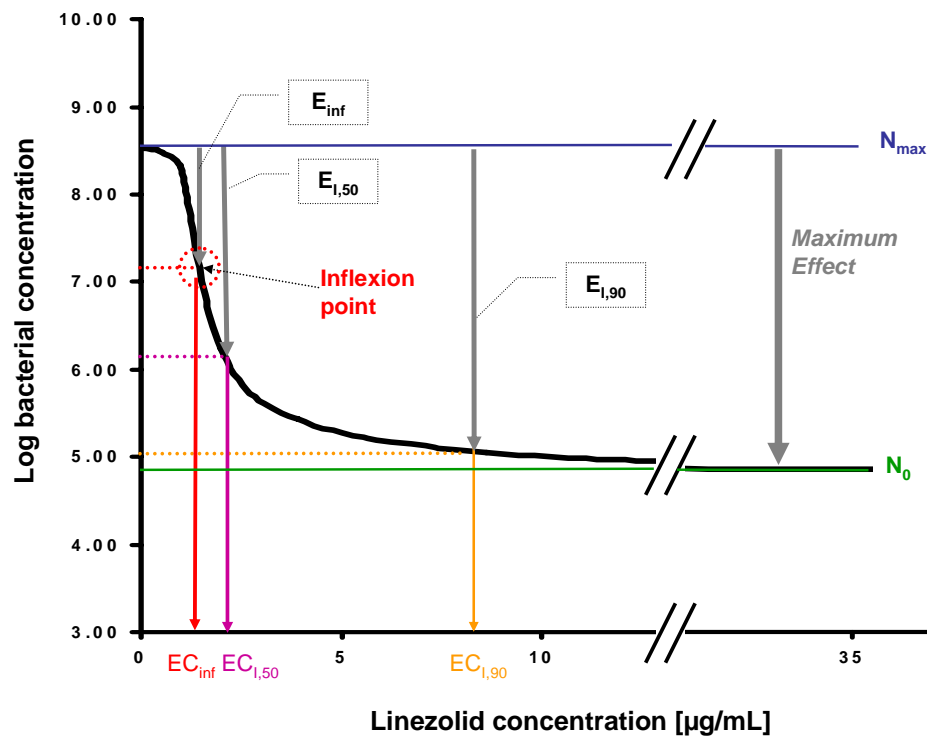
Figure 54 Schematic depiction of the curve of the inhibitory effect model and its characteristic parameters: N_{max} -maximum bacterial concentration, N_0 - minimum bacterial concentration, $E_{I,50}$ – half maximum effect, $EC_{I,50}$ – drug concentration with half maximum effect, $E_{I,90}$ – 90% of maximum effect, $EC_{I,90}$ – drug concentration with 90% of maximum effect, E_{inf} – effect at inflexion point, EC_{inf} – drug concentration, where inflexion of effect-concentration curve appears.

```
Sub PopPK_Sim_LZD_SD()

'data types
Dim t_PMs, t, t_s, t0, dt, t_(1 To 56), n, n0, Ntot, Numpoints, y, tau As Long '(long up to 10E9)

Dim t_1, A2, A3, A4, A2_(1 To 56), A3_(1 To 56), A4_(1 To 56), Cp, C3, Cl, V2, Q, V3, KA, ALAG1,
KIC, IC50, _
INH, IHN_1, R0, RX, R(1 To 56), TI, Ce, Ce_(1 To 56), keo, E_, E, E_1, E_2, Emax_, Emax_t,
Emax_t_2, EC50_, _
EC50_t, EC50_t_2, nf_, n_t, n_t_2, Emax, a_, EC50, b_, n_, z_, kA2_1_x, kA2_1_(1 To 56), _
kA3_1_x, kA3_1_(1 To 56), kA4_1_x, kA4_1_(1 To 56), kCe_1_x, kCe_1_(1 To 56), _
kA2_2_x, kA2_2_(1 To 56), kA3_2_x, kA3_2_(1 To 56), kA4_2_x, kA4_2_(1 To 56), kCe_2_x,
kCe_2_(1 To 56), _
kA2_3_x, kA2_3_(1 To 56), kA3_3_x, kA3_3_(1 To 56), kA4_3_x, kA4_3_(1 To 56), kCe_3_x,
kCe_3_(1 To 56), _
kA2_4_x, kA2_4_(1 To 56), kA3_4_x, kA3_4_(1 To 56), kA4_4_x, kA4_4_(1 To 56), kCe_4_x,
kCe_4_(1 To 56), AUCE As Single

'Parameter values


'PK-Parameter
```

```
'CL = 11.1 '[L/h]
Cl = 11.1 / 3600 '[L/s]
V2 = 20#  '[L]
'Q = 75 '[L/h]
Q = 75# / 3600  '[L/s]
V3 = 28.9 '[L]
'KA = 1.81 '[1/h]
'KA = 1.81 / 3600 '[1/s]
'ALAG1 = 1.27 '[h]
'ALAG1 = 1.27 * 3600 '[s]
'KIC = 0.0019 '[1/h]
KIC = 0.0019 / 3600 '[1/s]
IC50 = 0.1 '[mg/L]
RCLF = 0.764

'R0 = 1200 '[mg/h]
R0 = 1200# / 3600 '[mg/s]
'TI = 0.5 '[h]
TI = 0.5 * 3600 '[s]
tau = 12# * 3600 '[h]
'tau = 12 * 3600 '[s]
n0 = 1

'PD-Parameter:
'keo = 0.054 ' [1/h]
keo = 0.054 / 3600 '[1/s]
Emax = 42.733 ' [%]
EC50 = 1.765 ' [µg/mL]
n_ = 3.167
'a = 0.379 '[1/h]
a_ = 0.379 / 3600  '[1/s]
'b = 0.042 '[1/h]
b_ = 0.042 / 3600 '[1/s]
'z_ = 0.12 '[1/h]
z_ = 0.12 / 3600 '[1/s]

'Times
t0 = 0 '[s,h]
dt = 60 '[s]= 0.0167 '[h]

'Iterations
Ntot = 28
Numpoints = Ntot * (tau / dt) + 1
'Numpoints = 1000

'Initial values
n = n0
t_s = t0
t = t0
t_h_ = 0
t_PMs = t0

A2 = 0 '[mg]
A3 = 0 '[mg]
A4 = 0 '[mg]

A2_(1) = 0 '[mg]
A3_(1) = 0 '[mg]
A4_(1) = 0 '[mg]

RX = R0
```

```
R(1) = R0
R(2) = R0
R(3) = R0
R(4) = R0
R(5) = R0
R(6) = R0
R(7) = R0
R(8) = R0
R(9) = R0
R(10) = R0
R(11) = R0
R(12) = R0
R(13) = R0
R(14) = R0
R(15) = R0
R(16) = R0
R(17) = R0
R(18) = R0
R(19) = R0
R(20) = R0
R(21) = R0
R(22) = R0
R(23) = R0
R(24) = R0
R(25) = R0
R(26) = R0
R(27) = R0
R(28) = R0
R(29) = R0
R(30) = R0
R(31) = R0
R(32) = R0
R(33) = R0
R(34) = R0
R(35) = R0
R(36) = R0
R(37) = R0
R(38) = R0
R(39) = R0
R(40) = R0
R(41) = R0
R(42) = R0
R(43) = R0
R(44) = R0
R(45) = R0
R(46) = R0
R(47) = R0
R(48) = R0
R(49) = R0
R(50) = R0
R(51) = R0
R(52) = R0
R(53) = R0
R(54) = R0
R(55) = R0
R(56) = R0

Ce = 0 '[µg/mL]
E = 0 ' [%]
AUCE = 0
```

```
E_1 = 0
E_2 = 0

'Column names
  Range("A4").Value = "t_h_"
  Range("A4").Offset(0, 1).Value = "t_PMs"
  Range("A4").Offset(0, 2).Value = "n"
  Range("A4").Offset(0, 3).Value = "Cp"
  Range("A4").Offset(0, 4).Value = "Ce"
  Range("A4").Offset(0, 5).Value = "INH_1"
  Range("A4").Offset(0, 6).Value = "E"
  Range("A4").Offset(0, 7).Value = "Emax_t"
  Range("A4").Offset(0, 8).Value = "EC50_t"
  Range("A4").Offset(0, 9).Value = "n_t"
  Range("A4").Offset(0, 10).Value = "E_1"
  Range("A4").Offset(0, 11).Value = "E_2"
  Range("A4").Offset(0, 12).Value = "AUCE"


'For-Next Loop
  For I = 1 To Numpoints

    A2 = A2_(1) + A2_(2) + A2_(3) + A2_(4) + A2_(5) + A2_(6) + A2_(7) + A2_(8) + A2_(9) +
A2_(10) _
      + A2_(11) + A2_(12) + A2_(13) + A2_(14) + A2_(15) + A2_(16) + A2_(17) + A2_(18) + A2_(19)
+ A2_(20) _
      + A2_(21) + A2_(22) + A2_(23) + A2_(24) + A2_(25) + A2_(26) + A2_(27) + A2_(28) + A2_(29)
+ A2_(30) _
      + A2_(31) + A2_(32) + A2_(33) + A2_(34) + A2_(35) + A2_(36) + A2_(37) + A2_(38) + A2_(39)
+ A2_(40) _
      + A2_(41) + A2_(42) + A2_(43) + A2_(44) + A2_(45) + A2_(46) + A2_(47) + A2_(48) + A2_(49)
+ A2_(50) _
      + A2_(51) + A2_(52) + A2_(53) + A2_(54) + A2_(55) + A2_(56)


    A3 = A3_(1) + A3_(2) + A3_(3) + A3_(4) + A3_(5) + A3_(6) + A3_(7) + A3_(8) + A3_(9) +
A3_(10) _
      + A3_(11) + A3_(12) + A3_(13) + A3_(14) + A3_(15) + A3_(16) + A3_(17) + A3_(18) + A3_(19)
+ A3_(20) _
      + A3_(21) + A3_(22) + A3_(23) + A3_(24) + A3_(25) + A3_(26) + A3_(27) + A3_(28) + A3_(29)
+ A3_(30) _
      + A3_(31) + A3_(32) + A3_(33) + A3_(34) + A3_(35) + A3_(36) + A3_(37) + A3_(38) + A3_(39)
+ A3_(40) _
      + A3_(41) + A3_(42) + A3_(43) + A3_(44) + A3_(45) + A3_(46) + A3_(47) + A3_(48) + A3_(49)
+ A3_(50) _
      + A3_(51) + A3_(52) + A3_(53) + A3_(54) + A3_(55) + A3_(56)

    A4 = A4_(1) + A4_(2) + A4_(3) + A4_(4) + A4_(5) + A4_(6) + A4_(7) + A4_(8) + A4_(9) +
A4_(10) _
      + A4_(11) + A4_(12) + A4_(13) + A4_(14) + A4_(15) + A4_(16) + A4_(17) + A4_(18) + A4_(19)
+ A4_(20) _
      + A4_(21) + A4_(22) + A4_(23) + A4_(24) + A4_(25) + A4_(26) + A4_(27) + A4_(28) + A4_(29)
+ A4_(30) _
      + A4_(31) + A4_(32) + A4_(33) + A4_(34) + A4_(35) + A4_(36) + A4_(37) + A4_(38) + A4_(39)
+ A4_(40) _
      + A4_(41) + A4_(42) + A4_(43) + A4_(44) + A4_(45) + A4_(46) + A4_(47) + A4_(48) + A4_(49)
+ A4_(50) _
      + A4_(51) + A4_(52) + A4_(53) + A4_(54) + A4_(55) + A4_(56)


    Cp = A2 / V2
    C_3 = A3 / V3
```

```
Ce = Ce_(1) + Ce_(2) + Ce_(3) + Ce_(4) + Ce_(5) + Ce_(6) + Ce_(7) + Ce_(8) + Ce_(9) + Ce_(10) _
    + Ce_(11) + Ce_(12) + Ce_(13) + Ce_(14) + Ce_(15) + Ce_(16) + Ce_(17) + Ce_(18) + Ce_(19) +
Ce_(20) _
    + Ce_(21) + Ce_(22) + Ce_(23) + Ce_(24) + Ce_(25) + Ce_(26) + Ce_(27) + Ce_(28) + Ce_(29) +
Ce_(30) _
    + Ce_(31) + Ce_(32) + Ce_(33) + Ce_(34) + Ce_(35) + Ce_(36) + Ce_(37) + Ce_(38) + Ce_(39) +
Ce_(40) _
    + Ce_(41) + Ce_(42) + Ce_(43) + Ce_(44) + Ce_(45) + Ce_(46) + Ce_(47) + Ce_(48) + Ce_(49) +
Ce_(50) _
    + Ce_(51) + Ce_(52) + Ce_(53) + Ce_(54) + Ce_(55) + Ce_(56)

Emax_t = Emax * (1 - Exp(-a_ * t))
EC50_t = EC50 * (1 - Exp(-b_ * t))
n_t = n_ * (1 - Exp(-z_ * t))
E = (Emax_t * (Ce ^ n_t)) / ((EC50_t ^ n_t) + (Ce ^ n_t))
E_1 = E
AUCE = AUCE + (((E_1 + E_2) / 2) * dt)

    INH_1 = INH_(RCLF, A4, IC50)

    Range("A4").Offset(I, 0).Value = t_h_
    Range("A4").Offset(I, 1).Value = t_PMs
    Range("A4").Offset(I, 2).Value = n
    Range("A4").Offset(I, 3).Value = Cp
    Range("A4").Offset(I, 4).Value = Ce
    Range("A4").Offset(I, 5).Value = INH_1
    Range("A4").Offset(I, 6).Value = E
    Range("A4").Offset(I, 7).Value = Emax_t
    Range("A4").Offset(I, 8).Value = EC50_t
    Range("A4").Offset(I, 9).Value = n_t
    Range("A4").Offset(I, 10).Value = E_1
    Range("A4").Offset(I, 11).Value = E_2
    Range("A4").Offset(I, 12).Value = AUCE


  t_s = t_s + dt
  t = t_s
  t_h_ = t_h(t_s)
' Pace maker time
  t_PMs = t_PMs + dt
  If t_PMs >= tau Then
  t_PMs = 0
  n = n + 1
  End If
 If n > Ntot Then
Range("M3").Value = AUCE
End If

'nested loop
  For y = 1 To Ntot

  t_(y) = t - ((y - 1) * tau)

  If (y - 1) * tau >= t Then t_(y) = 0

A2_x = A2_(y)
A3_x = A3_(y)
A4_x = A4_(y)
RX = R(y)
R(y) = R0
```

```
Ce_x = Ce_(y)
If t_(y) > TI Then R(y) = 0


'4. order Runge-Kutta for solving coupled differential equations

kA2_1_x = dt * dA2dt(A2_x, A3_x, A4_x, RX, Q, V2, V3, Cl, INH_(RCLF, A4, IC50))
kA3_1_x = dt * dA3dt(A2_x, A3_x, A4_x, Q, V2, V3)
kA4_1_x = dt * dA4dt(A2_x, A3_x, A4_x, KIC, V2)
kCe_1_x = dt * dCedt(A2_x, A3_x, A4_x, Ce_x, keo, V2)

kA2_2_x = dt * dA2dt(A2_x + kA2_1_x / 2#, A3_x + kA3_1_x / 2#, A4_x + kA4_1_x / 2#, RX, Q, V2,
V3, Cl, INH_(RCLF, A4, IC50))
kA3_2_x = dt * dA3dt(A2_x + kA2_1_x / 2#, A3_x + kA3_1_x / 2#, A4_x + kA4_1_x / 2#, Q, V2, V3)
kA4_2_x = dt * dA4dt(A2_x + kA2_1_x / 2#, A3_x + kA3_1_x / 2#, A4_x + kA4_1_x / 2#, KIC, V2)
kCe_2_x = dt * dCedt(A2_x + kA2_1_x / 2#, A3_x + kA3_1_x / 2#, A4_x + kA4_1_x / 2#, Ce_x +
kCe_1_x / 2#, keo, V2)

kA2_3_x = dt * dA2dt(A2_x + kA2_2_x / 2#, A3_x + kA3_2_x / 2#, A4_x + kA4_2_x / 2#, RX, Q, V2,
V3, Cl, INH_(RCLF, A4, IC50))
kA3_3_x = dt * dA3dt(A2_x + kA2_2_x / 2#, A3_x + kA3_2_x / 2#, A4_x + kA4_2_x / 2#, Q, V2, V3)
kA4_3_x = dt * dA4dt(A2_x + kA2_2_x / 2#, A3_x + kA3_2_x / 2#, A4_x + kA4_2_x / 2#, KIC, V2)
kCe_3_x = dt * dCedt(A2_x + kA2_2_x / 2#, A3_x + kA3_2_x / 2#, A4_x + kA4_2_x / 2#, Ce_x +
kCe_2_x / 2#, keo, V2)

kA2_4_x = dt * dA2dt(A2_x + kA2_3_x, A3_x + kA3_3_x, A4_x + kA4_3_x, RX, Q, V2, V3, Cl,
INH_(RCLF, A4, IC50))
kA3_4_x = dt * dA3dt(A2_x + kA2_3_x, A3_x + kA3_3_x, A4_x + kA4_3_x, Q, V2, V3)
kA4_4_x = dt * dA4dt(A2_x + kA2_3_x, A3_x + kA3_3_x, A4_x + kA4_3_x, KIC, V2)
kCe_4_x = dt * dCedt(A2_x + kA2_3_x, A3_x + kA3_3_x, A4_x + kA4_3_x, Ce_x + kCe_3_x, keo, V2)

A2_(y) = A2_x + (kA2_1_x + 2 * (kA2_2_x + kA2_3_x) + kA2_4_x) / 6
A3_(y) = A3_x + (kA3_1_x + 2 * (kA3_2_x + kA3_3_x) + kA3_4_x) / 6
A4_(y) = A4_x + (kA4_1_x + 2 * (kA4_2_x + kA4_3_x) + kA4_4_x) / 6
Ce_(y) = Ce_x + (kCe_1_x + 2 * (kCe_2_x + kCe_3_x) + kCe_4_x) / 6



If (y - 1) * tau >= t Then
   A2_(y) = 0 '[mg]
   A3_(y) = 0 '[mg]
   A4_(y) = 0 '[mg]
   Ce_(y) = 0 '[µg/mL]
   End If

'Ce = Ce_(1) + Ce_(2) + Ce_(3) + Ce_(4) + Ce_(5) + Ce_(6) + Ce_(7) + Ce_(8) + Ce_(9) + Ce_(10) _
'      + Ce_(11) + Ce_(12) + Ce_(13) + Ce_(14) + Ce_(15) + Ce_(16) + Ce_(17) + Ce_(18) + Ce_(19) +
Ce_(20) _
'      + Ce_(21) + Ce_(22) + Ce_(23) + Ce_(24) + Ce_(25) + Ce_(26) + Ce_(27) + Ce_(28) + Ce_(29) +
Ce_(30) _
'      + Ce_(31) + Ce_(32) + Ce_(33) + Ce_(34) + Ce_(35) + Ce_(36) + Ce_(37) + Ce_(38) + Ce_(39) +
Ce_(40) _
'      + Ce_(41) + Ce_(42) + Ce_(43) + Ce_(44) + Ce_(45) + Ce_(46) + Ce_(47) + Ce_(48) + Ce_(49) +
Ce_(50) _
'      + Ce_(51) + Ce_(52) + Ce_(53) + Ce_(54) + Ce_(55) + Ce_(56)

Emax_t_2 = Emax * (1 - Exp(-a_ * (t - dt)))
EC50_t_2 = EC50 * (1 - Exp(-b_ * (t - dt)))
n_t_2 = n_ * (1 - Exp(-z_ * (t - dt)))
E_2 = (Emax_t_2 * (Ce ^ n_t_2)) / ((EC50_t_2 ^ n_t_2) + (Ce ^ n_t_2))


Next y
```

```
Next I

End Sub
```

Figure 55 Model script for deterministic effect simulations of various dosing regimens by an example of 600 mg twice a day over 14 days.
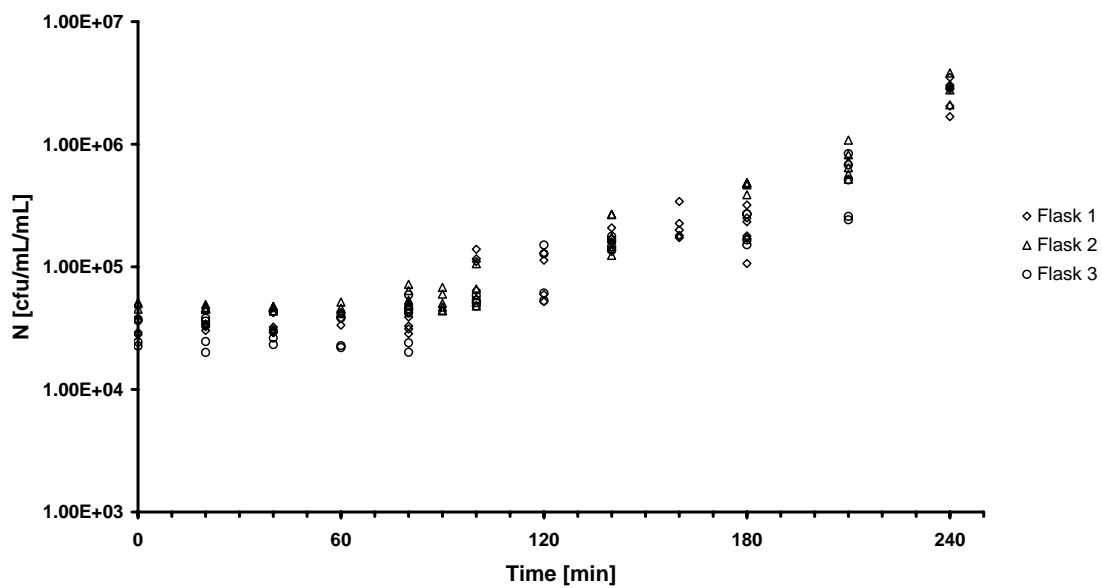
Figure 56 Observation of bacterial concentration after inoculation of medium to determine the lag-time of *E. faecium*; shown are single measurements per cell culture flask.
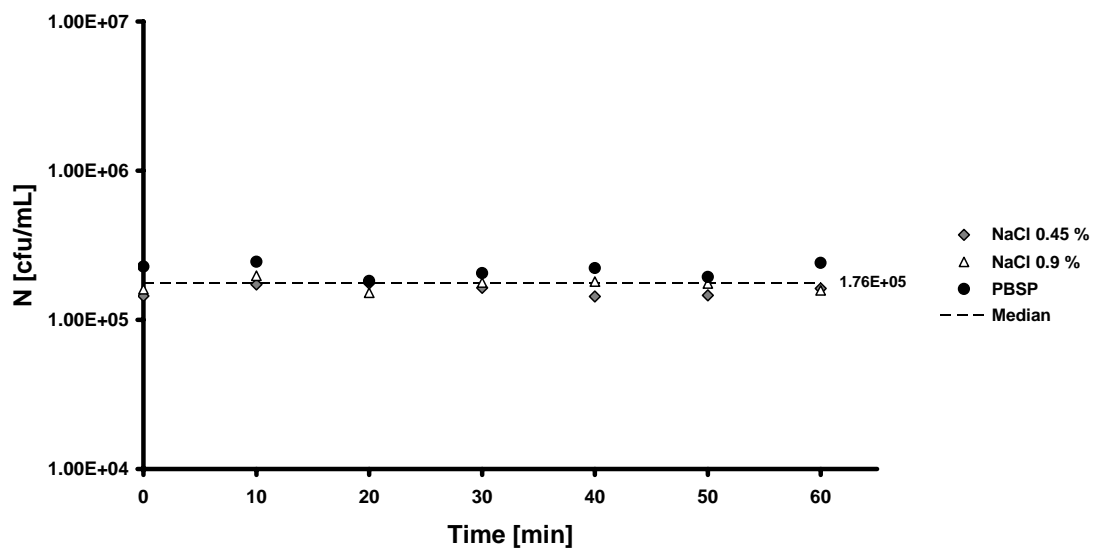
Figure 57 Bacterial survival in different dilution media over time; shown are geometric means of bacterial concentrations (n=3 cell culture flask each).
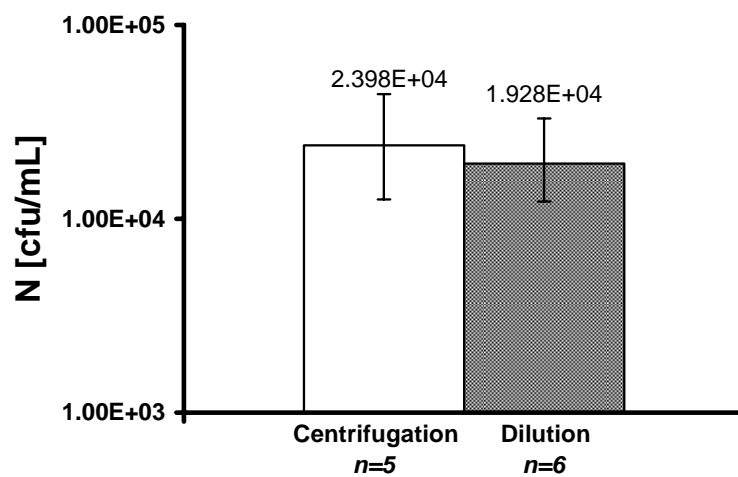
Figure 58 Comparison of centrifugation and dilution procedure for bacterial purification, shown are geometric means, error bars indicate minimum and maximum bacterial concentrations.
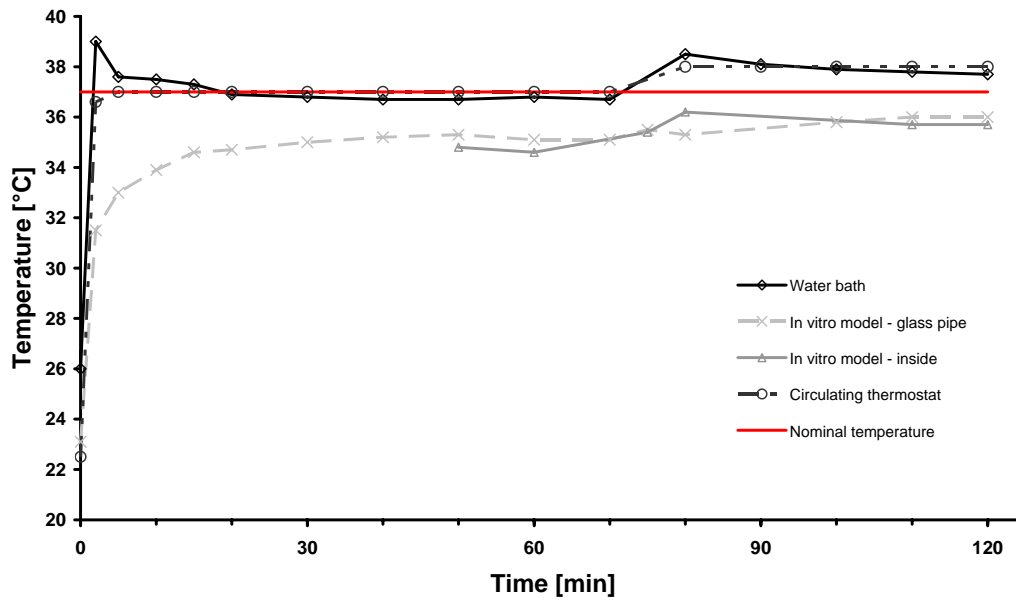
Figure 59 Progress of temperature in the dynamic *in vitro* model 1.
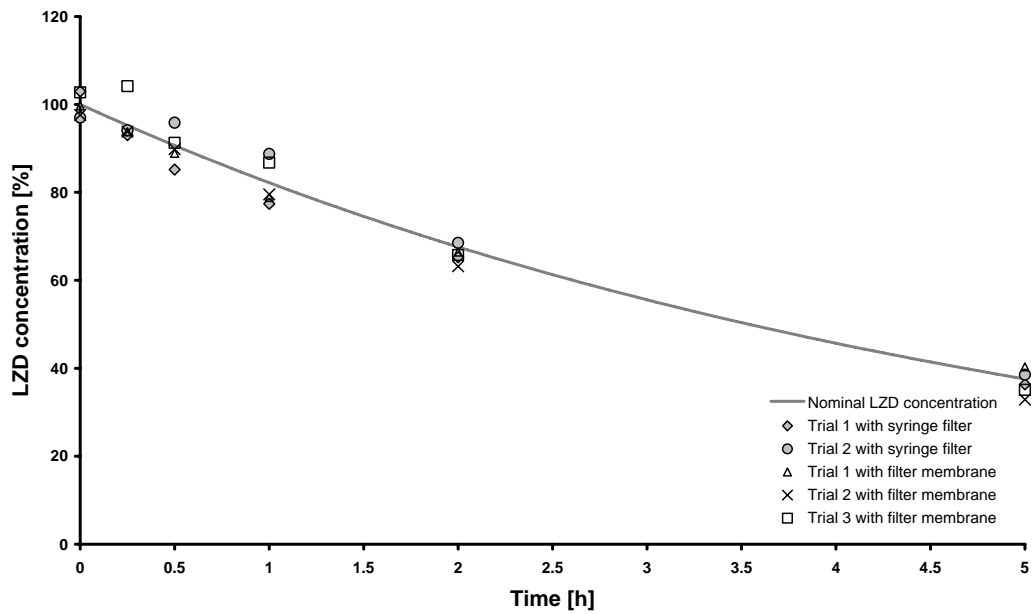
Figure 60 Comparison of the suitability of syringe and membrane filters for the simulation of LZD PK profiles.
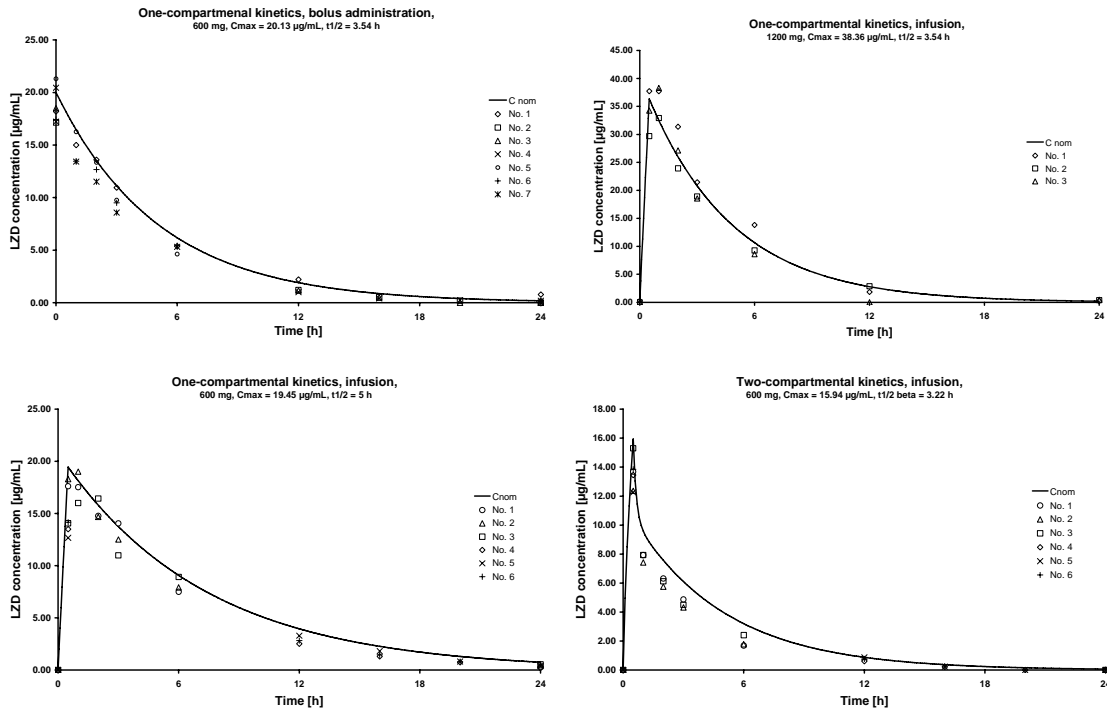
Figure 61 Single LZD concentrations in time kill experiments referring to nominal concentrations in the dynamic *in vitro* model.
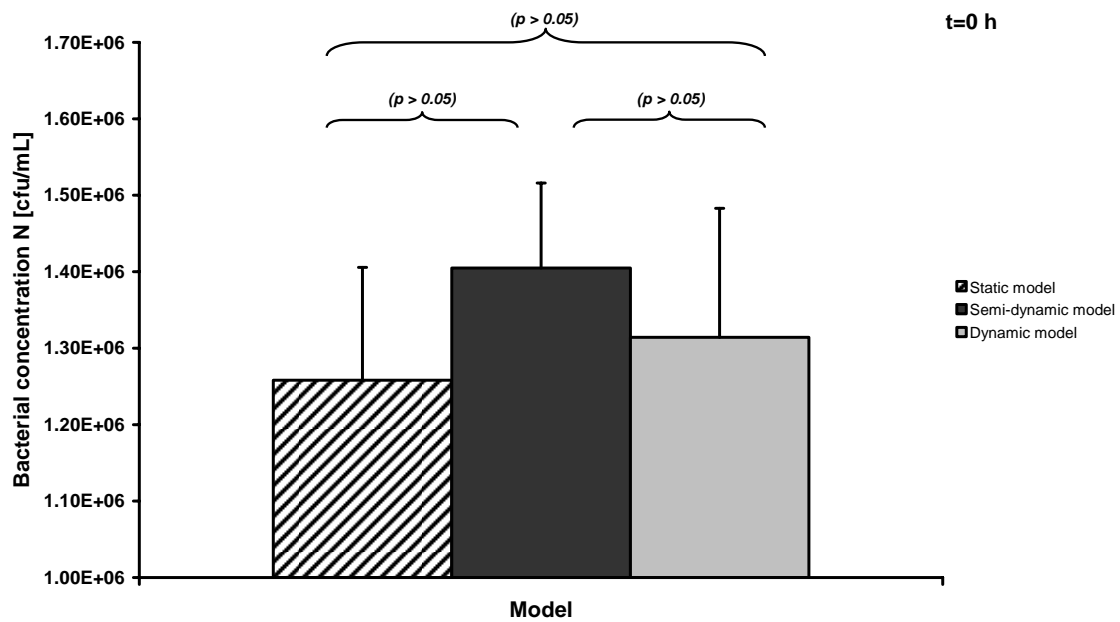
Figure 62 Differences between initial bacterial concentrations in the static, semi-dynamic and dynamic *in vitro* models (t = 0 h); shown are means + standard errors (error bars).

A

B

C
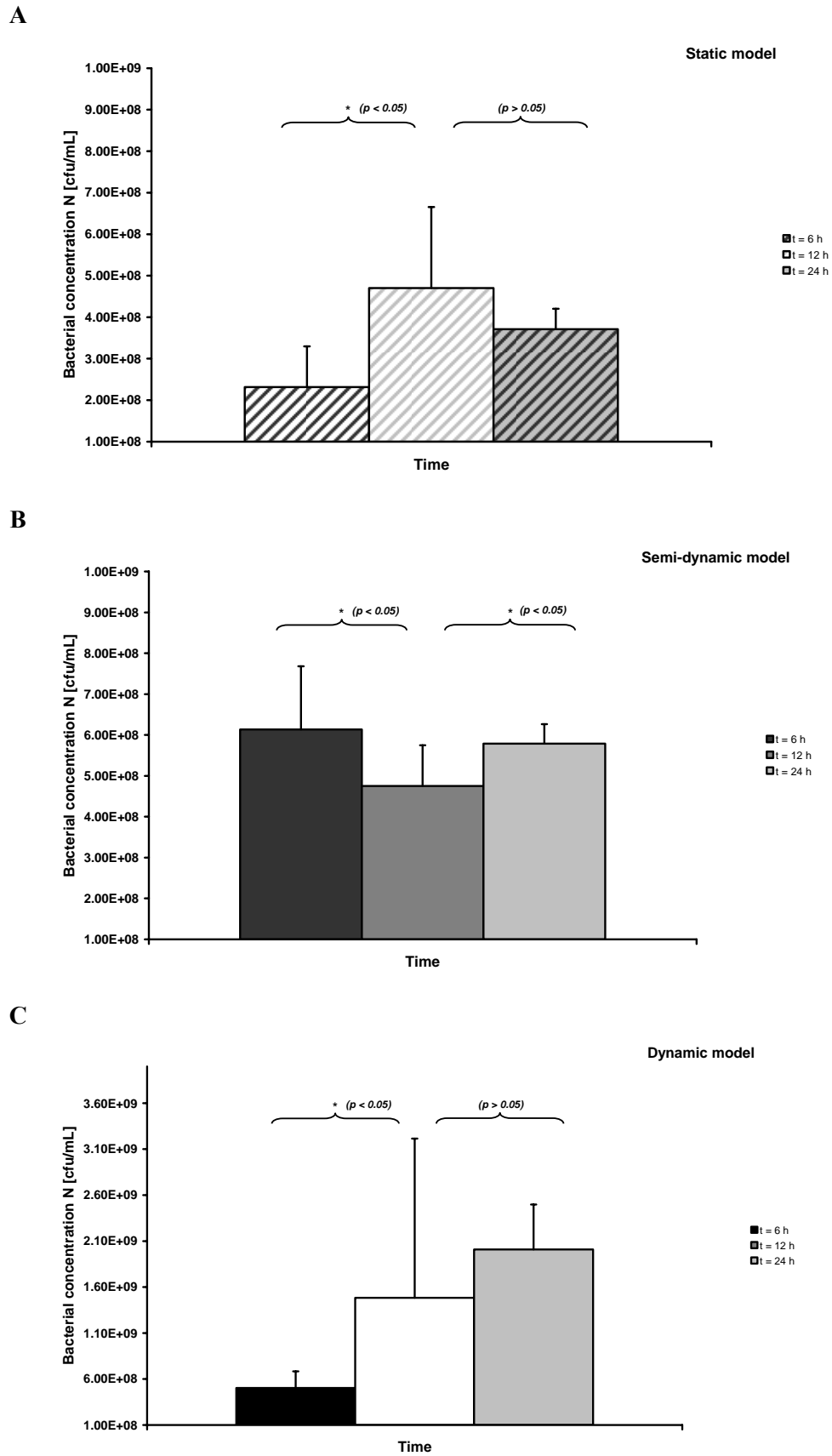
Figure 63 Comparison of bacterial concentrations over time (6, 12 and 24 h) in A) the static, B) the semi-dynamic and C) the dynamic *in vitro* model.
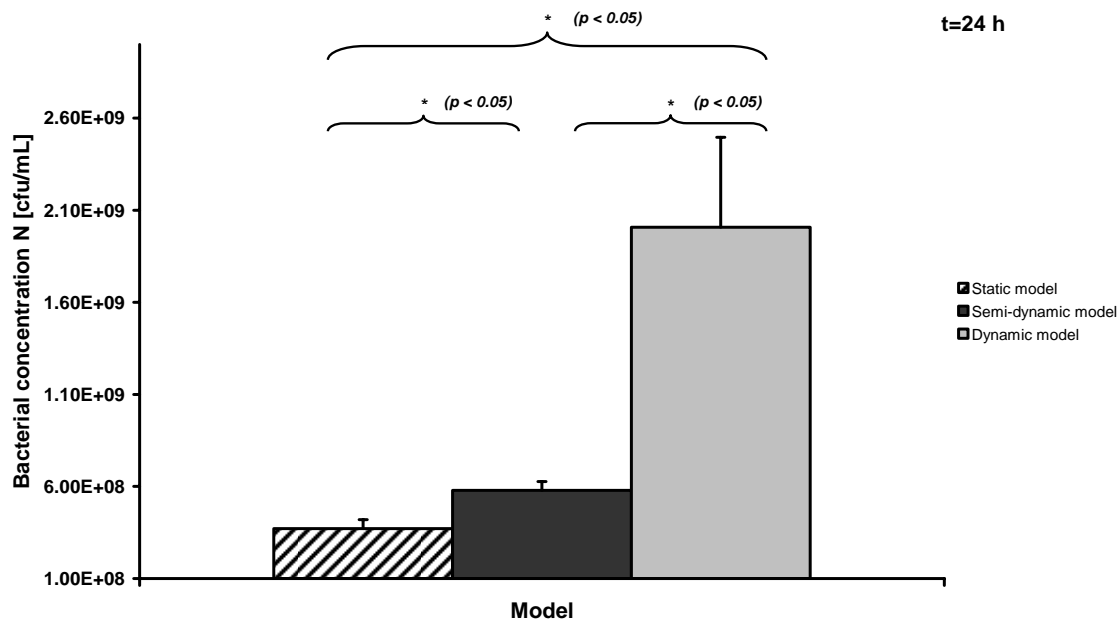
Figure 64 Differences between bacterial concentrations at the end of experiments (t=24 h) in the static, semi-dynamic and dynamic *in vitro* model, shown are means + standard errors (error bars).
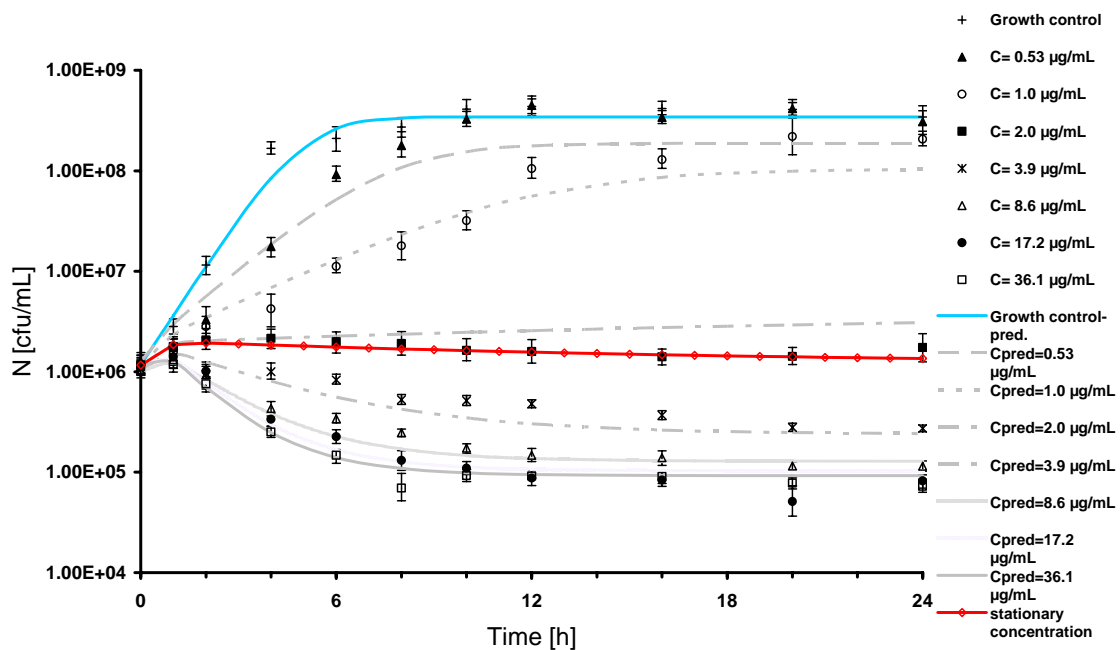
Figure 65 Bacterial concentration-time course under constant exposure of the stationary concentration (C=2.25 µg/mL) with the respective time-kill curves derived in the static model.
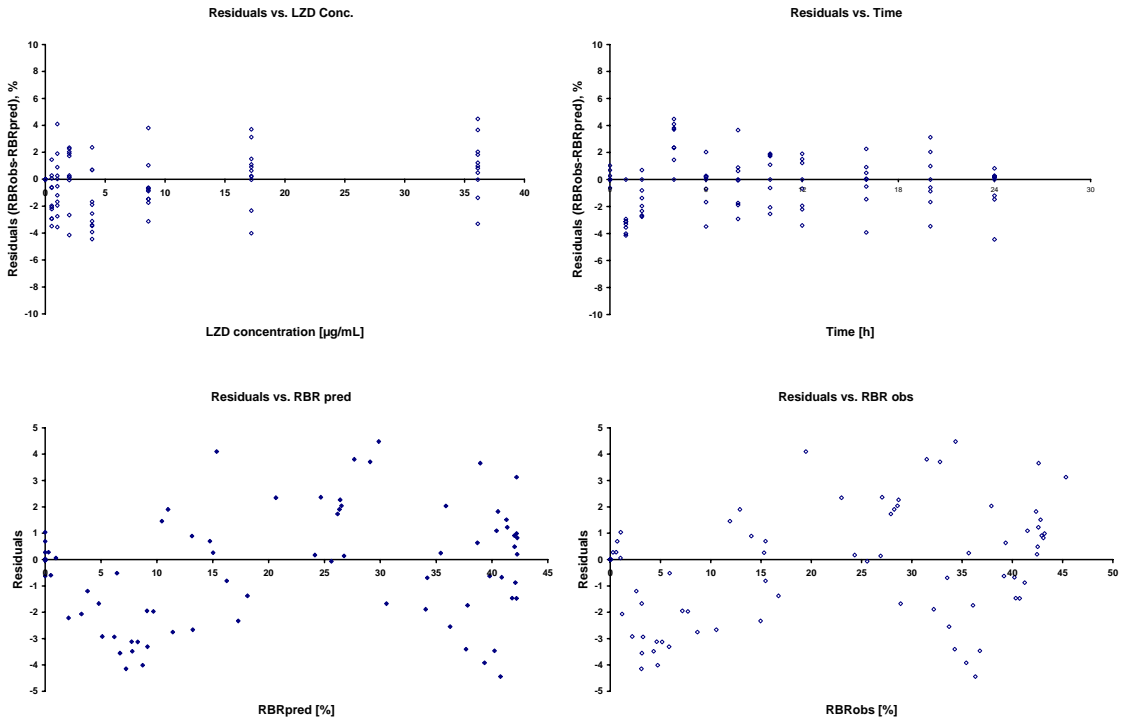
Figure 66 Residual plots for the basic RBR (sigmoidal E$_{max}$) model, shown are residuals between observed and model-predicted RBR values for the data of static model.
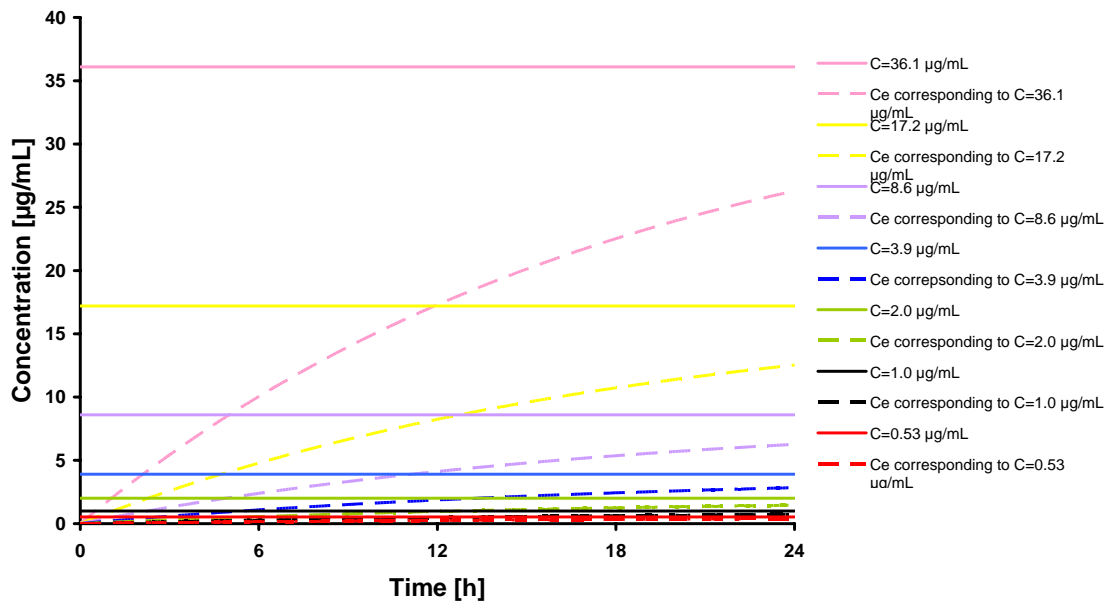
Figure 67 LZD concentrations in the static *in vitro* model and the respective effect compartmental concentrations assumed by the RBR model.
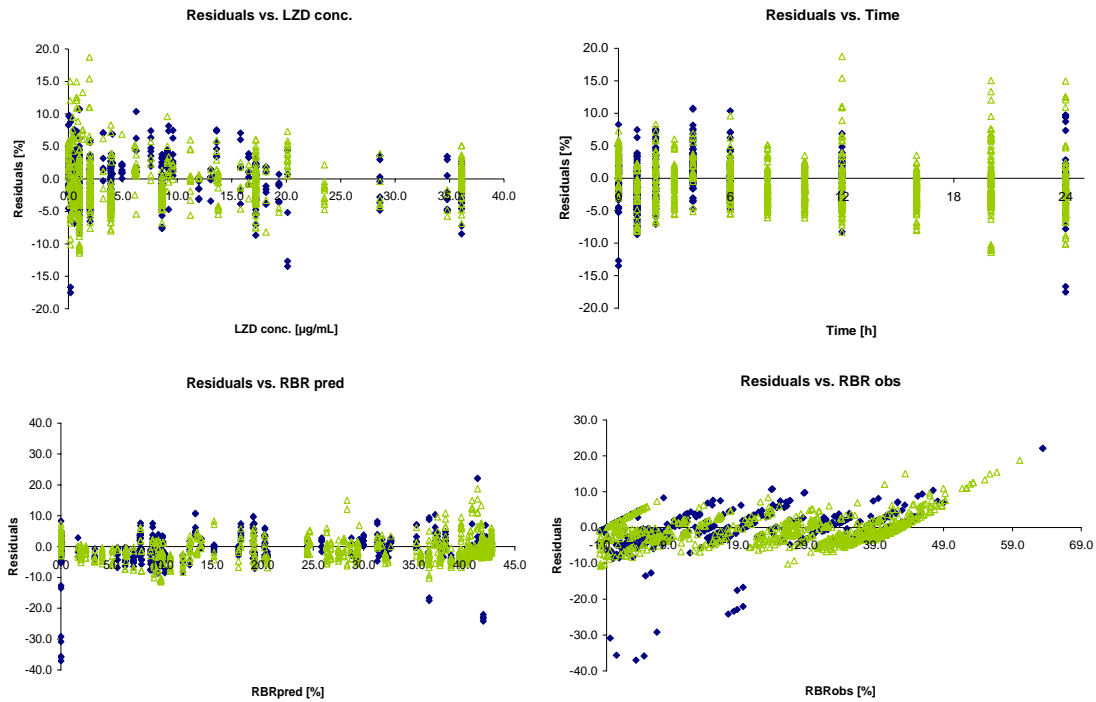
Figure 68 Residual plots for the final RBR (indirect link) model, shown are residuals between observed and model-predicted RBR values for the model data set (blue diamonds) and for the evaluation data set (green triangles).
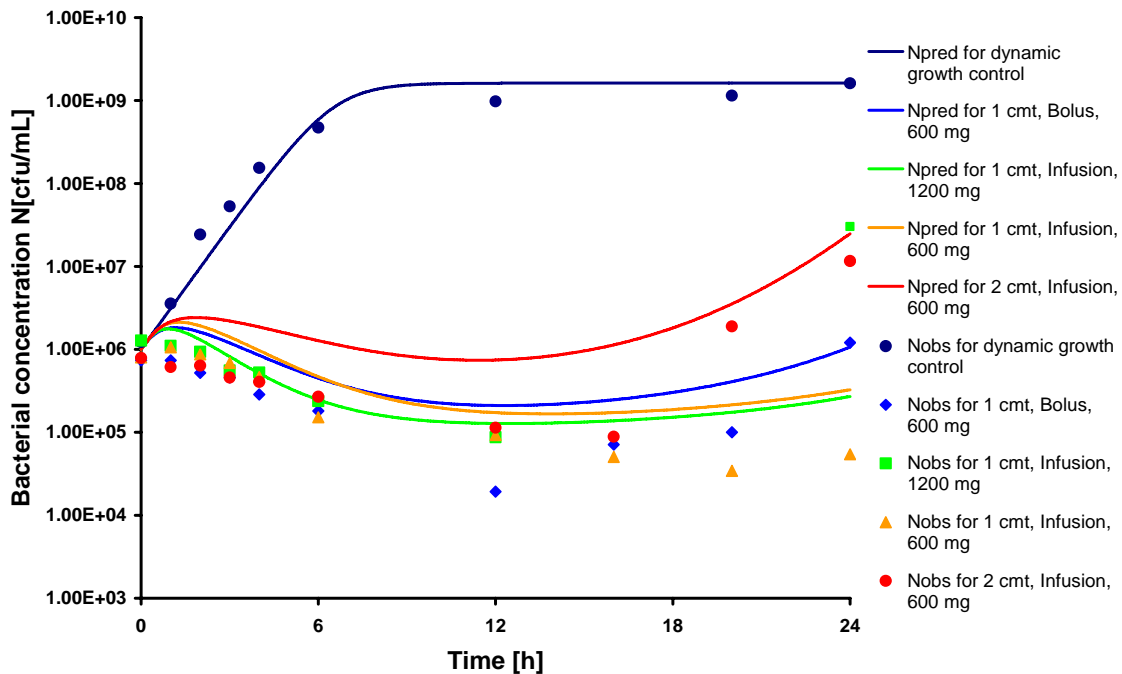
Figure 69 Modelling of time-kill curves using an indirect link model (E_{max} + effect compartment), shown are observed (single symbols) and model-predicted bacterial concentrations (full lines).
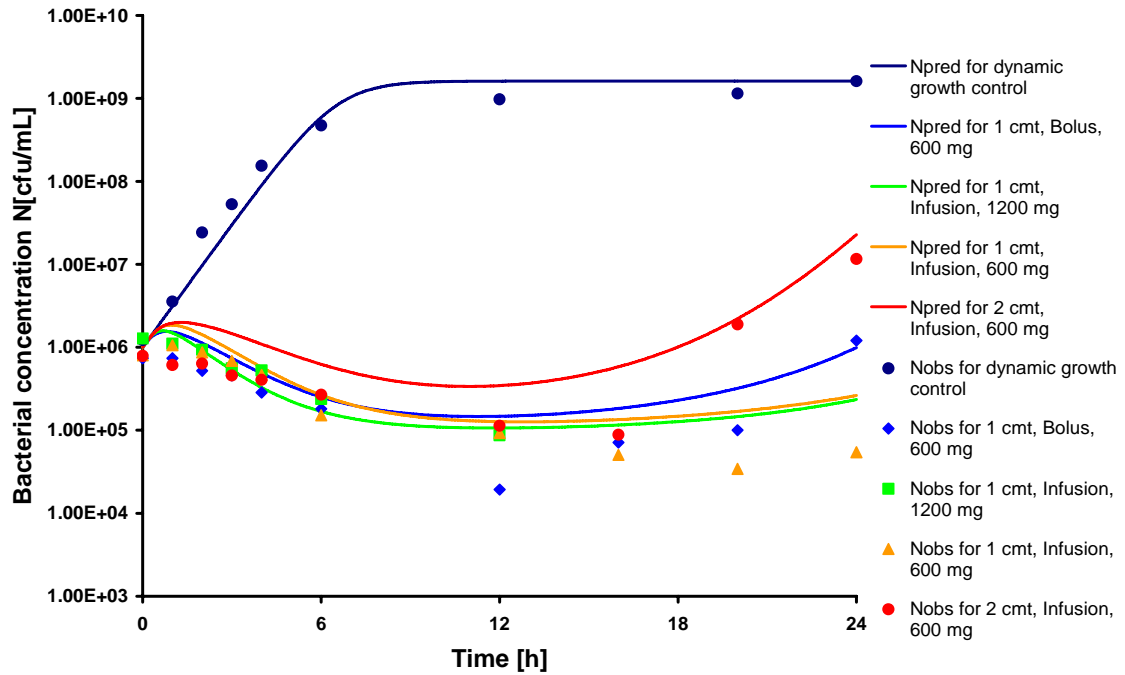
Figure 70 Modelling of time-kill curves using an indirect link model with Hill coefficient (sigmoidal E_{max} + effect compartment), shown are observed (single symbols) and model-predicted bacterial concentrations (full lines).
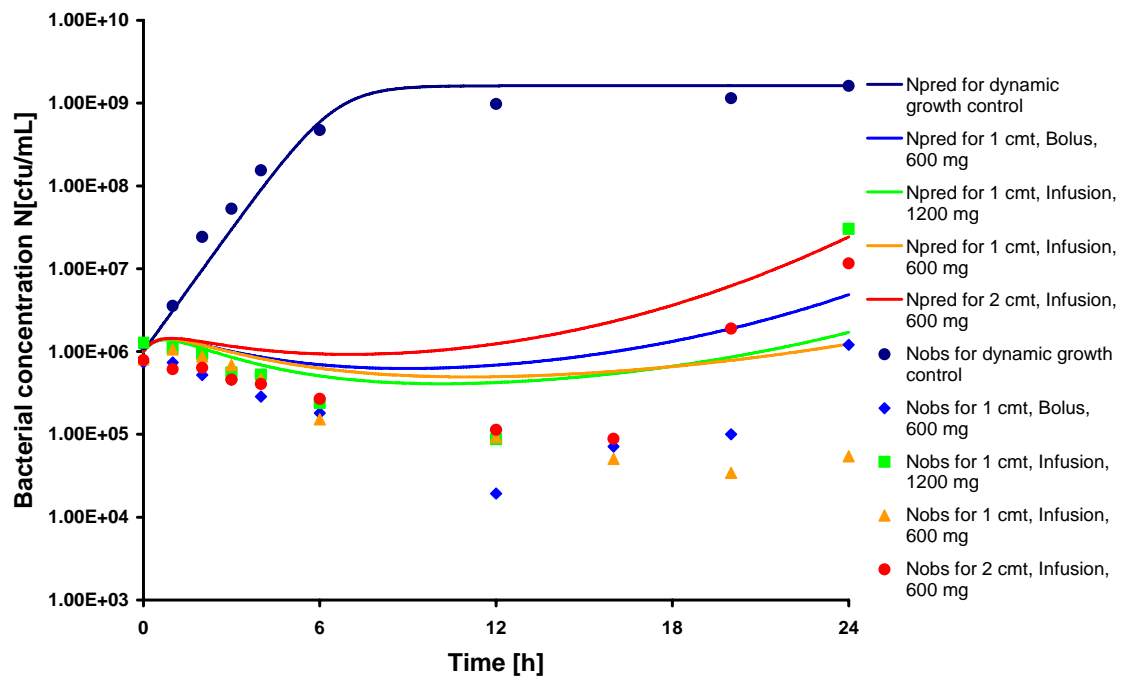
Figure 71 Modelling of time-kill curves using a sigmoidal E_{max} model, shown are observed (single symbols) and model-predicted bacterial concentrations (full lines).
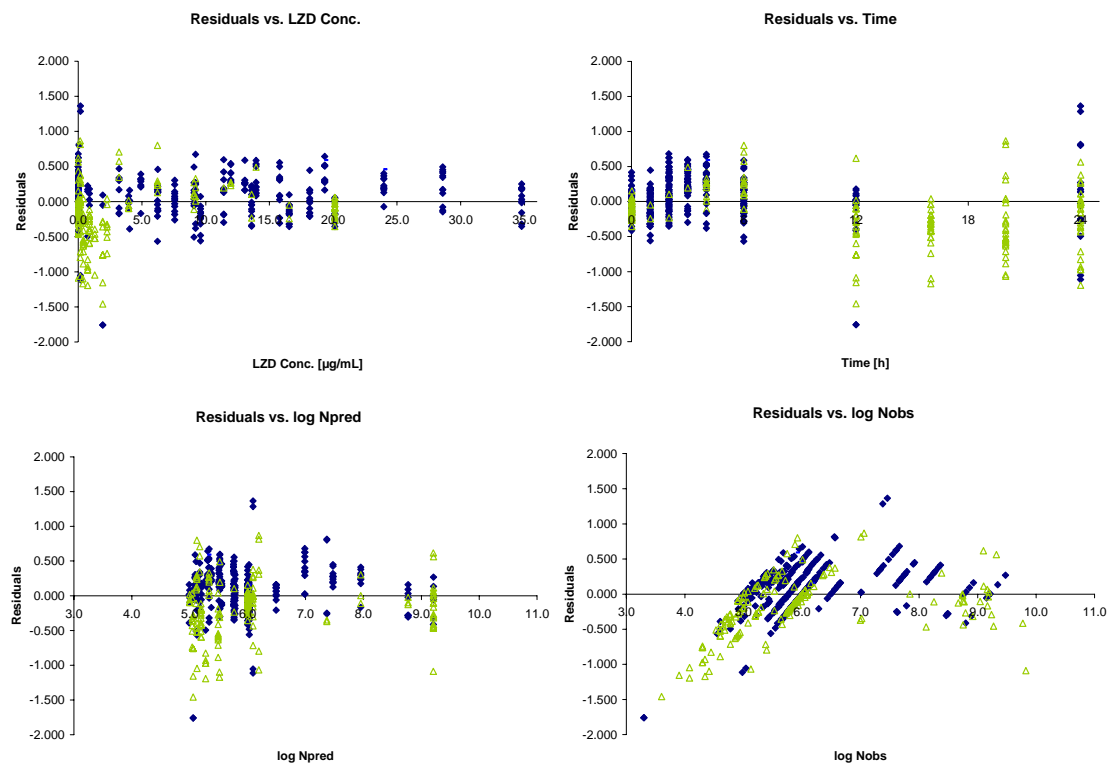
Figure 72 Residual plots for the final time-kill curve model, shown are residuals between logarithmic model-predicted and logarithmic observed values for the model data set (blue diamonds) and for the evaluation data set (green triangles).
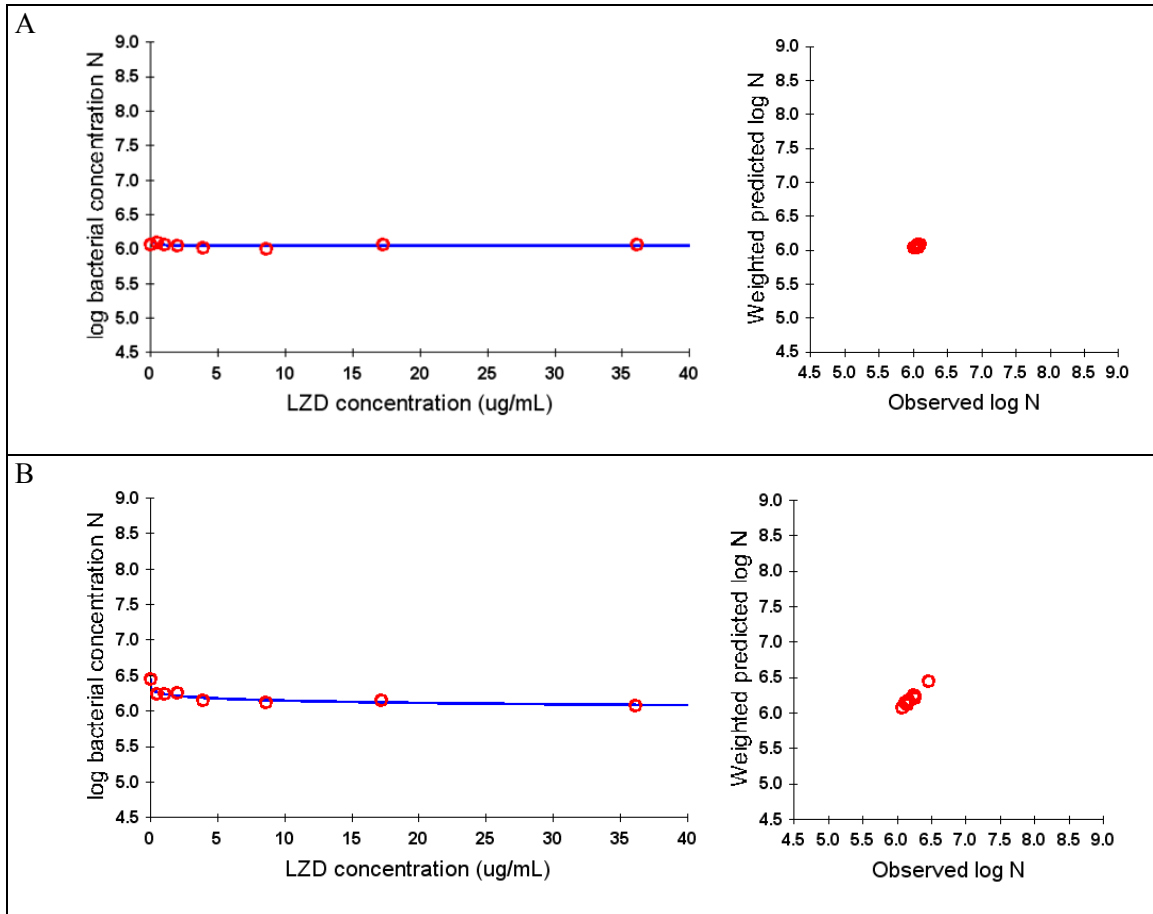
Figure 73 Left panel: Effect-drug concentration relationship for 0 and 1 h with red marks for observed logarithmic bacterial concentrations (static model) and blue line for model-predicted effect-concentration cause by the inhibitory effect model (effect at different time points); right panel: observed vs. model-predicted values (goodness of fit).
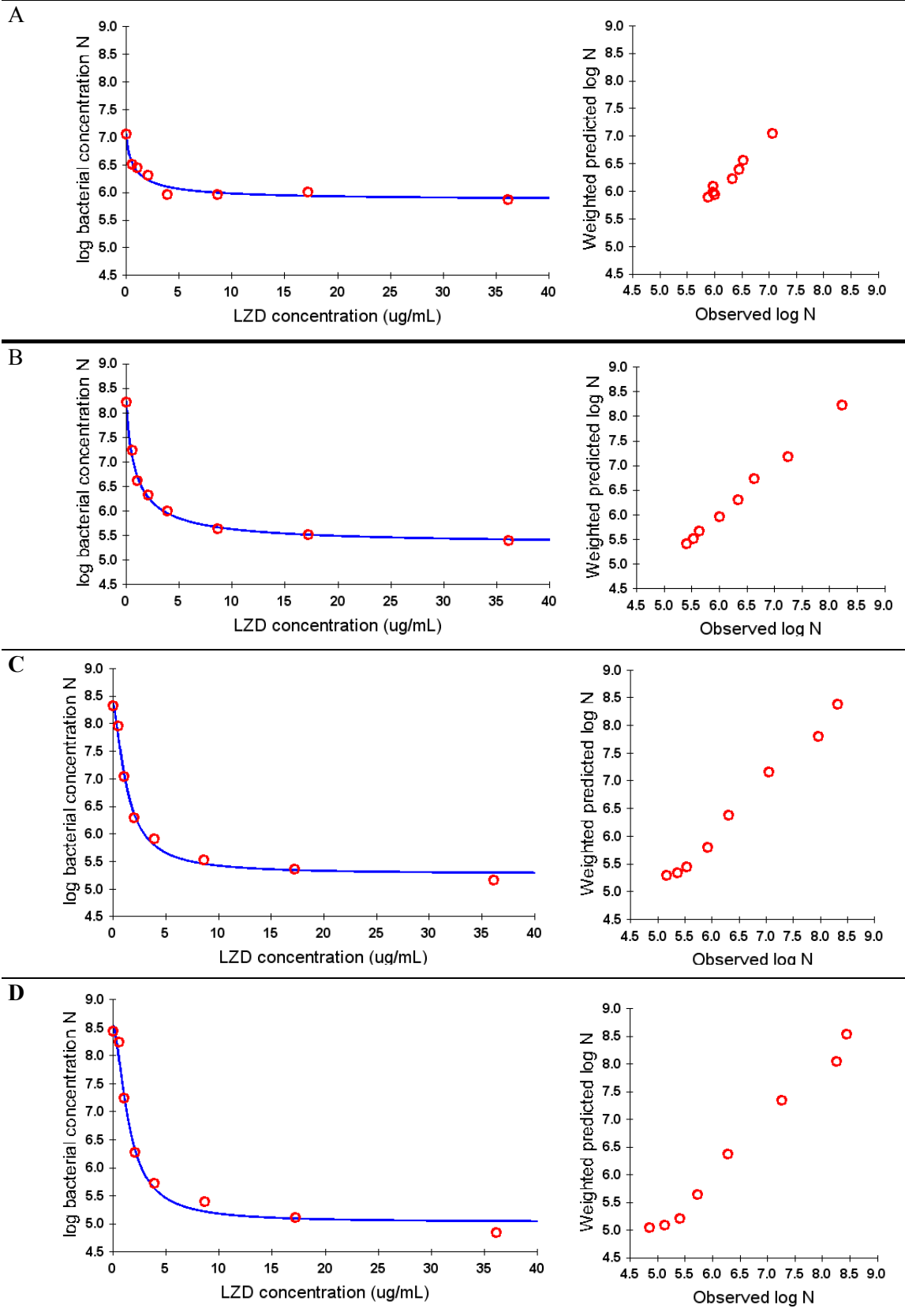
Figure 74 Effect at different time points modelling for A: 2 h, B: 4 h, C: 6 h, D: 8 h, E: 10 h, F: 12 h, G: 16 h and H: 20 h (left panel) with the respective goodness of fit plots (right panel) presenting model-predicted versus observed log bacterial concentrations.
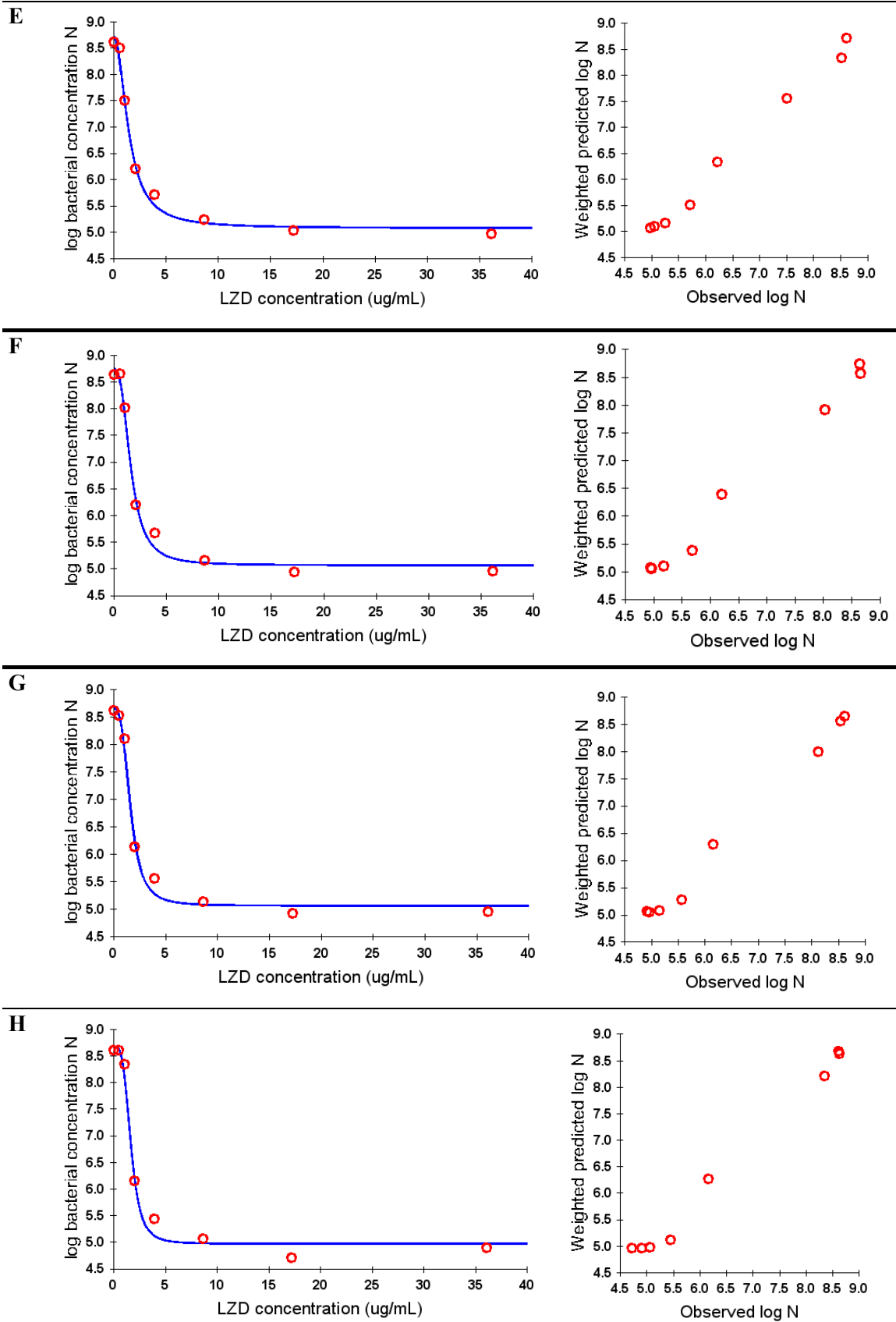
Figure 74 Effect at different time points modelling for A: 2 h, B: 4 h, C: 6 h, D: 8 h, E: 10 h, F: 12 h, G: 16 h and H: 20 h (left panel) with the respective goodness of fit plots (right panel) presenting model-predicted versus observed log bacterial concentrations. (continued)

Original inhibitory E$_{max}$ model for the effect at different time points $E_I(C)$:

$$E_I(C) = N_{max} - \frac{(N_{max} - N_0) \cdot C^H}{C^H + EC_{50}{}^H}$$

First derivative:

$$N_{max} - N_0 = a$$

$$EC_{50}{}^H = b$$

$$E_I(C) = N_{max} - \frac{a \cdot C^H}{C^H + b}$$

Apply quotient rule:
$$\left(\frac{u}{v}\right)' = \frac{u' \cdot v - u \cdot v'}{v^2}$$

$$u = -a \cdot C^H$$
$$u' = -a \cdot H \cdot C^{H-1}$$
$$v = C^H + b$$
$$v' = H \cdot C^{H-1}$$

$$E_I'(C) = \frac{-a \cdot H \cdot C^{H-1} \cdot (C^H + b) + a \cdot H \cdot C^{H-1} \cdot C^H}{(C^H + b)^2}$$

$$E_I'(C) = \frac{-a \cdot H \cdot C^{H-1} \cdot (C^H + b - C^H)}{(C^H + b)^2}$$

$$E_I'(C) = \frac{-a \cdot H \cdot C^{H-1} \cdot b}{(C^H + b)^2}$$

$$E_I'(C) = \frac{(N_0 - N_{max}) \cdot EC_{50}{}^H \cdot H \cdot C^{H-1}}{(C^H + EC_{50}{}^H)^2}$$

Second derivative:

$$E_I'(C) = \frac{-a \cdot H \cdot C^{H-1} \cdot b}{(C^H + b)^2}$$

Apply quotient rule, use
$$u = -a \cdot b \cdot H \cdot C^{H-1}$$
$$u' = -a \cdot b \cdot H \cdot (H-1) \cdot C^{H-2}$$
$$v = C^{2H} + 2 \cdot C^H \cdot b + b^2$$
$$v' = 2 \cdot H \cdot C^{2H-1} + 2 \cdot H \cdot b \cdot C^{H-1}$$

$$E_I''(C) = \frac{-a \cdot b \cdot H \cdot (H-1) \cdot C^{H-2} \cdot (C^{2H} + 2 \cdot C^H \cdot b + b^2) - (2 \cdot H \cdot C^{2H-1} + 2 \cdot H \cdot b \cdot C^{H-1}) \cdot (-a \cdot b \cdot H \cdot C^{H-1})}{(C^H + b)^4}$$

$$E_I''(C) = -a \cdot b \cdot H \cdot \frac{(H-1) \cdot C^{H-2} \cdot (C^{2H} + 2 \cdot C^H \cdot b + b^2) - 2 \cdot H \cdot C^{H-1} \cdot (C^{2H-1} + b \cdot C^{H-1})}{(C^H + b)^4}$$

$$E_I''(C) = -a \cdot b \cdot H \cdot \frac{(H-1) \cdot C^{H-2} \cdot (C^H + b)^2 - 2 \cdot H \cdot C^{H-1} \cdot (C^{2H-1} + b \cdot C^{H-1})}{(C^H + b)^4}$$

$$E_I''(C) = (N_0 - N_{max}) \cdot EC_{50}{}^H \cdot H \cdot \frac{(H-1) \cdot C^{H-2} \cdot (C^H + EC_{50}{}^H)^2 - 2 \cdot H \cdot C^{H-1} \cdot (C^{2H-1} + EC_{50}{}^H \cdot C^{H-1})}{(C^H + EC_{50}{}^H)^4}$$

Figure 75 Derivation of the second derivative of the inhibitory E_{max} model for the effect at different time points.
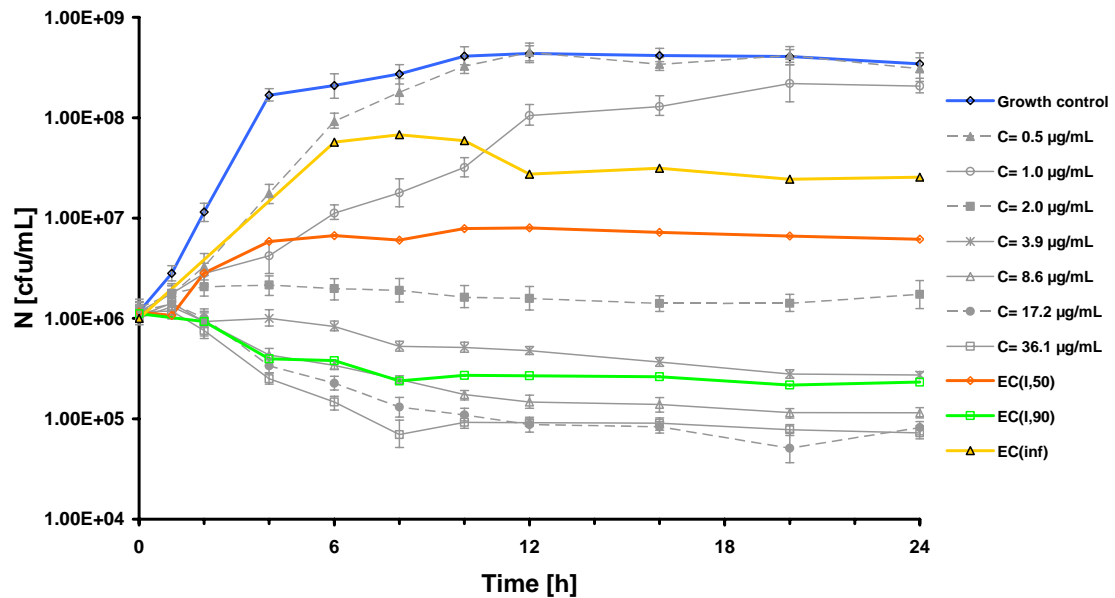
Figure 76 Bacterial concentration-time course under constant LZD concentrations at the height of $EC_{I,50}$, $EC_{I,90}$ and EC_{inf} compared to time-kill curves in the static model.
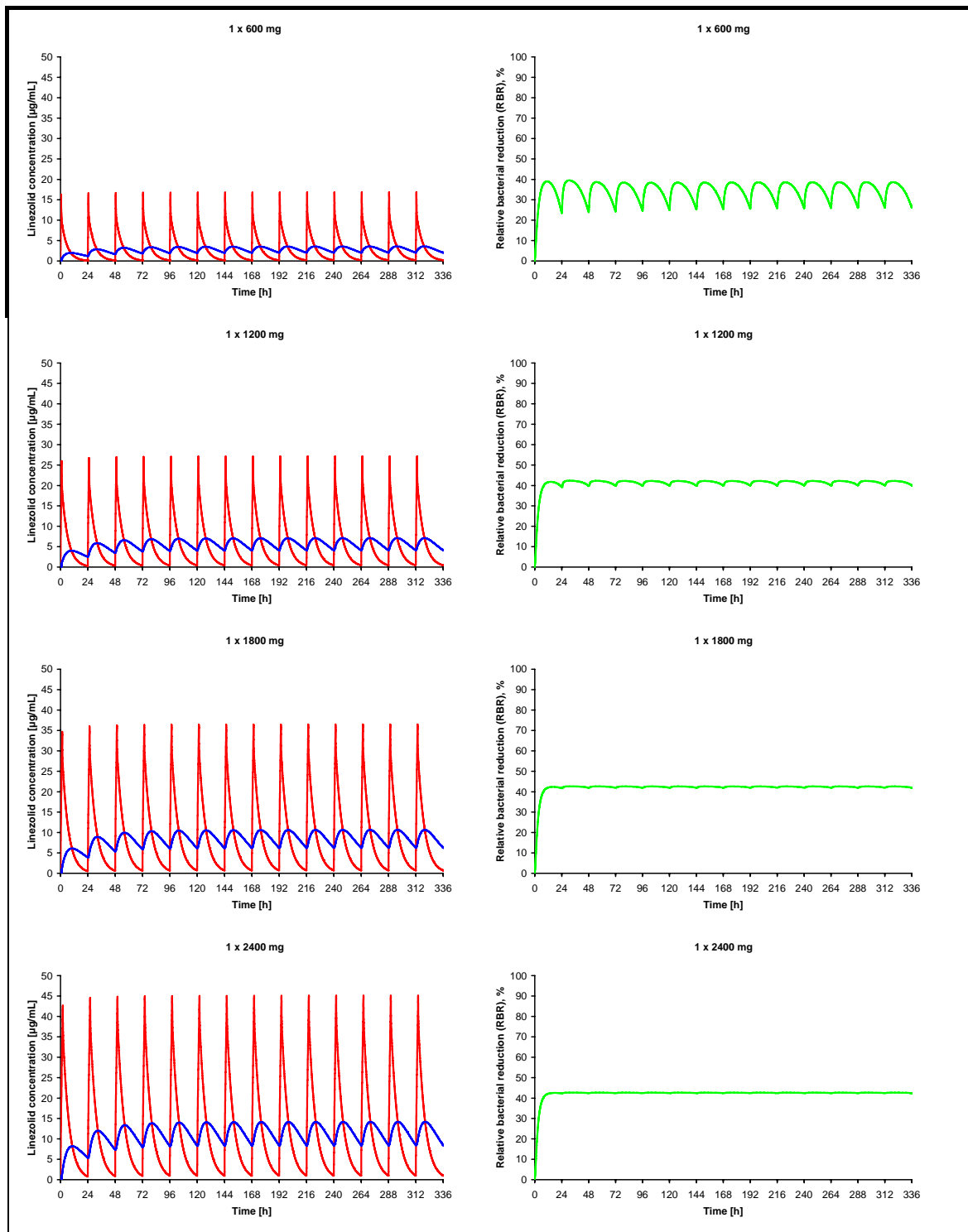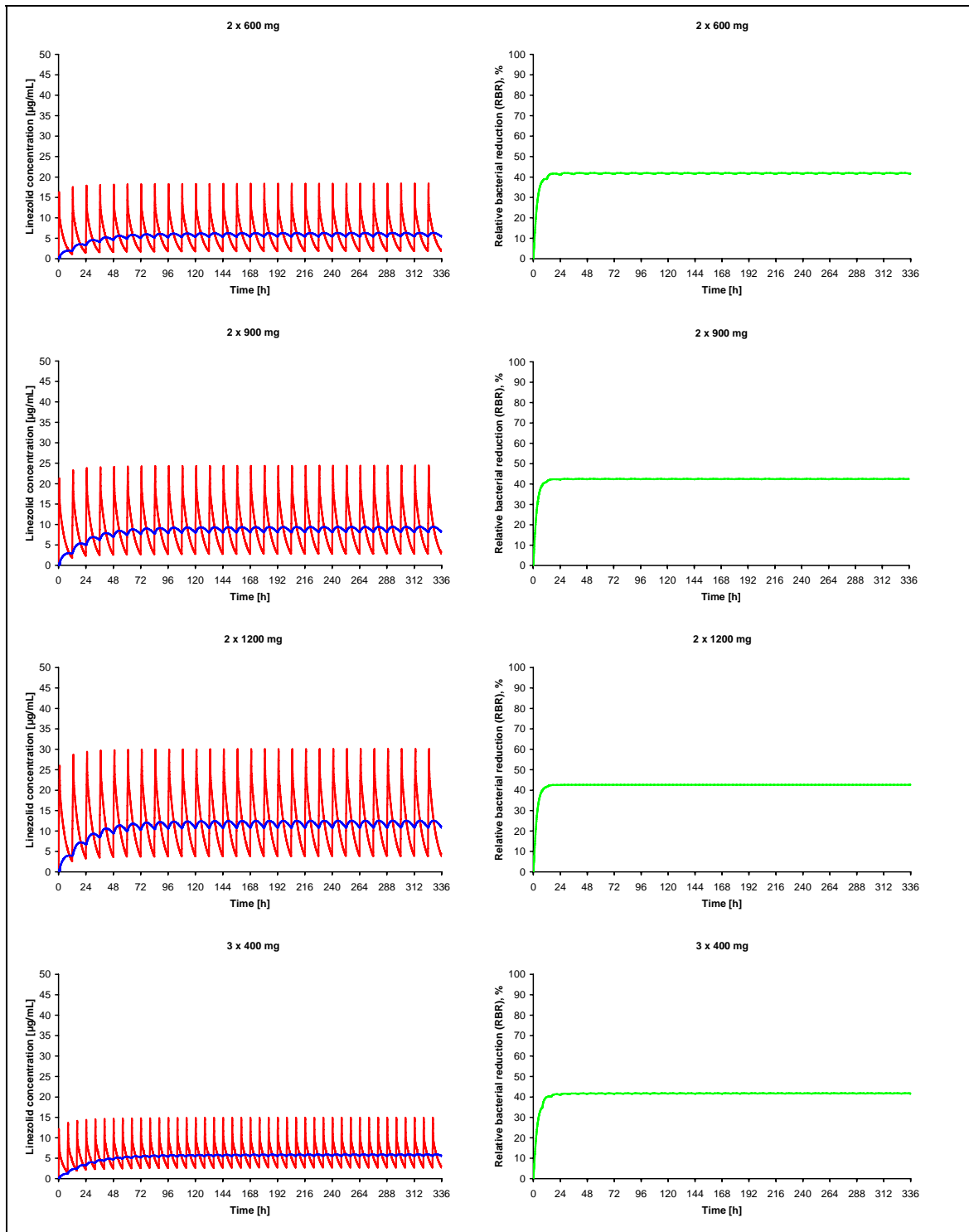
Figure 77 Deterministic simulations of dosing regimens: The left panel shows the LZD concentration-time course in plasma (red) and the effect compartment (blue). The right panel shows the resulting effect-time course.

Figure 77 Deterministic simulations of dosing regimens: The left panel shows the LZD concentration-time course in plasma (red) and the effect compartment (blue). The right panel shows the resulting effect-time course.

Figures

Figure 77 Deterministic simulations of dosing regimens: The left panel shows the LZD concentration-time course in plasma (red) and the effect compartment (blue). The right panel shows the resulting effect-time course.(continued)

146
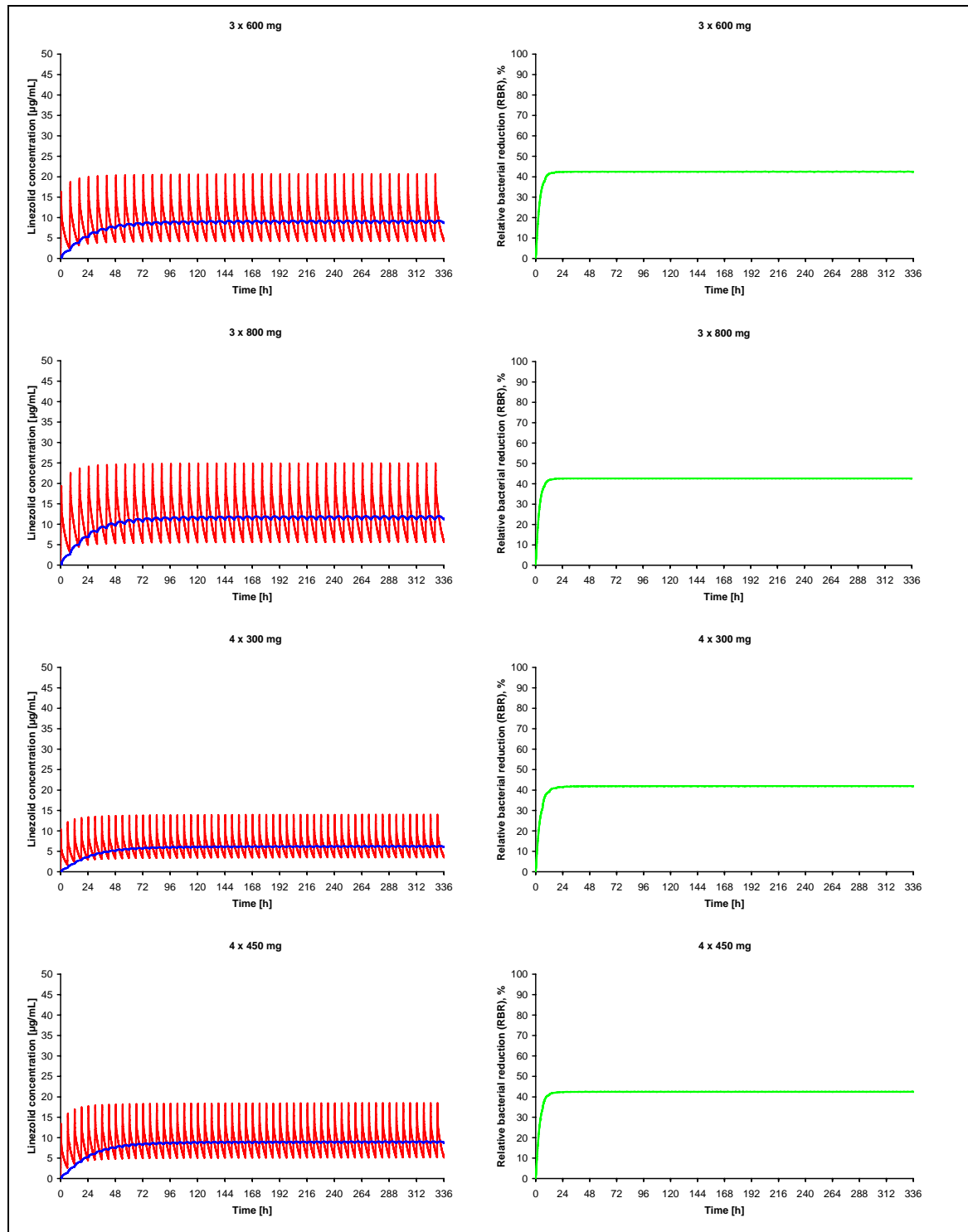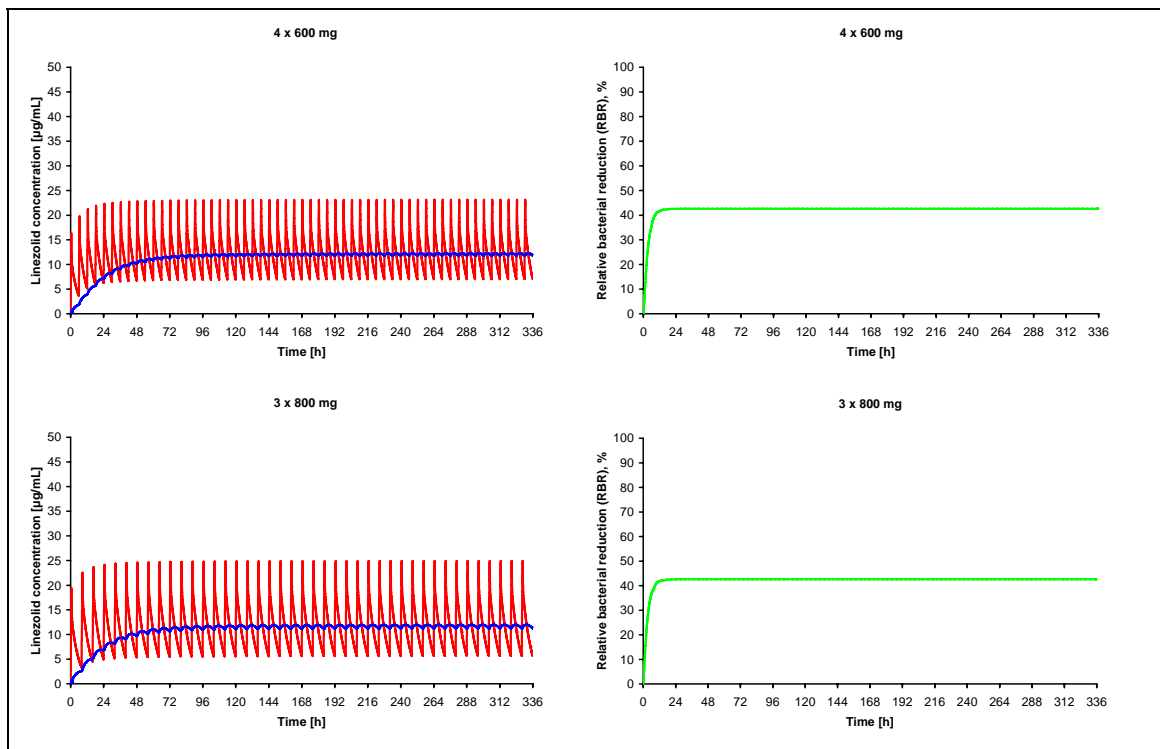
Figure 77 Deterministic simulations of dosing regimens: The left panel shows the LZD concentration-time course in plasma (red) and the effect compartment (blue). The right panel shows the resulting effect-time course. (continued)
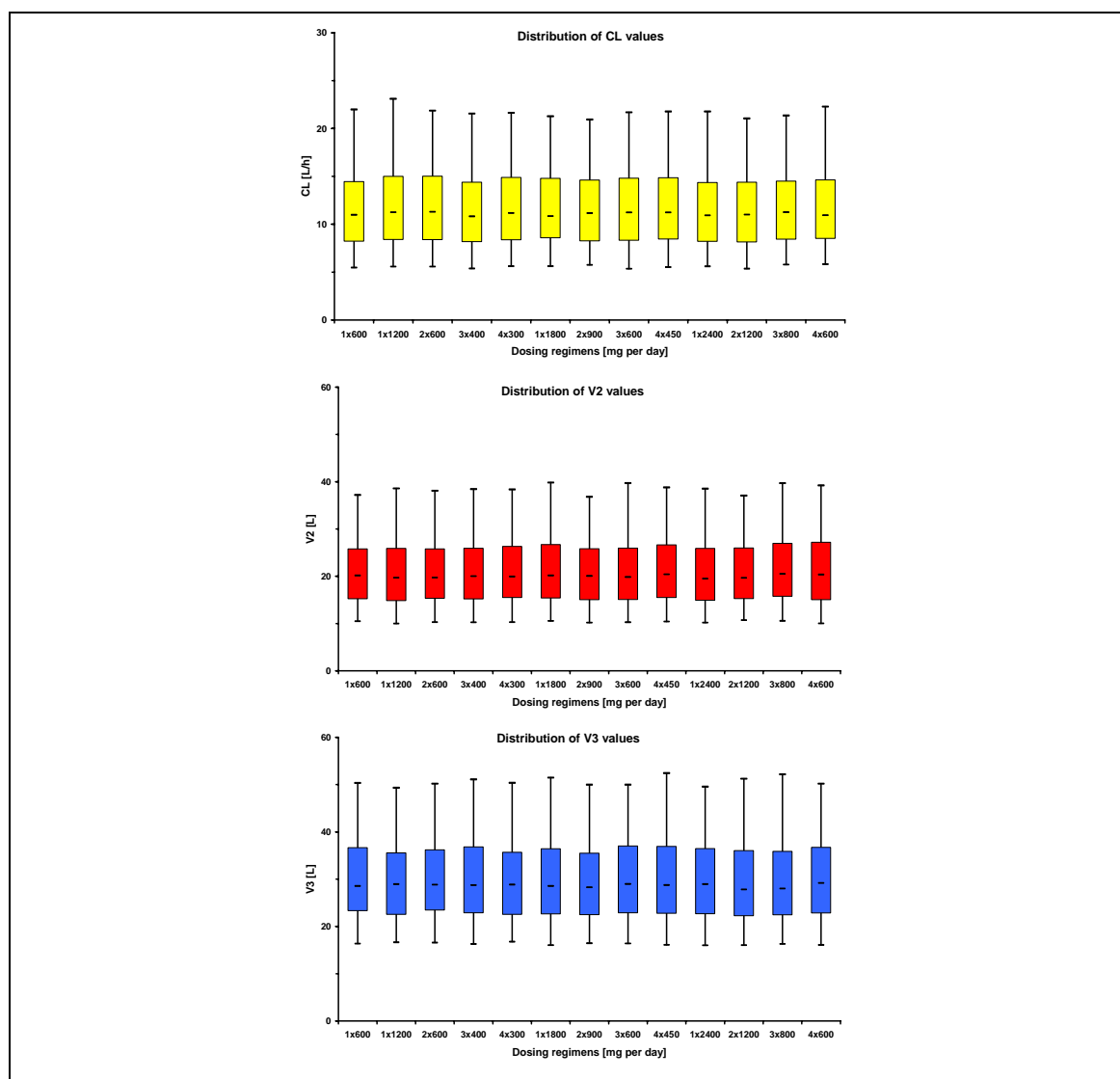
Figure 78 Distribution of clearance (CL), volume of distribution in the central (V2) and peripheral compartment (V3) values in stochastic simulations. Boxes present 25th to 75th percentiles, horizontal lines show medians, error bars indicate the respective 5th and 95th percentile.
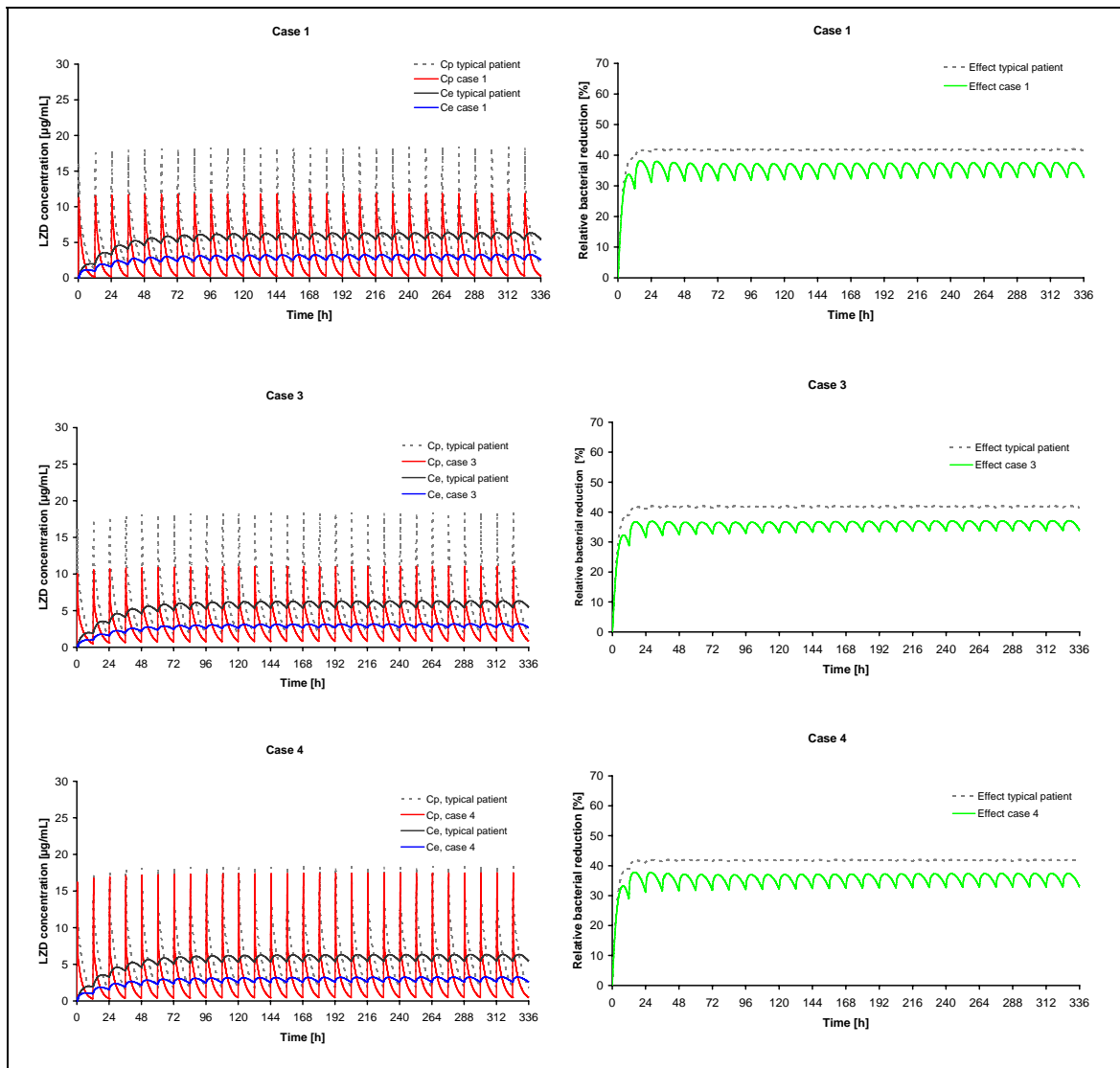
Figure 79 Simulations of the efficacy of standard LZD therapy against VRE for patients with worse PK conditions (case 2-4) compared to the typical patient; LZD concentrations in the central and effect compartment are shown on the left, the resulting effect-time course is shown on the right.
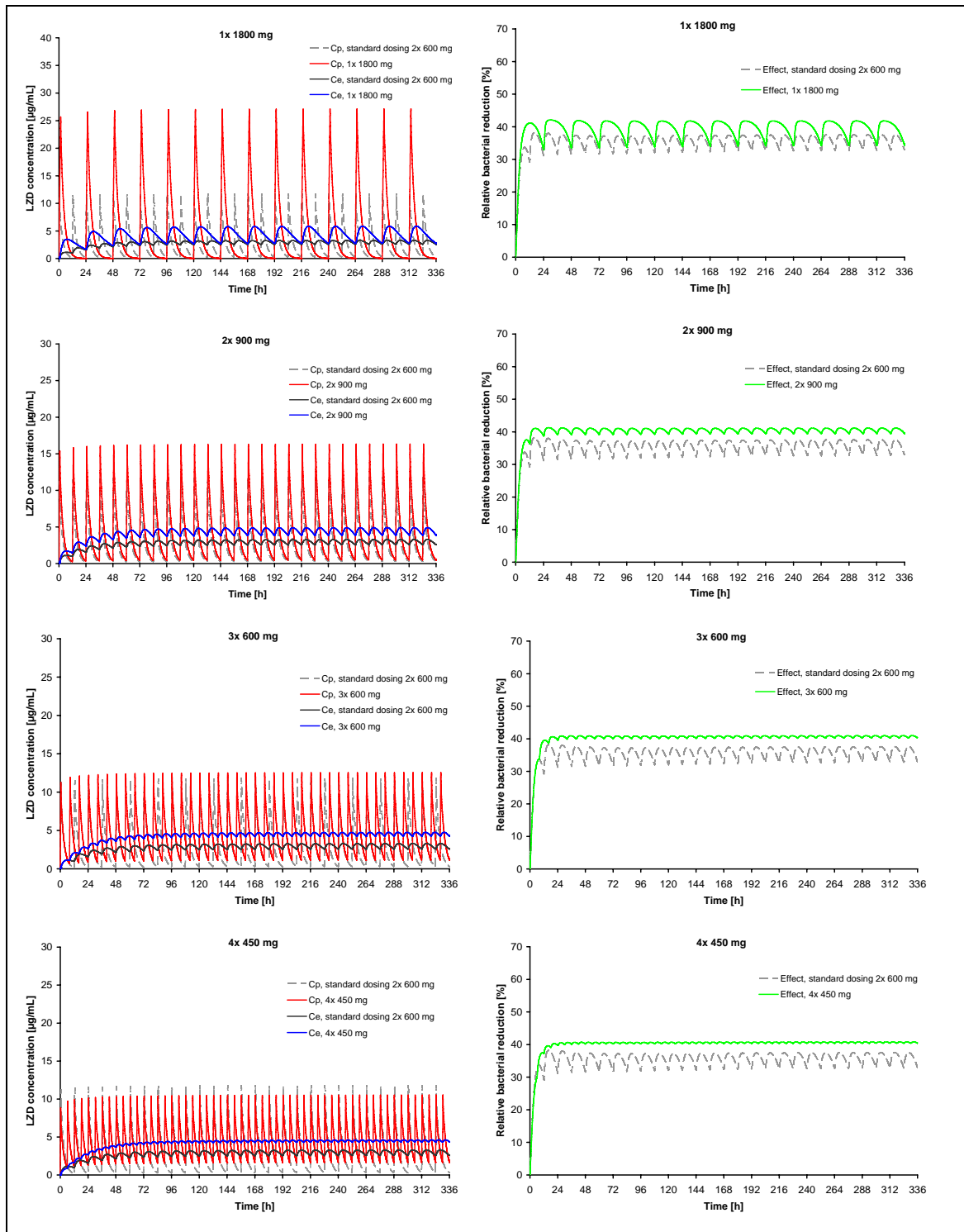
Figure 80 Dose optimisation for worst-case patient 1. The concentration-time course in plasma and the effect compartment with comparison to the typical patient is shown on the left. The resulting effect-time course is revealed on the right.
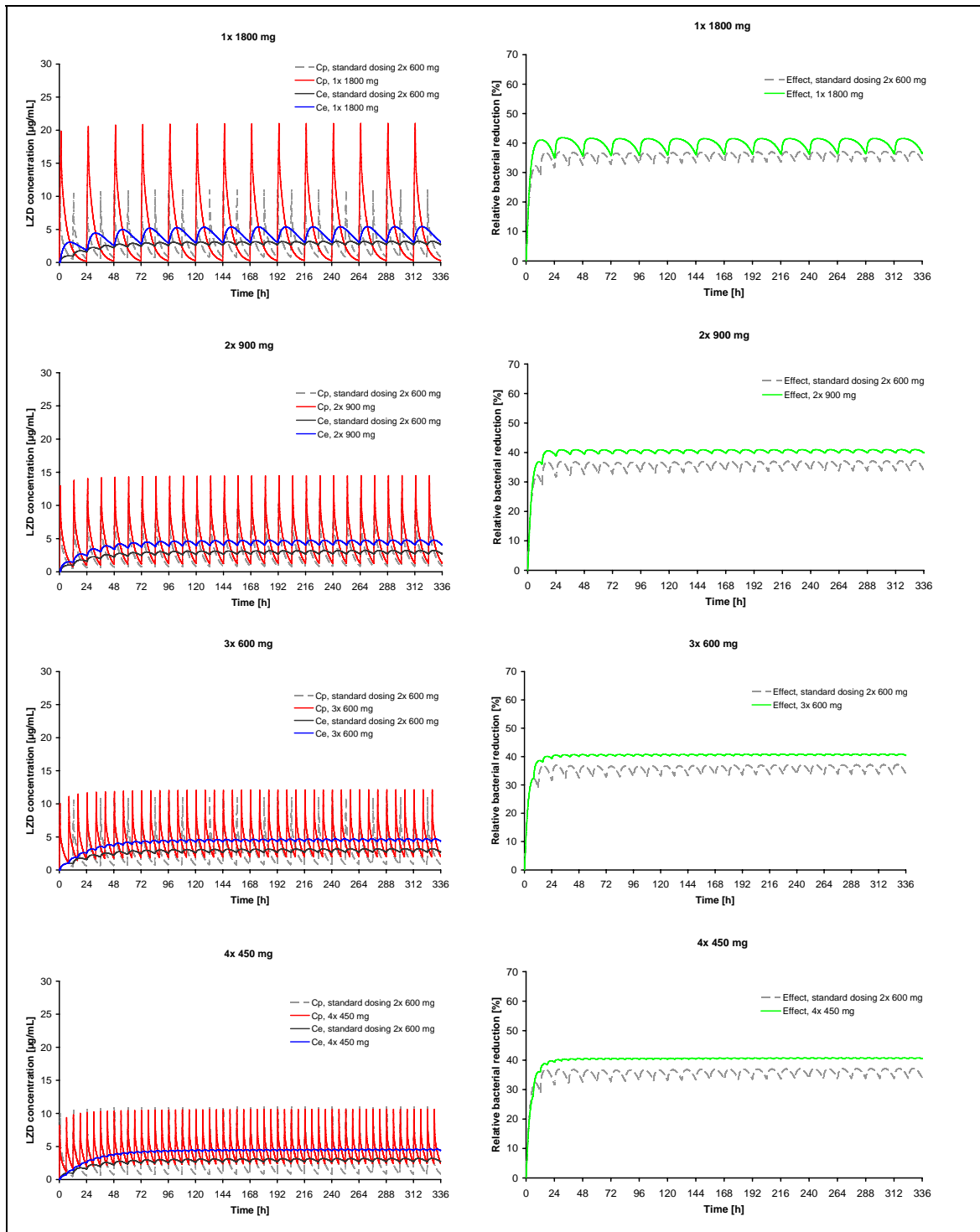
Figure 81 Dose optimisation for worst-case patient 3. The concentration-time course in plasma and the effect compartment with comparison to the typical patient is shown on the left. The resulting effect-time course is revealed on the right.
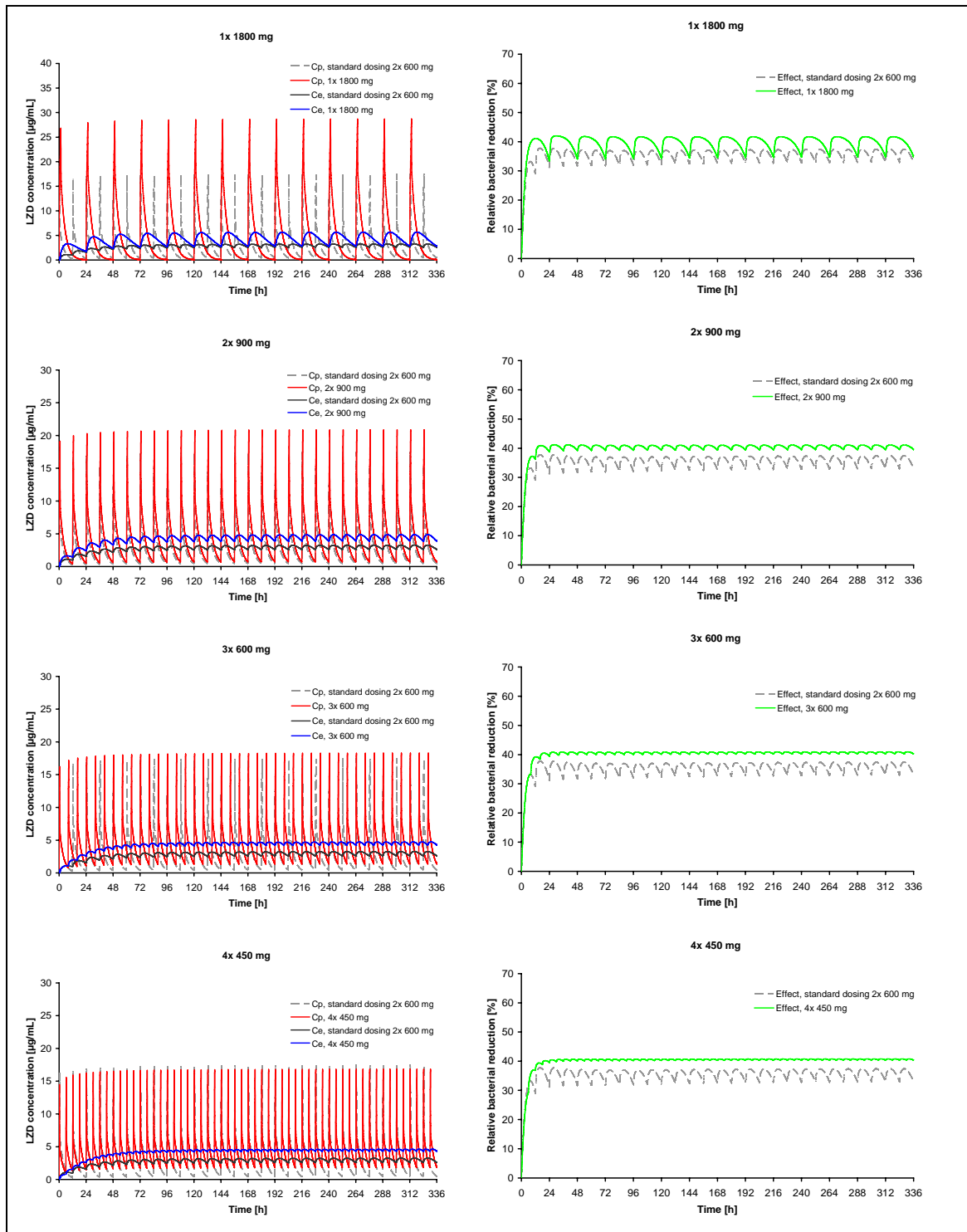
Figure 82 Dose optimisation for worst-case patient 4. The concentration-time course in plasma and the effect compartment with comparison to the typical patient is shown on the left. The resulting effect-time course is revealed on the right.
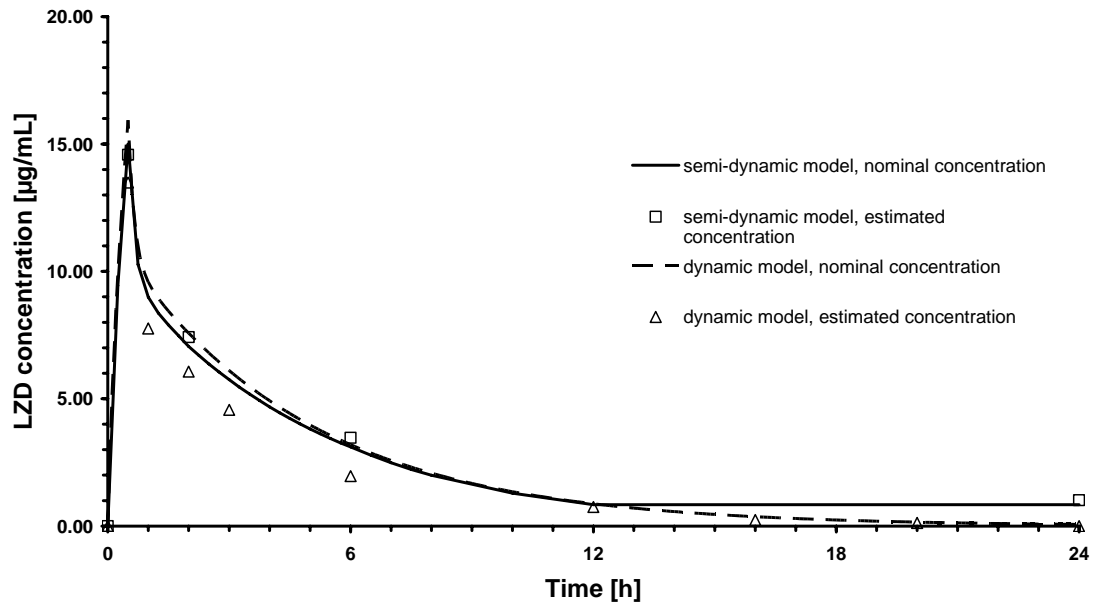
Figure 83 Comparison of LZD concentration-time courses in a semi-dynamic[111] and dynamic *in vitro* model with imitation of two-compartmental kinetics.
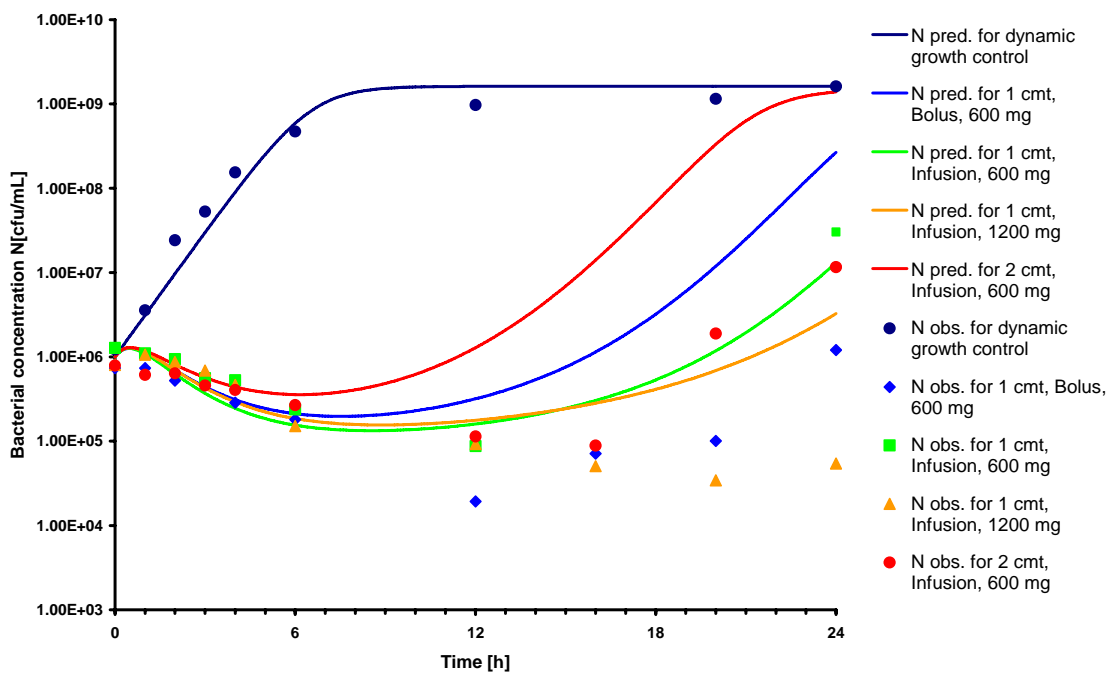
Figure 84 Simulations of the bacterial concentration-time course under changing LZD concentrations by use of the basic time-kill curve model.

7.2 Tables

Table 29 Bacterial concentrations from growth controls determined in the static, semi-dynamic and dynamic *in vitro* model.

Time	Static model			Semi-dynamic model (from [111])			Dynamic model		
	n1 $\times10^6$	n2 $\times10^6$	n3 $\times10^6$	n1 $\times10^6$	n2 $\times10^6$	n3 $\times10^6$	n1 $[\times10^6$	n2 $\times10^6$	n3 $\times10^6$
[h]	[cfu/mL]	[cfu/mL]	[cfu/mL]	[cfu/mL]	[cfu/mL]	[cfu/mL]	cfu/mL]	[cfu/mL]	[cfu/mL]
0	0.799	1.210	0.825	1.480	1.580	1.480	0.972	0.844	1.432
	0.694	0.851	0.908		1.080		0.986	0.900	1.240
	1.634	1.463	2.147				0.780	2.620	1.380
		1.425	1.881				1.280	2.020	
1	2.012	1.784	2.084	4.100	4.180	3.580	3.616	3.648	1.936
	2.164	2.052	2.216	3.620	4.540	5.120	3.100	4.532	3.240
	4.260	4.020	3.380	5.600	2.200	7.400	4.420	4.080	2.704
	3.960	3.600	4.060	6.600	5.200	4.000	4.500	4.120	4.020
2	6.140	9.700	10.42	17.60	17.80	18.80	35.52	40.84	10.28
	6.720	10.96	9.080	16.40	18.40	14.20	46.40	40.84	10.22
	20.80	12.40	20.20				19.00	30.20	21.20
	11.40	12.00	19.00				21.60	24.60	22.00
3				48.00	43.60	44.60	46.20	62.40	51.80
				38.60	43.00	46.20	57.40	56.60	46.00
				32.00	88.00	46.00	84.00	56.00	48.00
				50.00	58.00	56.00	40.00	80.00	30.00
4		1.300×10^2	1.492×10^2	1.300×10^2	1.760×10^2	2.400×10^2	1.344×10^2	1.572×10^2	61.20
		1.352×10^2	1.488×10^2	1.420×10^2	1.920×10^2	2.160×10^2	1.540×10^2	1.816×10^2	69.80
		1.880×10^2	2.340×10^2				1.900×10^2	2.160×10^2	1.800×10^2
		1.600×10^2	2.340×10^2				1.760×10^2	2.320×10^2	2.440×10^2
6	1.896×10^2	2.052×10^2	2.112×10^2	4.740×10^2	5.120×10^2	5.260×10^2	2.916×10^2	3.108×10^2	4.412×10^2
	2.016×10^2	2.252×10^2	1.848×10^2	4.820×10^2	5.520×10^2	5.180×10^2	3.080×10^2	3.068×10^2	4.692×10^2
	66.00	3.180×10^2	3.380×10^2	7.600×10^2	6.600×10^2	5.600×10^2	7.280×10^2	8.540×10^2	5.600×10^2
	1.040×10^2	3.760×10^2	3.600×10^2	6.400×10^2	6.600×10^2	1.020×10^3	5.580×10^2	6.340×10^2	5.580×10^2
8	1.532×10^2	3.088×10^2	1.824×10^2	5.340×10^2	4.300×10^2	4.780×10^2			
	1.336×10^2	2.392×10^2	1.992×10^2	5.560×10^2	5.260×10^2	6.320×10^2			
	2.560×10^2	4.300×10^2	4.100×10^2	6.000×10^2	6.800×10^2	5.400×10^2			
	4.040×10^2	3.780×10^2	4.100×10^2	4.800×10^2	6.200×10^2	7.000×10^2			
10	2.780×10^2	3.860×10^2	3.390×10^2						
	2.710×10^2	3.300×10^2	3.570×10^2						
	6.500×10^2	4.600×10^2							
	8.000×10^2	5.400×10^2							
12	2.780×10^2	3.030×10^2	3.760×10^2	5.480×10^2	5.600×10^2	5.020×10^2	6.250×10^2	5.510×10^2	5.910×10^2
	3.310×10^2	3.220×10^2	5.890×10^2	6.000×10^2	3.940×10^2	3.820×10^2	7.840×10^2	1.320×10^2	5.670×10^2
		5.100×10^2	7.400×10^2	6.000×10^2	5.400×10^2	3.600×10^2	1.640×10^3	6.700×10^3	1.880×10^3
		4.100×10^2	8.400×10^2		3.600×10^2	3.800×10^2	1.590×10^3	1.260×10^3	1.470×10^3
16	3.320×10^2	3.590×10^2	3.040×10^2						
	3.480×10^2	4.340×10^2	2.950×10^2						
	6.000×10^2	6.300×10^2	4.400×10^2						
	6.300×10^2	5.000×10^2	3.200×10^2						

20	3.160×10^2	3.250×10^2	3.110×10^2						7.800×10^2
	3.350×10^2	3.930×10^2	3.230×10^2						8.260×10^2
	6.900×10^2	5.900×10^2	3.400×10^2						1.730×10^3
	5.800×10^2	5.000×10^2	4.100×10^2						1.560×10^3
24	3.180×10^2	3.600×10^2	2.170×10^2	5.240×10^2	4.380×10^2	5.080×10^2	1.534×10^3	8.780×10^2	1.276×10^3
	2.970×10^2	3.350×10^2	2.450×10^2	4.720×10^2	5.260×10^2	6.000×10^2	1.422×10^3	6.240×10^2	1.108×10^3
		6.300×10^2	2.700×10^2	9.200×10^2	4.400×10^2	6.800×10^2	2.210×10^3	5.920×10^3	1.480×10^3
		6.700×10^2	3.700×10^2	7.400×10^2	6.200×10^2	5.600×10^2	3.010×10^3	2.100×10^3	1.530×10^3

Table 30 Mean RBR data calculated from bootstrapped geomeans of bacterial concentrations from the static *in vitro* model.

Time [h]	Mean RBR obtained under LZD concentrations of						
	0.53 µg/mL	1 µg/mL	2 µg/mL	3.9 µg/mL	8.6 µg/mL	17.2 µg/mL	36.1 µg/mL
0	-0.626	0.020	0.275	0.692	1.036	-0.034	-0.029
1	3.256	3.147	3.093	4.619	5.159	4.716	5.845
2	7.720	8.667	10.550	15.447	15.445	14.950	16.729
4	11.903	19.451	23.001	27.040	31.479	32.798	34.345
6	4.309	15.295	24.318	28.879	33.515	35.657	37.908
8	2.187	14.031	25.559	32.176	36.077	39.333	42.606
10	1.177	12.899	27.906	33.701	39.163	41.498	42.358
12	-0.128	7.169	28.248	34.268	40.201	42.802	42.586
16	1.014	5.905	28.672	35.412	40.336	42.913	42.510
20	-0.090	3.128	28.568	36.763	41.219	45.325	43.193
24	0.579	2.593	26.892	36.319	40.723	42.451	43.077

Table 31 RBR data set derived from bacterial concentrations in the static and dynamic model. Grey highlighted data present the modelling data set, used for the final RBR model; not highlighted data were used for the evaluation data set.

Time	Static model							Dynamic model			
[h]	RBR for 0.5 µg/mL	RBR for 1 µg/mL	RBR for 2 µg/mL	RBR for 3.9 µg/mL	RBR for 8.6 µg/mL	RBR for 17.2 µg/mL	RBR for 36.1 µg/mL	RBR, 1 cmt, bolus, 600 mg, t1/2 = 3.54 h	RBR, 1 cmt, infusion. 1200 mg, t1/2 = 3.54 h	RBR, 1 cmt, infusion, 600 mg, t1/2 = 5.00 h	RBR, 2 cmt, infusion, 600 mg, t1/2 beta = 3.22 h
0	1.389	3.332	0.737	1.207	2.491	2.120	1.086	0.711	0.711	3.739	3.526
	1.753	3.058	0.737	1.533	2.590	0.910	1.361	4.473	4.473	3.700	3.047
	-5.269	-3.357	-0.741	-0.741	1.934	-1.993	-2.081	5.668	-2.330	-2.245	-1.146
	-4.440	-4.687	0.037	-3.284	0.676	-1.723	-2.254	6.457	-4.547	3.603	1.040
	1.446	1.934	3.425	2.011	-0.635	1.738	2.231	0.521	-1.341	2.976	4.728
	1.634	3.733	1.029	3.276	2.057	1.828	2.231	1.455	2.035	4.528	4.227
	-0.948	-1.814	-2.747	-1.537	1.768	0.155	-1.442	5.465	-0.842	1.747	-0.079
	-1.442	-2.827	-2.338	0.910	3.332	-0.307	-2.422	4.270	-0.842	0.155	2.871
	0.751	1.319	1.139	1.263	-2.338	0.496	0.663	7.311	-0.842	8.282	5.123
	2.311	2.026	1.277	1.679	-1.723	1.194	2.726	4.419	2.498	4.751	3.507
	-3.357	-2.422				-2.905	0.037	3.720	-1.341	3.047	0.275
	-1.442	-0.635				-1.723	-2.827	3.959	-1.146	1.897	1.747
								5.851		2.019	5.147
								1.897		4.935	3.283
								2.802		1.314	4.000
								2.750		3.799	3.047
								5.099		5.147	5.219
								0.521		4.616	3.720
								4.594		5.851	1.897
								3.083		0.776	4.206
								7.311		3.338	5.591
								5.341		3.264	5.147
								2.019		-1.046	1.455
								2.958		2.531	3.799
								1.314			
								0.521			
1	5.055	3.956	3.540	5.713	6.605	6.258	7.724	13.033	13.033	8.321	11.758
	3.072	6.009	2.211	5.344	7.815	6.306	6.682	13.542	13.542	10.507	12.850
	1.261	0.005	1.926	3.905	3.217	0.924	3.027	12.954	5.407	7.807	9.594
	1.319	1.436	0.656	3.573	1.232	4.078	1.831	10.635	6.907	5.492	10.616
	5.302	5.690	5.768	7.162	7.232	6.331	8.063	9.918	10.579	11.274	15.359
	4.739	5.116	3.948	7.190	6.198	6.708	6.891	8.849	8.053	11.133	16.552
	-1.254	5.646	2.663	6.467	4.144	4.816	5.679	10.616	5.160	5.664	11.397
	2.953	2.054	2.879	2.251	1.451	4.255	6.554	10.784	5.242	7.342	10.258
	5.218	5.004	5.836	6.580	7.605	6.091		8.849	8.373	10.543	11.113
	4.437	4.511	7.066	6.405	5.974	6.174		6.599	7.688	11.233	10.452
		-1.054	-0.412	0.248		2.054		10.956	4.326	6.115	8.992
		-0.971	0.500	-0.043		2.119		9.167	5.242	1.247	11.397
								11.824			
								8.849			
2	9.836	10.883	11.245	15.657	16.582	17.234	17.541	23.774	23.774	17.195	21.380
	10.674	5.400	11.876	14.805	17.691	15.879	18.003	19.767	19.767	20.753	22.103
	4.953	4.448	8.024	15.535	15.023	13.699	18.813	24.764	17.397	20.853	20.687
	4.627	11.680	8.103	13.409	14.664	12.132	16.711	26.499	16.530	17.491	19.781
	11.497	11.245	12.883	15.338	15.535	14.998	17.129	22.601	23.146	26.096	24.173
	6.811	8.734	14.436	15.097	16.080	16.457	17.252	26.677	20.479	25.065	25.240
	5.717	8.103	6.811	14.217	17.395	16.095	17.216	22.534	15.365	15.170	22.601

		11.232	8.959	12.055	15.535	14.110	15.671	20.558	17.123	17.782	23.584
		11.538	13.922	22.347	15.767	15.377	16.551	19.119	24.056	21.567	20.142
		5.478	13.572	23.500	16.582	16.662	17.486	18.874	19.795	20.836	21.058
		6.779	9.005	13.222	10.821	13.601	13.601	23.373	16.293	14.393	17.586
			7.642	10.883	12.866	12.695	14.901	22.041	15.919	17.586	18.413
								25.100			
								20.526			
3								26.063	26.063	26.937	25.870
								24.473	24.473	26.448	26.174
								32.351	29.683	22.101	22.210
								30.938	25.786	21.785	26.219
								30.835	26.566	27.473	29.809
								26.786	26.264	25.891	29.895
								26.786	27.067	21.585	29.479
								20.760	23.576	20.933	25.384
								26.355	24.607	27.067	25.891
								26.355	23.999	25.807	26.448
								23.040	26.332	25.009	26.448
								25.998	22.790	22.210	
4	12.261	16.954	23.481	28.004	31.857	33.999	35.492	31.798	31.798	31.128	30.533
	11.770	16.907	23.930	28.550	33.129	34.241	35.041	31.583	31.583	31.743	31.743
	10.580	24.108	21.174	27.486	31.884	33.767	34.324	38.751	31.609	30.018	31.881
	8.810	23.971	21.533	25.660	33.767	32.440	34.670	39.518	33.134	31.351	30.426
	15.478	17.873	25.833	27.805	30.338	31.831	32.155	35.284	28.954	31.662	30.914
	14.699	19.543	26.189	28.564	30.280	31.309	34.159	33.732	31.351	29.940	31.556
	11.553	17.799	20.430	24.181	30.705	30.299	34.670	32.792	28.811	28.348	29.639
	10.675	18.380	23.229	25.909	30.107	31.626	33.882	26.646	28.938	28.493	30.643
	14.102		23.385			32.155	32.742	31.881	27.310	31.530	36.467
	13.436		21.037			32.211	36.100	34.017	27.934	31.743	
	9.760					34.159		32.440		32.168	
	9.881					35.544		30.868		31.609	
								34.779			
6	4.414	16.160	23.908	29.989	34.182	36.403	39.915	38.181	38.181	37.968	36.884
	3.405	16.549	24.626	29.850	34.542	38.085	37.869	38.181	38.181	39.636	36.654
	3.761	14.201	21.894	29.470	33.498	34.655	36.965	47.467	39.408	40.667	38.403
	1.679	13.237	22.414	28.334	32.501	34.395	37.462	43.345	34.497	41.438	34.933
	5.565	14.354	26.594	28.985	32.948	33.845	36.965	41.438	37.763	39.244	42.351
	6.161	16.362	26.578	28.934	33.977	34.542	38.546	38.881	38.269	41.784	42.252
	4.414	16.160	23.908	29.989	34.182	36.403	39.915	40.812	38.403	46.940	41.438
	3.405	16.549	24.626	29.850	34.542	38.085	37.869	38.881	39.408	35.410	36.434
	3.761	14.201	21.894	29.470	33.498	34.655	36.965	31.695		40.125	36.373
	1.679	13.237	22.414	28.334	32.501	34.395	37.462	39.464		39.754	33.725
	5.565	14.354	26.594	28.985	32.948	33.845	36.965	38.225		42.351	32.196
	6.161	16.362	26.578	28.934	33.977	34.542	38.546	37.968		37.968	
	4.900	16.105	22.715	28.112	33.911	36.566		37.567			
	4.188		22.638	26.610	31.729	36.790					
			28.255	29.442		36.298					
			27.536	28.947		34.929					
			21.796								
			23.373								
8	4.028	17.932	26.096	32.919	36.671	42.009	45.711				
	3.510	16.579	25.978	32.528	36.625	41.752	44.299				
	0.132	11.613	22.699	33.939	36.354	43.715	45.711				
	-0.947	11.759	22.761	33.517	37.535	40.628	44.097				
	4.512	16.742	27.526	33.858	38.059	36.625	39.966				
	4.299	16.016	27.929	32.874	34.742	36.814	40.628				
	-0.522	10.814	27.695	31.288	35.504	38.247	39.707				
	2.029	11.833	28.247	30.832	35.579	36.814	40.528				
		18.094	23.613	31.110	35.811	38.998					
		11.198	23.019	30.892	37.162	38.441					
		11.759		30.426	34.906	39.072					

				31.015	35.617	39.224					
				31.558	36.671						
				31.770	35.430						
				33.542	34.873						
				32.343	35.891						
10	2.108	14.860	30.010	34.676	39.225	42.838	43.084				
	3.205	14.380	30.577	34.653	41.478	42.490	41.761				
	0.538	11.629	24.983	34.629	38.940	42.165	42.719				
	0.538	11.071	24.745	34.724	40.483	43.211	42.490				
	3.742	14.439	29.752	34.724	37.893	39.782	41.761				
	1.302	13.459	29.672	33.097	39.225	40.559	40.874				
	2.515	11.366	26.240	34.114	38.414	40.335	40.263				
	-1.551	8.990	25.088	33.457	37.938	38.776	41.211				
	0.980	16.298	30.310	33.667	39.653	42.838	43.903				
	1.962	14.907	30.717	32.616	39.465	41.124	43.757				
	-0.668	11.342	26.285	32.295	38.365	41.571	43.903				
	-0.668	11.986	26.376	31.476	38.885	42.165					
12	-0.280	9.263	31.606	34.354	41.563	43.009	42.891	44.468	44.468	44.374	42.065
	-0.776	8.953	29.901	34.968	41.052	44.536	42.775	42.875	42.875	44.861	41.083
	2.610	3.829	26.689	34.944	41.746	45.420	42.552	63.400	48.975	45.638	40.347
	0.321	6.934	25.914	35.865	41.746	44.071	43.009	63.400	44.563	43.685	42.943
	-0.970	9.703	30.362	32.648	38.035	41.936	41.474	56.725		44.374	44.660
	-1.423	8.700	30.353	38.170	40.370	39.898	42.662	60.063		45.179	44.468
	-1.693	6.581	27.718	34.145	38.649	42.662	42.662	52.313		45.638	48.975
	-0.970	3.731	24.938	34.595	40.971	41.133	42.552	52.313		45.638	47.023
	-0.034	9.471	29.762	33.144	39.291	41.301		47.186			
	2.237	8.349	30.136	33.827	40.442	43.382		47.901			
		5.867	24.776	34.920	38.309	42.234		52.313			
		4.865	26.506	32.648		43.926		47.023			
				34.640							
				33.983							
				34.573							
				34.595							
				31.939							
				35.165							
16	2.654	8.226	30.080	35.540	39.032	42.872	41.333				
	1.144	7.050	30.979	36.458	39.380	43.511	41.700				
	-1.400	2.949	27.900	35.402	38.760	42.993	45.098				
	-0.041	3.500	27.487	37.417	40.595	46.130	41.700				
	2.414	7.312	29.507	35.267	40.750	41.513	40.992				
	2.074	7.011	28.910	38.501	41.513	41.700	41.796				
	1.174	7.834	27.106	35.653	42.638	42.095	44.915				
	1.654	5.214	27.601	34.984	40.371	42.753	42.305				
	2.002	7.926	30.453	34.934		41.700	41.796				
	1.638	6.755	30.780	36.770		43.118	42.753				
	0.205	3.956	25.898	36.458		43.937	42.872				
	-1.307	2.821	27.053	35.540		42.872	43.118				
				34.621							
				34.835							
				35.188							
				35.798							
				32.966							
				34.305							
20	2.659	7.494	30.261	37.313	41.641	46.075	42.579	46.128		54.976	28.215
	1.261	6.605	30.124	36.925	42.355	47.087	42.935	45.648		47.766	27.556
	-2.187	-0.623	26.979	38.004	41.546	48.729	42.036	49.205		48.535	22.643
	-0.816	-1.512	27.413	38.051	43.733	41.186	43.591	47.261		49.205	22.068
	1.691	7.798	29.582	35.762	40.932	41.737	42.355	42.441		49.205	40.420
	1.867	7.035	29.832	36.068	40.310	41.737	43.591	45.426			43.410
	-3.200	-0.319	27.827	35.588	40.690	41.737	42.935	38.947			
	-1.410	-1.082	25.906	35.645	40.769	46.815	42.036	43.939			

	1.555	7.249	30.921	36.100	39.890	48.729	43.880	46.387			
	1.104	6.966	30.444	35.883	41.546	47.681	45.636	41.490			
	-1.122	-0.868	25.660	35.202	40.769	47.087	44.859	45.882			
	-2.187	-1.151	27.586	36.228	40.611		42.036				
				36.851							
				38.193							
				36.394							
				37.519							
				37.519							
24	1.562	3.675	30.159	37.850	41.742	43.242	41.635	19.844	19.844	41.152	17.137
	4.536	2.136	29.995	36.807	42.563	44.562	42.692	18.984	18.984	40.298	17.272
	-0.089	4.221	25.520	37.190	40.500	44.954	43.698	45.888	17.676	40.839	28.676
	-1.589	1.423	25.259	37.370	42.315	43.390	42.563	45.246	18.487	48.105	28.832
	1.269	3.294	28.331	39.716	39.100	41.228	41.228	37.089		51.700	23.743
	1.916	3.645	27.951	37.901	40.416	41.742	43.698	38.497		55.696	24.011
	-1.801	2.509	24.475	36.766	39.939	41.228	40.672	41.566		53.287	
	-0.894	0.366	23.732	36.011	41.228	40.672	42.824	34.300		52.837	
		2.992		35.323	39.572	42.437	45.162	35.524		53.287	
		3.525		35.704	39.644	43.099	43.698	34.958			
		3.893		37.416	41.131	42.563	44.377	30.744			
		-0.894		36.974	40.585	41.530	44.377	30.947			
				35.606				33.489			
				35.976				33.935			
				36.337				29.684			
				36.766				32.617			
				34.636				33.819			
				35.510				33.896			
								31.072			
								30.666			
								32.444			
								32.501			
								27.262			
								26.336			

Table 32 Bootstrapped geometric means of bacterial concentrations derived from the static *in vitro* model for modelling of time-kill curves.

Time [h]		Bacterial concentration [cfu/mL] for linezolid concentrations [µg/mL] of						
		36.1	17.2	8.6	3.9	2.0	1.0	0.53
0	2.5th percentile	$1.005×10^6$	$1.033×10^6$	$8.668×10^5$	$9.217×10^5$	$9.687×10^5$	9.485E+05	$1.068×10^6$
	Median	$1.170×10^6$	$1.170×10^6$	$1.008×10^6$	$1.058×10^6$	$1.121×10^6$	$1.162×10^6$	$1.271×10^6$
	97.5th percentile	$1.380×10^6$	$1.336×10^6$	$1.190×10^6$	$1.251×10^6$	$1.304×10^6$	$1.448×10^6$	$1.554×10^6$
1	2.5th percentile	$9.894×10^5$	$1.218×10^6$	$1.080×10^6$	$1.163×10^6$	$1.515×10^6$	$1.449×10^6$	$1.464×10^6$
	Median	$1.185×10^6$	$1.401×10^6$	$1.312×10^6$	$1.421×10^6$	$1.783×10^6$	$1.768×10^6$	$1.740×10^6$
	97.5th percentile	$1.491×10^6$	$1.645×10^6$	$1.666×10^6$	$1.757×10^6$	$2.134×10^6$	$2.229×10^6$	$2.112×10^6$
2	2.5th percentile	$6.712×10^5$	$8.912×10^5$	$8.091×10^5$	$6.307×10^5$	$1.672×10^6$	$2.181×10^6$	$2.411×10^6$
	Median	$7.578×10^5$	$1.012×10^6$	$9.338×10^5$	$9.334×10^5$	$2.069×10^6$	$2.811×10^6$	$3.278×10^6$
	97.5th percentile	$8.629×10^5$	$1.179×10^6$	$1.132×10^6$	$1.248×10^6$	$2.681×10^6$	$3.550×10^6$	$4.437×10^6$
4	2.5th percentile	$2.214×10^5$	$2.853×10^5$	$3.630×10^5$	$8.404×10^5$	$1.696×10^6$	$2.802×10^6$	$1.394×10^7$
	Median	$2.510×10^5$	$3.364×10^5$	$4.318×10^5$	$1.001×10^6$	$2.151×10^6$	$4.213×10^6$	$1.759×10^7$
	97.5th percentile	$2.881×10^5$	$3.860×10^5$	$5.041×10^5$	$1.223×10^6$	$2.651×10^6$	$5.909×10^6$	$2.167×10^7$
6	2.5th percentile	$1.225×10^5$	$1.930×10^5$	$3.096×10^5$	$7.523×10^5$	$1.530×10^6$	$9.672×10^6$	$7.862×10^7$
	Median	$1.469×10^5$	$2.261×10^5$	$3.408×10^5$	$8.287×10^5$	$1.986×10^6$	$1.119×10^7$	$9.181×10^7$
	97.5th percentile	$1.678×10^5$	$2.647×10^5$	$3.848×10^5$	$9.436×10^5$	$2.485×10^6$	$1.353×10^7$	$1.112×10^8$
8	2.5th percentile	$5.191×10^4$	$1.039×10^5$	$2.253×10^5$	$4.728×10^5$	$1.462×10^6$	$1.296×10^7$	$1.371×10^8$
	Median	$6.946×10^4$	$1.312×10^5$	$2.469×10^5$	$5.268×10^5$	$1.905×10^6$	$1.788×10^7$	$1.785×10^8$
	97.5th percentile	$9.706×10^4$	$1.637×10^5$	$2.684×10^5$	$5.928×10^5$	$2.504×10^6$	$2.464×10^7$	$2.455×10^8$
10	2.5th percentile	$8.061×10^4$	$9.493×10^4$	$1.543×10^5$	$4.601×10^5$	$1.284×10^6$	$2.582×10^7$	$2.758×10^8$
	Median	$9.239×10^4$	$1.096×10^5$	$1.741×10^5$	$5.145×10^5$	$1.624×10^6$	$3.187×10^7$	$3.260×10^8$
	97.5th percentile	$1.065×10^5$	$1.273×10^5$	$1.920×10^5$	$5.803×10^5$	$2.125×10^6$	$3.998×10^7$	$3.899×10^8$
12	2.5th percentile	$8.746×10^4$	$7.371×10^4$	$1.271×10^5$	$4.377×10^5$	$1.217×10^6$	$8.410×10^7$	$3.702×10^8$
	Median	$9.138×10^4$	$8.752×10^4$	$1.469×10^5$	$4.781×10^5$	$1.584×10^6$	$1.049×10^8$	$4.482×10^8$
	97.5th percentile	$9.779×10^4$	$1.036×10^5$	$1.722×10^5$	$5.262×10^5$	$2.082×10^6$	$1.356×10^8$	$5.194×10^8$
16	2.5th percentile	$7.724×10^4$	$7.214×10^4$	$1.166×10^5$	$3.328×10^5$	$1.172×10^6$	$1.056×10^8$	$2.959×10^8$
	Median	$9.027×10^4$	$8.333×10^4$	$1.389×10^5$	$3.693×10^5$	$1.407×10^6$	$1.291×10^8$	$3.407×10^8$
	97.5th percentile	$1.021×10^5$	$9.370×10^4$	$1.630×10^5$	$4.088×10^5$	$1.684×10^6$	$1.654×10^8$	$3.973×10^8$
20	2.5th percentile	$6.812×10^4$	$3.655×10^4$	$1.017×10^5$	$2.545×10^5$	$1.174×10^6$	$1.440×10^8$	$3.362×10^8$
	Median	$7.792×10^4$	$5.105×10^4$	$1.152×10^5$	$2.788×10^5$	$1.416×10^6$	$2.196×10^8$	$4.157×10^8$
	97.5th percentile	$8.755×10^4$	$7.336×10^4$	$1.268×10^5$	$3.074×10^5$	$1.742×10^6$	$3.376×10^8$	$5.113×10^8$
24	2.5th percentile	$6.313×10^4$	$6.928×10^4$	$1.024×10^5$	$2.522×10^5$	$1.256×10^6$	$1.774×10^8$	$2.295×10^8$
	Median	$7.231×10^4$	$8.177×10^4$	$1.148×10^5$	$2.730×10^5$	$1.741×10^6$	$2.066×10^8$	$3.069×10^8$
	97.5th percentile	$8.498×10^4$	$9.392×10^4$	$1.293×10^5$	$2.947×10^5$	$2.387×10^6$	$2.476×10^8$	$3.959×10^8$

Table 33 Bacterial concentrations determined in time kill curve experiments in the static and dynamic *in vitro* model. Grey highlighted data present the modelling data set, used for the final time-kill curve modelling; not highlighted data were used for the evaluation data set.

	Static *in vitro* model							Dynamic *in vitro* model			
Time	N for C=36.1 µg/mL	N for C=17.2 µg/mL	N for C=8.6 µg/mL	N for C=3.9 µg/mL	N for C=2.0 µg/mL	N for C=1.0 µg/mL	N for C=0.53 µg/mL	N for 1 cmt, Bolus, 600mg	N for 1 cmt, Infusion, 1200 mg	N for 1 cmt, Infusion, 600 mg	N for 2 cmt, Infusion, 600 mg
[h]	×10⁶ [cfu/mL]	×10⁶ [cfu/mL]	×10⁶ [cfu/mL]	×10⁶ [cfu/mL]	×10⁶ [cfu/mL]	×10⁶ [cfu/mL]	×10⁶ [cfu/mL]	×10⁶ [cfu/mL]	×10⁶ [cfu/mL]	×10⁶ [cfu/mL]	×10⁶ [cfu/mL]
0	1.001	0.866	0.823	0.984	1.05	0.732	0.960	1.11	1.11	0.726	0.748
	0.963	1.03	0.811	0.941	1.05	0.760	0.912	0.655	0.655	0.730	0.800
	1.56	1.54	0.889	1.29	1.29	1.86	2.43	0.554	1.70	1.68	1.44
	1.60	1.48	1.06	1.84	1.16	2.24	2.17	0.496	2.32	0.740	1.06
	0.853	0.914	1.27	0.880	0.722	0.889	0.95	1.14	1.48	0.808	0.632
	0.853	0.903	0.874	0.737	1.01	0.692	0.93	1.00	0.922	0.650	0.678
	1.43	1.14	0.910	1.44	1.71	1.50	1.33	0.570	1.38	0.960	1.24
	1.63	1.22	0.732	1.03	1.62	1.73	1.43	0.674	1.38	1.20	0.820
	1.06	1.09	1.62	0.977	0.994	0.969	1.05	0.440	1.38	0.384	0.598
	0.796	0.986	1.48	0.922	0.975	0.878	0.844	0.660	0.864	0.630	0.750
	1.16	1.75				1.63	1.86	0.728	1.48	0.800	1.18
	1.73	1.48				1.27	1.43	0.704	1.44	0.940	0.960
								0.540		0.924	0.596
								0.940		0.614	0.774
								0.828		1.02	0.700
								0.834		0.720	0.800
								0.600		0.596	0.590
								1.14		0.642	0.728
								0.644		0.540	0.940
								0.796		1.100	0.680
								0.440		0.768	0.560
								0.580		0.776	0.596
								0.924		1.42	1.00
								0.810		0.860	0.720
								1.02			
								1.14			
1	0.896	1.11	1.06	1.21	1.67	1.57	1.33	0.500	0.500	1.02	0.606
	1.05	1.11	0.884	1.28	2.03	1.17	1.79	0.463	0.463	0.732	0.514
	1.80	2.46	1.75	1.58	2.12	2.82	2.34	0.506	1.58	1.10	0.840
	2.15	1.54	2.35	1.66	2.56	2.28	2.32	0.718	1.26	1.56	0.720
	0.852	1.10	0.964	0.974	1.20	1.21	1.28	0.800	0.724	0.652	0.352

Tables

	1.01	1.04	1.12	0.970	1.57	1.32	1.40	0.940	1.06	0.666	0.294
	1.21	1.38	1.53	1.08	1.90	1.22	3.40	0.720	1.64	1.52	0.640
	1.07	1.50	2.28	2.02	1.84	2.08	1.82	0.702	1.62	1.18	0.760
		1.14	0.912	1.06	1.19	1.34	1.30	0.940	1.01	0.728	0.668
		1.13	1.16	1.09	0.988	1.44	1.46	1.32	1.12	0.656	0.738
		2.08		2.72	3.00	3.30		0.684	1.86	1.42	0.920
		2.06		2.84	2.62	3.26		0.896	1.62	2.96	0.640
								0.600			
								0.940			
2	0.664	0.698	0.776	0.902	1.85	1.96	2.32	0.426	0.426	1.30	0.640
	0.616	0.870	0.648	1.04	1.67	4.78	2.03	0.842	0.842	0.712	0.566
	0.540	1.24	1.00	0.920	3.12	5.58	5.14	0.360	1.26	0.700	0.720
	0.760	1.60	1.06	1.30	3.08	1.72	5.42	0.268	1.46	1.24	0.840
	0.710	1.00	0.920	0.950	1.42	1.85	1.77	0.520	0.474	0.287	0.398
	0.696	0.792	0.842	0.988	1.10	2.78	3.80	0.260	0.746	0.342	0.332
	0.700	0.840	0.680	1.14	3.80	3.08	4.54	0.526	1.78	1.84	0.520
	0.900	1.16	0.920	1.62	2.68	1.85		0.736	1.32	1.18	0.440
	0.780	0.944	0.886	0.304	1.20	1.76		0.940	0.406	0.620	0.790
	0.670	0.766	0.776	0.252	1.27	4.72		0.980	0.838	0.702	0.676
	1.26	1.26	1.98	1.34	2.66	3.82		0.456	1.52	2.10	1.22
	1.02	1.46	1.42	1.96	3.32			0.572	1.62	1.22	1.06
								0.340			
								0.740			
3								0.514	0.514	0.440	0.532
								0.682	0.682	0.480	0.504
								0.168	0.270	1.04	1.02
								0.216	0.540	1.10	0.500
								0.220	0.470	0.400	0.264
								0.452	0.496	0.530	0.260
								0.452	0.430	1.14	0.280
								1.32	0.800	1.28	0.580
								0.488	0.666	0.430	0.530
								0.488	0.742	0.538	0.480
								0.880	0.490	0.620	0.480
								0.520	0.920	1.02	
4	0.202	0.268	0.402	0.834	1.96	6.76	16.4	0.386	0.386	0.438	0.490
	0.220	0.256	0.316	0.752	1.80	6.82	18.0	0.402	0.402	0.390	0.390
	0.252	0.280	0.400	0.920	3.040	1.74	22.6	0.104	0.400	0.540	0.380
	0.236	0.360	0.280	1.30	2.84	1.79	31.6	0.090	0.300	0.420	0.500
	0.380	0.404	0.536	0.866	1.26	5.68	8.94	0.200	0.660	0.396	0.456

	0.260	0.446	0.542	0.750	1.18	4.14	10.4	0.268	0.420	0.548	0.404
	0.236	0.540	0.500	1.72	3.50	5.76	18.8	0.320	0.678	0.740	0.580
	0.274	0.420	0.560	1.24	2.06	5.16	22.2	1.02	0.662	0.720	0.480
	0.340	0.380			2.00		11.6	0.380	0.900	0.406	0.160
	0.180	0.376			3.12		13.2	0.254	0.800	0.390	
		0.260					26.4	0.342		0.360	
		0.200					25.8	0.460		0.400	
								0.220			
6	0.100	0.196	0.300	0.670	2.15	9.48	90.0	0.230	0.230	0.240	0.298
	0.148	0.142	0.280	0.688	1.87	8.80	109	0.230	0.230	0.172	0.312
	0.176	0.274	0.342	0.740	3.16	13.8	102	0.036	0.180	0.140	0.220
	0.160	0.288	0.414	0.920	2.86	16.6	152	0.082	0.480	0.120	0.440
	0.176	0.320	0.380	0.812	1.28	13.4	72.2	0.120	0.250	0.186	0.100
	0.130	0.280	0.312	0.820	1.29	9.12	64.4	0.200	0.226	0.112	0.102
		0.190	0.316	0.960	2.70	9.58	82.0	0.136	0.220	0.040	0.120
		0.182	0.480	1.28	2.74		94.0	0.200	0.180	0.400	0.326
		0.200		0.744	0.934			0.840		0.156	0.330
		0.260		0.818	1.07			0.178		0.168	0.560
					3.22			0.228		0.100	0.760
					2.38			0.240		0.240	
								0.260			
8	0.038	0.078	0.220	0.456	1.72	8.38	125				
	0.050	0.082	0.222	0.492	1.76	10.9	138				
	0.038	0.056	0.234	0.374	3.32	28.6	266				
	0.052	0.102	0.186	0.406	3.28	27.8	328				
	0.116	0.222	0.168	0.380	1.30	10.6	113				
	0.102	0.214	0.320	0.460	1.20	12.2	118				
	0.122	0.162	0.276	0.626	1.26	33.4	302				
	0.104	0.214	0.272	0.684	1.13	27.4	184				
		0.140	0.260	0.648	2.78	8.12					
		0.156	0.200	0.676	3.12	31.0					
		0.138	0.310	0.740		27.8					
		0.134	0.270	0.660							
			0.220	0.594							
			0.280	0.570							
			0.312	0.404							
			0.256	0.510							
10	0.080	0.084	0.172	0.424	1.07	21.6	271				
	0.104	0.090	0.110	0.426	0.956	23.8	218				
	0.086	0.096	0.182	0.428	2.90	41.0	370				

	0.090	0.078	0.134	0.420	3.04	45.8	370				
	0.104	0.154	0.224	0.420	1.13	23.5	196				
	0.124	0.132	0.172	0.580	1.14	28.5	318				
	0.140	0.138	0.202	0.474	2.26	43.2	250				
	0.116	0.188	0.222	0.540	2.84	69.2	560				
	0.068	0.084	0.158	0.518	1.01	16.2	339				
	0.070	0.118	0.164	0.638	0.93	21.4	279				
	0.068	0.108	0.204	0.680	2.24	43.4	470				
		0.096	0.184	0.800	2.20	38.2	470				
12	0.086	0.084	0.112	0.470	0.812	69.2	462	0.102	0.102	0.104	0.168
	0.088	0.062	0.124	0.416	1.14	73.6	510	0.142	0.142	0.094	0.206
	0.092	0.052	0.108	0.418	2.16	204	260	0.002	0.040	0.080	0.240
	0.084	0.068	0.108	0.348	2.52	110	410	0.002	0.100	0.120	0.140
	0.114	0.104	0.226	0.660	1.04	63.4	530	0.008		0.104	0.098
	0.090	0.156	0.142	0.220	1.04	77.4	580	0.004		0.088	0.102
	0.090	0.090	0.200	0.490	1.76	118	612	0.020		0.080	0.040
	0.092	0.122	0.126	0.448	3.06	208	530	0.020		0.080	0.060
		0.118	0.176	0.598	1.17	66.4	440	0.058			
		0.078	0.140	0.522	1.09	83.0	280	0.050			
		0.098	0.214	0.420	3.16	136		0.020			
		0.070		0.660	2.24	166		0.060			
				0.444							
				0.506							
				0.450							
				0.448							
				0.760							
				0.400							
16	0.114	0.084	0.180	0.360	1.06	81.4	246	0.064		0.052	0.180
	0.106	0.074	0.168	0.300	0.89	103	332	0.048		0.034	0.182
	0.054	0.082	0.190	0.370	1.64	232	550	0.040		0.020	0.160
	0.106	0.044	0.132	0.248	1.78	208	420	0.060		0.100	0.160
	0.122	0.110	0.128	0.380	1.19	97.6	258	0.074		0.048	0.022
	0.104	0.106	0.110	0.200	1.34	104	276	0.100		0.041	0.026
	0.056	0.098	0.088	0.352	1.92	88.0	330	0.060		0.120	
	0.094	0.086	0.138	0.402	1.74	148	300	0.120			
	0.104	0.106		0.406	0.988	86.4	280	0.082			
	0.086	0.080		0.282	0.926	109	301	0.088			
	0.084	0.068		0.300	2.44	190	400	0.100			
	0.080	0.084		0.360	1.94	238	540	0.060			
				0.432							
				0.414							

				0.386							
				0.342							
				0.600							
				0.460							
20	0.088	0.044	0.106	0.250	1.01	92.4	241	0.076		0.012	3.19
	0.082	0.036	0.092	0.270	1.04	110	318	0.084		0.054	3.66
	0.098	0.026	0.108	0.218	1.94	462	630	0.040		0.046	10.2
	0.072	0.116	0.070	0.216	1.78	551	480	0.060		0.040	11.5
	0.092	0.104	0.122	0.340	1.16	87.0	292	0.164		0.040	0.250
	0.072	0.104	0.138	0.320	1.10	101	282	0.088			0.134
	0.082	0.104	0.128	0.352	1.64	435	770	0.340			
	0.098	0.038	0.126	0.348	2.40	506	540	0.120			
	0.068	0.026	0.150	0.318	0.888	97.0	300	0.072			
	0.048	0.032	0.108	0.332	0.976	102	328	0.200			
	0.056	0.036	0.126	0.380	2.52	485	510	0.080			
	0.098		0.130	0.310	1.72	513	630				
				0.274							
				0.210							
				0.300							
				0.240							
				0.240							
24	0.096	0.070	0.094	0.202	0.916	167	253	24.0	24.0	0.262	42.6
	0.078	0.054	0.080	0.248	0.946	226	141	28.8	28.8	0.314	41.4
	0.064	0.050	0.120	0.230	2.28	150	350	0.096	38.0	0.280	3.69
	0.080	0.068	0.084	0.222	2.40	260	470	0.110	32.0	0.060	3.57
	0.104	0.104	0.158	0.140	1.31	180	268	0.620		0.028	10.5
	0.064	0.094	0.122	0.200	1.41	168	236	0.460		0.012	9.92
	0.116	0.104	0.134	0.250	2.80	210	490	0.24		0.020	
	0.076	0.116	0.104	0.290	3.24	320	410	1.12		0.022	
	0.048	0.082	0.144	0.332		191		0.864		0.020	
	0.064	0.072	0.142	0.308		172		0.974			
	0.056	0.080	0.106	0.220		160		2.38			
	0.056	0.098	0.118	0.240		410		2.28			
	2.22			0.314				1.33			
	2.42			0.292				1.21			
	1.66			0.272				2.98			
	1.64			0.250				1.60			
	4.98			0.380				1.24			
	6.06			0.320				1.22			

Table 34 Variability of calibration samples in the validation of LZD in MHB with respect to mean, imprecision and inaccuracy.

C_nom [μg/mL]	C_est [μg/mL] Mean ± S.D.	Imprecision CV, %	Inaccuracy RE, %
Within-day (n = 3)			
0.204	0.214 ± 0.028	13.3	+ 4.83
0.510	0.482 ± 0.062	12.8	- 5.81
1.02	0.938 ± 0.054	5.7	- 8.75
5.10	5.394 ± 0.156	2.9	+ 5.46
20.4	20.839 ± 0.663	3.2	+ 2.11
30.6	30.909 ± 3.585	11.6	+ 1.00
35.7	38.335 ± 2.945	7.7	+ 6.87
Between-day (n = 9)			
0.204	0.215 ± 0.020	9.5	+ 5.12
0.510	0.480 ± 0.051	10.5	- 6.32
1.02	0.949 ± 0.048	5.1	- 7.48
5.10	5.360 ± 0.210	3.9	+ 4.86
20.4	20.942 ± 0.584	2.8	+ 2.95
30.6	30.818 ± 2.677	8.7	+ 0.71
35.7	37.867 ± 2.503	6.6	+ 5.72

C_{nom} – nominal LZD concentration, C_{est} – estimated LZD concentration

Table 35 Bacterial concentrations for the determination of the bacterial concentration corresponding to a McFarland index of 0.5; shown are manually (manual) and digitally (CQ) counted bacterial counts per plate.

Plate number	Bacterial counts per plate							
	Low I		Low II		Intermediate		High	
	Manual	CQ	Manual	CQ	Manual	CQ	Manual	CQ
Repeated counting of plate 1 on day 1								
1-1	1	0	16	15	192	182	1872	1895
1-2	1	0	15	15	196	180	1845	1873
1-3	1	1	15	15	185	184	1851	1945
1-4	1	1	15	15	186	182	1852	1856
1-5	1	1	15	15	183	179	1852	1829
1-6	1	1	15	15	195	177	1839	1891
Repeated sampling on day 1								
2	1	0	15	15	210	205	2248	2071
3	4	2	15	15	181	161	1957	1776
4	1	1	26	23	211	170	1990	1592
5	4	4	28	27	180	184	2019	1923
6	3	3	9	9	178	172	2012	1974
Repeated sampling on day 2								
1	3	3	24	23	261	231	1798	1892
2	3	3	27	24	214	213	1649	1654
3	4	3	18	17	232	212	1492	1786

4	3	3	21	20	222	214	1618	1731
5	1	1	30	27	254	237	1592	1681
6	2	2	31	27	205	189	1691	1736

Repeated sampling on day 3

1	1	1	24	22	211	148	2026	1941
2	2	2	20	20	220	211	2084	1796
3	4	4	20	18	277	255	1976	1592
4	5	5	17	17	232	220	2070	1414
5	1	2	24	24	252	238	1981	1740
6	3	3	19	18	213	209	2259	1807

Table 36 Single observations of bacterial concentrations for the determination of the lag-time of *E. faecium*.

Time [min]	Flask 1 [cfu/mL]	Flask 2 [cfu/mL]	Flask 3 [cfu/mL]
0	3.636E+04	5.012E+04	2.261E+04
	3.640E+04	5.142E+04	2.436E+04
	2.915E+04	4.520E+04	3.750E+04
	2.805E+04		3.650E+04
20	3.246E+04	4.558E+04	2.004E+04
	3.426E+04	4.670E+04	2.457E+04
	3.355E+04	4.500E+04	3.610E+04
	3.025E+04	4.920E+04	3.820E+04
40	2.928E+04	4.352E+04	2.322E+04
	2.978E+04	4.698E+04	2.622E+04
	3.080E+04	4.760E+04	4.340E+04
	3.223E+04	4.640E+04	4.340E+04
	2.904E+04		
	4.235E+04		
60	3.806E+04	4.242E+04	2.192E+04
	3.346E+04	5.152E+04	2.280E+04
		4.160E+04	3.820E+04
		4.600E+04	4.180E+04
80	3.288E+04	4.920E+04	2.012E+04
	3.114E+04	5.348E+04	2.401E+04
	2.849E+04	4.760E+04	4.470E+04
	3.894E+04	5.120E+04	4.540E+04
	4.235E+04	7.200E+04	5.900E+04
		6.400E+04	4.200E+04
90		4.702E+04	
		4.378E+04	
		5.040E+04	
		4.420E+04	
		6.800E+04	
		6.000E+04	
100	1.163E+05	5.500E+04	4.780E+04
	1.103E+05	4.800E+04	5.100E+04
	6.413E+04	6.600E+04	5.800E+04
	1.392E+05	1.060E+05	5.360E+04

120	1.133E+05		6.120E+04
	1.288E+05		1.280E+05
	5.929E+04		1.510E+05
	5.203E+04		5.310E+04
140	1.577E+05	2.684E+05	1.378E+05
	1.373E+05	2.670E+05	1.770E+05
	2.081E+05	1.740E+05	1.460E+05
	1.331E+05	1.240E+05	1.660E+05
	1.597E+05		
160	1.804E+05		
	2.263E+05		
	3.412E+05		
	1.730E+05		
	1.997E+05		
180	1.708E+05	4.664E+05	1.656E+05
	1.786E+05	4.864E+05	2.690E+05
	2.335E+05	3.880E+05	2.700E+05
	2.505E+05	4.820E+05	1.515E+05
	3.194E+05		
	1.065E+05		
210		5.696E+05	2.419E+05
		5.182E+05	2.581E+05
		7.240E+05	5.120E+05
		6.440E+05	6.800E+05
		1.080E+06	8.400E+05
		8.200E+05	
240	3.030E+06	3.052E+06	
	2.814E+06	3.820E+06	
	2.050E+06	2.780E+06	
	1.677E+06	2.100E+06	
	2.928E+06		
	3.514E+06		

Table 37 Bacterial concentrations in different dilution media concerning the bacterial survival.

Time	Bacterial survival in		
	NaCl 0.45%	NaCl 0.9%	PBSSP
[min]	[cfu/mL]	[cfu/mL]	[cfu/mL]
0	1.349×10^5	1.290×10^5	1.510×10^5
	1.490×10^5	1.330×10^5	2.790×10^5
	1.500×10^5	2.400×10^5	2.800×10^5
10	1.338×10^5	1.836×10^5	1.649×10^5
	1.600×10^5	1.740×10^5	2.360×10^5
	2.400×10^5	2.400×10^5	3.800×10^5
20	1.820×10^5	1.523×10^5	1.192×10^5
	1.700×10^5	1.650×10^5	1.740×10^5
		1.400×10^5	2.900×10^5
30	1.420×10^5	1.399×10^5	1.418×10^5
	1.410×10^5	1.390×10^5	2.270×10^5
	2.200×10^5	2.900×10^5	2.700×10^5
40	1.277×10^5	1.724×10^5	1.698×10^5
	1.360×10^5	1.360×10^5	1.850×10^5
	1.700×10^5	2.500×10^5	3.500×10^5
50	1.349×10^5	1.772×10^5	1.640×10^5
	1.440×10^5	1.730×10^5	2.230×10^5
	1.600×10^5		2.000×10^5
60	1.252×10^5	1.448×10^5	1.587×10^5
	1.620×10^5	1.800×10^5	2.380×10^5
	2.100×10^5	1.500×10^5	3.700×10^5

Table 38 Comparison of centrifugation and dilution method by bacterial concentrations.

Experiment No.	Centrifugation	Dilution
1	1.260E+04	1.639E+04
2	1.568E+04	1.229E+04
3	3.000E+04	1.970E+04
4	3.040E+04	2.180E+04
5	4.400E+04	3.300E+04
6		1.800E+04
Geometric mean:	2.398E+04	1.928E+04

Table 39 Digital counting methods to count E. faecium on MH agar plates with 5% sheep blood by the automated digital colony counter ColonyQuant®; the software parameter and their settings are taken from the ColonyQuant® software (German version).

Software parameter	<100 colonies (low)	>100 colonies (intermediate)	1000 – 2000 colonies (high)
Auswahl	schwarz	schwarz	schwarz
▪ Hintergrund			
Farbe			
	Stärke 50	Stärke 50	Stärke 50
Markierung			
▪ Empfindlichkeit	0.55	0.81	0.80
▪ Unterdrückung Hintergrund	17	17	17
Trennen			
▪ Trennfaktor	0.8	0.87	0.9
▪ Min Linie	0.360	0.4	0.358
▪ Max. Linie	16.9	16.9	16.9
▪ Trennung	mehrfach	mehrfach	mehrfach
Größe und Form			
▪ Min. Fläche	0.008	0.008	0.000
▪ Min. Durchmesser	0.1 mm	0.1 mm	0.0 mm
▪ Max. Fläche	3.0	79.0	1.9
▪ Max. Durchmesser	2.0	10.0	1.5
▪ Min U/F	0.9982	0.9982	0.1
▪ Max U/F	7.346	7.346	7.346

Table 40 Obtained LZD concentrations in the static *in vitro* model.

Time [h]	C_{nom} [µg/mL]	C_{obs} [µg/mL] Experiment 1	Experiment 2	Experiment 3	mean	SD	CV %	RE %
0 h	**32**	32.828	39.712	35.890	36.143	3.449	9.5	12.95
	16	17.150	17.535	16.801	17.162	0.367	2.1	7.26
	8	8.320	9.302	8.106	8.576	0.638	7.4	7.20
	4	4.230	4.038	3.555	3.941	0.348	8.8	-1.47
	2	2.100	2.038	1.916	2.018	0.093	4.6	0.89
	1	0.872	1.376	0.829	1.026	0.304	29.6	2.56
	0.5	0.432	0.705	0.452	0.529	0.152	28.7	5.89
24 h	**32**	35.625	30.177	32.122	32.641	2.761	8.5	2.00
	16	17.356	15.362	15.821	16.180	1.044	6.5	1.12
	8	8.579	7.510	7.070	7.720	0.776	10.0	-3.50
	4	4.306	3.375	3.683	3.788	0.474	12.5	-5.30
	2	2.136	1.988	1.853	1.992	0.141	7.1	-0.39
	1	0.854	0.977	1.018	0.950	0.085	9.0	-5.03
	0.5	0.476	0.569	0.456	0.500	0.060	12.0	0.05

Table 41 Comparison of suitability of syringe and membrane filters for simulations of LZD PK profiles.

Time [h]	Syringe filter Trial 1 Peak Area$_{mean}$[*] %	Trial 2 Peak Area$_{mean}$[*] %	Membrane filter Trial 1 Peak Area$_{mean}$[*] %	Trial 2 Peak Area$_{mean}$[*] %	Trial 3 Peak Area$_{mean}$[*] %
0	102.98	97.02	99.66	97.60	102.73
0.25	93.03	94.11	93.78	93.80	104.17
0.5	85.18	95.86	88.89	89.83	91.27
1	77.39	88.74	78.85	79.56	86.76
2	65.24	68.54	66.43	63.18	65.75
5	36.36	38.54	40.33	32.88	35.10

*determined from double injection

Table 42 Variability of applied PK profiles in the dynamic *in vitro* model.

PK profile	Time [h]	C_{nom}, %	C_{est}^{*}, %	RE, %
1 cmt, iv bolus	0.00	100.0	100.0	0.00
	0.50	90.7	92.4	1.90
	1.00	82.2	81.2	-1.24
	2.00	67.6	66.0	-2.37
	5.00	37.6	34.2	-8.97
1 cmt, continuous infusion	0.25	51.2	51.3	0.17
	0.50	100.0	100.0	0.00
	0.75	95.2	100.0	4.96
	1.00	90.7	90.2	-0.58
	2.00	74.5	79.5	6.58
	5.10	41.4	45.0	8.56
2 cmt, bolus	0.00	100.0	100.0	0.00
	0.08	75.1	73.2	2.61
	0.25	48.6	46.7	3.95
	0.50	37.4	35.3	6.01
	0.75	34.2	31.7	7.81
	1.00	31.6	29.7	6.39
	2.00	26.3	23.9	9.80
	5.00	14.4	12.5	14.59
2 cmt, continuous infusion	0.00	0	0.2	-
	0.08	25.7	22.9	-11.16
	0.25	62.6	59.2	-5.47
	0.50	100.0	97.9	-2.12
	0.58	84.7	91.8	8.49
	0.67	74.3	69.1	-7.09
	0.75	68.7	63.3	-7.83
	0.92	62.0	65.8	6.02
	1.08	58.7	58.1	-0.98
	1.68	50.9	47.6	-6.48
	2.00	47.5	46.1	-2.94
	5.00	24.9	19.3	-22.49

*mean of two measures

Table 43 Variability of drug concentrations in the dynamic model in time-kill experiments; No. presents the number of the culture vessel:

a) LZD concentrations in the dynamic model simulating a one-compartment model, bolus administration, $t_{1/2} = 3.54$ h, 600 mg dose, $C_{max} = 20.134$ µg/mL.

Time [h]	C_{nom} [µg/mL]	No. 1 [µg/mL]	No. 2 [µg/mL]	No. 3 [µg/mL]	No. 4 [µg/mL]	No. 5 [µg/mL]	No. 6 [µg/mL]	No. 7 [µg/mL]	Mean [µg/mL]	SD [µg/mL]	CV %
0	20.000	18.195	17.125	18.493	17.231	21.306	17.427	20.448	18.603	0.686	3.7
1	15.505	14.993				16.262	13.457	13.426	14.535	1.364	9.4
2	12.748	13.599				13.348	12.670	11.512	12.782	0.933	7.3
3	10.481	10.952				9.753	9.497	8.569	9.693	0.981	10.1
6	5.825	5.382				4.624	5.425	5.323	5.189	0.379	7.3
12	1.908	2.212	1.197	1.151	1.007				1.392	0.553	39.7
16	0.872		0.511	0.485	0.419				0.472	0.047	10.0
20	0.398		0.184*	n.a.*	0.241				0.142*		
24	0.182*	0.770	n.a.*	n.a.*	n.a.*	0.191*	0.186*	0.190*	0.191*		

*<LLOQ; n.a. = not analysable

b) LZD concentrations in the dynamic model simulating a one-compartment model, 30 minutes infusion, $t_{1/2} = 3.54$ h, 1200 mg dose, $C_{max} = 36.597$ µg/mL.

Time [h]	C_{nom} [µg/mL]	No. 1 [µg/mL]	No. 2 [µg/mL]	No. 3 [µg/mL]	Mean [µg/mL]	SD [µg/mL]	CV %
0	0.000*	0.272	0.015*	0.015*	0.101*		
0.5	36.325	37.725	29.697	34.264	33.895	4.027	11.9
1	32.489	37.704	32.905	38.297	36.302	2.956	8.1
2	25.991	31.357	23.931	27.151	27.480	3.724	13.6
3	20.792	21.456	18.897	18.565	19.639	1.582	8.1
6	10.645	13.819	9.252	8.611	10.561	2.840	26.9
12	2.790	1.844	2.860	n.a.*	2.352	0.718	30.5
24	0.192*	0.220	0.363	0.463	0.349	0.122	35.0

*<LLOQ; n.a. = not analysable

c) LZD concentrations in the dynamic model simulating a one-compartment model, 30 minutes infusion, $t_{1/2}$ = 5.00 h, 600 mg dose, C_{max} = 19.45 µg/mL.

Time [h]	C_{nom} [µg/mL]	No. 1 [µg/mL]	No. 2 [µg/mL]	No. 3 [µg/mL]	No. 4 [µg/mL]	No. 5 [µg/mL]	No. 6 [µg/mL]	Mean [µg/mL]	SD [µg/mL]	CV %
0	0.000*	n.a.*	n.a.*	n.a.*	n.a.*	n.a.*	0.194*	*		
0.5	19.452	17.617	18.300	14.070	13.496	12.679	14.155	15.053	2.322	15.42
1	18.150	17.530	19.017	16.005				17.517	1.506	8.60
2	15.800	14.770	14.687	16.440				15.299	0.989	6.46
3	13.755	14.058	12.511	10.990				12.520	1.534	12.25
6	9.075	7.501	7.925	8.922				8.116	0.729	8.99
12	3.950				2.515	3.291	2.818	2.875	0.391	13.60
16	2.269				1.311	1.819	1.458	1.529	0.262	17.11
20	1.303				0.736	0.821	0.802	0.786	0.044	5.64
24	0.748	0.261	0.467	0.545	0.237	0.382	0.564	0.409	0.140	34.25

*<LLOQ; n.a. = not analysable

d) LZD concentrations in the dynamic model simulating a two-compartment model, 30 minutes infusion, $t_{1/2}$ beta = 3.22 h, 600 mg dose, C_{max} = 15.94 µg/mL.

Time [h]	C_{nom} [µg/mL]	No. 1 [µg/mL]	No. 2 [µg/mL]	No. 3 [µg/mL]	No. 4 [µg/mL]	No. 5 [µg/mL]	No. 6 [µg/mL]	Mean [µg/mL]	SD [µg/mL]	CV %
0	0.000*	n.a.*	n.a.*	n.a.*	n.a.*	n.a.*	n.a.*	n.a.*		
0.5	15.935	13.687	12.365	15.303	13.451	12.263	13.849	13.486	1.116	8.3
1	9.587	7.927	7.422	7.936				7.762	0.294	3.8
2	7.573	6.318	5.758	6.124				6.067	0.284	4.7
3	6.105	4.870	4.319	4.503				4.564	0.281	6.2
6	3.198	1.691	1.784	2.405				1.960	0.388	19.8
12	0.878				0.612	0.875	0.766	0.751	0.132	17.6
16	0.371				0.215	0.229	0.268	0.237	0.027	11.4
20	0.157*				0.066*	n.a.*	0.179*	0.123*		
24	0.066*	n.a.*	n.a.*	n.a.*	n.a.*	n.a.*	n.a.*	n.a.*		

*<LLOQ; n.a. = not analysable

Table 44 Bootstrapped geometric means of bacterial concentrations derived from the dynamic *in vitro* model.

Time [h]		Bacterial concentration [cfu/mL] under PK simulation and dosing of			
		1 cmt, Bolus, 600 mg	1 cmt, Infusion, 1200 mg	1 cmt, Infusion, 600 mg	2 cmt, Infusion, 600 mg
0	2.5th percentile	6.629E+05	9.478E+05	7.106E+05	7.190E+05
	median	7.382E+05	1.100E+06	8.013E+05	7.900E+05
	97.5th percentile	8.242E+05	1.247E+06	9.112E+05	8.714E+05
1	2.5th percentile	6.356E+05	9.437E+05	8.320E+05	5.124E+05
	median	7.355E+05	1.140E+06	1.050E+06	6.145E+05
	97.5th percentile	8.531E+05	1.330E+06	1.390E+06	7.203E+05
2	2.5th percentile	4.229E+05	7.585E+05	6.078E+05	5.224E+05
	median	5.219E+05	9.410E+05	8.775E+05	6.375E+05
	97.5th percentile	6.511E+05	1.200E+06	1.220E+06	7.871E+05
3	2.5th percentile	3.333E+05	4.820E+05	6.760E+05	3.630E+05
	median	4.598E+05	5.520E+05	8.055E+05	4.596E+05
	97.5th percentile	6.238E+05	6.230E+05	9.538E+05	5.862E+05
4	2.5th percentile	2.019E+05	4.488E+05	4.112E+05	3.137E+05
	median	2.821E+05	5.290E+05	4.627E+05	4.101E+05
	97.5th percentile	3.912E+05	6.272E+05	5.364E+05	4.878E+05
6	2.5th percentile	1.231E+05	2.019E+05	1.091E+05	1.822E+05
	median	1.791E+05	2.370E+05	1.520E+05	2.689E+05
	97.5th percentile	2.568E+05	2.951E+05	2.035E+05	3.844E+05
12	2.5th percentile	8.501E+03	5.055E+04	8.435E+04	7.660E+04
	median	1.936E+04	8.720E+04	9.218E+04	1.134E+05
	97.5th percentile	4.177E+04	1.301E+05	1.027E+05	1.676E+05
16	2.5th percentile	5.927E+04		3.401E+04	3.589E+04
	median	7.105E+04		5.002E+04	8.848E+04
	97.5th percentile	8.338E+04		7.628E+04	1.703E+05
20	2.5th percentile	7.279E+04		1.997E+04	4.856E+05
	median	9.953E+04		3.530E+04	1.936E+06
	97.5th percentile	1.444E+05		4.905E+04	7.206E+06
24	2.5th percentile	8.654E+05	2.579E+07	2.465E+04	5.144E+06
	median	1.504E+06	3.030E+07	5.439E+04	1.158E+07
	97.5th percentile	2.502E+06	3.546E+07	1.232E+05	2.645E+07

Table 45 Mean RBR values calculated from bootstrapped geomeans of bacterial concentrations determined in the dynamic model.

Time	1 cmt, bolus, 600 mg, C_{max} = 20.13 µg/mL, $t_{1/2}$ = 3.45 h		1 cmt, infusion, 1200 mg, C_{max} = 36.68 µg/mL, $t_{1/2}$ = 3.45 h		1 cmt, infusion, 600 mg, C_{max} = 19.45 µg/mL, $t_{1/2}$ = 5 h		2 cmt, infusion, 600 mg, C_{max} = 15.94 µg/mL, $t_{1/2,beta}$ = 3.2 h	
	RBR	C_{nom}	RBR	C_{nom}	RBR	C_{nom}	RBR	C_{nom}
[h]	%	[µg/mL]	%	[µg/mL]	%	[µg/mL]	%	[µg/mL]
0	3.620	20.000	0.775	0.000	3.035	0.000	3.137	0.000
1	10.475	16.444	7.595	32.489	8.116	18.150	11.666	9.587
2	22.579	13.519	19.113	25.991	19.524	15.800	21.403	7.573
3	26.690	11.115	25.660	20.792	23.537	13.755	26.693	6.105
4	33.462	9.139	30.131	16.634	30.837	11.974	31.477	4.921
6	39.434	6.178	38.031	10.645	40.256	9.075	37.399	3.198
12	52.469	1.908	45.220	2.790	44.955	3.950	43.957	0.878
20	44.835	0.872		1.143	49.804	2.269	30.609	0.371
24	32.908	0.182		0.192	48.568	0.748	23.281	0.066

Table 46 Variability in the semi-dynamic *in vitro* model derived as logarithmic bacterial concentrations from three growth control experiments; shown are mean, standard deviation (SD), imprecision expressed as CV in %, minimum (Min) and maximum (Max) observed bacterial concentrations, median bacterial concentration and the number of bacterial counts (n) underlying the calculations. Calculations performed with data from [111].

Time [h]	Mean	SD	CV %	Min	Max	Median	n
0	6.143	0.074	1.21	6.033	6.199	6.170	4
1	6.651	0.139	2.08	6.342	6.869	7.248	6
2	7.234	0.045	0.62	7.152	7.274	7.248	6
3	7.681	0.107	1.40	7.505	7.944	7.664	12
4	8.252	0.103	1.25	8.114	8.380	8.264	6
6	8.777	0.096	1.10	8.676	9.009	8.745	12
8	8.747	0.065	0.74	8.633	8.845	8.739	12
12	8.668	0.093	1.07	8.556	8.778	8.701	11
24	8.757	0.096	1.10	8.641	8.964	8.735	12

Table 47 Overview on obtained effects by dosing optimisation for case 2-4; standard dosing is underlined in grey.

Case No.	Dosing regimen	$C_{p, max}$ [µg/mL]	$C_{e, max}$ [µg/mL]	$AUC_{E,max}/AUC_{E,max (typical)}$, %	$E_{max, ss}$, %	$E_{min, ss}$, %
1	2x 600 mg	11.83	3.31	84	37.6	32.7
	1x 1800 mg	27.14	5.88	93	41.2	34.3
	2x 900 mg	16.33	4.94	95	41.1	39.4
	3x 600 mg	12.55	4.77	95	41.0	40.2
	4x 450 mg	10.53	4.63	95	40.8	40.4
3	2x 600 mg	11.056	3.205	84	37.1	33.8
	1x 1800 mg	21.027	5.429	94	41.3	36.4
	2x 900 mg	14.495	4.786	95	41.0	39.8
	3x 600 mg	12.129	4.697	95	40.9	40.4
	4x 450 mg	10.631	4.596	94	40.8	40.4
4	2x 600 mg	17.471	3.265	84	37.4	32.9
	1x 1800 mg	28.705	5.690	93	41.2	34.8
	2x 900 mg	20.878	4.875	95	41.1	39.5
	3x 600 mg	18.296	4.743	95	40.9	40.2
	4x 450 mg	16.830	4.625	95	40.8	40.3

7.3 Equations

$$\frac{dA1}{dt} = -k_A \cdot A1$$

$$\frac{dA2}{dt} = k_A \cdot A1 - \frac{Q}{V2} \cdot A2 + \frac{Q}{V3} \cdot A3 - \frac{CL}{V3} \cdot INH \cdot A2$$

$$\frac{dA3}{dt} = \frac{Q}{V2} \cdot A2 - \frac{Q}{V3} \cdot A3$$

$$\frac{dA4}{dt} = k_{IC} \cdot \left(\frac{A2}{V2} - A4\right)$$

$$INH = RCLF + (1 - RCLF) \cdot \left(1 - \frac{A4}{IC_{50} + A4}\right)$$

Eq. 18 Differential equations for the applied PK model [32] A1 is the applied dose, A2, A3, A4 are the amounts of LZD in the respective compartments 2 to 4, central, peripheral and inhibition compartment. k_A is the absorption rate constant; k_{IC} is the elimination rate constant from the central into the inhibition compartment; CL is the drug clearance and Q the inter-compartmental clearance. V2 and V3 are volumes of distribution in the central and peripheral compartment. INH represents the inhibited drug fraction. RCLF is the remaining clearance fraction, which cannot be inhibited. IC_{50} is the drug concentration in the inhibition compartment yielding 50% of clearance inhibition.

7.4 Statistics for data evaluation

7.4.1 Descriptive statistics

The following parameters were consulted for the assessment of position and distribution of data.

Calculation of position parameters of data:

- o Arithmetic mean $\quad \overline{x}_{arithm} = \frac{1}{n}\sum_{i=1}^{n} x_i = \frac{x_1 + x_2 + \ldots + x_n}{n}$

- o Geometric mean $\quad \overline{x}_{geom} = \sqrt[n]{\prod_{i=1}^{n} x_i} = \sqrt[n]{x_1 \cdot x_2 \cdot \ldots \cdot x_n}$

- o Median $\quad \overline{x}_{median} = \begin{cases} n = odd : x_{\left(\frac{n+1}{2}\right)} \\ n = even : \frac{1}{2}\left(x_{\left(\frac{n}{2}\right)} + x_{\left(\frac{n}{2}+1\right)}\right) \end{cases}$

Calculation of distribution parameters of data:

o Standard deviation (SD)
$$SD = \sqrt{\frac{\sum_{i=1}^{n}(x_i - \bar{x})^2}{n-1}}$$

o Standard error (SE)
$$SE = \sqrt{\frac{1}{n-2}\left[\sum_{i=1}^{n}(y_i - \bar{y})^2 - \frac{\left[\sum_{i=1}^{n}(x_i - \bar{x})(y_i - \bar{y})^2\right]}{\sum_{i=1}^{n}(x_i - \bar{x})^2}\right]}$$

o Coefficient of variation (CV)
$$CV = \frac{SD}{\bar{x}_{arithm}} \cdot 100\%$$

The coefficient of variation reflects imprecision.

o Relative error (RE)
$$RE = \frac{x - x_{nominal}}{x_{nominal}} \cdot 100\%$$

The relative error reflects inaccuracy.

Precision and accuracy can be calculated by subtraction of 100% - *CV*, % and 100% - *RE*, %, respectively.

o 2.5[th] and 97.5[th] percentile: Values of a data set sorted by size, below which 2.5% and 97.5% of all data are, respectively. The difference between both values equates the 95% confidence interval.

o Coefficient of correlation (R)

$$R = \frac{\sum_{i=1}^{n} w_i (x_i - \bar{x})(y_i - \bar{y})}{\sqrt{\sum_{i=1}^{n} w_i (x_i - \bar{x})^2} \sqrt{\sum_{i=1}^{n} w_i (y_i - \bar{y})^2}}$$

x and y are dependent variables. $\bar{x}$ and $\bar{y}$ are means, w is a weighing factor. The coefficient of correlation reflects, how changes in one variable are related to changes in the other variable.

o Coefficient of determination (R^2)

$$R^2 = \frac{\sum_{i=1}^{n} w_i (y_{obs,i} - \bar{y}_{obs})^2 - \sum_{i=1}^{n} w_i (y_{obs,i} - y_{cal,i})^2}{\sum_{i=1}^{n} w_i (y_{obs} - \bar{y}_{obs})^2}$$

W is the weight applied to a data point, y_{obs} is the value of the observed data, y_{cal} is the value of the model calculation. The coefficient of determination is the measure of the fraction of the total variance constituted by a model.

7.4.2 Explorative statistics

o Statistical tests

The level of statistical significance was set to 0.05.

A two-sided Student's t-test was used to compare the means of two samples. A general linear model was accomplished for an analysis of variance of paired samples with repeated measures. The Kruskal-Wallis test (H-test) was used to find differences between bacterial survival in the different media and the duration of sampling. A distribution-free Mann-Whitney-Wilcoxon test was performed to detect differences between growth control experiments (in different models) at defined time points and to detect changes within one growth control (in one model) between two time points.

o Least square fit

The least square fit is a method to fit non-linear equations to data. It operates with the Powell algorithm and finds the minimum of sum of squared deviations between observed data and the model calculations. [172]

o Simplex fit

The simplex fit is a method based on a simplex algorithm with only a few numbers of iterations. It is especially used for complex models, when no good a priori approximations are available and/or initial estimates can not be intuitively found.[172]

o Akaike's information criterion (AIC)

$$AIC = n \cdot \ln\left[\frac{\sum_{i=1}^{n}\left(y_{obs,i} - y_{cal,i}\right)^2}{n}\right] + 2K$$

The AIC represents the information content of a given parameter set. It depends on the number of data points n and their magnitude. The variable K presents the number of parameters plus 1. Superior models have smaller AICs.[173]

o Corrected Akaike's information criterion (AIC$_c$)

$$AIC_c = AIC + \frac{2 \cdot K \cdot (K+1)}{n - K - 1}$$

A huge number of parameters for a small sample size cause bias and would predict false small AICs. The corrected AIC accounts for this bias with a small sample size adjustment. The larger the sample size, the lower becomes the second term and the correction becomes smaller.[100]

o Model selection criterion (MSC)

$$MSC = \ln\left[\frac{\sum_{i=1}^{n} w_i\left(y_{obs,i} - \overline{y}_{obs}\right)^2}{\sum_{i=1}^{n} w_i\left(y_{obs,i} - y_{cal,i}\right)^2}\right] - \frac{2p}{n}$$

The MSC is the scaled version of the AIC, and thus unaffected by the magnitude of the data. Superior models have larger MSC values.[173]

o **In silico resampling (Bootstrapping)**

To allow a statistical analysis of the bacterial data, the determined bacterial concentrations were amplified via bootstrapping with resampling in Microsoft Excel.[174] All bacterial concentrations at one specific time point and LZD concentration ($4 \leq n \leq 24$) worked as matrix. Thousand samples per time point and concentration were generated from the matrix by resampling with replacement and the 95% confidence intervals calculated.

Publications

Papers

J. Gloede, C. Scheerans, H. Derendorf, C. Kloft.
In vitro pharmacodynamic models to determine the effect of antibacterial drugs.
J. Antimicrob. Chemother., 65: 186-201 (2010).

J. Michael, C. Scheerans, C. Kloft
Modelling in vitro pharmacodynamics of linezolid against vancomycin resistant Enterococcus faecium.
Antimicrob. Agents and Chemotherapy, *in preparation.*

J. Michael, C. Scheerans, C. Kloft
Pharmacokinetic/Pharmacodynamic in silico simulation and analysis for dosing regimen evaluation of linezolid for critically ill patients with VRE infections.
British J. of Clinical Pharmacology, *in preparation*.

Presentations

J. Gloede
PK, PD und wie sich daraus eine Therapie optimieren lässt: Entwicklung eines In-vitro-Infektionsmodells
Martin-Luther Universitaet Halle-Wittenberg, Halle, 05.12.2007

J. Gloede
Development of an in vitro system of infection
University of Florida, Gainesville, USA, 29.02.2008

Conference Abstracts

J. Glöde, C. Scheerans, C. Kloft.
In vitro investigations to quantify the effects of antibiotics using linezolid as model drug.
Annual Meeting of the German Pharmaceutical Society (DPhG) 2007, Erlangen, 10.-13.10.2007. Abstract book, 138 (2007).

J. Gloede, C. Scheerans, C. Kloft.
Vancomycin resistant Enterococcus faecium under constant linezolid exposure.
Ehrlich II – 2nd World Conference on Magic Bullets, Nuernberg, 03.-05.10.08. Abstract book online [www.ehrlich-2008.org/scientificprogram.htm], A-106 (2008).

J. Gloede, C. Scheerans, C. Kloft.
PK/PD-modelling of vancomycin resistant Enterococcus growing under constant linezolid exposure.
Annual Meeting of the German Pharmaceutical Society (DPhG) 2008, Bonn, 08.-11.10.08. Abstract book, 275 (2008).

J. Gloede, C. Scheerans, C. Kloft.
PK/PD-Modelling of Vancomycin Resistant Enterococcus Faecium Growing Under Constant Linezolid Exposure.
Paul Ehrlich Society (PEG) Bad Honnef-Symposium 2009, Königswinter, 06.-07.04.2009. Chemother. J., 18: 70 (2009).

Lebenslauf

Name	Julia Michael (Dipl. Pharm.)
Geburtsdatum und -ort	05. August 1981, Halle
Geburtsname	Glöde
Nationalität	Deutsch

POSTGRADUIERTEN AUSBILDUNG

Seit 07/2011	**Wissenschaftlicher Mitarbeiter** Skinomics GmbH, Halle
05/2010 – 06/2011	**(Elternzeit)**
06/2006 – 09/2010	**Doktorand im Arbeitskreis von Frau Prof. Dr. Kloft** Institutsbereich Pharmazeutische Chemie und Klinische Pharmazie, Institut für Pharmacy, Martin-Luther-Universität Halle-Wittenberg (MLU)
01/2008 – 05/2008	**Forschungsaufenthalt in der Arbeitsgruppe von Herrn Prof. Dr. Derendorf,** University of Florida, Gainesville (Florida, USA)
07/2006	**Verteidigung der Diplomarbeit** Fachbereich Pharmazie, Institut für Pharm. Chemie, MLU, Halle; Titel: „Derivatisierung und weiterführende Untersuchungen von potentiellen MDR-Modulatoren"

PRÄGRADUIERTEN AUSBILDUNG UND BERUFSERFAHRUNG

05/2006	**3. Staatsexamen und Approbation als Apotheker**
11/2005 – 04/2006	**Pharmaziepraktikant** Apotheke am Rathenauplatz, Halle
04/2005 – 10/2005	**Pharmaziepraktikant** Institute of Pharmacy, MLU (Diploma thesis)
10/2004 – 03/2005	**Pharmaziepraktikant** Schering GmbH und Co. Produktions KG, Weimar
09/2004	**2. Staatsexamen Pharmazie**
08-09/2003	**Praktikum in der pharmazeutischen Industrie** Boehringer Ingelheim Pharma GmbH&Co.KG, Biberach
09/2002	**1. Staatsexamen Pharmazie**
08-09/2001	**Famulatur in einer öffentlichen Apotheke** Riebeck-Apotheke, Halle
03/2001	**Famulatur in einer Krankenhausapotheke** Martha-Maria Krankenhaus Halle-Dölau, Halle
10/2000 – 09/2004	**Pharmaziestudium an der MLU, Halle**

SCHULBILDUNG

09/1992 – 07/2000   Gymnasium (Abschluss: Abitur)
Adolf-Reichwein Gymnasium, Halle

MITGLIEDSCHAFTEN

Seit 10/2007   Gewähltes Mitglied der Kammerversammlung und des
Fortbildungsausschusses der Apothekerkammer Sachsen-
Anhalt)

Seit 2006   Deutsche Pharmazeutische Gesellschaft (DPhG)

Halle (Saale), 20.07.2011

Danksagung

Ohne die Unterstützung vieler Menschen, wäre es mir nicht möglich gewesen, diese Arbeit anzufertigen. Daher möchte ich mich an dieser Stelle bei Ihnen bedanken.

Mein besonderer Dank gilt Frau Prof. Kloft, die mir die Möglichkeit gab, eine vielseitige und interessante Doktorarbeit über In-vitro-Infektionsmodelle anzufertigen. Die Kombination von praktischer und theoretischer Arbeit, Organisation, Lehre und gleichzeitig eigener Fortbildung waren für mich äußerst ansprechend.

Des Weiteren möchte ich Prof. Kekulé vom Institut für Medizinische Mikrobiologie der Martin-Luther-Universität Halle-Wittenberg für die freundliche Aufnahme in seinen Räumlichkeiten und die großzügige Unterstützung mit Verbrauchsmaterialien und technischen Geräten danken.

Prof. Derendorf danke ich, dass er mich zu einem Forschungsaufenthalt an der University of Florida eingeladen hat. Der wissenschaftliche Austausch, sowie die örtlichen Fortbildungsmöglichkeiten haben für mich entscheidend zum Verständnis der Arbeit beigetragen.

Bei der Dr. August und Dr. Anni Lesmüller-Stiftung möchte ich mich für die finanzielle Förderung dieses Forschungsaufenthaltes bedanken.

Frau Dr. Hofmann und Frau Dr. Wilhelms danke ich dafür, dass sie mir stets hilfsbereit und kompetent als Ansprechpartner zu Verfügung standen. Ein Dank geht hier auch an die Nährbodenküche der Medizinischen Mikrobiologie für die Versorgung mit Nährmedium und Agarplatten.

Ein herzlicher Dank geht an Frau Frenzel für die Unterstützung bei den HPLC-Analysen und der entsprechenden Auswertung, sowie für die stets angenehme Schreibtischnachbarschaft.
Auch Sebastian Böhner sei herzlich gedankt für seine praktische Unterstützung im Labor bei der Durchführung der Versuche im dynamischen In-vitro-Modell während meiner Schwangerschaft.

Dr. Franziska Simmel, Dr. Christian Scheerans, Dr. Anne Drescher und Freya Binner danke ich für die vielen fachlichen Gespräche, Erörterungen und Motivationen.

Meinem Arbeitskreis danke ich für das angenehme Arbeitsumfeld und die gegenseitige Unterstützung.

Meinem Mann Thomas möchte recht herzlich für die vielen anregenden Gespräche und die konstruktive Kritik zu meiner Arbeit besonders zu den Modellierungen danken.

Meiner Mutter danke ich für das Vertrauen, dass sie immer in mich gesetzt hat, und die aufbauenden Gespräche.

Meiner Tochter Karoline danke ich für die vielen Stunden des Schlafens, in denen diese Arbeit geschrieben werden konnte.

Erklärung

Hiermit erkläre ich, dass ich mich mit der vorliegenden Dissertation erstmals um die Erlangung eines Doktorgrades bewerbe. Ferner erkläre ich, dass ich die vorliegende Arbeit selbständig und ohne fremde Hilfe angefertigt habe, sowie andere als die von mir angegebenen Quellen und Hilfsmittel nicht benutzt und die den verwendeten Werken wörtlich oder inhaltlich entnommenen Stellen als solche kenntlich gemacht habe.

Halle/Saale, 20.07.2011